Hawaii Ocean Time-series Program

DATA REPORT 12

2000

Rev 1.1: July 2004

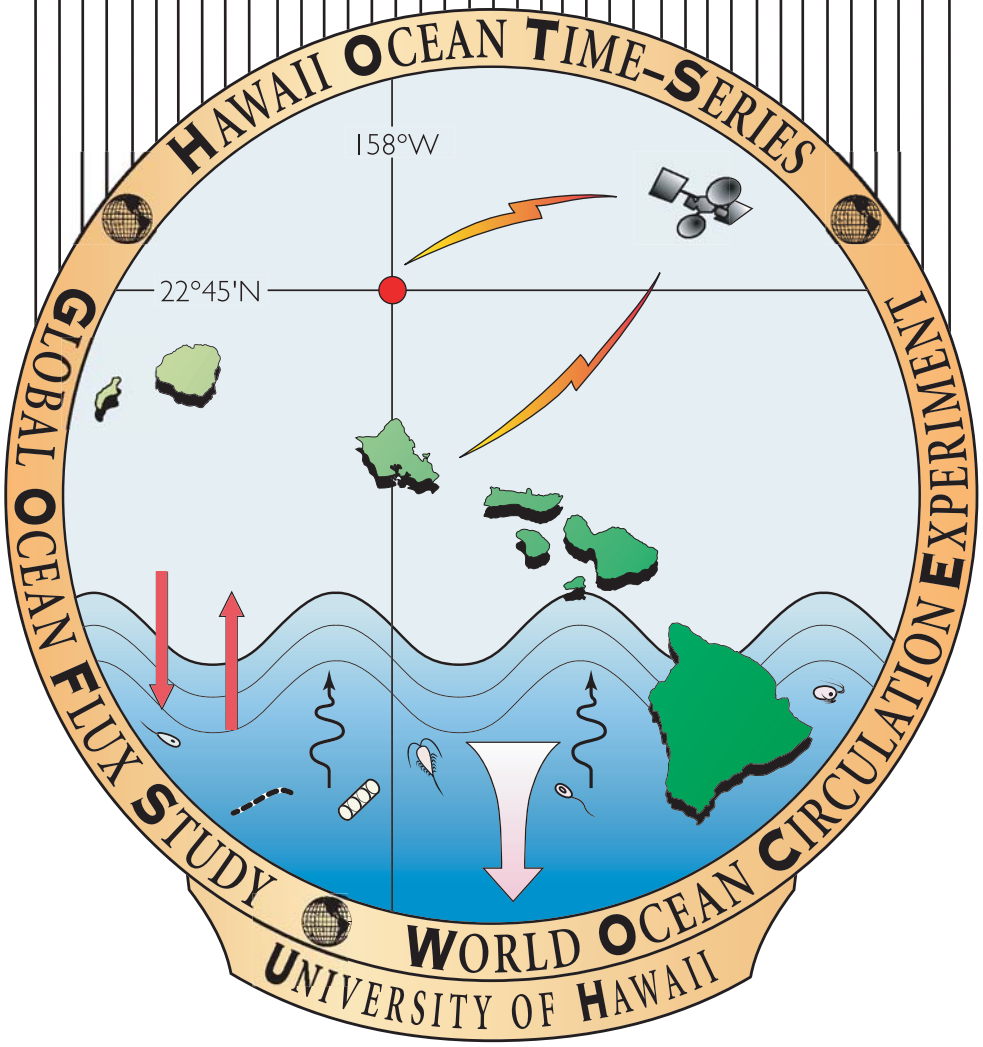

Hawaii Ocean Time-series
Data Report 12: 2000

Rev 1.1: July 2004

Lance A. Fujieki
Fernando Santiago-Mandujano
Jeremiah Johnson
Cecelia Sheridan
Roger Lukas
David Karl

with contributions by:
Robert Bidigare
John Dore
Eric Firing
Michael Landry

University of Hawaii
School of Ocean and Earth Science and Technology
1000 Pope Road
Honolulu, Hawaii 96822
U.S.A.

PREFACE

Scientists working on the Hawaii Ocean Time-series (HOT) program have been making repeated observations of the hydrography, chemistry and biology of the water column at a station north of Oahu, Hawaii since October 1988. The objective of this research is to provide a comprehensive description of the ocean at a site representative of the North Pacific subtropical gyre. Cruises are made approximately once per month to the deep-water station ALOHA (A Long-term Oligotrophic Habitat Assessment; 22° 45' N, 158° 00' W) located 100 km north of Oahu, Hawaii. Measurements of the thermohaline structure, water column chemistry, currents, primary production, plankton community structure, and particle sedimentation rates are made on each cruise.

This document reports the data collected in 2000. However, we have included some data from 1988-1999 to place the 2000 measurements within the context of our ongoing time-series observations. The data reported here are a subset of the complete data set. Summary plots are given for CTD, biogeochemical, optical, meteorological, thermosalinograph and ADCP observations. The complete data set resides on a Sun workstation at the University of Hawaii. These data are in ASCII format, and can easily be accessed using either anonymous file transfer protocol (FTP) ,the World Wide Web (WWW) or the Hawaii Ocean Time-series Data Organization and Graphical System (HOT-DOGS).

ACKNOWLEDGMENTS

Many people participated in the 2000 cruises sponsored by the HOT program. Special thanks are due to Colleen Allen, Karin Björkman, Matt Church, Dale Hebel, Lal Ratnapala and Mark Valenciano for the tremendous amount of time and effort they have put into the program. Special thanks are given to Lisa Lum and Andrea Matsuda for their excellent administrative support of the program, Sharon DeCarlo for computer support, Siang Chyn Lim and Ishuan Wu for CTD processing and June Firing for ADCP processing. Ursula Magaard performed many of the core chemical analyses. Karin Björkman, Ted Walsh and Terrence Houlihan performed the nutrient analyses, Don Wright and Jeremiah Johnson performed the salinity measurements & Douglas Herring provided additional technical support. We gratefully acknowledge the support from Nordeen Larson, Ken Lawson and Jim Carlson of Sea-Bird for helping us to maintain the quality of the CTD data throughout the HOT program. We also would like to thank the captains and crew members of the R/V *Ka'imikai-o-Kanaloa* and the UH Marine Center staff for their efforts. Without the assistance of these and the many technicians, students and ancillary investigators, the data presented in this report could not have been collected, processed, analyzed and reported. Weather buoy data used in this report were obtained by the NOAA National Data Buoy Center (NDBC) and were provided to us by the National Oceanographic Data Center (NODC). We thank Pat Caldwell for his assistance.

This data set was acquired with funding from the National Science Foundation (NSF) and State of Hawaii general funds. The specific grants which have supported our 2000 work are NSF grants OCE-9811921 (Lukas) and OCE-9617409 (Karl, Bidigare, Hebel, Landry and Tupas).

1.0 INTRODUCTION

In response to the growing awareness of the ocean's role in climate and global environmental change, and the need for additional and more comprehensive oceanic time-series measurements, the Board on Ocean Science and Policy (BOSP) of the National Research Council (NRC) sponsored a workshop on "Global Observations and Understanding of the General Circulation of the Oceans" in August 1983. The proceedings of this workshop (National Research Council 1984a) served as a prospectus for the development of the U.S. component of the World Ocean Circulation Experiment (WOCE). US-WOCE has the following objectives:

- To understand the general circulation of the global ocean, to model with confidence its present state and predict its evolution in relation to long-term changes in the atmosphere.
- To provide the scientific background for designing an observation system for long-term measurement of the large-scale circulation of the ocean.

In a parallel effort, a separate research program termed Global Ocean Flux Study (GOFS) focused on the ocean's carbon cycle and associated air-sea fluxes of carbon dioxide. In September 1984, NRC-BOSP sponsored a workshop on "Global Ocean Flux Study" which served as an eventual blueprint for the GOFS program (National Research Council 1984b). In 1986, the International Council of Scientific Unions (ICSU) established the International Geosphere-Biosphere Program: A Study of Global Change (IGBP), and the following year JGOFS (Joint GOFS) was designed as a Core Project of IGBP. US-JGOFS research efforts focus on the oceanic carbon cycle, its sensitivity to change and the regulation of the atmosphere-ocean CO_2 balance (Brewer et al., 1986). The broad objectives of US-JGOFS are:

- To determine and understand on a global scale the time-varying fluxes of carbon and associated biogenic elements in the ocean.
- To evaluate the related exchanges of these elements with the atmosphere, the sea floor and the continental boundaries (Scientific Committee on Oceanic Research 1990).

In order to achieve these goals, four separate program elements were defined: (1) process studies to capture key regular events, (2) long-term time-series observations at strategic sites, (3) a global survey of relevant oceanic properties (e.g., CO_2), and (4) a vigorous data interpretation and modeling effort to disseminate knowledge and to generate testable hypotheses.

In 1987, two separate proposals were submitted to the US-WOCE and US-JGOFS program committees, respectively, by scientists at the University of Hawaii at Manoa, to establish a multi-disciplinary, deep water hydrostation in Hawaiian waters. In July 1988, these proposals were funded by the National Science Foundation and Station ALOHA was officially on the map (Karl and Lukas 1996). A sister station in the western North Atlantic Ocean, near the historical Panulirus Station, was likewise funded by the US-JGOFS program and is operated by scientists at the Bermuda Biological Station for Research, Inc. (Michaels and Knap 1996).

The primary research objectives of these ocean measurement programs are to establish and maintain deep-water hydrostations for observing and interpreting physical and biogeochemical variability. The initial design called for repeat measurements of a suite of core parameters at approximately monthly intervals, compilation of the data and rapid distribution to the scientific community.

1.1 Hawaii Ocean Time-series Program

The Hawaii Ocean Time-series (HOT) Program consists of several research components led by scientists at the University of Hawaii at Manoa (Table 1.1). The hydrographic (WOCE) and biogeochemical (JGOFS) components are fully integrated operationally and are both involved in all aspects of planning and execution of HOT Program objectives.

Table 1.1: HOT Research Components in 2000

Principal Investigators	Project Title
Robert R. Bidigare	Phytoplankton community structure
John E. Dore	JGOFS Carbon Component
Eric Firing	ADCP Component
David M. Karl	JGOFS Core Component
Michael R. Landry	Zooplankton community structure
Roger B. Lukas	Physical Oceanography Component

1.2 Scientific objectives for HOT

The primary objective of HOT is to obtain a long time-series of physical and biogeochemical observations in the North Pacific subtropical gyre that will address the goals of the US Global Change Research Program. The objectives specific to the WOCE program are to:

- Document and understand seasonal and interannual variability of water masses.
- Relate water mass variations to gyre fluctuations.
- Determine the need and methods for monitoring currents at Station ALOHA.
- Develop a climatology of short-term physical variability.

In addition to these general primary objectives, the physical oceanographic component of HOT provides CTD/rosette sampling support for the JGOFS time-series sampling program, and supports development of new instrumentation for hydrographic observations.

The objectives of HOT specific to the JGOFS program are to:

- Document and understand seasonal and interannual variability in the rates of primary production, new production and particle export from the surface ocean.
- Determine the mechanisms and rates of nutrient input and recycling, especially for N and P in the upper 200 m of the water column.
- Measure the time-varying concentrations of DIC in the upper water column and estimate the annual air-to-sea CO_2 flux.

In addition to these primary objectives, the HOT Program provides logistical support for numerous complementary research programs (Table 1.2). A complete listing of these projects can be obtained from the HOT-JGOFS web page (hahana.soest.hawaii.edu/hot/ancillary.html).

Table 1.2: Ancillary Projects Supported by HOT in 2000

Principal Investigator(s)	Institution	Agency	Project Title
Mark Abbott/ Ricardo Letelier	Oregon State University	NASA	HALE ALOHA: biooptics
Claudia Benitez-Nelson	Univ. Hawaii	NSF	^{234}Th export
Edward Boyle	MIT	NSF	HALE ALOHA: trace metals
Steven Emerson	Univ. Washington	NSF	HALE ALOHA: dissolved gases
Hans Jannasch/ Ken Johnson	MBARI	MBARI	HALE ALOHA: automated nutrients
Charles Keeling	UCSD Scripps Inst. Oceanography	NSF	$^{13}C/^{12}C$ ratio of atmosphere carbon dioxide and oceanic carbon in relation to the global carbon cycle
Ricardo Letelier	Oregon State University	NASA	TSRB validation of satellite remote sensing at Station ALOHA
Brian Popp/ Nathaniel Ostrom	Univ. Hawaii/ Michigan State University	NSF	Origins of oceanic N_2O
John Porter	Univ. Hawaii	NASA	Aerosols at Station ALOHA
Paul Quay	Univ. Washington	NOAA	$^{13}C/^{12}C$ of dissolved inorganic carbon in the ocean
Ken Smith	UCSD Scripps Inst. Oceanography	NSF	Organic carbon utilization by deep-sea sediment communities
Jonathan Zehr	UC Santa Cruz	NSF	Nitrogen fixation genes

1.3 HOT Study Site

There are both scientific and logistical considerations involved with the establishment of any long-term, time-series measurement program. Foremost among these are site selection, choice of variables and general sampling design, including sampling frequency. Equally important design considerations are those dealing with the choice of analytical methods for a given candidate variable, especially an assessment of the desired accuracy and precision, and availability of suitable reference materials, the hierarchy of sampling replication and, for data collected at a fixed geographical location, mesoscale horizontal variability.

We evaluated several major criteria prior to selection of the site for the HOT oligotrophic ocean benchmark hydrostation. First, the station must be located in deep water (>4000 m), upwind (north-northeast) of the main Hawaiian islands and of sufficient distance from land to be free from coastal ocean dynamics and biogeochemical influences. On the other hand, the station should be close enough to the port of Honolulu to make relatively short duration (<5 d) monthly cruises logistically and financially feasible. A desirable, but less stringent criterion would locate the station at, or near, previously studied regions of the central North Pacific Ocean, in particular Station GOLLUM. Documentation of oceanic time-series measurements in the North Pacific Ocean can be found in Karl and Winn (1991), Karl et al. (1996b), Karl and Lukas (1996) and in the HOT-JGOFS web page (hahana.soest.hawaii.edu/hot/hot_jgofs).

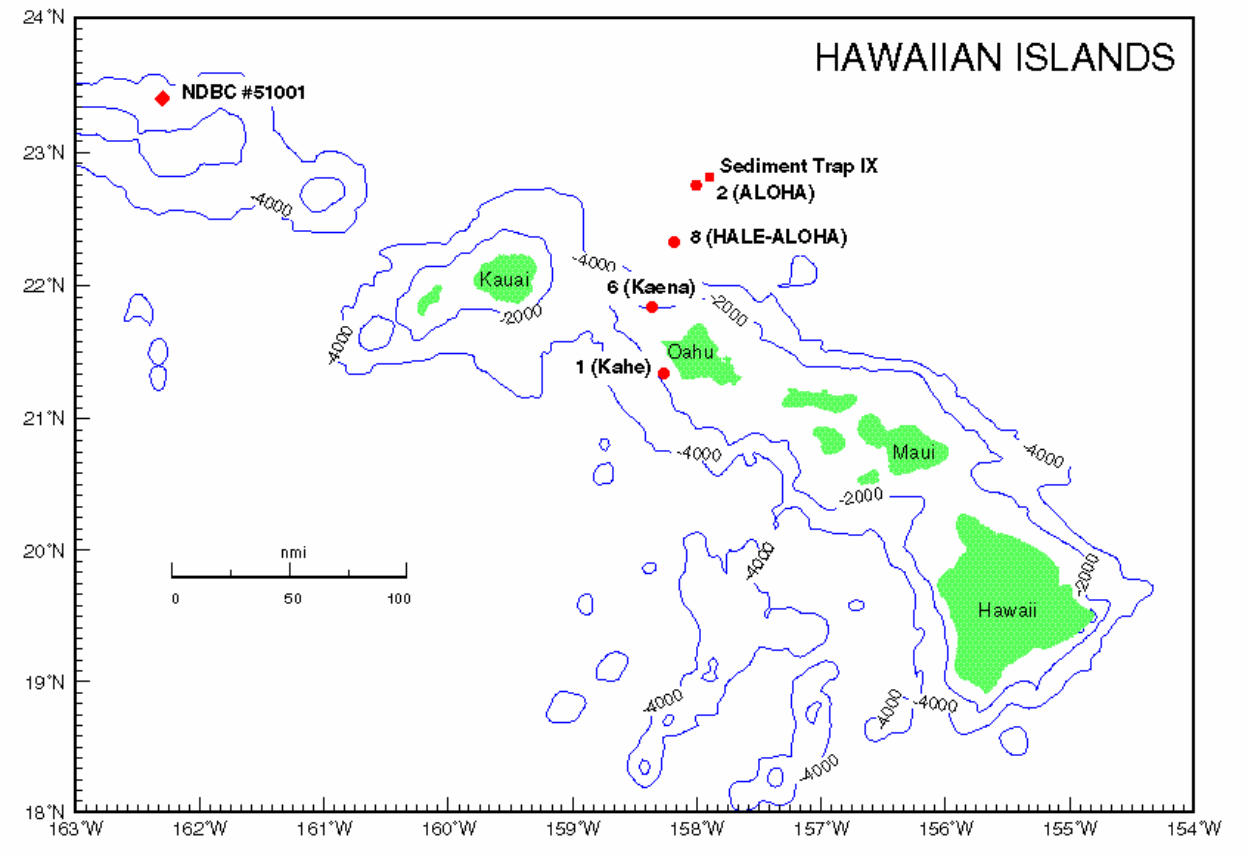

Figure 1.1: Map of the Hawaiian islands showing the locations of the HOT stations and the NOAA-NDBC weather buoy #51001. Depth contours are in meters.

After consideration of these criteria, we established our primary sampling site at 22° 45' N, 158° W at a location approximately 100 km north of the island of Oahu (Figure 1.1), and generally restrict our monthly sampling activities to a circle with an 10 km radius around this nominal site (Figure 1.2). Station ALOHA is in deep water (4750 m) and is more than one Rossby radius (50 km) away from steep topography associated with the Hawaiian Ridge. We also established a coastal station WSW of the island of Oahu, approximately 10 km off Kahe

Point (21° 20.6' N, 158° 16.4' W) in 1500 m of water. Station Kahe serves as a coastal analogue to our deep-water site and the data collected there provide a near-shore time-series for comparison to our primary open ocean site. Station Kahe is also used to test our equipment each month before departing for Station ALOHA, and to orient new personnel at the beginning of each cruise. In January 1997, a physical-biogeochemical mooring was deployed to obtain continuous measurements of various atmospheric and oceanographic parameters. The mooring is located at 22° 28' N, 158° 8' W and was designated as Station HALE-ALOHA. Locations and dates of occupancy of HOT water column and bottom recording stations are available on the HOT-JGOFS web page (hahana.soest.hawaii.edu/hot/locations.html).

1.4 Field Sampling Strategy

HOT program cruises are conducted at approximately monthly intervals; the exact timing is dictated by the availability of research vessels. From HOT-1 (October 1988) to HOT-65 (August 1995), with the exception of HOT-42 and HOT-43 (November and December 1992), each cruise was 5 d in duration (port to port). Beginning with HOT-66 (September 1995) the standard HOT cruise was reduced to 4 d in order to accommodate the additional mooring-based HOT field programs within a fixed per annum allocation of ship days.

From HOT-1 (October 1988) to HOT-32 (December 1991), underway expendable bathythermograph (XBT; Sippican T-7 probes) surveys were conducted at 13 km spacing on the outbound transect from Station Kahe to Station ALOHA. These surveys were later discontinued because the space-time correlation of the energetic, internal semi-diurnal tides made it difficult to interpret these data. From February 1995 until December 1997 we added an instrumented, 1.5 m Endeco towfish package (Sea-Bird CTD, optical plankton counter, fluorometer) to our sampling program (Tupas et al., 1997). Upper water column currents are measured both underway and on station using a hull-mounted Acoustic Doppler Current Profiler (ADCP), when available (Firing 1996). The majority of our sampling effort, approximately 60-72 h per standard HOT cruise, is spent at Station ALOHA. Underway near-surface measurement of a variety of physical, chemical and biological properties were made possible by sampling seawater through a pumped intake system positioned in the hull of the R/V *Moana Wave*. In May 1995, a thermosalinograph was installed in line to the ship's seawater intake system. In July 1996, the existing system was replaced with a non-contaminating PVC/ stainless steel system. A flow-through fluorometer was installed in 1996. R/V *Ka'imikai-o-Kanaloa* is outfitted with a similar seawater intake system to which the existing instruments were installed when R/V *Moana Wave* was retired.

High vertical resolution environmental data are collected with a Sea-Bird CTD having external temperature (T), conductivity (C), dissolved oxygen (DO) and fluorescence sensors and an internal pressure (P) sensor. A Sea-Bird 24-place carousel and an aluminum rosette that is capable of supporting 24 12-l PVC bottles are used to obtain water samples from desired depths.

The CTD and rosette are deployed on a 3-conductor cable allowing for real-time display of data and for tripping the bottles at specific depths of interest. The CTD system takes 24 samples s^{-1} and the raw data are stored both on the computer and, for redundancy, on VHS-format video tapes. We also routinely conduct a dedicated hydrocast to collect “clean” water samples for biological rate measurements, using General Oceanics Go-Flo bottles, Kevlar line, a metal-free sheave, Teflon messengers and a stainless steel bottom weight. A free-drifting sediment trap array, identical in design to the VERTEX particle interceptor trap (PIT) array

(Knauer et al., 1979), is deployed at Station ALOHA for an approximately 60 h period to collect sinking particles for chemical and microbiological analyses.

Sampling at Station ALOHA typically begins with sediment trap deployment followed by a deep (> 4700 m) CTD cast and a "burst series" of at least 13 consecutive 1000 m casts, on 3-h intervals, to span the local inertial period (~ 31 h) and three semidiurnal tidal cycles. The drift tracks of the sediment trap arrays and the location of the CTD casts for each cruise are shown in Figure 1.2. The repeated CTD casts enable us to calculate an average density profile from which variability on tidal and near-inertial time scales has been removed. These average density profiles are useful for the comparison of dynamic height and for the comparison of the depth distribution of chemical parameters from different casts and at monthly intervals. This sampling strategy is designed to assess variability on time scales of a few hours to a few years. Very high frequency variability (< 6 h) and variability on time scales of between 3-60 d are not adequately sampled with our ship-based operations.

Water samples for a variety of chemical and biological measurements are routinely collected from the surface to within 5 m of the seafloor. To the extent possible, we collect samples for complementary biogeochemical measurements from the same or from contiguous casts to minimize aliasing caused by time-dependent changes in the density field. This approach is especially important for samples collected in the upper 300 m of the water column. Furthermore, we attempt to sample from common depths and specific density horizons each month to facilitate comparisons between cruises. Water samples for salinity determinations are collected from every water bottle to identify sampling errors. Approximately 20% of the water samples are collected and analyzed in duplicate or triplicate to assess and track our precision in sample analyses.

The HOT program was initially conceived as being a deep ocean, ship and mooring based observation experiment that would have an approximately 20 y lifetime. Consequently, we selected a core suite of environmental variables that might be expected to display detectable change on time scales of several days to one decade. Except for the availability of existing satellite and ocean buoy sea surface data, the initial phase of the HOT program (Oct 1988 - Feb 1991) was entirely supported by research vessels. In February 1991, an array of five inverted echo sounders (IES) was deployed in an approximately 150 km^2 network around Station ALOHA (Chiswell 1996) and in June 1992, a sequencing sediment trap mooring was deployed a few km north of Station ALOHA (Karl et al., 1996a). In 1993, the IES network was replaced with two strategically-positioned instruments: one at Station ALOHA and the other at Station Kaena. The IES at Station Kaena was retired in October 1995. Between 1994 and 1999, a single IES was positioned and annually replaced at Station ALOHA. In January 1997, the Hawaii Air-sea Logging Experiment (HALE) was initiated with the deployment of a physical-biogeochemical mooring designated as HALE-ALOHA. Details of this mooring can be obtained from the HOT-JGOFS web site (hahana.soest.hawaii.edu/hot/hale-aloha/ha.html).

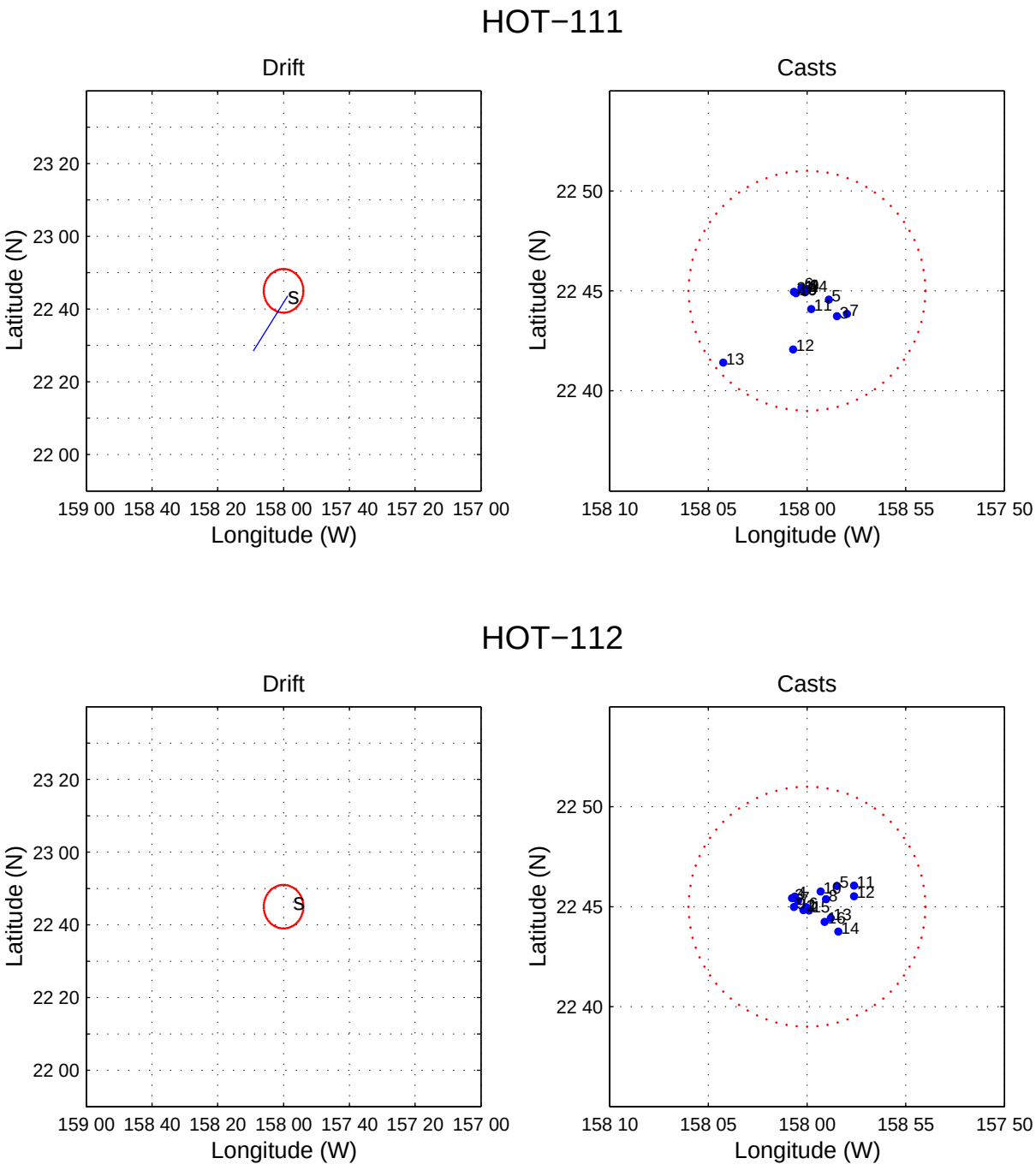

Figure 1.2: [Left panels] Drift tracks of the sediment trap array during each HOT cruise in 2000. Starting point of deployment indicated by "S". [Right panels] CTD cast locations during each HOT cruise in 2000. Location numbers correspond to cast numbers. Dashed line indicates the 10 km radius circle defining the station.

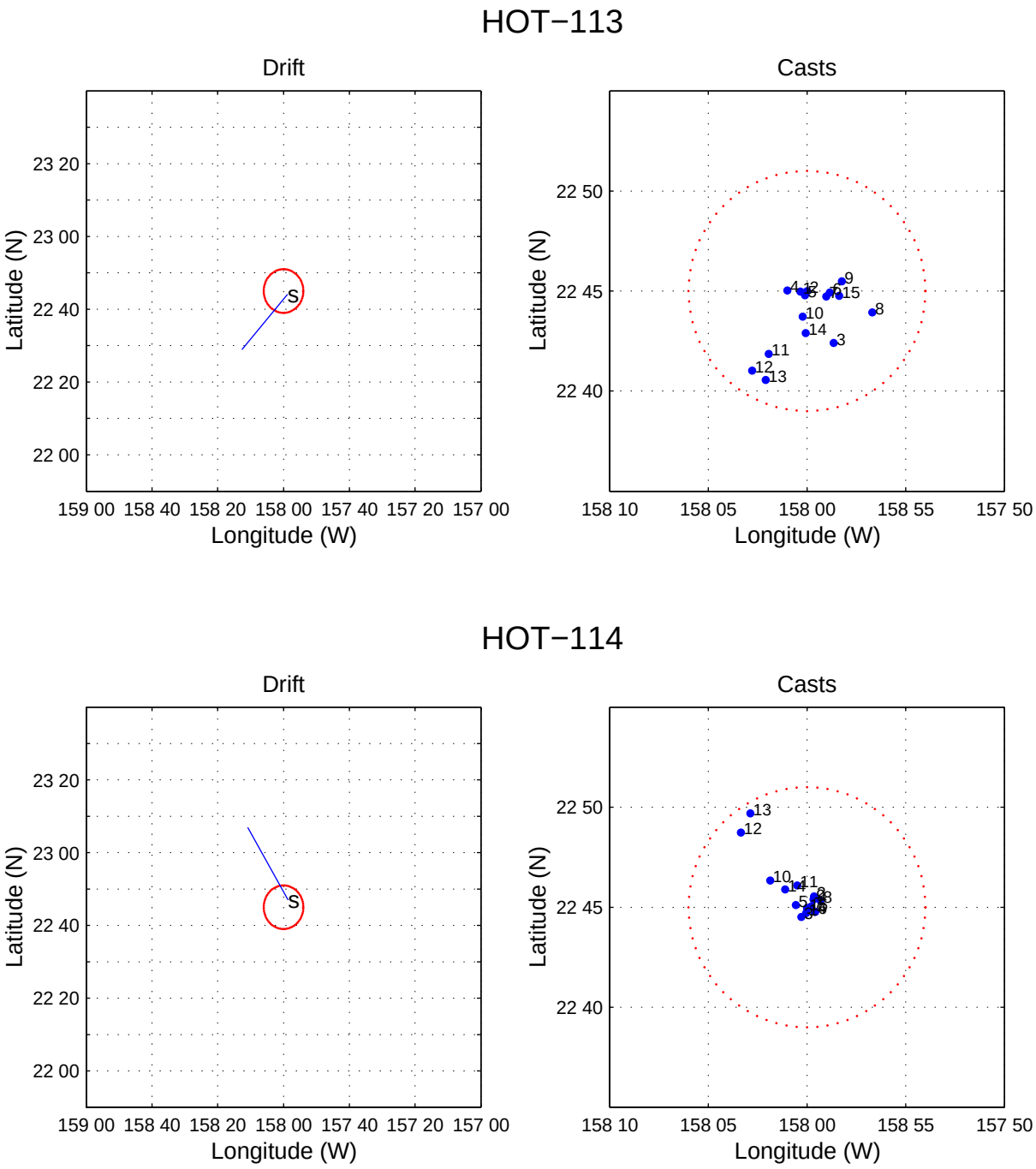

Figure 1.2: continued

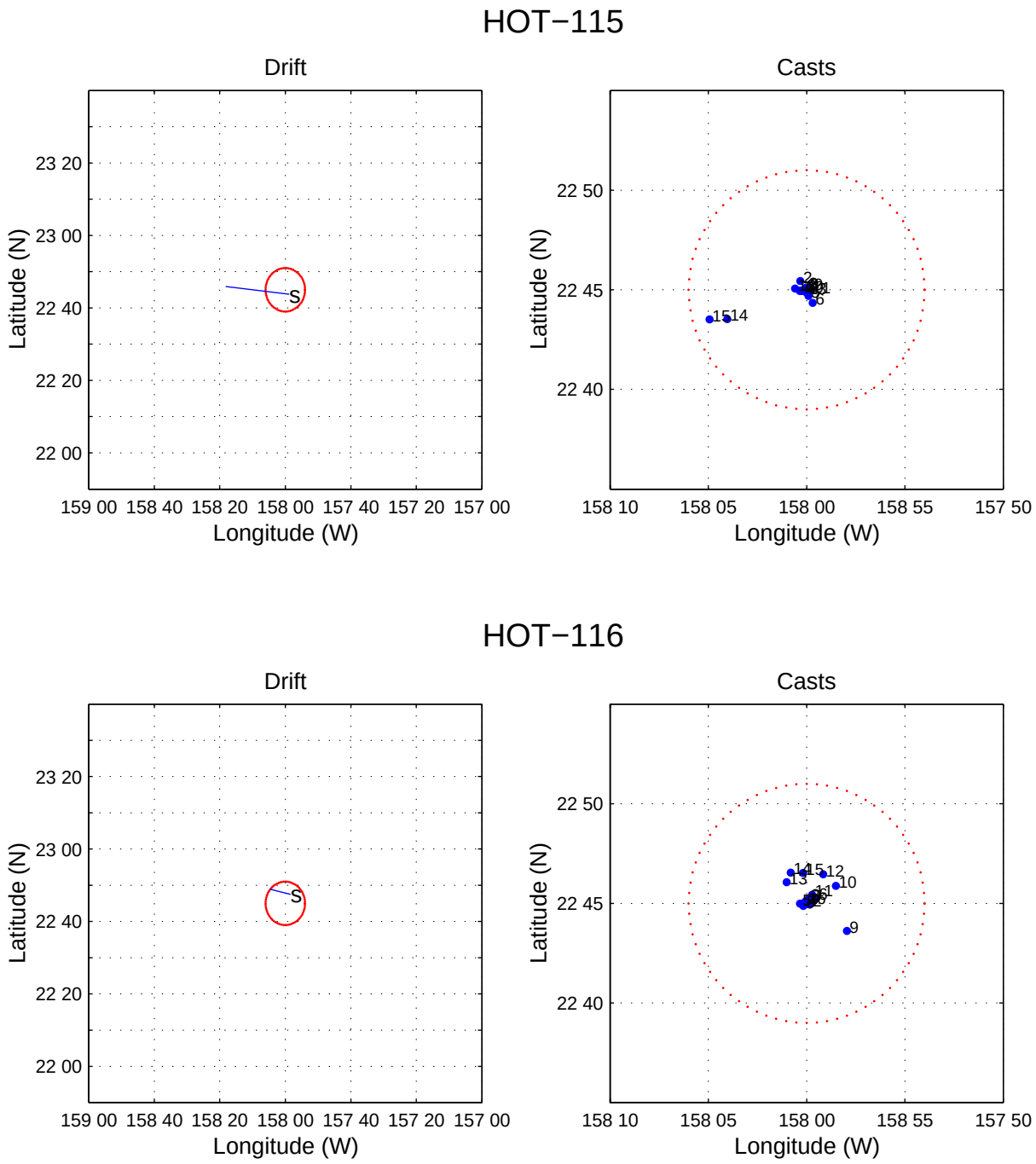

Figure 1.2: continued

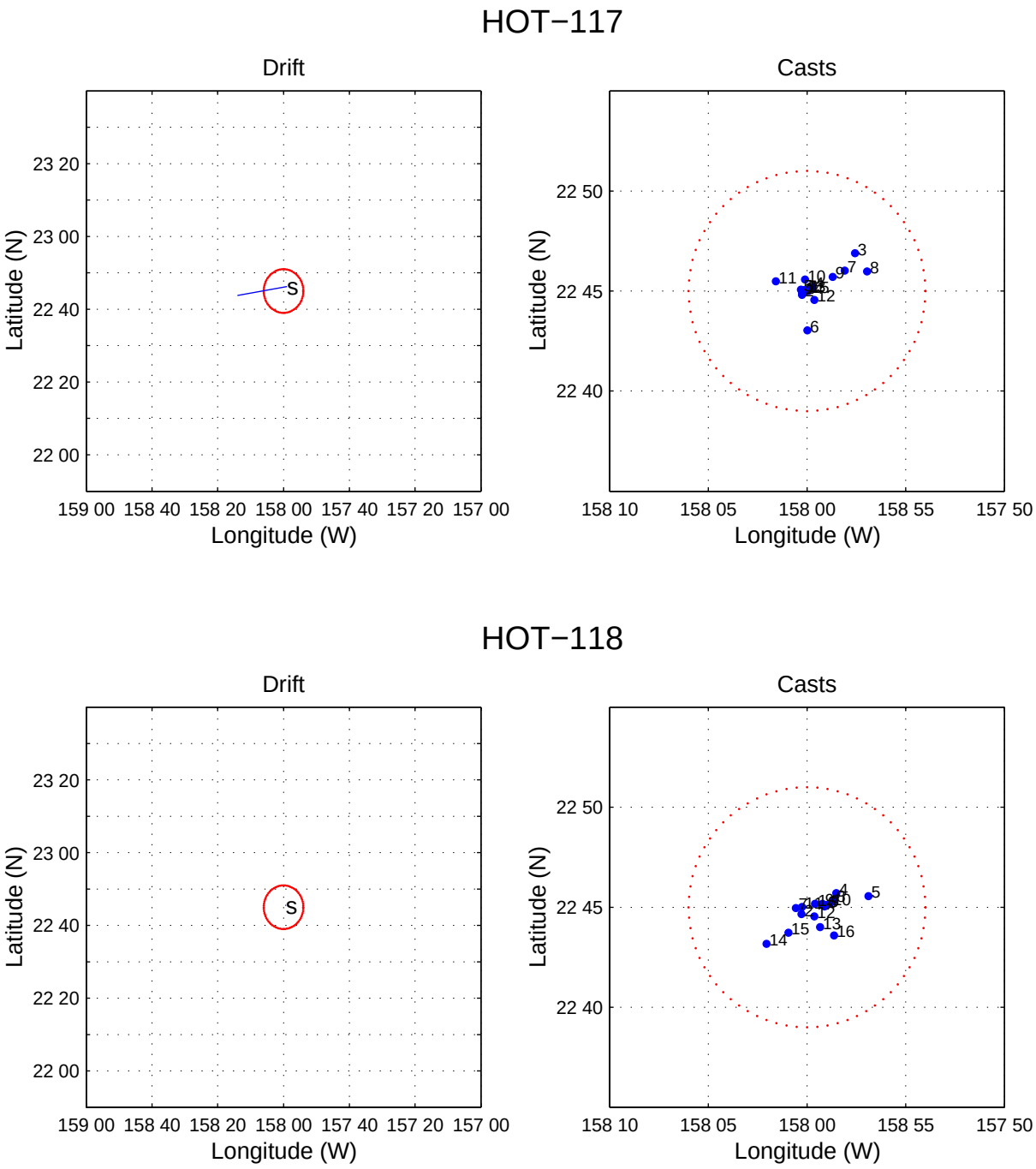

Figure 1.2: continued

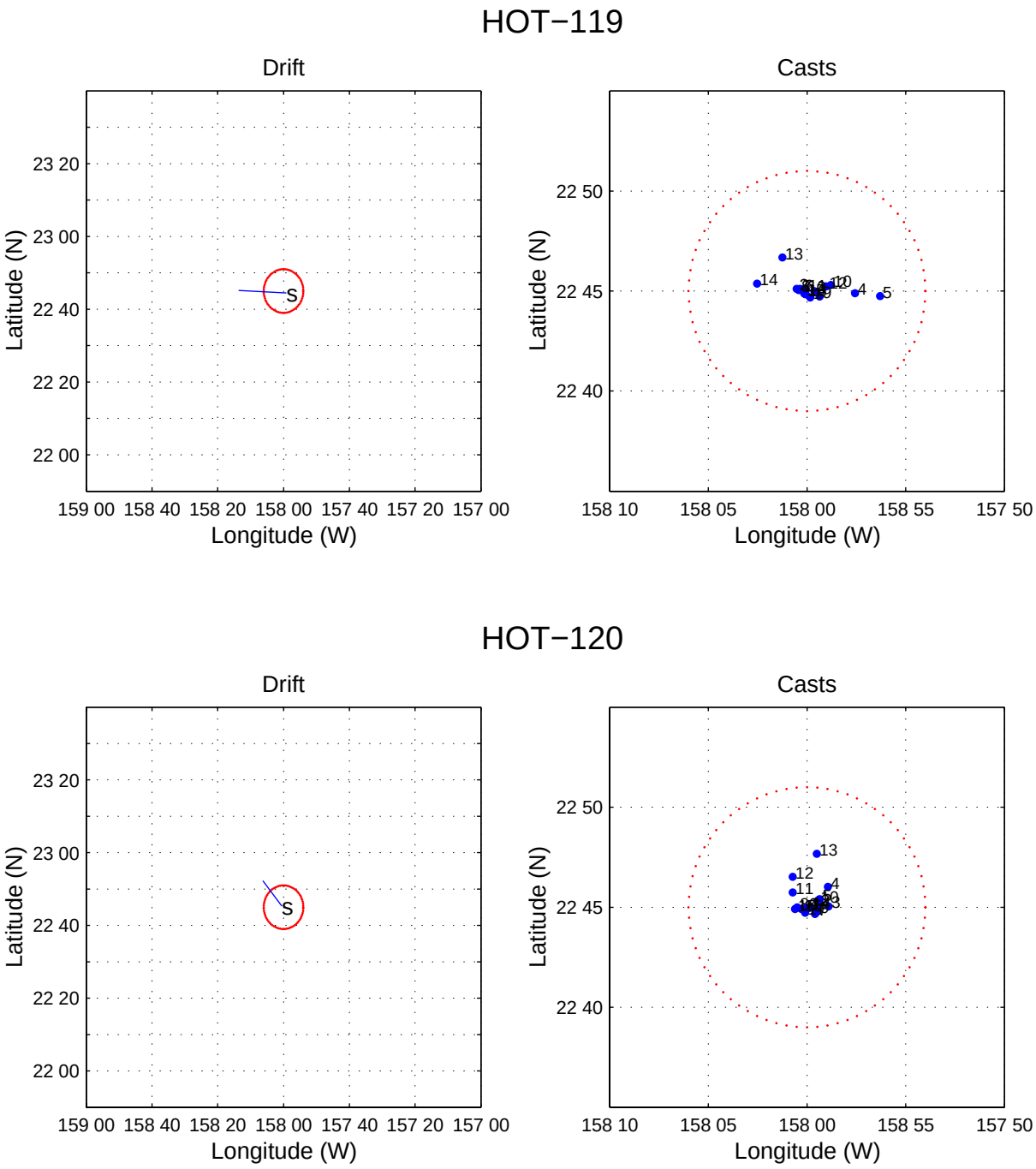

Figure 1.2: continued

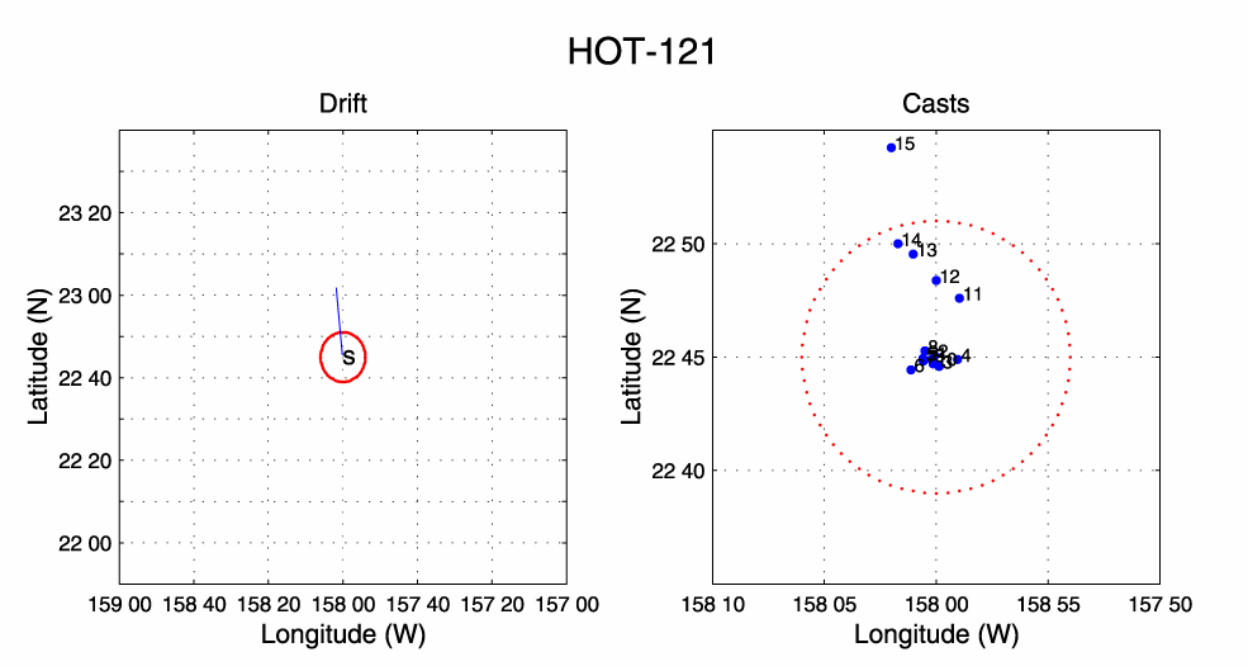

Figure 1.2: continued

1.5 Core Measurements, Experiments and Protocols

The suite of core measurements provides a database to validate existing biogeochemical models and to develop improved ones. Our list of core measurements has evolved since the inception of the HOT program in 1988, and now includes both continuous and discrete physical, biological and chemical ship-based measurements, *in situ* biological rate experiments, and observations and sample collections from bottom-moored instruments and buoys (Table 1.3). Continuity in the measurement parameters and their quality, rather than continuity in the methods employed, is of greatest interest. Detailed analytical methods are expected to change over time through technical improvements. In addition to the core data, specialized measurements and process-oriented experiments have also been conducted at Station ALOHA (Table 1.3).

Table 1.3: Parameters Measured at Station ALOHA during 2000

Parameter	Depth Range (m)	Analytical Procedure
I. Continuous Measurements		
Depth (Pressure)	0-4750	Pressure transducer on Sea-Bird CTD package
Temperature	0-4750	Thermistor on Sea-Bird CTD package
Conductivity (Salinity)	0-4750	Conductivity sensor on Sea-Bird CTD package, standardization with Guildline AutoSal using Wormley seawater standard
Dissolved Oxygen	0-4750	YSI or Sea-Bird sensor on Sea-Bird CTD package with Winkler standardization
Fluorescence (Chloropigment)	0-1000	Sea-Tech flash fluorometer
II. Water Column Chemical Measurements		
Oxygen	0-4750	Winkler titration
Dissolved Inorganic Carbon	0-4750	Coulometry
Total Alkalinity	0-4750	Automated Gran titration
Nitrate Plus Nitrite	0-4750	Autoanalyzer
Soluble Reactive Phosphorus (SRP)	0-4750	Autoanalyzer
Silicate	0-4750	Autoanalyzer
Low Level Nitrate Plus Nitrite	0-200	Chemiluminescence
Low Level SRP	0-200	Magnesium-induced coprecipitation
Dissolved Organic Carbon	0-1000	High temperature catalytic oxidation
Dissolved Organic Nitrogen	0-1000	UV oxidation of total nitrogen
Dissolved Organic Phosphorus	0-1000	UV oxidation of total phosphorus
Particulate Carbon	0-1000	High temperature combustion
Particulate Nitrogen	0-1000	High temperature combustion

Particulate Phosphorus	0-1000	High temperature combustion
Particulate Silica	0-200	Base Hydrolysis
III. Biomass Measurements		
Chlorophyll *a* and Pheopigments	0-200	Fluorometric analysis
Pigments	0-200	HPLC
Phycoerythrin	0-200	Fluorometric analysis
Adenosine 5′-triphosphate	0-1000	Firefly bioluminescence
Bacteria and Cyanobacteria	0-200	Flow cytometry
Mesozooplankton	0-175	Net tows, elemental analysis
IV. Carbon Assimilation and Particle Flux		
Primary Production	0-200	"Clean" ^{14}C incubations
Carbon, Nitrogen, Phosphorus	150	Free-floating particle traps
V. Currents		
Acoustic Doppler Current Profiler	10-300	Hull mounted, RDI #VM-150
VI. Bow Intake System		
Temperature	3	Sea-Bird remote temperature sensor
Conductivity (Salinity)	3	Sea-Bird temperature and conductivity sensors inside the thermosalinograph package
Fluorometry (Chloropigment)	3	Turner Designs 10-AU
VII. Optical Measurements		
Incident Irradiance	Surface	LI-COR and Biospherical collector
Upwelling radiance and downwelling irradiance	0-175	Biospherical Profiling Reflectance Radiometer PRR-600
Downwelling irradiance	0-3	Tethered Spectral Radiometer Buoy
VIII. Moored Instruments		
Inverted Echo Sounder	4750	Acoustic telemetry, CTD calibration
Sequencing Sediment Traps	2800, 4000	Parflux MK7-21
Physical-Biogeochemical Mooring	Surface-800	See HALE ALOHA web site

These selected measurements are part of a much larger HOT program data set on physical and biogeochemical variability at Station ALOHA that has been collected since October 1988. The complete data set is available to the community by several methods that are described in a subsequent section of this report.

This report presents selected core data collected during the twelfth full year of the HOT Program (January-December 2000). During this period, all regular HOT cruises were conducted using the University of Hawaii research vessel R/V *Ka'imikai-o-Kanaloa* (Table 1.4). University of Hawaii shipboard technical assistance personnel assisted a total field scientific crew of 44 HOT staff, students and visiting scientists (Table 1.5) in our 2000 field work.

Table 1.4: Chronology of 2000 HOT Cruises

Cruise	Ship	Depart	Return
HA-7B	R/V *Thompson*	26 January 2000	27 January 2000
111	R/V *KOK*	1 February 2000	4 February 2000
112	R/V *KOK*	28 February 2000	2 March 2000
113	R/V *KOK*	27 March 2000	30 March 2000
114	R/V *KOK*	24 April 2000	27 April 2000
115	R/V *KOK*	22 May 2000	26 May 2000
116	R/V *KOK*	19 June 2000	22 June 2000
HA-8A	R/V *KOK*	23 June 2000	24 June 2000
117	R/V *KOK*	24 July 2000	28 July 2000
118	R/V *KOK*	21 August 2000	25 August 2000
119	R/V *KOK*	16 October 2000	20 October 2000
120	R/V *KOK*	28 November 2000	2 December 2000
ST-9	R/V *KOK*	12 December 2000	15 December 2000
121	R/V *KOK*	18 December 2000	22 December 2000

Table 1.5: 2000 Cruise Personnel (shaded area = cruise participant)

Cruise Participants	HA-7B	111	112	113	114	115	116	HA-8A	117	118	119	120	121
Allen, Colleen		■	■	■	■	■	■		■	■	■	■	
Björkman, Karin			■	■	■	■			■	■	■	■	■
Benitez-Nelson, Claudia									■			■	
Breitbart, Mya													■
Bruhn, Regina				■									
Brum, Jennifer						■	■		■	■			
Church, Matt			■	■	■	■	■			■	■	■	■
Coleman, Albert				■									
Dickey, Tommy								■					
Dore, John						■			■			■	■
Eich, Michele		■	■	■	■								
Erickson, Matthew											■	■	■
Fujieki, Lance	■	■	■	■	■	■	■	■	■	■	■	■	■
Gasc, Anne											■	■	■
George, Russ								■					
Gregory, Tom		■	■	■		■	■			■	■		■
Gravatt, Dave	■	■	■	■	■	■	■	■	■	■	■	■	■
Hamm, Roberta									■	■			■
Hansen, Andrew						■		■					
Hebel, Dale	■	■	■	■	■		■	■		■	■	■	

Cruise Participants	HA-7B	111	112	113	114	115	116	HA-8A	117	118	119	120	121
Hervig, Will													
Houlihan, Terrence													
Johnson, Jeremiah													
Johnson, Steve													
Karner, Markus													
Lim, Siang Chyn													
Magaard, Ursula													
Mendez-Nuarez, Javier													
Manov, Derek													
Montoya, Joseph													
Orlando, Martin													
Poulos, Steve													
Ratnapala, Lal													
Sadler, Dan													
Sakimoto, Carole													
Santiago-Mandujano, Fernando													
Selph, Karen													
Stump, Chuck													
Thurber, Andrew													
Tupas, Louie													
Turner, Patti													
Valenciano, Mark													
Waterbury, John													
Wright, Don													

2.0 SAMPLING PROCEDURES AND ANALYTICAL METHODS

A comprehensive summary of all sampling and analytical methods currently used in the HOT program along with information on measurement accuracy and precision can be found in the "Hawaii Ocean Time-series Program Field and Laboratory Protocols" manual. This document is available on the World Wide Web (hahana.soest.hawaii.edu/hot/protocols/protocols.html). Brief summaries of methods as well as calibration specifications and quality control / quality assurance information for 2000 are presented in this report. Hydrographic sampling methods are included in "WOCE Hydrographic Sampling Procedure. A primer for ship-board operations at the Hawaii Ocean Time-series Station," and is also available on the web (www.soest.hawaii.edu/HOT_WOCE/manual/toc.html).

2.1 CTD Profiling

Continuous measurements of temperature, salinity, oxygen and fluorescence are made with a Sea-Bird SBE-9/11Plus CTD package with dual temperature, salinity and oxygen sensors and fluorometer described in Tupas *et al*. (1995).

CTD casts are made at Stations Kahe and ALOHA during each cruise. A CTD cast to 1000 m is made at Station Kahe. At Station ALOHA a burst of consecutive CTD casts to 1000 m is made over 36 hours to span the local inertial period and three semi-diurnal tidal cycles. One WOCE standard cast within 10 m of the bottom is made during each cruise. During all the 2000 cruises except HOT-115, 117 and 118 a second deep cast was obtained at Station ALOHA. Station HALE-ALOHA (site of the bottom moored array) was occupied during cruises HOT-117 through 121. One CTD cast to 1000 m is regularly made about 1 nm from the HALE-ALOHA mooring for calibration of Seacats and other instruments installed in the array.

2.1.1 Data Acquisition and Processing

CTD data were acquired at a rate of 24 samples per second. Digital data were stored on a laptop personal computer and, for redundancy, the analog signal was recorded on VHS video tapes. Backups of CTD data were made onto Zip™ disks and later onto compact disks. The raw CTD data were quality controlled and screened for spikes as described in Winn *et al*. (1993). Data alignment, averaging, correction and reporting were done as described in Tupas *et al*. (1993). Salinity spike rejection parameters were modified for some cruises in 2000 because of rough sea conditions. Spikes occur when the CTD samples the disturbed water of its wake, therefore, samples from the downcast are rejected when the CTD is moving upward or when its acceleration exceeds 0.5 m s^{-2} in magnitude. Cruises 112, 113, and 117 through 121 were conducted under rough sea conditions, with heavy ship rolling during some of the casts, causing large vertical velocity fluctuation of the CTD package. The acceleration cutoff value had to be increased to between 0.55 and 0.65 m s^{-2} to relax the data rejection criteria and avoid eliminating an excessive number of points.

The data were additionally screened by comparing the temperature and conductivity sensor pairs. These differences permitted identification of problems in the sensors. Only the data

from one set of T-C sensors and one oxygen sensor, whichever was deemed most reliable, is reported here. Temperature is reported in the ITS-90 scale. Salinity and all derived units were calculated using the UNESCO (1981) routines; salinity is reported in the practical salinity scale (PSS-78). Oxygen is reported in μmol kg^{-1}.

2.1.2 Sensor Corrections and Calibrations

2.1.2.1 Pressure

The pressure calibration strategy employed a high-quality quartz pressure transducer as a transfer standard. Periodic recalibrations of this lab standard were performed with a primary pressure standard. The transfer standard was used to check the CTD pressure transducers. The only correction applied to the CTD pressures was a constant offset determined at the time that the CTD first enters the water on each cast.

2.1.2.1.1 Transfer Standard Calibration

The transfer standard is a Paroscientific Model 760 pressure gauge equipped with a 10,000-PSI transducer. This instrument was purchased in March 1988, and was originally calibrated against a primary standard. Subsequent recalibrations have been performed every 2.5 years in average at the Northwest Regional Calibration Center and at the Scripps Institution of Oceanography. The latest calibration was conducted at the Scripps Institution of Oceanography in December 1998 (Santiago-Mandujano *et al*., 1999).

2.1.2.1.2 CTD Pressure Transducer Bench Tests

CTD pressure transducer bench tests were done using an Ametek T-100 pump and a manifold to apply pressure simultaneously to the CTD pressure transducer and to the transfer standard. All these tests had points at 6 pressure levels between 0 and 4500 dbar, increasing and decreasing pressures.

Our primary CTD (#91361) pressure sensor #75434 was installed in March 1999 after the previous sensor (#26448) failed apparently due to a vacuum leak (Santiago-Mandujano *et al*., 1999). The results of bench tests for sensors #75434 and #51412 (backup CTD #92859) are shown in Table 2.1. Tests before September 1998 do not include the 0 dbar offset because problems in the experimental settings during those tests deemed those data unreliable.

Pressure transducer #75434 was used for all the cruises during 2000. No correction was applied to the insignificant pressure offset at 0 dbar during data collection (however, a more accurate offset was later determined for the time that the CTD first enters the water on each cast). On-deck CTD pressures are regularly recorded during cruises at the beginning and at the end of each CTD cast, the mean of these pressures throughout each cruise are plotted in Figure 2.1. The before-cast pressures are about 0.3 dbar higher than the 0 dbar offset from the 2000 calibrations for sensor #75434. This may be due to the fact that during pressure tests the CTD is powered on

24 hr before calibration for full stabilization, while the on-deck pressures for each cast are taken only about 10 min after the CTD is powered on. Also, the mean difference between before-cast and after-cast on-deck pressures is about 0.5 dbar, larger than the hysteresis measured during the bench tests. This on-deck "hysteresis" is actually a residual temperature sensitivity effect of the pressure sensor caused when the CTD is submerged in cold water during casts, which has typical values of the order of 0.5 dbar (N. Larson, personal communication, 1999). Our bench tests do not show this effect because they are conducted at constant room temperature.

The 0-4500 dbar pressure span and hysteresis from the bench tests have been within expected values and nearly constant for the two sensors.

Table 2.1: CTD Pressure Calibrations against transfer standard (units are decibars)

Calibration Date	Offset @ 0 dbar	0-4500 dbar span	Hysteresis
Sea-Bird SBE-911 Plus #91361 / Pressure Transducer #75434			
1 August 2001	0.1	-0.1	
6 February 2001	0.24	-0.02	0.1
15 August 2000	0.18	0.12	0.1
13 January 2000	0.1	0.13	0.18
24 June 1999	-0.03	0.2	0.1
Sea-Bird SBE-911 Plus #92859 / Pressure Transducer #51412			
29 June 2001	1.14	0.5	0.1
5 February 2001	1.1	0.56	0.03
16 August 2000	1.05	0.6	0.05
14 January 2000	1.1	0.55	0.05
25 June 1999	1.0	0.47	0.05
26 January 1999	0.95	0.55	0.05
14 September 1998	1.25	0.55	0.05
12 June 1997	--	0.65	0.05
31 January 1997	--	0.5	0.08
30 August 1996	--	0.45	0.01
5 December 1995	--	0.65	0.07
21 August 1995	--	0.45	0.05
16 December 1994	--	0.45	0.05
21 August 1995	--	0.45	0.05
5 December 1995	--	0.65	0.07
30 August 1996	--	0.45	0.01
31 January 1997	--	0.5	0.08
12 June 1997	--	0.65	0.05
14 September 1998	1.25	0.55	0.05
26 January 1999	0.95	0.55	0.05
25 June 1999	1.0	0.47	0.05
14 January 2000	1.1	0.55	0.05

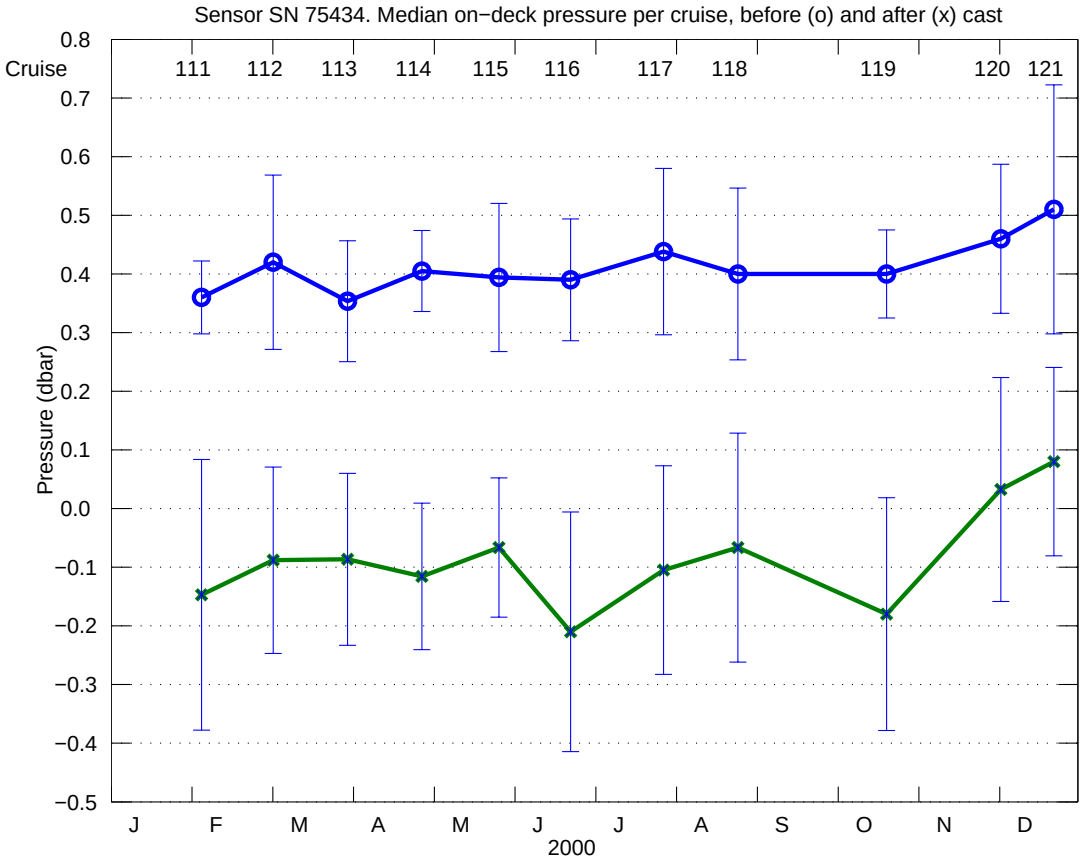

Figure 2.1: Median value of pressure on the ship's deck measured with the new CTD pressure sensor #75434, before (circles) and after (crosses) each cast for HOT cruises 111-121. Error bars are one standard deviation from the mean. Cruise numbers are shown below the upper x-axis.

2.1.2.2 Temperature

Three Sea-Bird SBE-3-Plus temperature sensors, #2242, #2700, and #2454 were used in 2000 and were calibrated at Sea-Bird after every cruise, except after the December cruise because the sensors were used in another project's cruise in early January 2001. Sensor #2700 showed large differences with respect to its paired sensor prior to cruise HOT-116 and was sent to Sea-Bird for evaluation; the sensor's power supply chip was found faulty and was replaced. SBE-3-02/F transducers #1591, #1416 and #741 were backup sensors also calibrated after every cruise. The history of the sensors, as well as the procedures followed to obtain the sensor drift from the Sea-Bird calibrations are well-documented in Santiago-Mandujano *et al*. (2001, 1999), Tupas *et al*. (1993, 1994a, 1995, 1997, 1998) and Karl *et al*. (1996). Calibration coefficients obtained at Sea-Bird for these sensors after 1999 and used in the drift estimates are presented in Table 2.2. These coefficients were used in the following formula that gives the temperature (in °C) as a function of the frequency signal (*f*):

$$temperature = 1/\{a+b[\ln(f_0/f)]+c[\ln^2(f_0/f)]+d[\ln^3(f_0/f)]\}-273.15$$

Table 2.2. Calibration coefficients for Sea-Bird temperature sensors. RMS residuals from calibration give an indication of quality of the calibration. Sensors #2045, #1496, #1392, and #2078 were used by the thermosalinograph (Section 2.2).

SN	*Date yymmdd*	*f0*	*a*	*b*	*c*	*d*	*RMS (m°C)*
2242	010427	3004.48	3.67981800e-03	6.02844978e-04	1.61423644e-05	2.12117524e-06	0.08
2242	010330	3004.24	3.67986794e-03	6.02847006e-04	1.61432885e-05	2.12393856e-06	0.08
2242	010227	3004.19	3.67987849e-03	6.02848506e-04	1.61468027e-05	2.12555215e-06	0.08
2242	010127	3003.98	3.67992331e-03	6.02852328e-04	1.61455037e-05	2.12106401e-06	0.08
2242	001102	3004.03	3.67991287e-03	6.02856205e-04	1.61718742e-05	2.15174044e-06	0.08
2242	000907	3004.07	3.67990413e-03	6.02851755e-04	1.61556299e-05	2.13457007e-06	0.08
2242	000804	3004.12	3.67989354e-03	6.02846970e-04	1.61434250e-05	2.12617155e-06	0.08
2242	000706	3004.17	3.67988527e-03	6.02849086e-04	1.61441545e-05	2.12579980e-06	0.08
2242	000607	3003.98	3.67992185e-03	6.02849595e-04	1.61391822e-05	2.12086886e-06	0.08
2242	000505	3003.80	3.67995866e-03	6.02849385e-04	1.61359695e-05	2.11837126e-06	0.09
2242	000407	3003.69	3.67998206e-03	6.02847310e-04	1.61257405e-05	2.11123568e-06	0.09
2242	000309	3003.74	3.67997393e-03	6.02857608e-04	1.61554887e-05	2.13399423e-06	0.09
2242	000215	3003.64	3.67999345e-03	6.02851230e-04	1.61257387e-05	2.10960043e-06	0.10
2454	001102	2891.96	3.67991392e-03	6.02085473e-04	1.67247348e-05	2.36470637e-06	0.07
2454	000907	2891.98	3.67990527e-03	6.02085787e-04	1.67212140e-05	2.35310160e-06	0.06
2454	000804	2892.03	3.67989466e-03	6.02087607e-04	1.67241737e-05	2.35790858e-06	0.07
2454	000706	2892.07	3.67988631e-03	6.02087759e-04	1.67235770e-05	2.35943634e-06	0.06
2454	000607	2891.89	3.67992287e-03	6.02086645e-04	1.67178313e-05	2.35412370e-06	0.06
2454	000505	2891.71	3.67995981e-03	6.02084592e-04	1.67083109e-05	2.34571279e-06	0.06
2454	000407	2891.59	3.67998326e-03	6.02089812e-04	1.67193405e-05	2.35646427e-06	0.07
2454	000309	2891.63	3.67997530e-03	6.02089492e-04	1.67112872e-05	2.34664486e-06	0.06
2454	000215	2891.53	3.67999477e-03	6.02090533e-04	1.67124002e-05	2.34904563e-06	0.07
2700	001102	2978.91	3.67991396e-03	6.04732549e-04	1.65107944e-05	2.35162824e-06	0.06
2700	000907	2978.93	3.67990527e-03	6.04733357e-04	1.65115293e-05	2.34299081e-06	0.06
2700	000804	2978.98	3.67989458e-03	6.04729015e-04	1.65013759e-05	2.33846367e-06	0.05
2700	000706	2979.01	3.67988627e-03	6.04729891e-04	1.65095878e-05	2.34652996e-06	0.06
2700	000607	2978.87	3.67992291e-03	6.04740494e-04	1.65431664e-05	2.37341369e-06	0.06
2700	000505	2978.69	3.67995996e-03	6.04744375e-04	1.65410019e-05	2.36679105e-06	0.06
2700	000407	2978.57	3.67998330e-03	6.04745800e-04	1.65430280e-05	2.37132759e-06	0.06
2700	000309	2978.61	3.67997544e-03	6.04742818e-04	1.65332706e-05	2.36045341e-06	0.06
2700	000215	2978.51	3.67999478e-03	6.04745439e-04	1.65364985e-05	2.36355707e-06	0.06
1591	001102	6259.39	3.68118020e-03	6.03650639e-04	1.47877082e-05	1.75535398e-06	0.25
1591	000907	6257.80	3.68133495e-03	6.03670391e-04	1.48270470e-05	1.78070263e-06	0.25
1591	000804	6257.55	3.68136103e-03	6.03663055e-04	1.48076317e-05	1.76318403e-06	0.26
1591	000607	6257.71	3.68135302e-03	6.03675291e-04	1.48380030e-05	1.79355869e-06	0.26
1591	000505	6257.52	3.68137472e-03	6.03669303e-04	1.48117110e-05	1.77198771e-06	0.27
1591	000406	6257.73	3.68135047e-03	6.03663137e-04	1.48141744e-05	1.77321937e-06	0.27
1591	000310	6257.28	3.68140012e-03	6.03673566e-04	1.48203649e-05	1.77890860e-06	0.26
1591	000217	6257.58	3.68136867e-03	6.03668626e-04	1.48358721e-05	1.79860587e-06	0.26
1591	000104	6257.82	3.68134669e-03	6.03654057e-04	1.48041892e-05	1.77017904e-06	0.28
1416	001102	6234.87	3.68118403e-03	6.01781688e-04	1.49372960e-05	2.05438128e-06	0.18
1416	000907	6233.23	3.68133894e-03	6.01776680e-04	1.49141777e-05	2.02975093e-06	0.20
1416	000804	6232.97	3.68136517e-03	6.01788760e-04	1.49380901e-05	2.04504982e-06	0.20
1416	000706	6233.57	3.68130945e-03	6.01779322e-04	1.49310673e-05	2.04864498e-06	0.17
1416	000607	6233.14	3.68135719e-03	6.01800309e-04	1.49613175e-05	2.06836468e-06	0.17

1416	000505	6232.96	3.68137878e-03	6.01812349e-04	1.49929327e-05	2.09670594e-06	0.16
1416	000406	6233.15	3.68135468e-03	6.01801664e-04	1.49864473e-05	2.09250171e-06	0.17
1416	000310	6232.67	3.68140416e-03	6.01788307e-04	1.49173100e-05	2.03240180e-06	0.19
1416	000217	6232.97	3.68137264e-03	6.01796436e-04	1.49675910e-05	2.07745560e-06	0.18
1416	000104	6233.20	3.68135059e-03	6.01767718e-04	1.48914139e-05	2.01317657e-06	0.19
741	001102	5941.12	3.68118325e-03	6.01963528e-04	1.55769284e-05	2.09529159e-06	0.05
741	000907	5939.55	3.68133817e-03	6.01971419e-04	1.55942573e-05	2.10721586e-06	0.05
741	000804	5939.29	3.68136406e-03	6.01967033e-04	1.55735737e-05	2.08761185e-06	0.04
741	000706	5939.84	3.68130783e-03	6.01950586e-04	1.55564177e-05	2.08486384e-06	0.03
741	000607	5939.44	3.68135602e-03	6.01975538e-04	1.55906353e-05	2.10308297e-06	0.04
741	000505	5939.26	3.68137784e-03	6.01973414e-04	1.55745531e-05	2.09164717e-06	0.04
741	000406	5939.45	3.68135367e-03	6.01961228e-04	1.55564184e-05	2.07772436e-06	0.04
741	000310	5939.02	3.68140341e-03	6.01973723e-04	1.55685148e-05	2.08609901e-06	0.04
741	000217	5939.29	3.68137170e-03	6.01962919e-04	1.55619593e-05	2.08670795e-06	0.03
741	000104	5939.52	3.68134988e-03	6.01953874e-04	1.55498171e-05	2.07567258e-06	0.03
2045	000908	2442.96	3.64763323e-03	5.89543392e-04	7.77856248e-06	-2.95111973e-6	0.38
2045	990810	2454.26	3.64491128e-03	5.89429698e-04	7.83780151e-06	-2.80829868e-6	0.34
2045	980728	2447.02	3.64664780e-03	5.89941753e-04	1.00854316e-05	-3.65949437e-7	0.43
1496	010118	5964.13	3.67991358e-03	5.89881380e-04	1.46683349e-05	2.91772668e-06	0.10
1496	980716	5947.26	3.68153908e-03	5.89975419e-04	1.46589621e-05	2.88623686e-06	0.20
1392	010117	2575.50	3.64764418e-03	5.86401349e-04	9.00471227e-06	2.257262161e-6	0.03
1392	000127	2575.59	3.64763375e-03	5.86545184e-04	9.78001159e-06	-1.67704522e-6	0.04
1392	981118	2578.63	3.64688995e-03	5.86286555e-04	9.04039578e-06	-2.36938641e-6	0.04
2078	000908	2773.99	3.67992125e-03	5.92809918e-04	1.61568922e-05	1.73539414e-06	0.02
2078	990812	2773.49	3.68001979e-03	5.92818163e-04	1.61678036e-05	1.73277527e-06	0.02
2078	990805	2773.38	3.68002759e-03	5.92815247e-04	1.61571052e-05	1.73369510e-06	0.03
2078	961217	2772.55	3.68022581e-03	5.92832713e-04	1.62002729e-05	1.77796339e-06	0.03
2078	951019	2772.32	3.68029270e-03	5.92819697e-04	1.61663533e-05	1.75679211e-06	0.03

For each sensor, the final calibration consists of two parts: first, a single "baseline" calibration is chosen from among the ensemble of calibrations during the year; second, for each cruise a temperature-independent offset is applied to remove the temporal trend due to sensor drift (Table 2.3). The offset, a linear function of time, is calculated by least squares fit to the 0-30 °C average of each calibration during the year. The maximum drift correction in 2000 was less than 0.5 x 10^{-3} °C. The baseline calibration is selected as the one for which the trend-corrected average from 0-5 °C is nearest to the ensemble mean of these averages.

A small residual pressure effect on the temperature sensors documented in Tupas *et al*. (1997) has been removed from measurements obtained with our sensors. Another correction to our temperature measurements was for the viscous heating of the sensor tip due to the water flow. This correction is thoroughly documented in Tupas *et al*. (1997).

Dual sensors were used during each of the 2000 cruises. The temperature differences between sensor pairs were calculated for each cast to evaluate the quality of the data, and to identify possible problems with the sensors. Means and standard deviations of the differences in 2-dbar bins were calculated from the ensemble of all casts at Station ALOHA for each cruise.

Both sensors performed correctly during the 2000 cruises, showing temperature differences within expected values. The mean temperature difference as a function of pressure was typically less than 1 x 10^{-3} °C, with a standard deviation of less than 0.5 x 10^{-3} °C below 500 dbar. The largest variability was observed in the thermocline, with standard deviation values of up to 5 x 10^{-3} °C.

Sensor #2242

This sensor was used during all cruises HOT-111 through -121, and HA-8A. The calibrations from December 1996 through January 2000 were used to calculate the sensor drift and the drift corrections. A linear fit to the 0-30 °C average offset from each calibration (Table 2.2) relative to 15 February 2000 gave an intercept of 1.32 x 10^{-4} °C with a slope of 1.7 x 10^{-7} °C day^{-1}. The RMS deviation of the offsets from this fit was 8.1 x 10^{-5} °C. The 2 November 2000 calibration was used as a baseline for the cruise. When corrected for linear drift to 30 June 2000 (the midpoint of the cruise date), this calibration gave the smallest deviation in the 0-5 °C temperature range from the set of all calibrations used to determine the drift (also corrected for linear drift to 30 June 2000). The mean deviation of this calibration was 2.0 x 10^{-5} °C with a range of variation of less than 2.5 x 10^{-5} °C. The set of all calibrations had deviations in the range ± 2 x 10^{-4} °C. The resulting drift corrections for the 2000 cruises were insignificant (Table 2.3).

Sensor #2454

The calibrations from March 1999 through January 2001 were used to calculate a sensor drift of –1.98 x 10^{-6} °C day^{-1} with a 2.3 x 10^{-5} °C intercept and 1.1 x 10^{-4} °C RMS residual. This drift was used to obtain the correction for cruises HOT-116, -117, -118, and HA-8A. The 6 July 2000 calibration was used as baseline for the cruises. This calibration yielded the smallest 0-5 °C mean deviation from the others, all drift-corrected to 15 July 2000 (midpoint date between the cruises). The deviation was 4.4 x 10^{-6} °C with less than 0.2 x 10^{-4} °C range of variation. The set of all calibrations had deviations in the range ± 2 x 10^{-4} °C. The resulting drift corrections for each cruise were insignificant (Table 2.3).

Sensor #2700

This sensor was used during cruises HOT-111 through 115, and 119 through 121. For an unknown reason, the sensor had a change in its drift rate after October 1999; it also suffered a jump in its calibration level after June 2000 when it was repaired due to a faulty power supply chip. The calibrations from October 1999 through June 2000 were used to calculate a sensor drift of –1.08 x 10^{-6} °C day^{-1} with a –2.0 x 10^{-5} °C intercept and 1.9 x 10^{-5} °C RMS residual. This drift was used to obtain the correction for cruises HOT-111 through -115. The 9 March 2000 calibration was used as baseline for the cruises. This calibration yielded the smallest 0-5 °C mean deviation from the others, all drift-corrected to 30 March 2000 (midpoint date between the cruises). The deviation was –5.2 x 10^{-6} °C with less than 0.1 x 10^{-4} °C range of variation. The set of all calibrations had deviations in the range ± 0.4 x 10^{-4} °C. The resulting drift corrections for each cruise were insignificant (Table 2.3).

The calibrations from July 2000 through January 2001 were used to calculate a sensor drift of -3.47×10^{-6} °C day^{-1} with a -8.6×10^{-6} °C intercept and 4.9×10^{-5} °C RMS residual. This drift was used to obtain the correction for cruises HOT-119 through -121. The 4 August 2000 calibration was used as baseline for the cruises. This calibration yielded the smallest 0-5 °C mean deviation from the others, all drift-corrected to 15 November 2000 (midpoint date between the cruises). The deviation was -3.2×10^{-6} °C with less than 0.1×10^{-4} °C range of variation. The set of all calibrations had deviations in the range $\pm 1.0 \times 10^{-4}$ °C. The resulting drift corrections for each cruise were very small (Table 2.3).

Sensor #1416

This sensor was not used during 2000. The calibrations from April 1996 through January 2001 yielded a linear drift of 2.59×10^{-6} °C day^{-1}, with an intercept of 1.91×10^{-5} °C, and 1.5×10^{-4} °C RSM residuals. This sensor has maintained a constant and uninterrupted drift for a long time compared to our other sensors.

Sensor #1591

This sensor was not used during 2000. The sensor showed a jump in its calibration level after April 1999. Calibrations after this date through January 2001 yielded a sensor drift of 5.38×10^{-6} °C day^{-1} with a -1.1×10^{-4} °C intercept and 1.2×10^{-4} °C RMS residual.

Sensor #741

This sensor was not used during 2000. The sensor showed a change in its drift rate after March 1999. Calibrations from June 1999 through January 2001 yielded a sensor drift of 2.20×10^{-6} °C day^{-1} with a -9.6×10^{-5} °C intercept and 1.9×10^{-4} °C RMS residual.

Table 2.3: Temperature (T) and Conductivity (C) sensor corrections including the thermal inertia parameter (α). Dual temperature and conductivity sensors were used in all cruises.

Cruise	*T sensor #*	*T Correction (° C)*	*C sensor #*	α	*Data reported*
HOT-111	2700	0.000039	2218	0.020	All casts
HOT-111	2242	0.000047	1336	0.028	
HOT-112	2700	0.000008	2218	0.028	All casts
HOT-112	2242	0.000042	1336	0.028	
HOT-113	2700	-0.000022	2218	0.028	All casts
HOT-113	2242	0.000037	1336	0.028	
HOT-114	2700	-0.000051	2218	0.028	All casts
HOT-114	2242	0.000032	1336	0.028	
HOT-115	2700	-0.000082	2218	0.028	All casts
HOT-115	2242	0.000028	1336	0.028	
HOT-116	2454	0.000032	2218	0.028	All casts
HOT-116	2242	0.000023	1336	0.028	

HA-8	2454	0.000026	2218	0.028	All casts
HA-8	2242	0.000022	1336	0.028	
HOT-117	2454	-0.000040	2218	0.028	All casts
HOT-117	2242	0.000017	1336	0.028	
HOT-118	2454	-0.000093	2218	0.028	All casts
HOT-118	2242	0.000012	1336	0.028	
HOT-119	2700	-0.000260	2218	0.028	All casts
HOT-119	2242	0.000003	1336	0.028	
HOT-120	2700	-0.000413	2218	0.028	All casts
HOT-120	2242	-0.000005	1336	0.028	
HOT-121	2700	-0.000479	2218	0.028	All casts
HOT-121	2242	-0.000008	1336	0.028	

2.1.2.3 Conductivity

Two sensors were used during the 2000 cruises, #2218 and #1336. The history of the sensors is well documented in Santiago-Mandujano *et al*. (2001, 1999), Tupas *et al*. (1993, 1994a, 1995, 1997, 1998) and Karl *et al*. (1996). The dual sensor configurations are shown in Table 2.3. As mentioned earlier, only the data from the most reliable sensor (and its corresponding temperature sensor pair, as shown in Table 2.3) are reported here.

For each sensor, the nominal calibrations were used for data acquisition, and a final calibration was determined empirically from salinities of discrete water samples acquired during each cast. Prior to empirical calibration, conductivity was corrected for thermal inertia of the glass conductivity cell as described in Chiswell *et al*. (1990). Table 2.3 lists the value of the α parameter used for each cruise.

Procedures for preliminary screening of bottle samples and empirical calibration of the conductivity cell are described in Tupas *et al*. (1993, 1994a). For cruises HOT-111 through -121, the standard deviation cutoff values for screening of bottle salinity samples were: 0.0035 (0-150 dbar), 0.0048 (151-500 dbar), 0.0021 (501- 1050 dbar), and 0.0011 (1051-5000 dbar).

The conductivity calibration coefficients (*b0*, *b1*, *b2*) derived from the least squares fit ($\Delta C = b0 + b1C + b2C^2$) to the CTD-bottle conductivity differences (ΔC) as a function of conductivity (C) are given in Table 2.4. The quality of the CTD calibration is illustrated in Figure 2.2, which shows the differences between the corrected CTD salinities and the bottle salinities used for calibration as a function of pressure for each cruise. The calibrations are best below 500 dbar because the weaker vertical salinity gradients at depth lead to less error when the bottle and CTD pressures are slightly mismatched.

The final step of conductivity calibration was a cast-dependent bias correction as described in Tupas *et al*. (1993) to allow for drift during each cruise or for sudden offsets due to fouling (Table 2.5). Note that a change of 1×10^{-4} Siemens m^{-1} in conductivity is approximately equivalent to 0.001 in salinity. Table 2.6 gives the mean and standard deviations for the final calibrated CTD minus bottle samples shown in Figure 2.2.

Conductivity differences between sensor pairs were calculated the same way as for the temperature sensors (Section 2.1.2.2). The range of variability as a function of pressure was about $\pm$ 1 x 10^{-4} Siemens m^{-1}, with a standard deviation of less than 0.5 x 10^{-4} Siemens m^{-1} below 500 dbar, from the ensemble of all the cruise casts. The largest variability was in the halocline, with standard deviations reaching up to 5 x 10^{-4} Siemens m^{-1} between 50 and 300 dbar.

Table 2.4: Conductivity calibration coefficients

Cruise	*Sensor #*	*b0*	*b1*	*b2*
HOT -111	2218	0.004709	-0.002197	0.000224
HOT -111	1336	0.000692	-0.000315	--
HOT -112	2218	0.000831	-0.000299	--
HOT -112	1336	0.000506	-0.000268	--
HOT -113	2218	0.007840	-0.003762	0.000399
HOT -113	1336	0.000706	-0.000356	--
HOT -114	2218	0.000876	-0.000325	--
HOT -114	1336	0.000425	-0.000263	--
HOT -115	2218	0.000872	-0.000290	--
HOT -115	1336	0.000520	-0.000224	--
HOT -116	2218	0.008176	-0.003941	0.000417
HOT -116	1336	0.000811	-0.000376	--
HA-8A	2218	-0.004522	0.002293	-0.000323
HA-8A	1336	-0.014246	0.006987	-0.000869
HOT -117	2218	0.008643	-0.004024	0.000440
HOT -117	1336	0.000922	-0.000242	--
HOT -118	2218	0.007245	-0.003334	0.000367
HOT -118	1336	0.000929	-0.000276	--
HOT -119	2218	0.001333	-0.000366	--
HOT -119	1336	0.001172	-0.000324	--
HOT -120	2218	0.001151	-0.000307	--
HOT -120	1336	0.000923	-0.000298	0.000197
HOT -121	2218	0.001139	-0.000284	--
HOT -121	1336	0.000979	-0.000293	--

Table 2.5: Individual cast conductivity corrections (units are Siemens m^{-1})

Cruise	*Station*	*Cast*	*C Correction*
HOT -111	2	1	-0.000067
HOT -111	2	14	0.000005
HOT -113	2	15	-0.000093
HOT -116	2	2	-0.000044
HOT -117	2	1	-0.000107
HOT -119	2	2	-0.000039

Table 2.6: CTD-Bottle salinity comparison for each cruise

		0-4800 dbar		*500-4800 dbar*	
Cruise	*Sensor #*	*Mean*	*SD*	*Mean*	*SD*
HOT -111	2218	0.0001	0.0015	0.0002	0.0009
HOT -111	1336	0.0000	0.0018	0.0002	0.0009
HOT -112	2218	0.0000	0.0014	0.0003	0.0011
HOT -112	1336	0.0000	0.0019	0.0003	0.0011
HOT -113	2218	0.0001	0.0018	0.0001	0.0012
HOT -113	1336	0.0000	0.0020	0.0003	0.0013
HOT -114	2218	0.0000	0.0018	0.0004	0.0013
HOT -114	1336	0.0000	0.0020	0.0003	0.0015
HOT -115	2218	0.0000	0.0026	0.0003	0.0016
HOT -115	1336	0.0001	0.0026	0.0005	0.0018
HOT -116	2218	0.0001	0.0017	0.0002	0.0011
HOT -116	1336	0.0000	0.0017	0.0003	0.0012
HA-8A	2218	0.0000	0.0038	-0.0005	0.0000
HA-8A	1336	0.0000	0.0028	-0.0004	0.0000
HOT -117	2218	0.0001	0.0019	0.0003	0.0013
HOT -117	1336	0.0000	0.0018	0.0003	0.0012
HOT -118	2218	-0.0000	0.0018	-0.0001	0.0012
HOT -118	1336	0.0000	0.0019	0.0003	0.0011
HOT -119	2218	0.0001	0.0019	0.0005	0.0014
HOT -119	1336	0.0000	0.0017	0.0000	0.0014
HOT -120	2218	0.0000	0.0017	0.0004	0.0011
HOT -120	1336	0.0000	0.0018	0.0000	0.0013
HOT -121	2218	0.0000	0.0017	0.0006	0.0007
HOT -121	1336	0.0000	0.0015	0.0002	0.0009

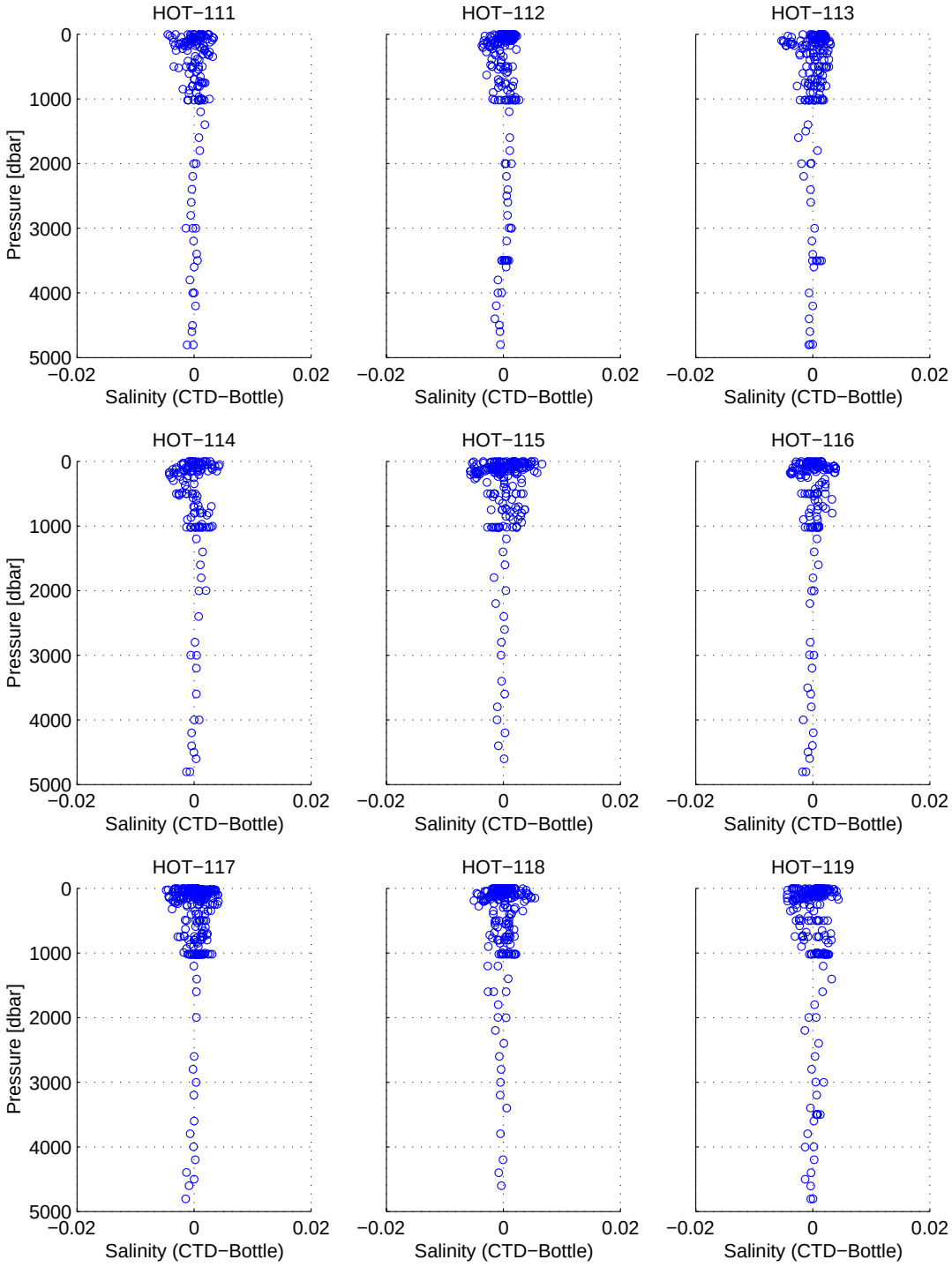

Figure 2.2: Difference between calibrated CTD salinities and bottle salinities for each cruise and all casts at Station ALOHA in 2000.

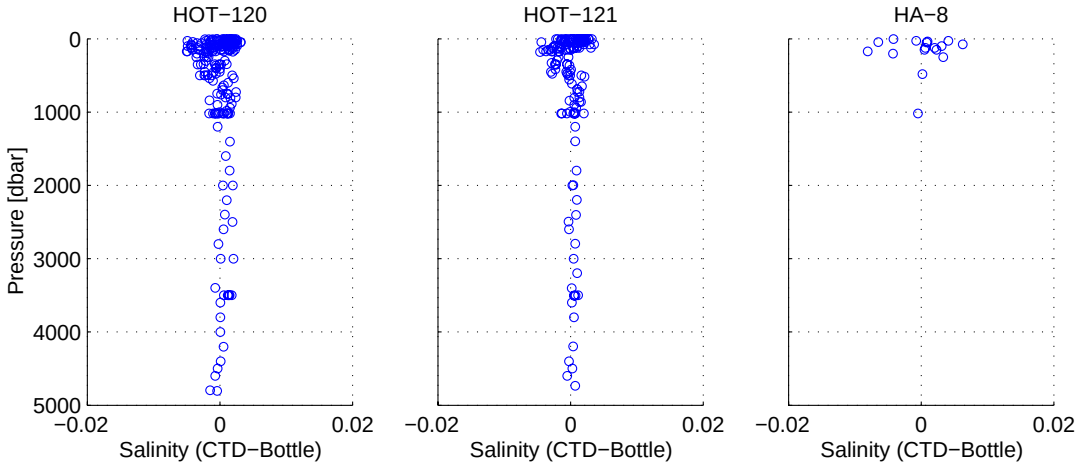

Figure 2.2: continued

2.1.2.4 Oxygen

During the 2000 cruises two developmental versions of the Sea-Bird SBE-43 oxygen sensor were used (#43071 and #43081). These sensors were calibrated at Sea-Bird before each cruise. In addition, two YSI Inc. probes (#13434 and #13251) were used during the 2000 cruises; the history of these sensors is documented in Santiago-Mandujano *et al*. (2001, 1999), Tupas *et al*. (1995, 1997, 1998) and Karl *et al*. (1996).

The regular maintenance procedure for the YSI sensors includes inspection of their electrolyte level and membrane before each cruise. Sensor #13434 had its membrane and electrolyte replaced prior to HOT-114.

Water bottle oxygen data were screened and the sensors were empirically calibrated following procedures described previously (Winn *et al*., 1991; Tupas *et al*., 1993). The analysis of water bottle samples is described in Section 2.4.1. The calibration procedure follows Owens and Millard (1985), and consists of fitting a non-linear equation to the CTD oxygen current and oxygen temperature. The bottle values of dissolved oxygen and the downcast CTD observations at the potential density of each bottle trip were grouped together for each cruise to find the best set of parameters with a non-linear least squares algorithm. Three sets of parameters were usually obtained per HOT cruise, corresponding to the casts at Stations 1, 2 and 8. Casts from HA-8A were calibrated with bottle data obtained during that cruise. The calibration procedure for the Sea-Bird SBE-43 sensors was modified because these sensors do an internal temperature compensation and do not output the oxygen probe internal temperature data as in the case of the YSI sensors (Santiago-Mandujano *et al*., 2001).

Table 2.7 gives the means and standard deviations for the final calibrated CTD oxygen minus water sample values. Dual sensors were used during cruises, but only the sensor whose data were deemed more reliable is reported.

Table 2.7a: CTD-Bottle dissolved oxygen per cruise at Station Kahe (µmol kg^{-1})

		0 to 1500 dbar	
Cruise	*Sensor*	*Mean*	*SD*
HOT-111	43071	0.01	1.30
HOT-112	13434	0.01	1.20
HOT-113	43071	0.02	1.54
HOT-114	13434	0.02	0.97
HOT-115	43081	0.00	0.62
HOT-116	43081	0.00	1.32
HOT-117	43081	0.00	0.96
HOT-118	43081	0.00	1.05
HOT-119	43081	0.00	0.28
HOT-120	13434	0.01	1.13
HOT-121	13434	0.01	0.70

Table 2.7b: CTD-Bottle dissolved oxygen per cruise at Station ALOHA (µmol kg^{-1})

		0 to 4800 dbar		*500 to 4800 dbar*	
Cruise	*Sensor*	*Mean*	*SD*	*Mean*	*SD*
HOT-111	43071	0.09	1.18	0.13	1.07
HOT-112	13434	0.07	0.98	0.15	0.81
HOT-113	43071	0.13	1.25	0.18	1.03
HOT-114	43081	0.01	0.80	-0.02	0.77
HOT-115	43081	0.09	0.83	0.11	0.75
HOT-116	43081	0.01	0.81	-0.02	0.69
HOT-117	43081	0.09	0.85	0.10	0.76
HOT-118	43081	0.01	0.83	-0.01	0.78
HOT-119	43081	0.02	0.95	0.00	0.86
HOT-120	13434	0.04	1.13	0.01	1.21
HOT-121	13434	0.04	1.03	0.02	1.09

Table 2.7c: CTD-Bottle dissolved oxygen at Station HALE-ALOHA (µmol kg^{-1})

		0-1500 dbar	
Cruise	*Sensor*	*Mean*	*SD*
HA-8A	43081	0.00	0.95
HOT-117	43081	-0.06	0.96
HOT-118	43081	0.00	0.27
HOT-119	43081	0.00	0.83
HOT-120	13434	0.00	0.58
HOT-121	13434	0.00	0.49

2.1.3 Discrete salinity

Salinity samples were collected, stored and analyzed as described in Tupas *et al*. (1993). Samples from a large batch of "secondary standard" seawater were measured after every 12 to 24 bottle samples to detect drift in the salinometer for each cruise. Standard deviations of the secondary standard measurements were less than ± 0.001 for most of the cruises (Table 2.8). Samples from mooring cruise HA-8A were measured together with samples from HOT-116.

The secondary standard seawater batches are made from 60 liters of seawater taken from a depth of 1000 m from Station ALOHA. Secondary standard batch #21 was prepared on December 12, 1999, batch #22 was prepared on June 14, 2000, and batch #23 was prepared on November 1, 2000.

Table 2.8: Precision of salinity measurements using lab standards

Cruise	*Mean Salinity ± SD*	*# Samples*	*Substandard Batch #*	*IAPSO Batch #*
HOT-111	34.4810 ± 0.0005	15	21	p135
HOT-112	34.4780 ± 0.0007	19	21	p135
HOT-113	34.4773 ± 0.0006	20	21	p135
HOT-114	34.4767 ± 0.0008	16	21	p135
HOT-115	34.4734 ± 0.0019	27	21	p135
HOT-116	34.4789 ± 0.0014	23	21	p135, p136
HOT-117	34.4790 ± 0.0004	39	22	p136
HOT-118	34.4786 ± 0.0003	22	22	p136
HOT-119	34.4772 ± 0.0004	21	22	p136
HOT-120	34.4714 ± 0.0004	23	23	p136
HOT-121	34.4702 ± 0.0003	22	23	p136

2.2 Thermosalinograph

2.2.1 Data acquisition

A SBE-21 Seacat thermosalinograph system was used aboard R/V *Ka'imikai-o-Kanaloa* for the HOT-111 through HOT-121 cruises, and buoy deployment cruise HA-8A. (see Section 2.2.2.2).

Seacat thermosalinograph sensor #2045 (comprised of one temperature and one conductivity sensor) was used for HOT-111 through HOT-118 and HA-8A. Cruises HOT-119 through HOT-121, used Seacat thermosalinograph sensor #1392 (also comprised of one temperature and one conductivity sensor). The thermosalinograph is installed in a pumped intake line in the hull of the R/V *Ka'imikai-o-Kanaloa* with an intake depth of about 3 m. This thermosalinograph is used to calculate salinity using internal sensors' temperature and conductivity, and the pressure of the pump on the intake flow, this pressure was 10 dbar. Conductivities are calibrated using bottle salinity samples periodically taken from the intake line. Near the start of the intake line, a Sea-Bird remote temperature sensor, installed in a sea chest in the bow of the ship, recorded temperature data. This location allows for relatively undisturbed water to enter the thermosalinograph. Sea-Bird remote or external temperature sensor #2078 was used for HOT-111 through HOT-118 and HA-8A. HOT-119 through HOT-121 used Sea-Bird external temperature sensor #1496. Data were obtained every 10 seconds.

2.2.2 Data processing and sensor calibration

2.2.2.1 Nominal Calibration

2.2.2.1.1 Temperature

The Sea-Bird internal temperature sensors (#1392 and #2045) and external temperature sensors (#1496 and #2078) have been calibrated at Sea-Bird (calibration coefficients in Table 2.2). Since these sensors are the same type as used for the CTD measurements, the same procedure for drift estimation was followed (see Section 2.1.2.2).

A temperature drift rate of -6.32×10^{-6} °C day^{-1} was determined for internal temperature sensor #1392 using the 29 September 1994, 13 October 1995, 20 August 1997, 28 August 1997, 18 November 1998, 27 January 2000 and 17 January 2001 calibrations. Temperatures were calculated with the 27 January 2000 baseline calibration, and temperature drift corrections for the cruises conducted with this sensor are presented in Table 2.9.

For internal temperature sensor #2045, a drift rate of -1.24×10^{-7} °C day^{-1} was determined using the 11 October 1995, 30 July 1996, 28 July 1998, 10 August 1999 and 8 September 2000 calibrations. Temperatures were calculated with the 10 August 1999 baseline calibration. Drift corrections were not applied to the data for this temperature sensor, as they are very small and inconsequential.

A drift rate of 4.32×10^{-6} °C day^{-1} was determined using the 2 November 1993, 18 January 1996 16 July 1998, 13 January 2000, and 18 January 2001 calibrations for remote temperature sensor #1496. Temperatures were calculated with the 13 January 2000 baseline calibration. Drift corrections were not applied to the data for this temperature sensor, as they are very small and inconsequential.

For remote temperature sensor #2078 a drift rate of 9.74×10^{-7} °C day^{-1} was determined using the 19 October 1995 and 17 December 1996, 5 August 1999, and 8 September 2000 calibrations. Temperatures were calculated with the 5 of August 1999 baseline calibration. Drift corrections were not applied to the data for this temperature sensor, as they are very small and inconsequential.

Table 2.9: Thermosalinograph temperature drift corrections

Cruise	*Sensor #2045*	*Sensor #1392*	*Sensor #2078*	*Sensor #1496*
HOT-111	No correction	Not used	No correction	Not used
HOT-112	No correction	Not used	No correction	Not used
HOT-113	No correction	Not used	No correction	Not used
HOT-114	No correction	Not used	No correction	Not used
HOT-115	No correction	Not used	No correction	Not used
HOT-116	No correction	Not used	No correction	Not used
HOT-117	No correction	Not used	No correction	Not used
HA-8A	No correction	Not used	No correction	Not used

HOT-118	No correction	Not used	No correction	Not used
HOT-119	Not used	0.0017°C	Not used	No correction
HOT-120	Not used	0.0019°C	Not used	No correction
HOT-121	Not used	0.0021°C	Not used	No correction

2.2.2.1.2 Conductivity

Sea-Bird conductivity sensor #2045 was used to collect thermosalinograph conductivity data for HOT-111 through HOT-118 and HA-8A. Conductivity sensor #1392 was used for HOT-119 through HOT-121. For sensor #2045, all conductivity data were nominally calibrated with coefficients obtained at Sea-Bird on 10 August 1999. For sensor #1392, all conductivity data were nominally calibrated with coefficients obtained at Sea-Bird on 8 September 2000. However, all the final salinity data reported here were calibrated against bottle data as explained below (Section 2.2.2.3).

2.2.2.2 Processing

The thermosalinograph data were screened for gross errors with upper and lower bounds of 35 °C and 18 °C for temperature and 6 and 3 Siemens m^{-1} for conductivity. There were 23 gross errors detected during the 2000 cruises, a typical cruise contains approximately 40,000 data points. Despite the small number of gross errors, some data have been deemed suspicious or bad. These could be ascribed to factors such as biological fouling of the thermosalinograph, air bubbles in the thermosalinograph system, etc. Hence, a quality control system has been established so that each temperature and salinity point is given a flag to determine whether the data are good, suspect or bad. A 5-point running median filter was used to detect one or two point temperature and conductivity glitches in the thermosalinograph data. Glitches in temperature and conductivity detected by the 5-point median filter were immediately replaced by the median. Threshold values of 0.3 °C for temperature and 0.1 Siemens m^{-1} for conductivity were used for the median filter. No more than a few points were replaced after running the median filter. A 3-point triangular running mean filter was used to smooth the temperature and conductivity data from all the cruises after they had gone through glitch detection. A visual inspection of the temperature and conductivity record was also done to flag suspect and bad data.

The number of thermosalinograph data points flagged as suspicious or bad per cruise ranged from 76 (HOT-112) to over 3000 (HOT-113), with the majority of the flags applied to the conductivity data. Most sections of flagged data were relatively small and were associated with bottle glitches (data spikes during bottle sampling due to a defective draining pump) or with air bubbles entering the thermosalinograph plumbing during transit. Heavy winds and rough seas can amplify the bubble effect and result in large tracts of suspect data. In particular, the thermosalinograph data from HOT-111, HOT-113, HOT-115, and HOT-120 had relatively large sections of suspect data attributed to the extreme weather conditions encountered during transit between stations. HOT-121 contained a section of 2079 points during the middle of the cruise that were flagged as bad due to a malfunctioning external temperature sensor (S/N #1496).

An estimate of the noise in the thermosalinograph data was performed to evaluate the quality of the thermosalinograph data. A 101-point running mean (about 17 min at 10 sec sampling) was applied to the thermosalinograph salinities and external temperatures, and the standard deviations of the residuals from the original data were used as an estimate of the data noise. Only data taken during near-constant salinity or temperature periods were included in the estimates to avoid large residuals resulting in sections of large variability. Noise estimates were obtained for cruises HOT-111 through -121 (Table 2.10).

Table 2.10: Thermosalinograph data noise estimates during HOT cruises.

Cruise	Noise estimate	
	Salinity	Temperature (°C)
HOT-111	0.0017	0.0041
HOT-112	0.0029	0.0047
HOT-113	0.0030	0.0039
HOT-114	0.0031	0.0047
HOT-115	0.0020	0.0043
HOT-116	0.0016	0.0033
HOT-117	0.0019	0.0034
HOT-118	0.0012	0.0032
HOT-119	0.0019	0.0039
HOT-120	0.0010	0.0043
HOT-121	0.0008	0.0041

2.2.2.3 Conductivity Calibration

The thermosalinograph salinity was calibrated by comparing it to bottle salinity samples drawn from the plumbing near the thermosalinograph. Bottle salinity samples were analyzed as described in Section 2.1.3.

For R/V *Ka'imikai-o-Kanaloa*, the thermosalinograph used to calculate salinity was located immediately next to the bottle sampling area. Thus, thermosalinograph data were extracted within ± 15 seconds around the sample time.

As in previously reported cruises (Tupas *et al.,* 1997) a cubic spline was fit to the time-series of the differences between the bottle conductivity and the thermosalinograph conductivity separately for all the 2000 cruises. The correction of the thermosalinograph conductivities was obtained from this fit. Salinity was calculated using these corrected conductivities, thermosalinograph temperatures and a pressure of 10 dbar. The mean values for the salinity bottle minus final calibrated thermosalinograph were less than $\pm 2 \times 10^{-5}$ for each cruise except cruise 111 which had a mean value of 2.7×10^{-5}.

Table 2.11 gives the standard deviation for the salinity bottle minus final calibrated thermosalinograph values for all the cruises.

Table 2.11: Bottle-Thermosalinograph salinity comparison during HOT 2000 cruises.

Cruise	Sensor #	Standard Deviation
HOT-111	2045	0.0036
HOT-112	2045	0.0021
HOT-113	2045	0.0046
HOT-114	2045	0.0019
HOT-115	2045	0.0022
HOT-116	2045	0.0055
HOT-117	2045	0.0023
HOT-118	2045	0.0042
HOT-119	1392	0.0059
HOT-120	1392	0.0013
HOT-121	1392	0.0036

2.2.2.4 Comparison with CTD Data

The calibrated thermosalinograph salinity data collected during CTD casts were compared with the downcast CTD salinity at 4 dbar as an additional quality control. This procedure was conducted in the same manner as previously reported HOT cruises (Tupas *et al.,* 1997). The thermosalinograph data were averaged using data sampled one minute after the acquisition time of the CTD sample. Mean comparisons with the CTD were smaller than ± 0.007°C for all cruises.

2.3 Meteorology

Wind speed and direction, atmospheric pressure, wet- and dry-bulb air temperature, sea surface temperature (SST), cloud cover and weather code were recorded at four-hour intervals while at Station ALOHA by the science personnel.

Meteorological observations were also obtained every 4 hours by the ship's officers on the bridge of the R/V *Ka'imikai-o-Kanaloa* throughout each cruise.

Also available were hourly atmospheric pressure, air temperature, SST, and wind velocities obtained from NDBC buoy #51001 (23.4°N, 162.3°W).

The time-series of shipboard observations obtained by the science group was plotted and obvious outliers were identified and flagged. The SST-dry air temperature and wet-dry air temperature plots also helped to identify outliers. Bad data points were often replaced with the bridge data. Outliers in the shipboard pressure, air temperature, SST, and wind observations were detected by comparison with the buoy data.

Comparison of the shipboard atmospheric pressure against the buoy data showed an offset in the data taken on the R/V *Ka'imikai-o-Kanaloa* during cruises HOT-111 through -117. The magnitude of the offset was 5 mbar, and was obtained by comparisons against our lab pressure standard (Section 2.1.2.1). These comparisons were obtained before the barometer was calibrated by National Weather Service personnel on 31 July 2000. This offset was added to the shipboard atmospheric pressures for the affected cruises.

2.4 Biogeochemical Measurements

At Stations Kahe, ALOHA, KAENA and HALE-ALOHA, water samples for chemical analyses were collected from discrete depths using 12 liter PVC bottles with teflon coated internal springs as closing mechanisms. Sampling strategies and procedures are well documented in the previous data reports and in the HOT Program Field and Laboratory Protocols manual. This report contains only a subset of the total database, which can be extracted electronically over the Internet (hahana.soest.hawaii.edu/hot/hot_jgofs.html). To assist in the interpretation of these data and to save users the time to estimate the precision of individual chemical analysis, we have summarized precision estimates from replicate determinations for selected constituents on each HOT cruise in 2000.

2.4.1 Dissolved Oxygen

Dissolved oxygen samples were collected and analyzed using a computer-controlled potentiometric end-point titration procedure as described in Tupas et al. (1997). As in previous years we measured, using a calibrated digital thermistor, the temperature of the seawater sample at the time the iodine flask was filled. This was done to evaluate the magnitude of sample temperature error that affects the calculation of oxygen concentrations in units of μmol kg^{-1}. Figure 2.3 (upper panel) shows a plot of the difference between sample temperature and potential temperature computed from the *in situ* temperature measured at the time of bottle trip, versus pressure. The lower panel of the same figure shows a plot of the difference between oxygen concentration using on-deck and potential temperatures versus pressure. The depth dependent variability in Δ oxygen is a result of the absolute magnitude of the oxygen concentration and the standard procedures we employ for sampling the water column.

Precision of the Winkler titration method is presented in Table 2.12. The mean precision of our oxygen analyses in 2000 was 0.12 %. Oxygen concentrations measured over the 12 years of the program are plotted at three constant potential density horizons in the deep ocean along with their mean and 95 % confidence intervals (Figure 2.4). These results indicate that analytical consistency has been maintained over the past 12 years of the HOT program.

Table 2.12: Precision of Winkler titration method

HOT	Dissolved O_2	
	Mean CV (%)	Mean SD ($\mu mol\ kg^{-1}$)
111	0.09	0.169
112	0.14	0.244
113	0.11	0.205
114	0.09	0.160
115	0.11	0.172
116	0.08	0.150
117	0.12	0.204
118	0.12	0.215
119	0.10	0.173
120	0.13	0.241
121	0.25	0.405

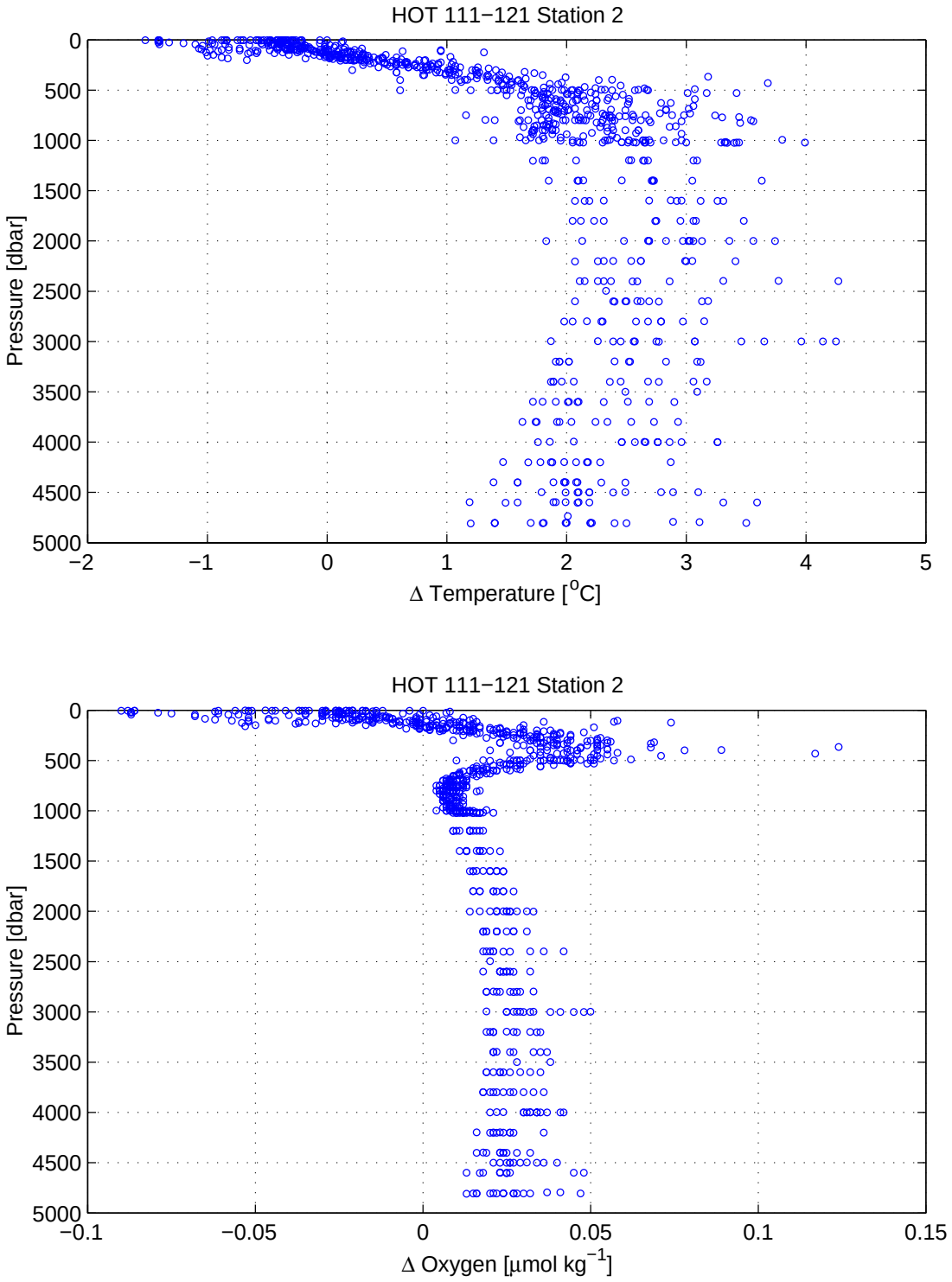

Figure 2.3: [Upper panel] Difference between sample temperature at the time of sample collection and potential temperature calculated from *in situ* temperature at the time of bottle trip. [Lower panel] Difference in oxygen concentration corrected for temperatures measured at the time of sample collection and potential temperature calculated from *in situ* temperature.

2.4.2 Dissolved Inorganic Carbon and Titration Alkalinity

Samples for dissolved inorganic carbon (DIC) were measured using a Single Operator Multi-parameter Metabolic Analyzer (SOMMA) which was manufactured at the University of Rhode Island and standardized at the Brookhaven National Laboratory. Analyses of replicate samples yielded a mean precision of 1.82 µmol kg^{-1} (Table 2.13). Total (titration) alkalinity (TAlk) was determined using the modified Gran titration method as described in Tupas et al. (1997). The mean precision of the alkalinity analyses during 2000 was 4.51 µeq kg^{-1} (Table 2.14). The accuracy of DIC and alkalinity measurements was established with certified reference materials (CRMs) obtained from Andrew Dickson at Scripps Institution of Oceanography.

Table 2.13: Precision of DIC analyses

	DIC	
HOT	Mean CV (%)	Mean SD (µmol kg^{-1})
111	0.06	1.32
112	0.06	1.29
113	0.04	0.82
114	0.15	3.51
115	0.04	0.99
116	0.20	4.33
117	0.02	0.47
118	0.10	2.13
119	0.07	1.49
120	0.06	1.23
121	0.11	2.40

Table 2.14: Precision of Total Alkalinity analyses

	Talk	
HOT	Mean CV (%)	Mean SD (µeq kg^{-1})
111	0.15	3.49
112	0.23	5.24
113	0.11	2.62
114	0.42	9.82
115	0.15	3.39
116	0.15	3.42
117	0.22	5.19
118	0.20	4.67
119	0.18	4.27
120	0.16	3.75
121	0.16	3.78

2.4.3 Inorganic Nutrients

2.4.3.1 Standard Methods

Samples for the determination of dissolved inorganic nutrient concentrations (soluble reactive phosphorus, [nitrate+nitrite] and silicate) were collected as described in Tupas et al. (1993). Analyses were conducted on a four-channel Technicon Autoanalyzer II continuous flow system at the University of Hawaii Analytical Services Facility. A summary of the precision of replicate analyses for 2000 is shown in Table 2.15. Figures 2.4-2.5 show the mean and 95% confidence limits of nutrient concentrations measured at three potential density horizons for the 12 years of the program. In addition to standard automated nutrient analyses, specialized chemical methods are used to determine concentrations of nutrients that are normally below the detection limits of autoanalyzer methods.

2.4.3.2 High Sensitivity Methods

The chemiluminescent method of Cox (1980) as modified for seawater by Garside (1982) was used to determine the [nitrate+nitrite] content of near surface (0-200 m interval) water samples. The limit of detection for [nitrate+nitrite] was approximately 2 nM with a precision and accuracy of ±1 nM (Dore et al., 1996).

Low level soluble reactive phosphorus (SRP) concentrations in the euphotic zone were determined according to the magnesium induced coprecipitation (MAGIC) method of Karl and Tien (1992). Typical precision estimates for triplicate determinations of SRP are from 1-3 % with a detection limit of 2 nM. The MAGIC SRP measurement is also corrected for arsenate interference of the molybdenum blue colorimeteric procedure (Johnson 1971), unlike the standard autoanalytical method.

2.4.4 Dissolved Organic Matter

Dissolved organic carbon (DOC) was determined by the high temperature catalytic oxidation method using an automated DOC analyzer (Qian and Mopper 1996). Dissolved organic nitrogen (DON) was calculated as the difference between total dissolved fixed nitrogen (TDN) and [nitrate+nitrite] concentrations. DON by this definition also includes ammonium, however, ammonium concentrations in these waters are below the detection limit of standard nutrient analyses (~50 nM). Dissolved organic phosphorus (DOP) was calculated as the difference between total dissolved phosphorus (TDP) and SRP concentrations. DOP, by this definition includes inorganic polyphosphates. TDN and TDP were determined by the UV oxidation method as described in Tupas et al. (1997). A summary of the precision of these analyses is given in Table 2.16.

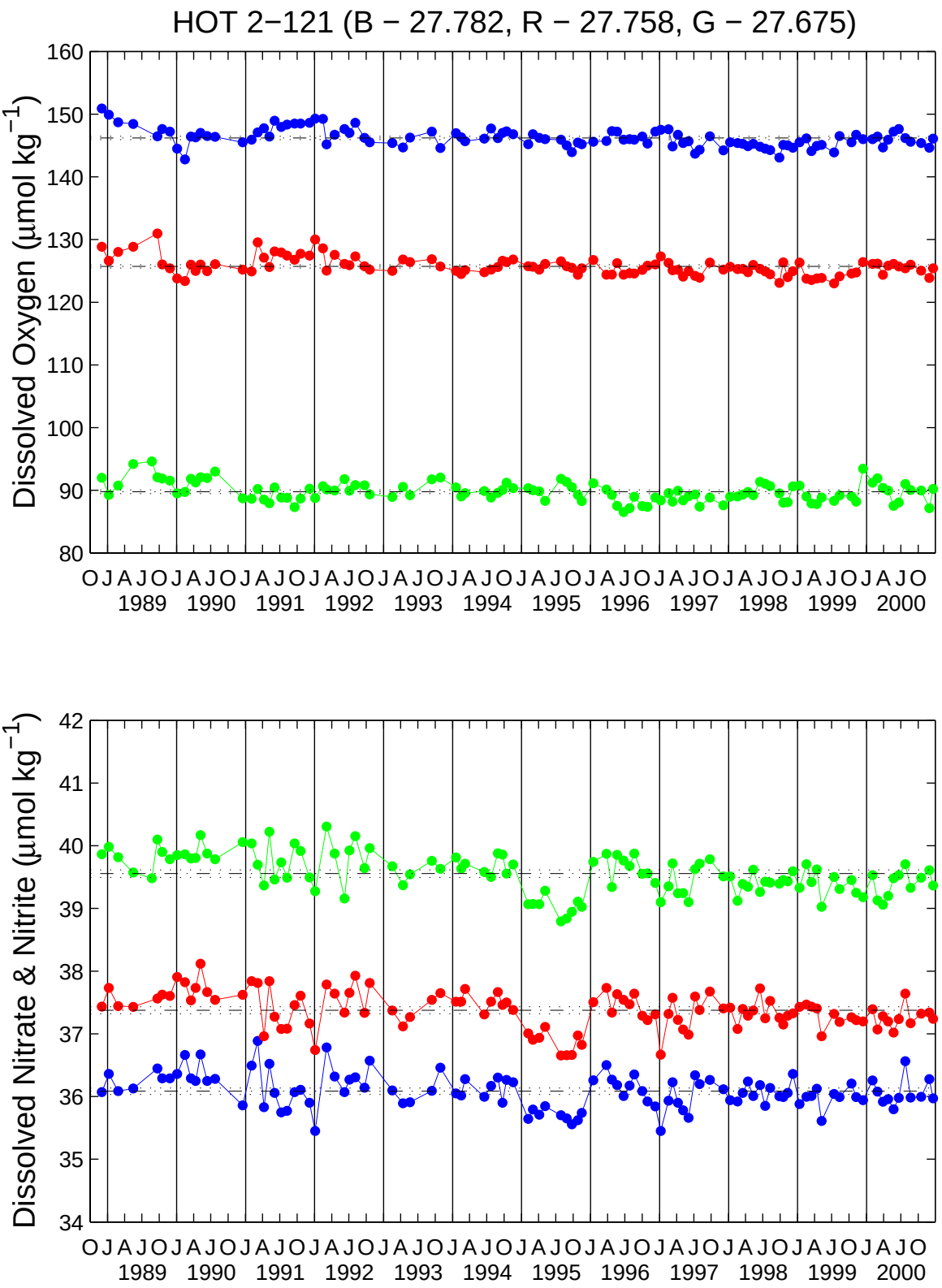

Figure 2.4: Concentrations at potential density horizons of 27.782, 27.758 and 27.675 (approx. 4000m, 3000m and 2000m) at Station ALOHA. [Upper panel] Dissolved oxygen. [Lower panel] Nitrate + nitrite.

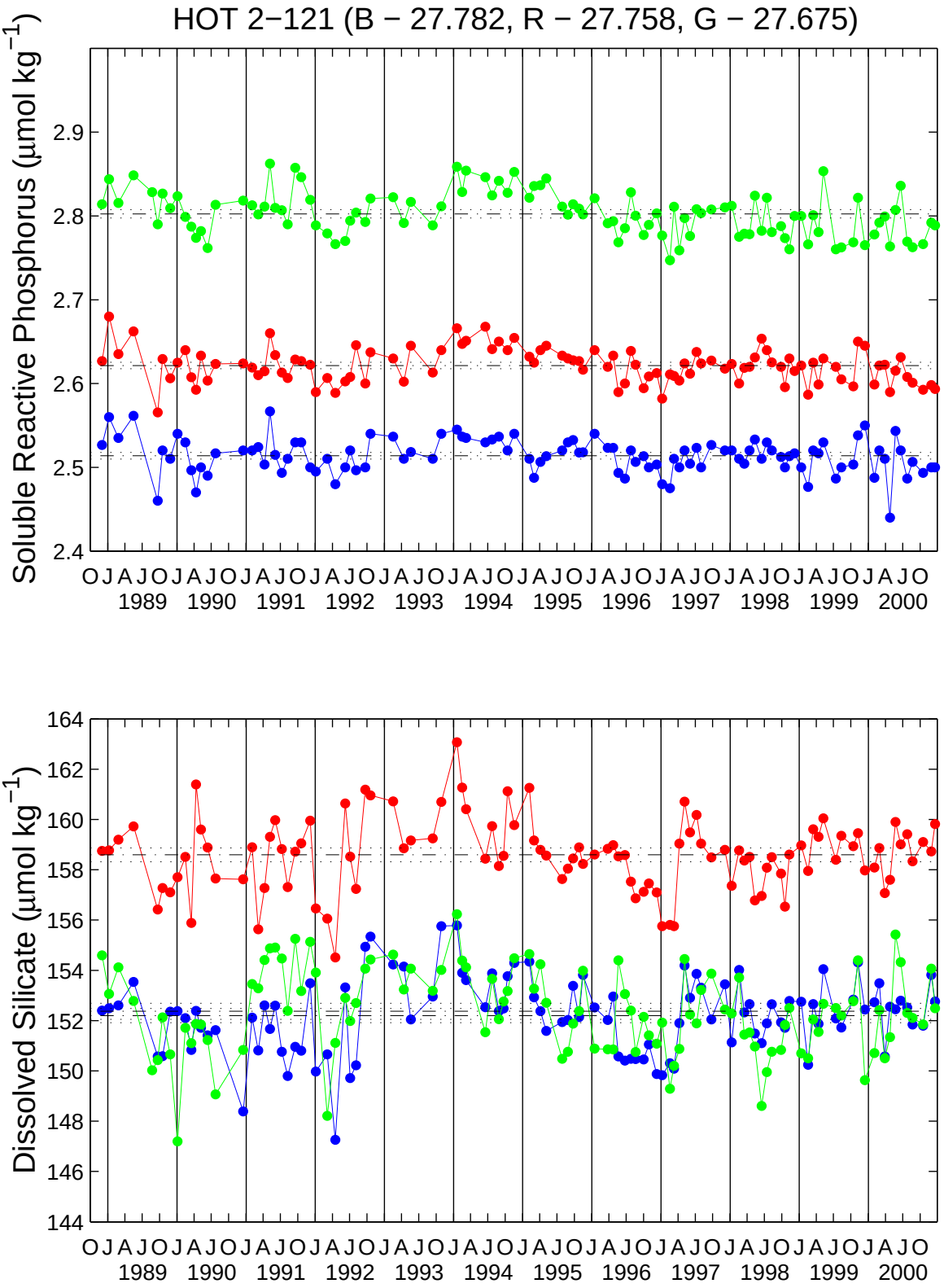

Figure 2.5: Concentrations at potential density horizons of 27.782, 27.758 and 27.675 (approx. 4000m, 3000m and 2000m) at Station ALOHA. [Upper panel] Soluble reactive phosphorus. [Lower panel] Silicate.

Table 2.15: Precision of dissolved inorganic nutrient analyses

	[Nitrate + Nitrite]		SRP		Silicate	
HOT	Mean CV (%)	Mean SD (µM)	Mean CV (%)	Mean SD (µM)	Mean CV (%)	Mean SD (µM)
111	0.2	0.032	0.4	0.006	0.3	0.274
112	0.2	0.063	0.4	0.010	5.4	0.309
113	0.3	0.068	1.1	0.012	1.6	0.381
114	0.6	0.078	0.3	0.009	3.4	0.184
115	0.2	0.033	1.1	0.031	1.2	0.313
116	0.6	0.135	0.8	0.016	1.2	0.169
117	0.5	0.078	0.4	0.008	3.7	0.341
118	0.3	0.049	0.6	0.013	1.6	0.358
119	0.6	0.057	0.2	0.004	3.0	0.211
120	0.6	0.049	0.2	0.004	0.4	0.274
121	0.4	0.030	0.4	0.008	2.0	0.307

Table 2.16: Precision of dissolved organic nutrient analyses

	DOC		DON		DOP	
HOT	Mean CV (%)	Mean SD (µM)	Mean CV (%)	Mean SD (µM)	Mean CV (%)	Mean SD (µM)
111	1.3	0.85	2.4	0.03	7.1	0.014
112	1.3	0.98	4.4	0.10	16.3	0.018
113	1.9	1.53	3.4	0.16	14.4	0.011
114	1.3	0.92	6.7	0.20	21.3	0.012
115	1.1	0.89	8.1	0.33	37.1	0.035
116	1.5	1.03	9.1	0.27	30.4	0.034
117	NA	NA	10.1	0.34	4.2	0.007
118	NA	NA	6.1	0.58	16.0	0.012
119	4.6	2.12	4.8	0.17	8.6	0.011
120	8.5	4.95	3.5	0.11	12.2	0.008
121	15.4	7.25	9.7	0.55	15.3	0.051

2.4.5 Particulate Bioelements

Samples for elemental analyses of particulate matter were prefiltered through 202 µm Nitex mesh to remove large zooplankton and collected onto combusted GF/F glass fiber filters (acid washed for particulate phosphorus). Particulate carbon (PC) and nitrogen (PN) on the filters were analyzed using a Europa automated nitrogen and carbon analyzer. Particulate

phosphorus (PP) was analyzed using high temperature ashing followed by acid hydrolysis and subsequent determination of the liberated orthophosphate by colorimetry. These procedures are detailed in Karl et al. (1991). The average precisions during 2000 determined from replicate particulate matter elemental analyses are presented in Table 2.17.

Table 2.17: Precision of particulate matter elemental analyses

	PC		PN		PP	
HOT	Mean CV (%)	Mean SD ($\mu g\ l^{-1}$)	Mean CV (%)	Mean SD ($\mu g\ l^{-1}$)	Mean CV (%)	Mean SD ($\mu g\ l^{-1}$)
111	3.7	0.85	3.0	0.11	4.3	0.018
112	1.7	0.35	4.7	0.18	10.7	0.039
113	9.1	2.47	4.6	0.17	6.7	0.025
114	14.0	4.60	2.3	0.09	5.0	0.018
115	NA	NA	NA	NA	8.1	0.028
116	NA	NA	NA	NA	1.4	0.004
117	12.8	3.65	6.7	0.33	7.0	0.035
118	2.1	0.34	1.5	0.05	12.3	0.046
119	5.8	1.01	8.1	0.29	17.7	0.053
120	5.1	1.27	7.9	0.32	12.1	0.042
121	5.5	1.00	3.9	0.12	17.5	0.064

2.4.6 Pigments

2.4.6.1 Standard Fluorometric Method

Chlorophyll a (chl *a*) and pheopigments were measured fluorometrically on a Turner Designs Model 10-AU fluorometer with 100% acetone as the solvent using standard techniques (Strickland and Parsons 1972). The precision for this analysis during 2000 is presented in Table 2.18.

2.4.6.2 High Performance Liquid Chromatography

Chlorophyll *a* and photosynthetic accessory pigments were also measured by high performance liquid chromatography (HPLC) according to Wright et al. (1991). The response factors and retention times yielded by this method during 2000 are presented in Table 2.19. Figure 2.6 shows the relationship between chlorophyll *a* measured by fluorometry and chlorophyll *a* measured by HPLC during 2000.

2.4.6.3 Underway Surface Fluorometry

Continuous *in vivo* chlorophyll (fluorescence) from surface seawater was measured using a Turner Designs Model 10-AU fluorometer installed on the ship's seawater intake system. The

underway measurements are calibrated by taking discrete samples from the outflow of the fluorometer and extracting the pigments according to standard methods.

Table 2.18: Precision of fluorometric chlorophyll *a* and pheopigment analyses

	Chlorophyll *a*		Pheopigments	
HOT	Mean CV (%)	Mean SD ($\mu g\ l^{-1}$)	Mean CV (%)	Mean SD ($\mu g\ l^{-1}$)
111	3.2	0.006	4.6	0.013
112	2.6	0.004	4.4	0.012
113	2.9	0.004	4.2	0.008
114	5.4	0.007	8.9	0.012
115	4.1	0.007	4.0	0.010
116	6.7	0.015	7.1	0.022
117	5.1	0.008	5.2	0.009
118	6.3	0.009	5.9	0.016
119	5.3	0.005	11.7	0.019
120	6.5	0.013	9.7	0.039
121	7.5	0.009	9.8	0.014

Table 2.19: 2000 HPLC Pigment Analysis Response Factors and Retention Times

Pigment	RF[a]	RT[b]
Chlorophyll c & Mg 3,8D[c]	0.250	
Peridinin	0.578	0.368
19'-Butanoyloxyfucoxanthin	0.466	0.397
Fucoxanthin	0.399	0.434
19'-Hexanoyloxyfucoxanthin	0.504	0.473
Violaxanthin	0.268	0.573
Diadinoxanthin	0.320	0.646
Alloxanthin	0.344	0.717
Lutein	0.311	0.791
Zeaxanthin	0.372	0.806
Monovinyl Chlorophyll b	1.049	0.939
Monovinyl Chlorophyll a	0.714	1.000
Divinyl Chlorophyll a	0.515	1.000
α-Carotene	0.379	1.180
β-Carotene	0.361	1.188

[a]RF - Response Factor ($ng\ l^{-1}$ pigment per unit absorbance peak area at 436 nm).
[b]RT - Retention Time (minutes, relative to chlorophyll a)
[c]Chlorophyll c = ($c_1 + c_2 + c_3$), Mg 3,8D = Mg 3,8 divinyl pheoporphyrin a_5 monomethyl ester.

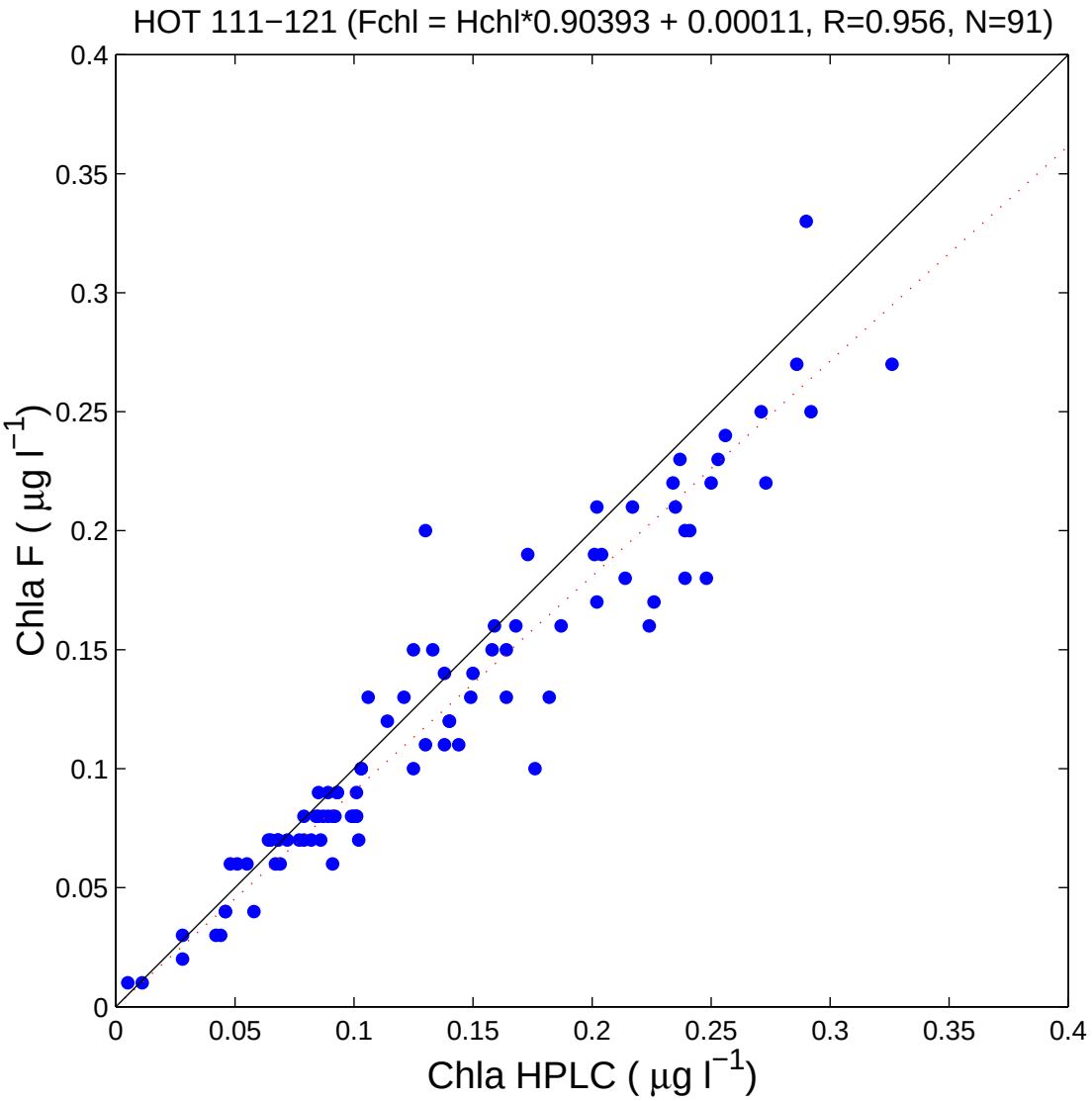

Figure 2.6: Chlorophyll a measured by fluorometry (Chla F) versus chlorophyll a measured by HPLC (Chla HPLC) for all data collected in 2000. The solid line shows the 1:1 x-y relationship while the dashed line is a model II linear regression analysis of the data set. The regression equation is at the top of the figure.

2.4.7 Adenosine 5'-triphosphate

Water column particulate adenosine 5'-triphosphate (ATP) concentrations were determined using the firefly bioluminesence technique as described by Karl and Holm-Hansen (1978). The precision of ATP determinations in 2000 is presented in Table 2.20.

Table 2.20: Precision of ATP Analyses during 2000

HOT	Particulate ATP	
	Mean CV (%)	Mean SD (ng l^{-1})
111	15.6	1.79
112	5.9	1.19
113	16.0	1.92
114	9.2	1.19
115	12.4	1.47
116	13.0	2.24
117	8.0	1.64
118	14.7	2.01
119	19.0	2.36
120	18.0	4.11
121	15.5	2.81

2.5 Biogeochemical Rate Measurements

2.5.1 Primary Production

Photosynthetic production of organic matter was measured by a trace-metal clean, ^{14}C tracer method. All incubations since 1990 were conducted *in situ* at eight depths over one daylight period using a free-drifting array as described by Winn et al. (1991). Some incubations during 1988-1990 were carried out *in situ*, and some on deck under simulated *in situ* light and temperature conditions. Integrated carbon assimilation rates were calculated using the trapezoid rule with the shallowest value extended to 0 m and the deepest extrapolated to a value of zero at 200 m.

2.5.2 Particle Flux

Particle flux was measured at a standard reference depth of 150 m using multiple cylindrical sediment traps deployed on a free-floating array for approximately 60 h during each cruise. Sediment trap design and collection methods are described in Winn et al. (1991). Samples were analyzed for particulate C, N and P. Typically three traps are analyzed for PC and PN, and another three traps for PP.

2.6 Optical Measurements

2.6.1 Solar Irradiance

Incident irradiance (400-700 nm wavelength band) at the sea surface was measured on each HOT cruise with a LI-COR LI-200 data logger and cosine collector. The instrument recorded data from the time the ship departed Snug Harbor until its return.

2.6.2 Downwelling Irradiance and Upwelling Radiance

Vertical profiles of upwelling radiance and downwelling irradiance were made using a Biospherical Profiling Reflectance Radiometer (PRR-600). This instrument measures downwelling irradiance (Ed) and upwelling radiance (Lu) as well as surface irradiance from a deck unit on 7 wavelength channels. The radiance channels comply with the SeaWIFS satellite optical parameters. The instrument is lowered by hand and depending on the subsurface currents, is deployed to a depth between 140 and 170 meters.

2.6.3 Tethered Spectral Radiometer Buoy (TSRB)

The TSRB was used to make continuous measurements of downwelling irradiance just above the sea surface, upwelling radiance just below the sea surface, and sea surface temperature at the sea surface. The instrument measures downwelling irradiance at 489nm and upwelling radiance at 410, 444, 489, 511, 553, 668 and 684nm. All wavelengths except the 684nm waveband have bandpasses of approximately 20nm. The 684nm waveband has a bandpass of 10nm. The sampling frequency is 1 Hz.

2.6.4 Chloropigment by Flash Fluorescence

Flash fluorescence was measured with a Sea Tech Model ST0250 flash fluorometer and the data collected with the Sea-Bird CTD system. Flash fluorescence traces were collected on as many casts as possible. Because an absolute radiometric standard is not available for flash fluorometers, instrument drift was corrected via calibration with the fluorometric chlorophyll plus accessory pheopigments. A linear relationship of the form, $V_n = b \cdot V_o + a$, was used to convert all fluorescence data to chloropigment.

2.7 Microbial Community Structure

Analysis of microbial numbers was made using an EPICS 753 flow cytometer (Coulter Electronics Corporation, Hialeah, FL, USA) which has been upgraded with a Cicero Data Acquisition System (Cytomation Inc., Boulder, Colorado). Prior to analysis by flow cytometry, samples were prepared using standard protocols (Monger & Landry 1993; Campbell et al., 1994). Enumeration efficiency was tracked using fluorescent beads. Cyanobacteria of the genera *Prochlorococcus* and *Synechococcus* were separately enumerated, as well as non-pigmented bacteria/archaea and pigmented eukaryotes.

2.8 Zooplankton Community Structure

2.8.1 Mesozooplankton Collection

Samples for the quantification of mesozooplankton were collected using a 1 m^2 plankton net with a 202 μm Nitex mesh. The net is towed obliquely at a speed of 1.0-1.5 knots while deploying and retrieving the tow line at a constant speed (about 20 meters min^{-1}; total line out = 200 meters; 20 minute tow duration; average depth of tow ≈ 175 meters). Three midnight (between 2200-0200 local time) and three mid-day (between 1000-1400 local time) tows are conducted on each cruise. This sampling scheme allows maximal collection of vertical migrants during the night and minimal collection of vertical migrants during the day.

2.8.2 Sample Processing

Immediately after the net tows, contents of the collecting buckets (cod ends) are divided using a Folsom splitter. One-half of each tow is preserved in 4% buffered formaldehyde, with 2 mg l^{-1} strontium sulfate added to prevent acantharians from dissolving. Approximately one-fourth of each tow, depending on sample density, is further size-fractionated through nested screens of 5, 2, 1, 0.5 and 0.2 mm Nitex mesh. Each size fraction is filtered onto a preweighed 0.2μm Nitex filter, rinsed with isotonic ammonium formate to remove salts, sucked dry under low vacuum, and flash frozen in liquid nitrogen. In the lab, frozen samples are defrosted at room temperature and weighed wet (moist) on an analytical balance. After a wet weight is obtained random subsamples of the zooplankton mass are removed and set aside for enumeration, and the remaining sample is dried at 60 °C. Dry samples are reweighed to obtain a total sample dry weight [total sample dry weight = measured dry weight/fraction of total wet weight dried]. The dry samples are analyzed for carbon and nitrogen.

3.0 CRUISE SUMMARIES

The cruise summaries presented here give an overview of the activities conducted during the 2000 HOT cruises. The official Chief Scientist's reports can be found on the HOT-JGOFS (hahana.soest.hawaii.edu/hot/cruises.html) and HOT-WOCE web pages.

3.1 HALE-ALOHA 7B Mooring Recovery

Chief Scientist: T. HOULIHAN
R/V *Thomas Thompson*
26-27 Jan. 2000

Due to the uncertainty of the availability of the *Ka'imikai-o-Kanaloa* we were able to charter the R/V *Thomas Thompson* which had recently ended a science cruise from San Diego to Honolulu.

The Thompson left Pier 2 at approximately 2000 on 26 January with 6 scientists from Hawaii on board. Equipment was also trucked from the Marine Center to the pier to aid in the recovery. We transited overnight and arrived at an intercept point south of the projected drift track at 0600. Captain Gray plotted out a dead reckoning projected location of the buoy from the Argos drift track and at about 0800 the buoy was sighted right where predicted, 22 44.4'N, 158 3.24'W. The winds were trades at 20-30 kts, seas rough, swell 8-10 ft, under mostly cloudy skies.

During the recovery the PVC ring was damaged and at least one anemometer was lost. Some of the instruments faired very well, many were lost. One UW Seacat/GTD was totally lost, one was recovered in somewhat damaged condition. One MBARI Nitrate sensor was totally lost, one sustained considerable damage. Both MIT trace metal samplers looked in good condition although a few of the individual samplers were damaged. The UH/Karl Seacats were recovered with the external sensors gone. All the UH/Karl thermistors and UH/Lucas Seacats were recovered and looked like they may have sustained some superficial external damage. The meteorological sensors were a near total loss as was the surface buoy and tower. We are fairly confident that the flotation hardhats and dual releases are in recoverable condition and will be retrieved at an appropriate time.

The line parted at the termination between the top two 500m nylon sections. It appeared that the damage to the instruments was due to the failure of the stainless bolts that held the base on to the buoy. This frame was missing upon recovery and it is guessed that as this frame fell through the water column it damaged the instruments and possibly caused the abrasion at the point where the line parted.

3.2 HOT-111

Chief Scientist: D. HEBEL
R/V *Ka'imikai-o-Kanaloa*
1-4 Feb. 2000

HOT-111 was conducted aboard the R/V *Ka'imikai-o-Kanaloa* 1-4 Feb. 2000. Captain Hayes was the master of the vessel. There were a total of 14 participants in the scientific party

composed of 4 WOCE, 6 JGOFS, 2 Ancillary and 2 STAG. We departed Snug on 1 Feb. occupying stations at Kahe Pt. (sta. 1) and Station ALOHA (sta. 2). All scheduled work was completed and all samples collected, however, a number of samples from the JGOFS-2 cast were compromised when they were discovered (7 Feb) at room temperature still in the collection box. These samples were latter re-taken by subsampling from our low-level phosphorus samples which were collected in excess. CTD operations were conducted at stations 1 & 2. One ~1000m CTD cast was conducted at station 1 and 14 casts at Station ALOHA with 2 deep casts (~4750 m). The HPLC cast (s2c14) was incorporated into the second WOCE deep cast. Other over-the-side operations included 3 light casts, 12 net tows, 2 *in situ* pumping operations, 1 Go-Flo cast, floating sediment traps and productivity operations. All operations were routine with the exception of additional net tows for C. Benitez-Nelson, a rosette Go-Flo primary productivity experiment comparison, and collection of atmospheric particutale material.

The underway/continous thermosalinograph and ADCP were operable and functioned properly. No continuous pCO_2 or fluorometry were measured on HOT-111 as well as limited meterological instrumentation.

The weather was variable with high winds, seas and mostly sunny skies at the beginning of the cruise with light winds, seas and mostly cloudy skies at the end of the cruise.

3.3 HOT-112

Chief Scientist: D. HEBEL
R/V *Ka'imikai-o-Kanaloa*
28 Feb.-3 Mar. 2000

HOT-112 was conducted aboard the R/V *Ka'imikai-o-Kanaloa* 28 Feb.-3 Mar. 2000. Captain Hayes was the master of the vessel. There were a total of 16 participants in the scientific party composed of 4 WOCE, 7 JGOFS, 3 Ancillary and 2 STAG. We departed Snug on 1 February occupying stations at Kahe Pt. (sta. 1), and Station ALOHA (sta. 2). All scheduled work was completed and all samples collected with the exception of two net tows due to engine problems. CTD operations were conducted at stations 1 & 2. One ~1000 m CTD cast was conducted at station 1, with 14 ~1000 m CTD casts at Station ALOHA and 2 near-bottom deep casts (~4750 m). S2c3 was aborted due to a faulty fluorometer, which stopped working for no apparent reason. Other over-the-side operations included 3 light casts, 10 net tows, 2 *in situ* pumping operations, 1 Go-Flo cast, floating sediment traps and productivity operations. All operations were routine with the exception of additional net tows for C. Benitez-Nelson, a rosette Go-Flo primary productivity experiment comparison, collection of atmospheric particulate material, *in situ* pump operations and rosette/Go-Flo primary production comparison.

The underway/continuous thermosalinograph and ADCP were operable and functioned properly. No continuous pCO_2 or fluorometry were measured on HOT 112 as well as limited meterological instrumentation. Overall the weather was partly cloudy with moderate to rough seas.

3.4 HOT-113

Chief Scientist: L. TUPAS
R/V *Ka'imikai-o-Kanaloa*
27-30 March 2000

All objectives of the JGOFS and WOCE programs were accomplished. All planned stations were occupied. Weather and sea conditions were rough but within limits of safety for deck operations. All core samples were taken and the 36 hour CTD burst sampling period was not interrupted. All samples for ancillary projects were taken. Guest scientists and students were able to accomplish their work. Floating sediment trap array and primary production array deployed and recovered successfully. No samples were lost during the *in-situ* incubations. ADCP measurements were made throughout the cruise. There was no HALE-ALOHA station because the mooring has not yet been deployed.

3.5 HOT-114

Chief Scientist: F. SANTIAGO-MANDUJANO
R/V *Ka'imikai-o-Kanaloa*
24-27 April 2000

Operations were conducted as planned without any incidents. All the primary JGOFS and WOCE objectives were accomplished. One 1000 m CTD cast was obtained at Station Kahe, and a total of 15 were conducted at Station ALOHA including two deep casts.

One 8-bottle Go-Flo cast was successfully obtained at station ALOHA, and the primary productivity array was deployed for 12 hr and recovered without problems. The array of floating sediment traps was also deployed for about 52 hr and recovered without incidents. C. Allen completed successfully 6 plankton net tows.

A strong near-surface northwestward current of about 1 kt was present during the cruise as indicated by the ADCP and by the drift of the primary productivity array and the sediment traps. This strong current caused some difficulties during the deployment of the primary productivity array and during the recovery of the sediment traps. The difficulties were resolved and in the future measures will be taken to adjust deployment procedures when strong currents are present.

Conditions were slightly rough during the transit to Station ALOHA due to the big swell, but improved afterwards.

The ADCP ran without interruption throughout the cruise, as well as the thermosalinograph. Some tests were conducted by the WOCE group on the continuous water supply system to investigate their effect on the thermosalinograph.

3.6 HOT-115

Chief Scientist: L. TUPAS
R/V *Ka'imikai-o-Kanaloa*
22-26 May 2000

All objectives of the JGOFS and WOCE programs were completed. All planned stations were occupied. Weather and sea conditions were good. All core samples were taken. The 36 hour CTD burst sampling period was interrupted in order to transport Mr. Hansen to shore after he injured himself through a chemical spill. All samples for ancillary projects were taken. Guest scientists and students were able to accomplish their work. Floating sediment trap array and primary production array deployed and recovered successfully. No samples were lost during the *in-situ* incubations. ADCP measurements were made throughout the cruise. There was no HALE ALOHA station because the mooring has not yet been deployed.

3.7 HOT-116

Chief Scientist: D. HEBEL
R/V *Ka'imikai-o-Kanaloa*
19-22 June 2000

HOT 116 was conducted aboard the R/V *Ka'imikai-o-Kanaloa*, 19 to 22 June, 2000. Captain Hayes was the master of the vessel. There was a total of 16 participants in the scientific party composed of 4 WOCE, 8 JGOFS, 2 ancillary and 2 STAG. We departed Snug on 19 June occupying stations at Kahe Pt. (sta. 1), and Station ALOHA (sta. 2). All scheduled work was completed and all samples collected. CTD operations were conducted at stations 1&2. One ~1000 m CTD cast was conducted at station 1, with 14 ~1000 m CTD casts at Station ALOHA and 2 near-bottom deep casts (~4750 m). Other over-the-side operations included 3 light casts, 12 net tows, 1 *in situ* pumping operations, 1 Go-Flo cast, floating sediment traps and productivity operations. All operations were routine with the exception of additional net tows for C. Benitez-Nelson, a rosette Go-Flo primary productivity experiment comparison, collection of atmospheric particulate material, *in situ* pump operation and rosette/Go-Flo primary production comparison.

The underway/continuous thermosalinograph, fluorometer and ADCP were operable and functioned properly. No continuous pCO_2 were measured on HOT 116 as well as limited meterological instrumentation. Overall the weather was partly cloudy with moderate to rough seas.

3.8 HALE-ALOHA 8A

Chief Scientist:T. HOULIHAN
R/V *Ka'imikai-o-Kanaloa*
23-24 June 2000

The loading of the ship for the mooring deployment was conducted on the morning of 23 June after the *Ka'imikai-o-Kanaloa* had returned from HOT-116 the previous evening. The loading was completed by 1200 and the back deck was subsequently secured.

A total of 11 scientists participated in the cruise aboard the *Ka'imikai-o-Kanaloa* . The HALE-ALOHA mooring was successfully deployed. Andrew Hanson was able to collect water for John Zehr at UCSC.

3.9 HOT-117

Chief Scientist: L. TUPAS
R/V *Ka'imikai-o-Kanaloa*
24-28 July 2000

All objectives of the JGOFS and WOCE programs were completed. All planned stations were occupied. Weather and sea conditions were good. All core samples were taken. The 36 hour CTD burst sampling period was interrupted twice to reterminate the CTD package. The second deep cast was aborted due to concerns with the CTD cable. All samples for ancillary projects were taken. Guest scientists and students were able to accomplish their work. Floating sediment trap array and primary production array deployed and recovered successfully. No samples were lost during the *in-situ* incubations. ADCP measurements were made throughout the cruise. A CTD cast and asmples were taken at the recently deployed HALE-ALOHA mooring.

3.10 HOT-118

Chief Scientist: D. HEBEL
R/V *Ka'imikai-o-Kanaloa*
21-25 August 2000

HOT 118 was conducted aboard the R/V *Ka'imikai-o-Kanaloa*, 21-25 August, 2000. Captain Hayes was the master of the vessel. There was a total of 16 participants in the scientific party composed of 4 WOCE, 8 JGOFS, 2 ancillary investigators and 2 STAG. We departed Snug on 21 August occupying stations at Kahe Pt. (sta. 1), Station ALOHA (sta. 2), HALE ALOHA (sta. 8) and Kaena Pt. (sta. 6). All scheduled work was completed and all samples collected. CTD operations were conducted at stations 1, 2, 6 and 8. One ~1000 m CTD cast was conducted at station 1&8; 2 <250m, 13 ~1000 m, one ~2000m and one ~4800 m CTD casts at Station ALOHA; one ~2500m CTD cast at Kaena Pt. (sta.6). Other over-the- side operations included 3 light casts, 12 net tows, 2 *in situ* pumping operations, 1 Go-Flo cast, floating sediment traps and primary productivity measurements. All operations were routine with the exception of additional net tows for C. Benitez-Nelson (which by now are routine), an external Niskin /Go-Flo primary

productivity comparison, *in situ* pump operations (again almost routine) and addition of sta. 6 with secondary CTD testing.

The underway/continuous thermosalinograph, ADCP, and fluorometer were operable and functioned properly. WOCE met. obs and limited ship met. data were collected as well as aerosol measurements on 23 Aug. Overall the weather was partly cloudy with moderate to rough seas and 15-30 kt Trades.

3.11 HOT-119

Chief Scientist: D. HEBEL
R/V *Ka'imikai-o-Kanaloa*
16-20 October 2000

HOT 119 was conducted aboard the R/V *Ka'imikai-o-Kanaloa*, 16-20 October, 2000.. Captain Hayes was the master of the vessel. There was a total of 17 participants in the scientific party composed of 5 WOCE, 8 JGOFS, 2 ancillary investigators and 2 STAG. We departed Snug on 16 Oct., occupying stations at Kahe Pt. (sta. 1), Station ALOHA (sta. 2), HALE ALOHA (sta. 8) and Kaena Pt. (sta. 6). All scheduled work was completed and all samples collected. CTD operations were conducted at stations 1, 2, 8 and 6. One ~1000 m CTD cast was conducted at stations 1&8; 1 <250m, 14 ~1000 m, and 2 ~4800 m CTD casts at Station ALOHA; one ~2500m CTD cast at Kaena Pt. (sta.6). Other over-the-side operations included 3 light casts, 13 net tows, 2 *in situ* pumping operations, 1 Go-Flo cast, floating sediment traps and primary productivity array. All operations were routine with the exception of an external closing General Oceanics bottle primary productivity experiment and addition of sta. 6. The underway/continuous thermosalinograph, ADCP, and fluorometer were operable and functioned properly. WOCE met. Obs and limited ship met. data were collected as well as aerosol measurements. Overall the weather was mostly cloudy with moderate seas and wind.

3.12 HOT-120

Chief Scientist: F. SANTIAGO-MANDUJANO
R/V *Ka'imikai-o-Kanaloa*
28 Nov. – 2 Dec. 2000

Operations were conducted as planned without major interruptions. Fifteen 1000-m CTD casts and two deep casts were obtained at station ALOHA. One 1000-m CTD cast was obtained at each of stations Kahe and HALE-ALOHA. One near-bottom cast (~2500 m) was obtained at station 6. Both deep casts at ALOHA indicated the presence of a "cold event" with near-bottom potential temperatures reaching 1.089 C.

The primary productivity array was deployed and recovered without problems. The array of floating sediment traps was deployed without incidents, but the recovery was delayed when the array's line got tangled on the ship's propellers (although the engine was not engaged). One of the crew members had to swim under the ship using SCUBA gear to untangle the line.

The ADCP ran without interruption throughout the cruise, as well as the thermosalinograph, the fluorometer, and the ship's anemometer. The thermosalinograph recorded

noisy salinity data during the transit to station ALOHA, apparently due to bubbles introduced in the system because of the rough ride. C. Allen and C. Benitez-Nelson completed successfully 6 plankton net tows. Weather conditions during the cruise were rough at the beginning, but improved considerably after the first day with winds less than 5 kt and flat seas.

3.13 HOT-121

Chief Scientist: F. SANTIAGO-MANDUJANO
R/V *Ka'imikai-o-Kanaloa*
18-22 December 2000

Operations were conducted as planned without major interruptions. Twelve 1000-m CTD casts, one 100-m, and two deep casts were obtained at station ALOHA. One 1000-m CTD cast was obtained at each of stations Kahe and HALE-ALOHA. One near-bottom cast (~2500 m) was obtained at station 6. The CTD wire developed a kink near the package on the third day of the cruise and had to be reterminated.

The primary productivity array was deployed as planned on December 20, but its recovery was delayed until the next morning because it could not be found in the dark given that its strobe light was not working. The array of floating sediment traps was deployed and recovered without incidents. K. Selph and T. Gregory completed successfully 6 plankton net tows.

The ADCP ran without interruption throughout the cruise, as well as the fluorometer, and the ship's anemometer. The thermosalinograph external temperature sensor had problems and had to be replaced during the cruise, compromising about 6 hours of temperature data.

Weather conditions were favorable during the first two days of the cruise, with light winds and flat seas, but conditions deteriorated after the second day, with winds increasing to 20-25 kt and sea state 4, with large swells.

4.0 RESULTS

4.1 Hydrography

4.1.1 2000 CTD Profiling Data

Profiles of temperature, salinity, oxygen and potential density (σ_θ) were obtained from data collected at Stations Kahe, ALOHA, and HALE-ALOHA. The downcast CTD profiles from Station ALOHA during 2000 are presented in Figure 6.1.1, together with the results of bottle determinations of oxygen, salinity and inorganic nutrients. Stack plots of CTD temperature and salinity profiles for all 1000 m casts conducted at Station ALOHA are also presented (Figure 6.1.2). The offset between bottle salinities and CTD profiles apparent in some of the cruise's salinity vs. pressure plots (e.g. HOT-111 and -115, Figs. 6.1.1a and 6.1.1e) is due to the mismatch between the downcast CTD profile and the bottle salinities, which are taken during the upcast. This salinity mismatch is caused mostly by vertical displacements of the density structure and disappears when plotted against potential temperature (lower right panel in Figs. 6.1.1). In some instances mismatches are caused by freshening of the surface water due to rain during the cast (e.g. HOT-120, Figure 6.1.1j lower right panel).

Profiles of the data collected for Stations Kahe and HALE-ALOHA during 2000 are presented in Figures 6.1.3. Station HALE-ALOHA was not visited during HOT-111 through 116 because the mooring was not installed during these cruises.

The potential temperature, salinity and oxygen profiles obtained from the deep casts at Station ALOHA during 2000 are presented in Figures 6.1.4-6. A cold-water anomaly developed near the bottom in late November 2000 during HOT-120 (Figure 6.1.4, the coldest profile near the bottom) and started warming up in the following cruise. Similar anomalies have been observed in previous years; this is the 7th major cold-water anomaly observed since the beginning of the time-series (Lukas et. al., 2001).

4.1.2 Time-series Hydrography, 1988-2000

The hydrographic data collected during the first twelve years of HOT are presented in a series of contour plots (Figures 6.1.7-22). These figures show the data collected in 2000 within the context of the longer time-series. The CTD data used in these plots are obtained by averaging the data collected during the 36-hour period of burst sampling. Therefore, much of the variability, which would otherwise be introduced by internal tides, has been removed. Figures 6.1.7 and 6.1.8 show the contoured time-series for potential temperature and density (σ_θ) in the upper 1000 dbar for all HOT cruises through 2000. Seasonal variation in temperature for the upper ocean is apparent in the maximum of near-surface temperature of about 26 °C and the minimum of approximately 23 °C. Oscillations in the depth of the 5 °C isotherm below 500 dbar appear to be relatively large with displacements up to 100 dbar. The main pycnocline is observed between 100 and 600 dbar, with a seasonal pycnocline developing between June and December in the 50-100 dbar range (Figure 6.1.8). The cruise-to-cruise changes between February and July

1989 in the upper pycnocline illustrate that variability in density is not always well resolved by our quasi-monthly sampling.

Figures 6.1.9-12 show the contoured time-series record for salinity in the upper 1000 dbar for all HOT cruises through 2000. The plots show both the CTD and bottle results plotted against pressure and potential density. Most of the differences between the contoured sections of bottle salinity and CTD salinity are due to the coarse distribution of bottle data in the vertical as compared to the CTD observations. Some of the bottles in Figure 6.1.12 are plotted at density values lower than the indicated sea surface density. This is due to surface density changing from cast to cast within each cruise, and even between the downcast and the upcast during a single cast.

Surface salinity is variable from cruise-to-cruise, with no obvious seasonal cycle and some substantial interannual variability. Relatively low surface salinities occurred during 1989, the early part of 1995, and during 1996. A relative increase in surface salinity that started in the late months of 1997 has continued throughout 1998, 1999 and 2000, intensifying in the first half of 1999 and during the major part of 2000. This increase is also present in deeper layers reaching 200 dbar (Fig 6.1.9).

The salinity maximum is generally found between 50 and 150 dbar, and within the range 24-25 σ_θ. A salinity maximum region extends to the sea surface in the later part of 1990, 1993 and during 1998, 1999 and 2000, as indicated by the 35.2 contour reaching the surface. The maximum shows salinities lower than normal in early 1995 and 1996, and throughout these two years the values are below 35.2. During 1997 the salinities decrease even further, with values below 35.1, to recover rapidly after February 1998 to values prior to 1995. The increase continues throughout 2000 reaching record values of up to 35.45 in the first half of 1999.

The maximum value of salinity in the salinity maximum region is subject to short-term variations of about 0.1, which is probably due to the proximity of Station ALOHA to the region where this water is formed at the sea surface (Tsuchiya, 1968). The variability of this feature is itself variable. Throughout 1989 there were extreme variations of a couple of months duration with 0.2 amplitude. The variability was much smaller and slower thereafter, except for a few months of rapid variation in earlier 1992.

The salinity minimum is found between 400 and 600 dbar (26.35-26.85 σ_θ). There is no obvious seasonal variation in this feature, but there are distinct periods of higher than normal minimum salinity in early 1989, in the fall of 1990, in early 1992 and in the summer of 1996. These variations are related to the episodic appearance at Station ALOHA of energetic fine structure and submesoscale water mass anomalies (Lukas and Chiswell, 1991; Kennan and Lukas, 1995).

Figures 6.1.13 and 6.1.14 show contoured time-series data for oxygen in the upper 1000 dbar at Station ALOHA. The oxygen data show a strong oxycline between 400 and 625 dbar (26.25-27.0 σ_θ), and an oxygen minimum centered near 800 dbar (27.2 σ_θ). Recurrent drops in the oxygen concentration can be seen throughout the time-series between 25 and 26.25 σ_θ. This features are accompanied by a decrease in salinity and an increase in the nutrient concentration (see discussion below).

The oxygen minimum exhibits some interannual variability, with values less than 30 μmol kg^{-1} appearing frequently during the time-series. This variability can be seen in a plot of the mean oxygen in the intermediate waters spanning the oxygen minimum (27-27.8 σ_θ, Figure 6.1.23). Superimposed to this variability is a general trend towards lower oxygen values from 1989 throughout 1998, which started increasing in 1999.

The surface layer shows a seasonality in oxygen concentrations, with highest values in the winter. This pattern corresponds roughly to the minimum in surface layer temperature (Figure 6.1.7).

Figures 6.1.15-22 show [nitrate + nitrite], SRP, and silica at Station ALOHA plotted against both pressure and potential density. The nitricline is located between about 200 and 600 dbar (25.75-27 σ_θ; Figs. 6.1.15-16). Most of the variations seen in these data are associated with vertical displacements of the density structure, and when [nitrate + nitrite] is plotted versus potential density, most of the contours are level. Recurrent events with increasing [nitrate + nitrite] can be seen throughout the series between 25-26.25 σ_θ (Figure 6.1.16). These events are accompanied by a decrease in the oxygen concentration mentioned above (Figure 6.1.14). The most obvious events occurred in March-April 1990, January 1992, May 1992, February-March 1995, early 1996, mid- to late 1997, and July-September 1999. These events can likely be attributed to mesoscale features such as eddies. It is possible for eddies to transport water with different biogeochemical characteristics from distant sources into the region of Station ALOHA (Lukas and Santiago-Mandujano, 2001). The SRP variability is similar to the [nitrate + nitrite] in the upper water column (Figure 6.1.19-20).

During 1996, the intermediate waters between 27.0-27.8 σ_θ recovered from anomalously low [nitrate + nitrite] which was observed during 1995 (Figure 6.1.17). This anomaly is apparent in a time series of mean [nitrate + nitrite] between 27.0-27.8 σ_θ (Figure 6.1.23). A decrease in [nitrate + nitrite] began in late 1994, with a comparable increase from mid-1995 through early 1996. The maximum decrease appears to be about 1 μmol kg^{-1} below 27.5 σ_θ where nitrate concentrations are about 40 μmol kg^{-1}. This decrease appears to be real as it does have coherence over time. A precision estimate of 0.3% has been made for [nitrate + nitrite] measurements involving the high concentration samples associated with intermediate water (Dore et al., 1995). This translates to a precision of roughly 0.12 μmol kg^{-1} for samples with a concentration of 40 μmol kg^{-1}. Hence, the 1 μmol kg^{-1} decrease seen during 1995 is well within the precision level for the concentrations observed. However, the amount of the decrease could be approaching the accuracy limits of [nitrate + nitrite] measurements. This low [nitrate + nitrite] episode is accompanied by an increase in oxygen concentration (Figure 6.1.23).

Intermediate water SRP (between 27.0-27.8 σ_θ) reached lowest values in early 1997, after a decreasing trend established in early 1994 (Figure 6.1.18). A time series of mean SRP in this layer shows this trend clearly (Figure 6.1.23). Decreases in phosphate in the deeper waters could persist for long periods of time as the oceanic ecosystem associated with Station ALOHA has been hypothesized to be phosphorous limited in recent years (Karl et al., 1999). Oxygen concentrations between 27.0-27.8 σ_θ vary during the decrease of phosphate from early 1994 through 1997 (Figure 6.1.23) without any apparent correlation.

4.2 Thermosalinograph data

Thermosalinograph measurements of near-surface temperature (NST) and near-surface salinity (NSS), as well as navigation for the 2000 HOT and mooring cruises are presented in Figures 6.2.1a to l. Thermosalinograph data recorded while on station can be compromised by ship effects such as temperature changes in the water due to the ship's hull and engine temperatures. Salinity can also be influenced by the ship when on station as the ship provides a potential source of contamination and disturbs the water being sampled.

In general, cooler near-surface temperatures, and in most cases saltier near-surface salinities were observed at Station ALOHA compared to the data recorded near Oahu. Salinities at station ALOHA started above 35.2 for year 2000 but dropped to below 35.0 by the spring. The surface salinity then rose to above 35.4 by August and then dropped again to below 35.0 by the end of the year. These fluctuations are consistent with the salinity increases and decreases seen in the CTD data in the upper 200 dbar of the water column (see Section 4.1).

Cruise HOT-120 (November-December) was conducted under very light wind conditions, and shows large variability in temperature and salinity mainly during mid-day hours. This variability was apparently caused by water patches heated by solar radiation that were sampled by the thermosalinograph.

4.3 Meteorology

The meteorological data collected at 4-hour intervals by HOT program scientists include atmospheric pressure, sea-surface temperature and wet and dry bulb air temperature. These data are presented in Figures 6.3.1 to 6.3.3. As described by Winn et al. (1991), parameters show evidence of annual cycles, although the daily and weekly ranges are nearly as high as the annual range for some variables. Wind speed and direction are also collected on HOT cruises. These data are presented in Figures 6.3.4a to k.

One National Data Buoy Center (NDBC) meteorological buoy (#51001) is located 400 km west of ALOHA at 23.4°N, 162.3°W (Figure 1.1). This buoy collects hourly observations of air temperature, sea surface temperature, atmospheric pressure, wind speed and direction and significant wave height. The coherence of the data from Buoy #51001 with the data collected on HOT cruises was examined and reported in Tupas et al. (1993). We concluded from these analyses, that the data from this buoy can be used to get useful estimates of air temperature, sea-surface temperature and atmospheric pressure at Station ALOHA when the station is not occupied. These data are also plotted in Figures 6.3.1 through 6.3.3. Because of the geographic separation between the buoy and station ALOHA, the buoy sea-surface temperatures are higher than at ALOHA by up to 1 °C, particularly during the summer and fall (Figure 6.3.1, lower panel). The buoy had problems during January, November and part of December, and recorded data at 3-hour intervals.

The thermosalinograph temperatures obtained at Station ALOHA during cruises are also plotted together with the sea-surface meteorological observations in Figure 6.3.1 (lower panel) and show good agreement with these measurements. Cruise HOT-120 was conducted under very light wind conditions and showed large variability in the thermosalinograph temperatures (see Section 4.2)

The wind vectors from buoy #51001 are plotted together with the ship wind observations in Figures 6.3.4a to k. Problems with the buoy in November yielded gaps in the data file (Figure 6.3.4j).

4.4 Biogeochemistry

4.4.1 Dissolved oxygen

A contour plot of dissolved oxygen in the upper 200 dbar of the water column from 1988-2000 analyses of water samples collected at discrete depths is shown in Figure 6.4.1. Dissolved oxygen shows a seasonal maximum between 60 and 100 m depth that develops during the summer-fall. This maximum, presumably of biological origin, is typically eroded during the winter.

4.4.2 Inorganic carbon

Time-series of mixed-layer titration alkalinity and DIC from 1988-2000 are presented in Figure 6.4.2. Titration alkalinity normalized to 35 ppt salinity averages approximately 2303 µeq kg^{-1} and, within the precision of the analysis, appears to remain relatively constant at Station ALOHA. This observation is consistent with the results of Weiss et al. (1982) who concluded that titration alkalinity normalized to salinity remains constant in both the North and South Pacific subtropical gyres. In contrast to titration alkalinity, the concentration of DIC varies seasonally and interannually. DIC in the mixed layer is highest in March and April and lowest in September and October. This oscillation is consistent with an exchange of carbon dioxide across the air-sea interface driven by temperature dependent changes in mixed layer pCO_2. Superimposed on the seasonal signal is a long-term increasing trend, consistent with rising atmospheric CO_2.

4.4.3 Inorganic nutrients

Mixed layer nutrient concentrations at Station ALOHA are at or well below the detection limits of the autoanalyzer methods. Alternative high-sensitivity analytical techniques were used to measure the nanomolar levels of [nitrate + nitrite] and SRP in the upper water column. Figure 6.4.3 shows the profiles obtained from our low level [nitrate + nitrite] analyses at Station ALOHA during 2000. The upper 100 m is generally depleted in [nitrate + nitrite] with only an occasional value exceeding 5 nmol kg^{-1}. Figure 6.4.4 presents the low-level SRP data from 2000. At depths shallower than 100 m, SRP is typically less than 100 nmol kg^{-1}. The depths of the nitracline and phosphacline can be seen to vary substantially between cruises.

4.4.4 Organic nutrients

Contour plots (0-1000 dbar) of dissolved organic carbon (DOC), nitrogen (DON) and phosphorus (DOP) over the 1988-2000 time period are presented in Figures 6.4.5-6.4.7. DOC concentrations are typically about 80-110 µmol kg^{-1} at the surface and decrease to about 40-50 µmol kg^{-1} at 800 m. DON is typically 5-6 µmol kg^{-1} at the surface, decreasing to about 2 µmol kg^{-1} at 800 m. DOP is about 0.2-0.3 µmol kg^{-1} at the surface and decreases to <0.05 µmol kg^{-1} at 800 m. All three organic nutrients exhibit substantial interannual variability.

4.4.5 Particulate matter

Particulate carbon (PC), nitrogen (PN) and phosphorus (PP) concentrations in the surface ocean over the 12 years of the program are shown in Figures 6.4.8. PC ranges from about 1-3 µmol kg^{-1}, PN from 0.1-0.6 µmol kg^{-1} and PP from 10-25 nmol kg^{-1} in the upper 100 m of the water column. An annual cycle is suggested with the greatest particulate bioelement concentrations in summer/fall and the lowest in winter. Substantial interannual variability is also noted, especially for PP.

4.4.6 Chlorophyll *a*

A contour plot of chlorophyll *a* concentrations measured using standard fluorometric techniques from 0 to 200 dbar during 1988-2000 is shown in Figure 6.4.9. A chlorophyll maximum with concentrations up to about 0.3 mg m^{-3} is observed at approximately 100 m depth. The magnitude of this feature exhibits significant interannual variability, with a pronounced period of low chlorophyll concentration lasting from 1992-1998. Chlorophyll *a* concentrations at depths shallower than 50 m display an annual cycle with winter maxima and summer minima.

4.4.7 Adenosine 5'-triphosphate

The concentration of particulate ATP resembles those of the particulate bioelements, showing maximum concentration near the surface and a decreasing profile with depth (Figure 6.4.10). Surface ocean ATP varies between years more than three-fold, with conspicuously high levels noted in 1994-1995.

4.5 Biogeochemical Rate Measurements

4.5.1 Primary Productivity

The depth-integrated (0-200 m) results of the ^{14}C incubations and pigment determinations for samples collected from Go-Flo casts in 2000 are presented in Table 4.1. Also included for each cruise is the incubation duration and the total incident irradiance (400-700 nm) measured on

the deck of the ship during the incubation period. Integrated primary production rates measured over all 12 years of the program are shown in Figure 6.4.11 in order to place the 2000 results within the context of the time-series data set. Depth-integrated rates of primary production vary seasonally, with summer maxima and winter minima. Overall, primary production varies by a factor of five, from about 200-1000 mg C m^{-2} d^{-1}. However, a large majority of the primary production estimates are between 300 and 600 mg C m^{-2} d^{-1}, and the overall mean value (± sd) is 491 ± 147 mg C m^{-2} d^{-1}. Although this value is higher than historical measurements for the oceanic central gyres (Ryther 1969), it is consistent with more recent measurements using modern methodology (Martin et al., 1987; Laws et al., 1989; Knauer et al., 1990).

Table 4.1: Primary production and pigment summary integrated values (0-200 m)

HOT	Incident Irradiance (E m^{-2} d^{-1})	Pigments (mg m^{-2})		Incubation Duration (hrs)	Assimilation Rates (mg C m^{-2} d^{-1})	
		Chl a	Pheo		Light	Dark
111	26.7	18.0	28.7	12.0	353	24
112	39.6	19.6	35.3	12.0	607	17
113	43.8	19.2	28.2	11.8	470	22
114	50.1	20.5	39.4	13.8	710	20
115	46.3	21.7	36.7	14.0	477	23
116	58.7	30.8	41.7	14.0	1077	22
117	54.6	26.9	41.0	13.5	895	25
118	49.4	20.0	42.2	12.8	664	27
119	30.6	19.2	36.4	12.0	370	NA
120	35.9	26.3	45.1	12.0	525	NA
121	25.6	26.0	45.0	25.0	265	NA

4.5.2 Particle Flux

Particulate carbon (PC), nitrogen (PN) and phosphorus (PP) fluxes at 150 m are presented in Table 4.2 and Figure 6.4.12 for the 1988-2000 time period. All three fluxes show large month-to-month and interannual variations. The magnitudes of PC and PN fluxes vary by about a factor of five, while PP flux varies by about a factor of 20. These particle flux measurements are consistent in magnitude with those measured in the central North Pacific Ocean during the VERTEX program (Martin et al., 1987; Knauer et al., 1990). However, the HOT data set reveals interannual changes not documented by earlier studies. Of particular note is the change from a high-flux high-variability regime (1988-1991) to a low-flux low-variability regime (1992-1996). There is a suggestion in the 1997-2000 data that the high flux and variability may be returning.

Table 4.2: Station ALOHA sediment trap flux data

	PC Flux (mg m^{-2} d^{-1})		PN Flux (mg m^{-2} d^{-1})		PP Flux (mg m^{-2} d^{-1})	
HOT	Mean	SD	Mean	SD	Mean	SD
111	19.0	3.8	3.30	0.65	0.187	0.014
112	28.4	3.3	4.40	0.28	0.456	0.139
113	36.0	1.4	5.12	0.74	0.316	0.046
114	42.9	4.2	5.25	0.47	0.529	0.244
115	21.4	2.3	3.44	0.62	0.277	0.072
116	29.7	5.4	4.50	0.77	0.364	0.066
117	39.8	2.2	5.63	0.26	0.451	0.063
118	19.0	1.9	4.02	0.27	0.538	0.226
119	35.4	2.9	5.94	0.63	0.432	0.084
120	16.8	2.1	3.15	0.29	0.319	0.021
121	16.1	5.4	2.00	0.59	0.216	0.024

4.6 Microbial Community Structure

Depth profiles of counts of heterotrophic bacteria (actually non-pigmented bacteria and archaea) and photosynthetic (pigmented) bacteria for each cruise are presented in Figure 6.4.13. At the surface, heterotrophic bacterial numbers range from 3 to 6 x 10^5 cells ml^{-1}. In some cases bacterial numbers decrease with depth although there are some profiles where the numbers remain fairly constant with depth throughout the euphotic zone. *Prochlorococcus* cells are found at concentrations of about 2 x 10^5 ml^{-1} at the surface and usually decrease with depth but with a subsurface maximum between 50 and 100 m.

4.7 Zooplankton Community Structure

Temporal variation in mesozooplankton biomass during 2000 are presented in Figure 6.4.14. The biomass of mesozooplankton collected during night (mean = 0.719 g DW m^{-2} (standard deviation, s = 0.313 g DW m^{-2})) is generally greater than the biomass of mesozooplankton collected during day (mean = 1.148 g DW m^{-2} (s = 0.253 g DW m^{-2})), due to the upward migration of deep-living zooplankton and micronekton after sunset. Although the percent contribution of 0.2 – 5 mm size classes to total biomass is remarkably similar at Station ALOHA (Table 4.3, Landry, 2001), the inclusion of diel vertical migrators does increase the contribution of > 5 mm mesozooplankton to total biomass at night (Table 4.3).

Mesozooplankton biomass averages during 2000 are slighty higher than averages for all seven years of the zooplankton program (1994 – 2000; night mean = 0.987 g DW m^{-2} (s = 0.322 g DW m^{-2}); day mean = 0.987 g DW m^{-2} (s = 0.322 g DW m^{-2})).

Table 4.3: Percent contribution of different size classes to total biomass of mesozooplankton collected at Station ALOHA

Size Fraction	Contribution to Total Biomass	
	Day (%)	Night (g DW m^{-2})
> 5 mm	3	10
2 - 5 mm	19	24
1 - 2 mm	29	26
0.5 - 1 mm	26	22
0.2 - 0.5 mm	23	19

5.0 REFERENCES

Brewer, P.G., K.W. Bruland, R.W. Eppley and J.J. McCarthy. 1986. The Global Ocean Flux Study (GOFS): Status of the US-GOFS program. *EOS, Transactions of the American Geophysical Union*, 67, 827-832.

Campbell, L., H. Nolla and D. Vaulot. 1994. The importance of *Prochlorococcus* to community structure in the central North Pacific Ocean. *Limnology and Oceanography*, 39, 954-961.

Chiswell, S.M. 1996. Intra-annual oscillations at Station ALOHA, north of Oahu, Hawaii. *Deep-Sea Research II*, 43, 305-319.

Chiswell, S.M., E. Firing, D. Karl, R. Lukas, C. Winn. 1990. *Hawaii Ocean Time-series Program Data Report 1, 1988-1989*. School of Ocean and Earth Science and Technology, University of Hawaii, SOEST 90-1, 269 pp.

Cox, R.D. 1980. Determination of nitrate at the parts per billion level by chemiluminescence. *Analytical Chemistry*, 52, 332-335.

Dore, J.E., T. Houlihan, D.V. Hebel, G. Tien, L.M. Tupas and D.M. Karl. 1996. Freezing as a method of sample preservation for the analysis of dissolved inorganic nutrients in seawater. *Marine Chemistry,* 53, 173-185.

Firing, E. 1996. Currents observed north of Oahu during the first 5 years of HOT. *Deep-Sea Research*, 43, 281-303.

Garside, C. 1982. A chemiluminescent technique for the determination of nanomolar concentrations of nitrate and nitrite in seawater. *Marine Chemistry*, 11, 159-167.

Johnson, D.L. 1971. Simultaneous determination of arsenate and phosphate in natural waters. *Environmental Science and Technology*, 5, 411-414.

Karl, D.M., J.R. Christian, J.E. Dore, D.V. Hebel, R.M Letelier, L.M. Tupas and C.D. Winn. 1996a. Seasonal and interannual variability in primary production and particle flux at Station ALOHA. *Deep-Sea Research,* 43, 539-568.

Karl, D. M., J. E. Dore, D. V. Hebel, and C. Winn. 1991. Procedures for particulate carbon, nitrogen, phosphorus and total mass analyses used in the US-JGOFS Hawaii Ocean Time-series program, p. 71-77. In D. Spencer and D. Hurd [eds.], Marine Particles: Analysis and Characterization. Geophysical Monograph 63, American Geophysical Union.

Karl, D.M. and O. Holm-Hansen. 1978. Methodology and measurement of adenylate energy charge ratios in environmental samples. *Marine Biology*, 48, 185-197.

Karl, D.M., R. Letelier, D. Hebel, L. Tupas, J. Dore, J. Christian and C. Winn. 1995 Ecosystem changes in the North Pacific subtropical gyre attributed to the 1991-92 El Niño. *Nature,* 373, 230-234.

Karl, D.M. and R. Lukas. 1996. The Hawaii Ocean Time-series (HOT) program: Background, rationale and field implementation. *Deep-Sea Research*, 43, 129-156.

Karl, D.M. and G. Tien. 1992. MAGIC: A sensitive and precise method for measuring dissolved phosphorus in aquatic environments. *Limnology and Oceanography*, 37, 105-116.

Karl, D., L. Tupas, F. Santiago-Mandujano, C. Nosse, D. Hebel, E. Firing and R. Lukas, 1996b. *Hawaii Ocean Time-series Program Data Report 7, 1995.* School of Ocean and Earth Science and Technology, University of Hawaii, SOEST 96-09, 228 pp.

Karl, D.M. and C.D. Winn, 1991. A sea of change: Monitoring the oceans carbon cycle. *Environmental Science and Technology*, 25, 1967-1981.

Kennan, S.C. and R. Lukas. 1995. Saline intrusions in the intermediate waters north of Oahu, Hawaii. *Deep-Sea Research*, 43, 215-241.

Knauer, G.A., J.H. Martin and K.W. Bruland. 1979. Fluxes of particulate carbon, nitrogen and phosphorus in the upper water column of the northeast Pacific. *Deep-Sea Research*, 26, 97-108.

Knauer, G.A., D.G. Redalje, W.G. Harrison and D.M. Karl. 1990. New production at the VERTEX time-series site. *Deep-Sea Research*, 37, 1121-1134.

Landry, M.R., H. Al-Mutairi, K.E. Selph, S. Christensen and S, Nunnery. 2001. Seasonal patterns of mesozooplankton abundance and biomass at Station ALOHA. *Deep-Sea Research II,* 48, 2037-2062.

Laws, E.A., G.R. DiTullio, P.R. Betzer, D.M. Karl and K.L. Carder. 1989. Autotrophic production and elemental fluxes at 26° N, 155° W in the North Pacific subtropical gyre. *Deep-Sea Research*, 36, 103-120.

Lukas, R. and S. Chiswell. 1991. Submesoscale water mass variations in the salinity minimum of the north Pacific near Hawaii. *WOCE Notes*, 3(1), 6-8.

Lukas, R., F. Santiago-Mandujano, F. Bingham and A. Mantyla. 2001. Cold bottom water events observed in the Hawaii Ocean Time-series: implications for vertical mixing. *Deep-Sea Research I*, 48: 995-1021.

Lukas R. and F. Santiago-Mandujano. Eddy Transport of Anomalous Waters in the Hawaii Ocean Time-series. *Geophys. Res. Lett.*, 28, 2931-2934.

Martin, J.H., G.A. Knauer, D.M. Karl and W.W. Broenkow. 1987. VERTEX: Carbon cycling in the northeast Pacific. *Deep-Sea Research*, 34, 267-285.

Michaels, A. and A. Knap. 1996. Overview of the U.S.-JGOFS Bermuda Atlantic Time-series Study and Hydrostation S program. *Deep-Sea Research*, 43, 157-198.

Monger, B,C, and M.R. Landry. 1993. Flow cytometry analysis of marine bacteria with Hoechst 3342. *Applied and Environmental Microbiology*, 59, 905-911.

National Research Council. 1984a. *Global Observations and Understanding of the General Circulation of the Oceans: Proceedings of a Workshop*, National Academy Press, Washington, DC, 418 pp.

National Research Council. 1984b. *Global Ocean Flux Study: Proceedings of a Workshop*, National Academy Press, Washington, DC, 360 pp.

Ortner, P.B. E.M. Hulbert and P.H. Wiebe. 1979. Gulf Stream rings, phytohydrography and herbivore habitat contrasts. *Journal of Experimental Marine Biology and Ecology*, 39, 101-124.

Owens, W.B. and R.C. Millard. 1985. A new algorithm for CTD oxygen calibration. *Journal of Physical Oceanography*, 15, 621-631.

Qian, J. and K. Mopper. 1996. Automated high-performance, high-temperature combustion total organic carbon analyzer. *Analytical Chemistry*, 68, 3090-3097.

Ryther, J.H. 1969. Photosynthesis and fish production in the sea. The production of organic matter and its conversion to higher forms of life vary throughout the world ocean. *Science,* 166, 72-76.

Santiago-Mandujano, F., L. Tupas, C. Nosse, D. Hebel, L. Fujieki, R. Lukas, D. Karl, 1999. Hawaii Ocean Time-series Data Report 10, 1998, School of Ocean and Earth Science and Technology, University of Hawaii, 246 pp. *In*: R. Lukas and D. Karl, 1999. Hawaii Ocean Time-series. A Decade of Interdisciplinary Oceanography. SOEST 99-5. University of Hawaii CD-ROM.

Santiago-Mandujano, F., J. Dore, L. Tupas, D. Hebel, L. Fujieki, R. Lukas, D. Karl, 2001. Hawaii Ocean Time-series Data Report 11, 1999, School of Ocean and Earth Science and Technology, University of Hawaii, 191 pp..

Scientific Committee on Oceanic Research. 1990. *The Joint Global Ocean Flux Study (JGOFS) Science Plan.* JGOFS Report No. 5. International Council of Scientific Unions, 61 pp.

Strickland, J.D.H. and T.R. Parsons. 1972. *A Practical Handbook of Seawater Analysis*. Fisheries Research Board of Canada, 167 pp.

Tsuchiya, M. 1968. *Upper Waters of the Intertropical Pacific Ocean*. Johns Hopkins Oceanographic Studies, 4, 49 pp.

Tupas, L., F. Santiago-Mandujano, D. Hebel, E. Firing, F. Bingham, R. Lukas and D. Karl. 1994. *Hawaii Ocean Time-series Program Data Report 5, 1993.* School of Ocean and Earth Science and Technology, University of Hawaii, 156 pp.

Tupas, L., F. Santiago-Mandujano, D. Hebel, E. Firing, R. Lukas and D. Karl. 1995. *Hawaii Ocean Time-series Data Report 6: 1994*. School of Ocean and Earth Science and Technology, University of Hawaii, 199 pp.

Tupas, L., F. Santiago-Mandujano, D. Hebel, R. Lukas, D. Karl and E. Firing. 1993. *Hawaii Ocean Time-series Program Data Report 4, 1992*. School of Ocean and Earth Science and Technology, University of Hawaii, 248 pp.

Tupas, L., F. Santiago-Mandujano, D. Hebel, C. Nosse, L. Fujieki, E. Firing, R. Lukas and D. Karl. 1997. *Hawaii Ocean Time-series Program Data Report 8, 1996*. School of Ocean and Earth Science and Technology, University of Hawaii, SOEST 96-4, 296 pp.

UNESCO. 1981. *Tenth Report of the Joint Panel on Oceanographic Tables and Standards*. UNESCO Technical Papers in Marine Science, No. 36., UNESCO, Paris.

Weiss, R.F., R.A. Jahnke and C.D. Keeling. 1982. Seasonal effects of temperature and salinity on the partial pressure of CO_2 in seawater. *Nature*, 300, 511-513.

Winn, C., S.M. Chiswell, E. Firing, D. Karl, R. Lukas. 1991. *Hawaii Ocean Time-series Program Data Report 2, 1990*. School of Ocean and Earth Science and Technology, University of Hawaii, SOEST 92-01, 175 pp.

Winn, C., R. Lukas, D. Karl, E. Firing. 1993. *Hawaii Ocean Time-series Program Data Report 3, 1991*. School of Ocean and Earth Science and Technology, University of Hawaii, SOEST 93-3, 228 pp.

Wright, S.W., S.W. Jeffrey, R.F.C. Mantoura, C.A. Llewellyn, T. Bjornland, D. Repeta and N. Welschmeyer. 1991. Improved HPLC method for the analysis of chlorophylls and carotenoids from marine phytoplankton. *Marine Ecology Progress Series*, 77, 183-196.

6.0 FIGURES

6.1 Hydrography

Figure 6.1.1a-k: [Upper left panel] Temperature, salinity, oxygen and potential density (σ_θ) as a function of pressure for the WOCE deep cast at Station ALOHA for each HOT cruise. [Upper right panel] Plot of [nitrate + nitrite], soluble reactive phosphorus, silicate, and bottle dissolved oxygen as a function of potential temperature for all water samples. [Lower left panel] CTD temperature and salinity plotted as a function of pressure to 1000 dbar. [Lower right panel] Salinity and oxygen from CTD and water samples plotted as a function of potential temperature. Only the CTD oxygen traces in which bottle oxygen samples were obtained are included.

Figure 6.1.2a-k: [1st panel] Stack plots of temperature versus pressure to 1000 dbar at Station ALOHA. Offset is 2 °C. [2nd panel] Stack plots of salinity versus pressure to 1000 dbar at Station ALOHA. Offset is 0.1.

Figure 6.1.3a-f: [Upper left panel] Temperature, salinity, oxygen and potential density (σ_θ) as a function of pressure for the cast at Station Kahe for each HOT cruise. [Upper right panel] Plot of [nitrate + nitrite], soluble reactive phosphorus, silicate, and bottle dissolved oxygen as a function of potential temperature. [Lower right panel] Plot of CTD and bottle salinity and oxygen as a function of potential temperature.

Figure 6.1.3g-k: [Upper left panel] Temperature, salinity, oxygen and potential density (σ_θ) as a function of pressure for the cast at Station Kahe for each HOT cruise. [Upper right panel] Plot of [nitrate + nitrite], soluble reactive phosphorus, silicate, and CTD and bottle dissolved oxygen and salinity as a function of potential temperature for water samples at Station Kahe. [Lower left panel] Plot of temperature, salinity, oxygen, and σ_θ as a function of pressure at Station HALE ALOHA. [Lower right panel] Plot of CTD and bottle salinity and oxygen as a function of potential temperature at Station HALE ALOHA.

Figure 6.1.4: [Upper panel] Potential temperature versus pressure for all deep casts in 2000. [Lower panel]: Potential temperature versus pressure deeper than 2500 dbar for all deep casts in 2000.

Figure 6.1.5: [Upper panel] Salinity versus potential temperature for all deep casts in 2000. [Lower panel]: Salinity versus potential temperature for all deep casts in 2000 in the 1-5 °C range.

Figure 6.1.6: [Upper panel] Oxygen concentrations from calibrated oxygen sensor data versus potential temperature for all deep casts in 2000. [Lower panel] Oxygen versus potential temperature for all deep casts in 2000 in the 1-5 °C range.

Figure 6.1.7: Contour plot of CTD potential temperature versus pressure for HOT cruises 1-121.

isopycnals for HOT cruises 1-121. The smooth line is the spline fit to the data. The asterisks indicate the annual mean.

6.2 Thermosalinograph

Figure 6.2.1a-k: Thermosalinograph data for each HOT cruise in 2000. Continuous near-surface temperature, salinity and sigma-theta (continuous lines), CTD data at 4 dbar (circles), and salinity bottle data (crosses). Station ALOHA was occupied during the time period bound by the vertical dashed lines.

Figure 6.2.1l: Same as in Fig 6.2.1a-k, but for HALE-ALOHA-8A mooring cruise.

Figure 6.2.2a-k: Navigation data for each HOT cruise in 2000: latitude, longitude and ship speed. Station ALOHA was occupied during the time period bound by the vertical dashed lines.

Figure 6.2.2l: Same as in Fig 6.2.2a-k, but for HALE-ALOHA-8A mooring cruise.

6.3 Meteorology

Figure 6.3.1: [Upper panel] Atmospheric pressure while at Station ALOHA for 2000 HOT cruises (open circles), and NDBC buoy #51001 hourly measurements throughout the year (thin line). Buoy data were recorded every 3 hours during January, November and part of December (see text). [Lower panel] Sea surface temperature measured from a bucket sample while at Station ALOHA for 2000 HOT cruises (open circles), NDBC buoy #51001 hourly measurements throughout the year (thin line), and near-surface temperatures from the thermosalinograph while at Station ALOHA during HOT cruises (thick line).

Figure 6.3.2: [Upper panel] Dry bulb air temperature while at Station ALOHA for 2000 HOT cruises (open circles), and NDBC buoy #51001 hourly measurements throughout the year (thin line). [Lower panel] Wet bulb air temperature while at Station ALOHA for 2000 HOT cruises.

Figure 6.3.3: [Upper panel] Sea surface temperature minus dry air temperature while at Station ALOHA for 2000 HOT cruises (open circles), and NDBC buoy #51001 hourly measurements throughout the year (thin line). [Lower panel] Relative humidity while at Station ALOHA for 2000 HOT cruises.

Figures 6.3.4a to k: [Upper panel] True winds measured at Station ALOHA for 2000 HOT cruises. [Lower panel] True winds measured by NDBC buoy #51001. The orientation of the arrows indicate the wind direction; up is northward, right is eastward.

6.4 Biogeochemistry

Figure 6.4.1: Contour plot of bottle dissolved oxygen versus pressure for HOT cruises 1-121 from 0-200 dbar. Solid dots indicate water column sample locations.

Figure 6.4.2: [Upper panel] Time series of mean mixed layer titration alkalinity (normalized to 35 ppt salinity) for HOT cruises 1-121. [Lower panel] Mixed layer dissolved inorganic carbon (normalized to 35 ppt salinity) for HOT cruises 1-121. Error bars represent standard deviation of pooled samples collected between 0 and 50 dbar.

Figure 6.4.3: Depth profiles from 0-150 dbar of low-level [nitrate + nitrite] at Station ALOHA for 2000 HOT cruises by the high-sensitivity chemiluminescence method.

Figure 6.4.4: Depth profile from 0-250 dbar of low-level soluble reactive phosphorus at Station ALOHA for 2000 HOT cruises by the high-sensitivity magnesium induced coprecipitation (MAGIC) method.

Figure 6.4.5: Contour plot from 0-1000 dbar of dissolved organic carbon at Station ALOHA for HOT cruises 1-121.

Figure 6.4.6: Contour plot from 0-1000 dbar of dissolved organic nitrogen at Station ALOHA for HOT cruises 1-121.

Figure 6.4.7: Contour plot from 0-1000 dbar of dissolved organic phosphorus at Station ALOHA for HOT cruises 1-121.

Figure 6.4.8a: [Upper panel] Mean concentrations of particulate carbon at Station ALOHA for HOT cruises 1-121 from 0-50 dbar. [Lower panel] Mean concentrations of particulate carbon at Station ALOHA for HOT cruises 1-121 from 50-100 dbar. Error bars represent standard deviation of pooled samples within specified depth ranges.

Figure 6.4.8b: Same as Figure 6.4.8a except for particulate nitrogen.

Figure 6.4.8c: Same as Figure 6.4.8a except for particulate phosphorus.

Figure 6.4.9: Contour plot from 0-200 dbar of fluorometric chlorophyll a concentrations at Station ALOHA for HOT cruises 1-121.

Figure 6.4.10: Contour plot from 0-500 dbar of particulate adenosine 5'-triphosphate concentrations at Station ALOHA for HOT cruises 1-121.

Figure 6.4.11: [Upper panel] Integrated (0-200 m) primary production rates from 1988-2000. Filled circles and crosses indicate *in situ* and on deck incubations, respectively. Solid line represents the average production (491 mg C m^{-2} d^{-1}), dashed lines are ± one standard deviation (147 mg C m^{-2} d^{-1}). [Lower panel] 3-point running mean of integrated primary production rates. Symbols as in upper panel.

Figure 6.4.12: [Upper panel] Particulate carbon flux at 150 m measured on all HOT cruises from 1988-2000. [Center panel] Particulate nitrogen flux at 150 m measured on all HOT cruises from 1988-2000. [Lower panel] Particulate phosphorus flux at 150 m measured on all HOT cruises from 1988-2000. Error bars represent the standard deviation of determinations from triplicate traps.

Figure 6.4.13: Depth profiles (0-200 m) of heterotrophic bacteria (blue) and *Prochlorococcus* numbers (red) measured by flow cytometry at Station ALOHA for 2000.

Figure 6.4.14: Total mesozooplankton biomass (dry weight, DW) at Station ALOHA during 2000. Data presented are the means of triplicate day or night tows, and error bars represent the standard errors of the means.

7.0 HOT PROGRAM PRESENTATIONS AND PUBLICATIONS

The following is a listing of Presentations & Publications as of August 2002, for an up-to-date listing please refer to our Web site (hahana.soest.hawaii.edu/hot/hotpub.html).

7.1 Invited Presentations and Published Abstracts

1. 1988 Karl, D. NSF-sponsored symposium on Dissertations in Chemical Oceanography, "Research opportunities in Hawaiian waters", Honolulu, Hawaii, November 1988.
2. 1988 Karl, D. NSF/GOFS-sponsored workshop on sediment traps, "Determination of total C, N, P flux" and "Screens: A potential solution to the problem of swimmers", Gulf Coast Research Laboratory, Mississippi, November 1988.
3. 1989 Winn, C. D., S. Chiswell, D. M. Karl and R. Lukas. Long time-series research in the Central Pacific Ocean. The Oceanography Society 1st Annual Meeting, Monterey, California.
4. 1990 Karl, D., R. Letelier, D. Bird, D. Hebel, C. Sabine and C. Winn. An Oscillatoria bloom in the oligotrophic North Pacific Ocean near the GOFS station ALOHA. EOS, Transactions of the American Geophysical Union 71, 177-178.
5. 1990 Winn, C. D., D. Hebel, R. Letelier, D. Bird and D. Karl. Variability in biogeochemical fluxes in the oligotrophic central Pacific: Results of the Hawaii Ocean Time- Series Program. EOS, Transactions of the American Geophysical Union 71, 190.
6. 1990 Chiswell, S. M. and R. Lukas. The Hawaii Ocean Time-series (HOT). EOS, Transactions of the American Geophysical Union 71, 1397.
7. 1990 Karl, D. "JGOFS time-series programs," San Francisco, California, December 1990.
8. 1991 Winn, C., C. Sabine, D. Hebel, F. Mackenzie and D. M. Karl. Inorganic carbon system dynamics in the central Pacific Ocean: Results of the Hawaii Ocean Time-series program. EOS, Transactions of the American Geophysical Union 72, 70.
9. 1991 Lukas, R. Water mass variability observed in the Hawaii Ocean Time Series. EOS, Transactions of the American Geophysical Union 72, 70.
10. 1991 Letelier, R., D. Karl, R. Bidigare, J. Christian, J. Dore, D. Hebel and C. Winn. Temporal variability of phytoplankton pigments at the U.S.-JGOFS station ALOHA (22 45'N, 158 W). EOS, Transactions of the American Geophysical Union 72, 74.
11. 1991 Karl, D. "The Hawaii Ocean Time-series program: Carbon production and particle flux", The Oceanography Society 2nd Annual Meeting, St. Petersburg, Florida, March 1991.
12. 1991 Karl, D. NATO symposium on Biology and Ecology of Diazotrophic Marine Organisms, "Trichodesmium blooms and new nitrogen in the North Pacific gyre", Bamberg, Germany, May 1991.
13. 1992 Anbar, A. D. Rhenium in seawater: Confirmation of generally conservative behavior. EOS, Transactions of the American Geophysical Union 73, 278.

14. 1992 Schudlich, R. and S. R. Emerson. Modelling dissolved gases in the subtropical upper ocean: JGOFS/WOCE Hawaiian Ocean Time-series. EOS, Transactions of the American Geophysical Union 73, 287.

15. 1992 Tupas, L. M., B. N. Popp and D. M. Karl. Dissolved organic carbon in oligotrophic waters: experiments on sample preservation, storage and analysis. EOS, Transactions of the American Geophysical Union 73, 287.

16. 1992 Karl, D., C. Winn, D. Hebel, R. Letelier, J. Dore and J. Christian. The U.S.- JGOFS Hawaii Ocean Time-Series (HOT) program. American Society for Limnology and Oceanography Aquatic Sciences Meeting, Santa Fe, NM, February 1992.

17. 1992 Campbell, L., R. R. Bidigare, R. Letelier, M. Ondrusek, S. Hall, B. Tsai and C. Winn. Phytoplankton population structure at the Hawaii Ocean Time-series station. American Society for Limnology and Oceanography Aquatic Sciences Meeting, Santa Fe, NM, February 1992.

18. 1992 Karl, D. NSF-sponsored GLOBEC scientific steering committee meeting, "Hawaii Ocean Time-series (HOT) program: A GLOBEC 'Blue Water' initiative", Honolulu, Hawaii, March 1992.

19. 1992 Karl, D. IGBP International Symposium on Global Change, "Oceanic ecosystem variability: Initial results from the JGOFS Hawaii Ocean Time-series (HOT) experiment", Tokyo, Japan, March 1992.

20. 1992 Karl, D. Conoco HOT Topics Seminar Series, "The U.S.-JGOFS Hawaii Ocean Time- Series (HOT) Program: Biogeochemical Vignettes from the Oligotrophic North Pacific Ocean" and "Temporal Variability in Bioelement Flux at Station ALOHA (22 45'N, 158 W)", Woods Hole, Massachusetts, May 1992

21. 1992 Bidigare, R. R., L. Campbell, M. Ondrusek, R. Letelier and D. Vaulot. Characterization of picophytoplankton at Station ALOHA (22 45'N, 158 W) using HPLC, flow cytometry and immunofluorescence techniques. PACON 1992 Meeting, June 1992.

22. 1992 Winn, C. D., D. Hebel, R. Letelier, J. Christian, J. Dore, R. Lukas and D. M. Karl. Long time-series measurements in the central North Pacific: Results of the Hawaii Ocean Time-series program. PACON conference, Kona, Hawaii, June 1992.

23. 1993 Atkinson, M. J. A potentiometric solid state sensor for oceanic CTDs, Abstract of The Oceanography Society Annual Meeting, Seattle, Washington, April 1993.

24. 1993 Campbell, L., H. A. Nolla and D. Vaulot. Microbial biomass in the subtropical central North Pacific Ocean (Station ALOHA): The importance of Prochlorococcus, Abstract of The Oceanography Society Annual Meeting, Seattle, Washington, April 1993.

25. 1993 Emerson, S., P. Quay, C. Stump, D. Wilbur and R. Schudlich. Oxygen cycles and productivity in the oligotrophic subtropical Pacific Ocean. Abstract of of the Oceanography SocietyAnnual Meeting, Seattle, Washington, April 1993.

26. 1993 Sharp, J. H., R. Benner, L. Bennett, C. A. Carlson, S. E. Fitzwater, E. T. Peltzer, and L. Tupas. Dissolved organic carbon: Intercalibration of analyses with equatorial Pacific samples. Abstract of The Oceanography Society Annual Meeting, Seattle, Washington, April 1993.

27. 1993 Winn, C. D., C. J. Carrillo, F. T. Mackenzie and D. M. Karl. Variability in the inorganic carbon system parameters in the North Pacific subtropical gyre. Abstract of The Oceanography Society Annual Meeting, Seattle, Washington, April 1993.

28. 1993 Yanagi, K. and D. M. Karl. Note on the fractional determination of TDP in seawater by an UV-irradiation method combined with the MAGIC procedure. Abstract of the Oceanography Society of Japan annual meeting, Tokyo, Japan, April 1993.

29. 1993 Campbell, L., H. Liu, R. R. Bidigare and D. Vaulot. Immunochemical characterization of Prochlorococcus. Abstract of the American Society of Limnology and Oceanography 1993 Annual Meeting, Edmonton, Alberta, Canada, May 1993.

30. 1993 Christian, J. R. and D. M. Karl. Bacterial exoenzymes in marine waters: Implications for global biogeochemical cycles. Abstract of the American Society of Limnology and Oceanography 1993 Annual Meeting, Edmonton, Alberta, Canada, May 1993.

31. 1993 Moyer, C. L., L. Campbell, D. M. Karl and J. Wilcox. Restriction fragment length polymorphism (RFLP) and DNA sequence analysis of PCR-generated clones to assess diversity of picoeukaryotic algae in the subtropical central North Pacific Ocean (Station ALOHA). Abstract of the American Society of Limnology and Oceanography 1993 Annual Meeting, Edmonton, Alberta, Canada, May 1993.

32. 1993 Sharp, J. H., R. Benner, L. Bennett, C. A. Carlson, S. E. Fitzwater and L. Tupas. The equatorial Pacific intercalibration analyses of dissolved organic carbon in seawater. Abstract of the American Society of Limnology and Oceanography 1993 Annual Meeting, Edmonton, Alberta, Canada, May 1993.

33. 1994 Yuan, J., C. I. Measures and J. A. Resing. Rapid determination of iron in seawater: In-line preconcentration flow injection analysis with spectrophotometric detection. EOS, Transactions of the American Geophysical Union 75, 25.

34. 1994 Smith, C. R., S. Garner, D. Hoover and R. Pope. Macrobenthos, mechanisms of bioturbation and carbon flux proxies at the abyssal seafloor along the JGOFS Equatorial Pacific Transect. EOS, Transactions of the American Geophysical Union 75, 70.

35. 1994 Farrenkopf, A. M., G. W. Luther, III and C. H. Van Der Weijden. Vertical distribution of dissolved iodine species in the northwest Indian Ocean. EOS, Transactions of the American Geophysical Union 75, 78.

36. 1994 Campbell, L., C. D. Winn, R. Letelier, D. Hebel and D. M. Karl. Temporal variability in phytoplankton fluorescence at Station ALOHA. EOS, Transactions of the American Geophysical Union 75, 100.

37. 1994 Winn, C., F. T. Mackenzie, C. Carrillo, T. Westby and D. M. Karl. Air-sea carbon dioxide exchange at Station ALOHA. EOS, Transactions of the American Geophysical Union 75, 112.

38. 1994 Lukas, R., F. Bingham and A. Mantyla. An anomalous cold event in the bottom water observed north of Oahu. EOS, Transactions of the American Geophysical Union 75, 205.

39. 1994 Tupas, L. M., B. N. Popp and D. M. Karl. Dissolved organic carbon in oligotrophic waters; experiments on sample preservation, storage and analysis. EOS, Transactions of the American Geophysical Union 75, 287.

40. 1994 Bingham, F.M. Drifter observations of the North Hawaiian Ridge Current. EOS, Transactions of the American Geophysical Union 75, 307.

41. 1994 HOT Program P.I.s, staff and students. The Hawaii Ocean Time-series (HOT) program: The first five years, p. 59. Abstract of The Oceanography Society Pacific Basin Meeting, Honolulu, Hawaii, July 1994.

42. 1994 HOT Program P.I.s, staff and students. HOT: a time-series study of carbon cycling in the oligotrophic North Pacific, p. 24. Abstract of The Oceanography Society Pacific Basin Meeting, Honolulu, Hawaii, July 1994.

43. 1994 Bidigare, R. R., L. Campbell, M. E. Ondrusek, R. Letelier, D. Vaulot and D. M. Karl. Phytoplankton community structure at station ALOHA (22 45'N, 158 W) during fall 1991, p. 58. Abstract of The Oceanography Society Pacific Basin Meeting, Honolulu, Hawaii, July 1994.

44. 1994 Bingham, F. M. and B. Qiu. Interannual varibility of surface and mixed layer properties observed in the Hawaii Ocean Time-series, p. 89. Abstract of The Oceanography Society Pacific Basin Meeting, Honolulu, Hawaii, July 1994.

45. 1994 Bingham, F. M. and R. Lukas. Seasonal cycles of temperature, salinity and dissolved oxygen observed in the Hawaii Ocean Time-series, p. 90. Abstract of The Oceanography Society Pacific Basin Meeting, Honolulu, Hawaii, July 1994.

46. 1994 Christian, J. Vertical fluxes of carbon and nitrogen at Station ALOHA, p. 61. Abstract of The Oceanography Society Pacific Basin Meeting, Honolulu, Hawaii, July 1994.

47. 1994 Dore, J. E. and D. M. Karl. Nitrite distributions and dynamics at Station ALOHA, p. 60. Abstract of The Oceanography Society Pacific Basin Meeting, Honolulu, Hawaii, July 1994.

48. 1994 Firing, E. Currents observed north of Oahu during the first five years of HOT, p. 90. Abstract of The Oceanography Society Pacific Basin Meeting, Honolulu, Hawaii, July 1994.

49. 1994 Fujieki, L. A., D. V. Hebel, L. M. Tupas and D. M. Karl. Hawaii Ocean Time-series Data Organization and Graphical System (HOT-DOGS), p. 61. Abstract of The Oceanography Society Pacific Basin Meeting, Honolulu, Hawaii, July 1994.

50. 1994 Hebel, D. V., F. P. Chavez, K. R. Buck, R. R. Bidigare, D. M. Karl, M. Latasa, M. E. Ondrusek, L. Campbell and J. Newton. Do GF/F filters underestimate particulate chlorophyll a and primary production in the oligotrophic ocean?, p. 62. Abstract of The Oceanography Society Pacific Basin Meeting, Honolulu, Hawaii, July 1994.

51. 1994 Houlihan, T., J. E. Dore, L. Tupas, D. V. Hebel, G. Tien and D. M. Karl. Freezing as a method of preservation for seawater dissolved nutrient and organic carbon samples, p. 62. Abstract of The Oceanography Society Pacific Basin Meeting, Honolulu, Hawaii, July 1994.

52. 1994 Kennan, S. C. and R. Lukas. Saline intrusions in the intermediate waters north of Oahu, p. 91. Abstract of The Oceanography Society Pacific Basin Meeting, Honolulu, Hawaii, July 1994.

53. 1994 Letelier, R. M., J. Dore, C. D. Winn and D. M. Karl. Temporal variations in photosynthetic carbon assimilation efficiencies at Station ALOHA (22 45'N; 158 00'W), p. 60. Abstract of The Oceanography Society Pacific Basin Meeting, Honolulu, Hawaii, July 1994.

54. 1994 Liu, H. and L. Campbell. Growth and grazing rates of Prochlorococcus and Synechococcus at Station ALOHA measured by the selective inhibitor technique, p. 59. Abstract of The Oceanography Society Pacific Basin Meeting, Honolulu, Hawaii, July 1994.

55. 1994 Lukas, R. Interannual variability of Pacific deep and bottom waters observed in the Hawaii Ocean Time-series, p. 91. Abstract of The Oceanography Society Pacific Basin Meeting, Honolulu, Hawaii, July 1994.

56. 1994 Lukas, R., F. Bingham and E. Firing. Seasonal-to-interannual variability observed in the Hawaii Ocean Time-series, p. 28. Abstract of The Oceanography Society Pacific Basin Meeting, Honolulu, Hawaii, July 1994.

57. 1994 Tupas, L. M., B. N. Popp, D. V. Hebel, G. Tien and D. M. Karl. Dissolved organic carbon measurements at Station ALOHA measured by high temperature catalytic oxidation: Characteristics and variation in the water column, p. 63. Abstract of The Oceanography Society Pacific Basin Meeting, Honolulu, Hawaii, July 1994.

58. 1994 Winn, C. D., F. T. Mackenzie, C. Carrillo and D. M. Karl. Air-sea carbon dioxide exchange at Station ALOHA, p. 58. Abstract of The Oceanography Society Pacific Basin Meeting, Honolulu, Hawaii, July 1994.

59. 1994 Liu, H. and L. Campbell. Measurement of growth and mortality rate of Prochloroccus and Synechococcus at Station ALOHA using a new selective inhibitor technique. Fifth International Phycological Congress, Qingdao, China, July 1994.

60. 1994 Winn, C., F. T. Mackenzie, C. Carrillo, T. Westby and D. M. Karl. Air-sea carbon dioxide exchange at Station ALOHA, p. 112. Abstract of the American Society of Limnology and Oceanography 1994 Ocean Sciences Meeting, San Diego, California.

61. 1994 Measures, C. I., J. Yuan and J. A. Resing. The rapid determination of iron in seawater at sub-nanomolar concentrations using in-line preconcentration and spectrophotometric detection. Sixth Winter Conference on Flow Injection Analysis, San Diego, CA.

62. 1994 Measures, C.I., J. Yuan and J. A. Resing. Determination of iron in seawater using in-line preconcentration and spectrophotometric detection. Workshop on Iron Speciation and its Biological Activity, Bermuda Biological Station for Research, Bermuda.

63. 1995 Cortés, M. Y. and H. R. Thierstein. Coccolithophore dynamics during 1994 at the JGOFS time series Station ALOHA, Hawaii. 5th International Conference on Paleoceanography, Halifax, Canada, Abstract, p. 121.

64. 1995 Campos, M. L. A. M., T. D. Jickells, A. M. Farrenkopf and G. W. Luther, III. A comparison of dissolved iodine cycling at the Bermuda Atlantic Time Series station and Hawaii Ocean Time-series station. EOS, Transactions of the American Geophysical Union 76, S175.

65. 1995 Yuan, J. Collecting iron samples from well mounted on CTD rosette. EOS, Transactions of the American Geophysical Union 76, S175.

66. 1995 Michaels, A. F., D. Karl and A. H. Knap. Insights on ocean variability from the JGOFS time-series stations. Invited plenary lecture, The Oceanography Society Biennial Meeting, April 1995.

67. 1995 Emerson, S., P. Quay, L. Tupas and D. Karl. Chemical tracers of productivity and respiration in the upper ocean at U.S. JGOFS station ALOHA, 10th Anniversary JGOFS Science Conference, Villefranche, France, May 1995.

68. 1995 Michaels, A. F., D. Karl and A. H. Knap. Insights on ocean variability from the JGOFS time-series stations. Invited lecture, 10th Anniversary JGOFS Science Conference, Villefranche, France, May 1995.

69. 1995 Karl, D. M. Oceanic carbon cycle and global environmental change: A microbiological perspective. Invited plenary talk, 7th International Symposium on Microbial Ecology, Santos, Brazil, August 1995.

70. 1995 Winn, C., D. Sadler and D. M. Karl. Carbon dioxide dynamics at the Hawaii JGOFS/WOCE time-series station. International Association for the Physical Sciences of the Oceans, Honolulu, Hawaii, August 1995.

71. 1996 Campbell, L., H. Liu and H. A. Nolla. Picophytoplankton population dynamics at Station ALOHA, p. OS65. AGU-ASLO Ocean Sciences Meeting, San Diego, CA, February 1996.

72. 1996 Christian, J. R., J. E. Dore and D. M. Karl. Mixing and nutrient fluxes at the US-JGOFS Station ALOHA ((22 45'N, 158 00'W), p. OS65. AGU-ASLO Ocean Sciences Meeting, San Diego, CA, February 1996.

73. 1996 Dulaney, T. S. and L. R. Sautter. Sedimentation of planktonic foraminifera: Seasonal changes in shell flux north of Oahu, Hawaii, p. OS85. AGU-ASLO Ocean Sciences Meeting, San Diego, CA, February 1996.

74. 1996 Emerson, S. Chemical tracers of biological processes: O2, Ar and N2 mass balance in the subtropical Pacific at the HOT station, p. OS85. AGU-ASLO Ocean Sciences Meeting, San Diego, CA, February 1996.

75. 1996 Hebel, D. V., D. M. Karl, J. R. Christian, J. E. Dore, R. M. Letelier, L. M. Tupas and C. D. Winn. Seasonal and interannual variability in primary production and particle flux at Station ALOHA, p. OS85. AGU-ASLO Ocean Sciences Meeting, San Diego, CA, February 1996.

76. 1996 Karl, D. M.. Alternation of N and P control of new and export production in the North Pacific gyre: A hypothesis based on the HOT program data set, p. OS86. AGU- ASLO Ocean Sciences Meeting, San Diego, CA, February 1996.

77. 1996 Lawson, L. M., E. E. Hofmann and Y. H. Spitz. Time series sampling and data assimilation in a simple marine ecosystem model, p. OS86. AGU-ASLO Ocean Sciences Meeting, San Diego, CA, February 1996.

78. 1996 Lopez, M. D. G., Y. Zhu and M. E. Huntley. Space-time variability of zooplankton-sized particle concentrations at the Hawaii Ocean Time-series station (Station ALOHA), p. OS85. AGU-ASLO Ocean Sciences Meeting, San Diego, CA, February 1996.

79. 1996 Quay, P. D. and H. Anderson. Organic carbon export rates in the subtropical N. Pacific, p. OS85. AGU-ASLO Ocean Sciences Meeting, San Diego, CA, February 1996.

80. 1996 Richman, J. G., R. M. Letelier, M. R. Abbott and D. Pillsbury. Expandable optical mooring test at Station ALOHA (22 45'N; 158 00'W), p. OS64. AGU-ASLO Ocean Sciences Meeting, San Diego, CA, February 1996.

81. 1996 Scharek, R., M. Latasa, D. M. Karl and R. R. Bidigare Diatom abundance and vertical flux at the US-JGOFS/WOCE Station "ALOHA" in the oligotrophic North Pacific gyre, p. OS85. AGU-ASLO Ocean Sciences Meeting, San Diego, CA, February 1996.

82. 1996 Selph, K. E., M. R. Landry, R. J. Miller and H. A. Al-Mutairi. Temporal variability in the mesozooplankton community at ocean Station ALOHA, p. OS85. AGU-ASLO Ocean Sciences Meeting, San Diego, CA, February 1996.

83. 1996 Tersol, V., S. Vink, J. Yuan and C. I. Measures. Variations in iron, aluminium and berylium concentrations in surface waters at Station ALOHA, p. OS65. AGU-ASLO Ocean Sciences Meeting, San Diego, CA, February 1996.

84. 1996 Tupas, L. M., M P. Sampson and D. M. Karl. Stable nitrogen isotopic analysis of sinking particulate matter at the Hawaii Ocean Time-series site, p. OS86. AGU-ASLO Ocean Sciences Meeting, San Diego, CA, February 1996.

85. 1996 Venrick, E. L.. A comparison between the phytoplankton species from Station ALOHA and from the Climax region, p. OS65. AGU-ASLO Ocean Sciences Meeting, San Diego, CA, February 1996.

86. 1996 Winn, C. D. Carbon dioxide dynamics at the Hawaii JGOFS/WOCE time-series station: Annual and interannual variability, p. OS64. AGU-ASLO Ocean Sciences Meeting, San Diego, CA, February 1996.

87. 1996 Lukas, R. Low-frequency climate signals emerge in the Hawaii Ocean Time-series. WOCE Pacific Workshop. Hyatt Newporter, Newport Beach, CA, 19-23 August 1996.

88. 1996 Santiago-Mandujano, F. Cold bottom water events observed in the Hawaii Ocean Time-series. WOCE Pacific Workshop. Hyatt Newporter, Newport Beach, CA, 19-23 August 1996.

89. 1997 Lukas, R. Physical studies at the Hawaii Ocean Time-series (HOT) Station. Ocean Climate Time-Series Workshop. Johns Hopkins University, Baltimore, MD, 18-20 March 1997.

90. 1997 Bird, D.F., R. Maranger and D.M. Karl. The importance of bacterial consumption by algae to marine systems. ASLO-Aquatic Sciences Meeting, Santa Fe, NM, February 1997.

91. 1997 Karl, D.M., D.V. Hebel and L.M. Tupas. Biogeochemical studies at the Hawaii Ocean Time- series (HOT) station ALOHA. Joint GCOS GOOS WCRP Ocean Observations Panel for Climate (OOPC), GCOS Report No. 41.

92. 1998 Letelier, R.M., M.R. Abbott, M.H. Freilich, D.M. Karl, P.J. Flament and R. Lukas. Euphotic zone biogeochemical response to a wind-induced upwelling event in the North Pacific subtropical gyre. AGU-Ocean Sciences Meeting, San Diego, CA, February 1998.

93. 1998 Letelier, R.M. and D.M. Karl. The US-JGOFS Hawaii ocean Time-series (HOT) Program; What we have learned over the first decade. AGU-Ocean Sciences Meeting, San Diego, CA, February 1998.

94. 1998 Karl, D. The subtropical North Pacific: New views on an old ocean. Ocean Optics XIV Meeting, Kailua-Kona, HI, November 1998.

95. 1998 Ondrusek, M.E., R.R. Bidigare, D. M. Karl and K. Waters. Predictive models for estimating rates of primary production in the subtropical North Pacific Ocean. Ocean Optics XIV Meeting, Kailua-Kona, HI, November 1998.

96. 1999 Karl, D.M., K. Bjorkman, D. Hebel, T. Houlihan and L. Tupas. Seasonal and interannual variability in C-N-P stoichiometry of dissolved and particulate matter in the subtropical North Pacific Ocean. ASLO Aquatic Sciences meeting, Santa Fe, NM, February 1999.

97. 1999 Karner, M.B., L.T. Taylor, E.F. DeLong and D.M. Karl. Bacterial and archaeal distributions at the Hawaii Ocean Time-series Station, ALOHA, in the North Pacific Ocean. ASLO Aquatic Sciences meeting, Santa Fe, NM, February 1999.

98. 1999 Karl, D. M. The subtropical North Pacific: New views on an old ocean. JGOFS North Pacific Workshop & SEATS Planning Meeting, Taipei, Taiwan, March 1999.

99. 2000 Benitez-Nelson, C. R., D. M. Karl and K. O. Buesseler. ^{234}Th derived carbon export at Station ALOHA. Ocean Sciences Meeting, San Antonio, TX, January 2000.

100. 2000 Benitez-Nelson, C. R. and D. M. Karl. Phosphorus cycling in the North Pacific gyre. Amirican Geophysical Union Meeting, San Francisco, CA, December 2000.

101. 2000 Bidigare, R. R., M. E. Ondrusek, M. R. Landry, K. Selph, D. M. Karl and R. Leteleir. Seasonal and interannual variations in phytoplankton community structure at Station ALOHA. JGOFS Open Sciences Conference on Ocean Biogeochemistry: A New Paradigm, Bergen, Norway, April 2000.

102. 2000 Karl, D. M., D. V. Hebel and L. M. Tupas. Biogeochemical studies at the Hawaii Ocean Time-series (HOT) Station ALOHA. International Symposium on Carbon Cycle in the North Pacific, Nagoya, Japan, February 2000.

103. 2000 Karl, D. M., S. Emerson, P. J. Harrison, A. F. Michaels and Y. Nojiri. Temporal variability of biogeochemistry. JGOFS Open Science Conference on Ocean Biogeochemistry: A New Paradigm, Bergen, Norway, April 2000.

104. 2000 Letelier, R. M., M. R. Abbott and D. M. Karl. Nutrient supply into the euphotic zone as a result of the seasonal solar irradiance cycle: Station ALOHA as a case study. Ocean Sciences Meeting, San Antonio TX, January 2000.

105. 2000 Russ, M. E., N. E. Ostrom, B. Popp, T. M. Rust and D. M. Karl. Mechanisms of N_2O production in the subtropical North Pacific based on determination of the isotopic abundance of N_2O and O_2. Ocean Sciences Meeting, San Antonio, TX, January 2000.

106. 2001 Neuer, S., R. Davenport, T. Freudenthal, G. Wefer, O. Llinas, M. J. Rueda, D. K. Steinberg, M. H. Conte and D. M. Karl. Differences in Redfield ratios between open ocean time series stations and implications for carbon export. ASLO Aquatic Sciences Meeting, Albuquerque, NM, February 2001.

107. 2001 Smith, JR., K. L., R. J. Baldwin, D. M. Karl and A. Boetius. Benthic community responses to seasonal pulses in pelagic food supply: Central North Pacific gyre. ASLO Aquatic Sciences Meeting, Albuquerque, NM, February 2001.

7.2 Invited/Contributed Book Chapters and Refereed Publications

1. 1990 Firing, E. and R. L. Gordon. Deep ocean acoustic Doppler current profiling. In: G. F. Appell and T. B. Curtin (eds.), Proceedings of the Fourth IEEE Fourth Working Conference on Current Measurement, pp. 192-201. IEEE, New York.
2. 1990 Giovannoni, S. J., E. F. DeLong, T. M. Schmidt and N. R. Pace. Tangential flow filtration and preliminary phylogenetic analysis of marine picoplankton. Applied and Environmental Microbiology, 56, 2572-2575.
3. 1991 Chiswell, S. M. Dynamic response of CTD pressure sensors to temperature. Journal of Atmospheric and Oceanic Technology 8, 659-668.
4. 1991 Karl, D. M., J. E. Dore, D. V. Hebel and C. Winn. Procedures for particulate carbon, nitrogen, phosphorus and total mass analyses used in the US-JGOFS Hawaii Ocean Time-Series Program. In: D.C. Hurd and D. Spencer (eds.), Marine Particles: Analysis and Characterization, pp. 71-77. American Geophysical Union, Geophysical Monograph 63.
5. 1991 Karl, D. M., W. G. Harrison, J. Dore et al. Chapter 3. Major bioelements workshop report. In: D. C. Hurd and D. W. Spencer (eds.), Marine Particles: Analysis and Characterization, pp. 33-42. American Geophysical Union, Geophysical Monograph 63.
6. 1991 Karl, D. M. and C. D. Winn. A sea of change: Monitoring the oceans' carbon cycle. Environmental Science & Technology 25, 1976-1981.
7. 1991 Laws, E. A. Photosynthetic quotients, new production and net community production in the open ocean. Deep-Sea Research 38, 143-167.
8. 1991 Sabine, C. L. and F. T. Mackenzie. Oceanic sinks for anthropogenic CO2. International Journal of Energy, Environment, Economics 1, 119-127.
9. 1991 Schmidt, T. M., E. F. DeLong and N. R. Pace. Analysis of a marine picoplankton community by 16S rRNA gene cloning and sequencing. Journal of Bacteriology 173, 4371-4378.
10. 1992 Anbar, A. D., R. A. Creaser, D. A. Papanastassiou and G. J. Wasserburg. Rhenium in seawater: Confirmation of generally conservative behavior. Geochimica et Cosmochimica Acta 56, 4099-4103.
11. 1992 Benner, R., J. D. Pakulski, M. McCarthy, J. I. Hedges and P. G. Hatcher. Bulk chemical characteristics of dissolved organic matter in the ocean. Science 255, 1561-1564.
12. 1992 Chen, R. F. and J. L. Bada. The fluorescence of dissolved organic matter in seawater. Marine Chemistry 37, 191-221.
13. 1992 Karl, D. M. The oceanic carbon cycle: Primary production and carbon flux in the oligotrophic North Pacific Ocean. In: Y. Oshima (ed.), Proceedings of the IGBP

Symposium on Global Change, pp. 203-219. Japan National Committee for the IGBP, Waseda University, Tokyo, Japan.

14. 1992 Karl, D. M., R. Letelier, D. V. Hebel, D. F. Bird and C. D. Winn. *Trichodesmium* blooms and new nitrogen in the North Pacific gyre. In: E. J. Carpenter et al. (eds.), Marine Pelagic Cyanobacteria: Trichodesmium and Other Diazotrophs, pp. 219-237. Kluwer Academic Publishers, Netherlands.

15. 1992 Karl, D. M. and G. Tien. MAGIC: A sensitive and precise method for measuring dissolved phosphorus in aquatic environments. Limnology and Oceanography 37, 105-116.

16. 1992 Quay, P. D., B. Tilbrook and C. S. Wong. Oceanic uptake of fossil fuel CO_2: Carbon-13 evidence. Science 256, 74-79.

17. 1993 Campbell, L. and D. Vaulot. Photosynthetic picoplankton community structure in the subtropical North Pacific Ocean near Hawaii (station ALOHA). Deep-Sea Research 40, 2043- 2060.

18. 1993 Coble, P. G., C. A. Schultz and K. Mopper. Fluorescence contouring analysis of DOC intercalibration experiment samples: a comparison of techniques. Marine Chemistry 41, 173-178.

19. 1993 Emerson, S., P. Quay, C. Stump, D. Wilbur and R. Schudlich. Determining primary production from the mesoscale oxygen field. ICES Marine Science Symposium 197, 196-206.

20. 1993 Hedges, J. I., B. A. Bergamaschi and R. Benner. Comparative analyses of DOC and DON in natural waters. Marine Chemistry 41, 121-134.

21. 1993 Karl, D. M. Total microbial biomass estimation derived from the measurement of particulate adenosine-5'-triphosphate. In: P. F. Kemp, B. F. Sherr, E. B. Sherr and J. J. Cole (eds.), Handbook of Methods in Aquatic Microbial Ecology, pp. 359-368. Lewis Publishers, Boca Raton.

22. 1993 Karl, D. M., G. Tien, J. Dore and C. D. Winn. Total dissolved nitrogen and phosphorus concentrations at US-JGOFS Station ALOHA: Redfield reconciliation. Marine Chemistry 41, 203-208.

23. 1993 Keeling, C. D. Lecture 2: Surface ocean CO2. NATO ASI Series I(15), 413-429.

24. 1993 Letelier, R. M., R. R. Bidigare, D. V. Hebel, M. Ondrusek, C. D. Winn and D. M. Karl. Temporal variability of the phytoplankton community structure based on pigment analyses. Limnology and Oceanography 38, 1420-1437.

25. 1993 Mopper, K. and C. A. Schultz. Fluorescence as a possible tool for studying the nature and water column distribution of DOC components. Marine Chemistry 41, 229- 238.

26. 1993 Selph, K. E., D. M. Karl and M. R. Landry. Quantification of chemiluminescent DNA probes using liquid scintillation counting. Analytical Biochemistry 210, 394-401.

27. 1993 Sharp, J. H., E. T. Peltzer, M. J. Alperin, G. Cauwet, J. W. Farrington, B. Fry, D. M. Karl, J. H. Martin, A. Spitzy, S. Tugrul and C. A. Carlson. Procedures subgroup report. Marine Chemistry 41, 37-49.

28. 1993 Winn, C. D., R. Lukas, D. Hebel, C. Carrillo, R. Letelier and D. M. Karl. The Hawaii Ocean Time-series program: Resolving variability in the North Pacific. In: N. Saxena (ed.), Recent Advances in Marine Science and Technology, pp. 139-150. Proceedings of the Pacific Ocean Congress (PACON).

29. 1994 Baines, S. B., M. L. Pace and D. M. Karl. Why does the relationship between sinking flux and planktonic primary production differ between lakes and oceans? Limnology and Oceanography 39, 213-226.

30. 1994 Bjorkman, K. and D. M. Karl. Bioavailability of inorganic and organic phosphorus compounds to natural assemblages of microorganisms in Hawaiian coastal waters. Marine Ecology Progress Series 111, 265-273.

31. 1994 Campbell, L., H. A. Nolla and D. Vaulot. The importance of *Prochlorococcus* to community structure in the central North Pacific Ocean (Station ALOHA). Limnology and Oceanography 39, 954-961.

32. 1994 Campbell, L., L. P.Shapiro and E. Haugen. Immunochemical characterization of the eukaryotic ultraplankton from the Atlantic and Pacific Oceans. Journal of Plankton Research 16, 35-51.

33. 1994 Christian, J. R. and D. M. Karl. Microbial community structure at the U.S.-Joint Global Ocean Flux Study Station ALOHA: Inverse methods for estimating biochemical indicator ratios. Journal of Geophysical Research 99, 14,269-14,276.

34. 1994 Karl, D. M. Accurate estimation of microbial loop processes and rates. Microbial Ecology 28, 147-150.

35. 1994 Karl, D. M. and B. D. Tilbrook. Production and transport of methane in oceanic particulate organic matter. Nature 368, 732-734.

36. 1994 Tupas, L. M., B. N. Popp and D. M. Karl. Dissolved organic carbon in oligotrophic waters: experiments on sample preservation, storage and analysis. Marine Chemistry 45, 207- 216.

37. 1994 Winn, C. D., F. T. Mackenzie, C. J. Carrillo, C. L. Sabine and D. M. Karl. Air- sea carbon dioxide exchange in the North Pacific subtropical gyre: Implications for the global carbon budget. Global Biogeochemical Cycles 8, 157-163.

38. 1995 Atkinson, M. A., F. I. M. Thomas, N. Larson, E. Terrill, K. Morita and C. Liu. A micro-hole potentiostatic oxygen sensor for oceanic CTDs. Deep-Sea Research 42, 761-771.

39. 1995 Chavez, F. P., K. R. Buck, R. R. Bidigare, D. M. Karl, D. Hebel, M. Latasa, L. Campbell and J. Newton. On the chlorophyll *a* retention properties of glass- fiber GF/F filters. Limnology and Oceanography 40, 428-433.

40. 1995 Christian, J. R. and D. M. Karl. Bacterial ectoenzymes in marine waters: Activity ratios and temperature responses in three oceanographic provinces. Limnology and Oceanography 40, 1042-1049.

41. 1995 Christian, J. R. and D. M. Karl. Measuring bacterial ectoenzyme activities in marine waters using mercuric chloride as a preservative and a control. Marine Ecology Progress Series 123, 217-224.

42. 1995 Emerson, S., P. D. Quay, C. Stump, D. Wilbur and R. Schudlich. Chemical tracers of productivity and respiration in the subtropical Pacific Ocean. Journal of Geophysical Research 100, 15,873-15,887.

43. 1995 Jones, D. R., D. M. Karl and E. A. Laws. DNA:ATP ratios in marine microalgae and bacteria: Implications for growth rate estimates based on rates of DNA synthesis. Journal of Phycology 31, 215-223.

44. 1995 Karl, D. M. A reply to a comment by J. A. McGowan "HOT and the North Pacific gyre." Nature 378, 21-22.

45. 1995 Karl, D. M., R. Letelier, D. Hebel, L. Tupas, J. Dore, J. Christian and C. Winn. Ecosystem changes in the North Pacific subtropical gyre attributed to the 1991-92 El Nino. Nature 373, 230-234.

46. 1995 Liu, H., L. Campbell and M. R. Landry. Growth and mortality rates of *Prochlorococcus* and *Synechococcus* measured with a selective inhibitor technique. Marine Ecology Progress Series 116, 277-287.

47. 1995 Maranger, R. and D. F. Bird. Viral abundance in aquatic systems: a comparison between marine and fresh waters. Marine Ecology Progress Series 121, 217-226.

48. 1995 Sabine, C. L. and F. T. Mackenzie. Bank-derived carbonate sediment transport and dissolution in the Hawaiian Archipelago. Aquatic Geochemistry 1, 189-230.

49. 1995 Sabine, C. L., F. T. Mackenzie, C. Winn and D. M. Karl. Geochemistry of carbon dioxide in seawater at the Hawaii Ocean Time-series station, ALOHA. Global Biogeochemical Cycles 9, 637-651.

50. 1995 Sharp, J. H., R. Benner, L. Bennett, C. A. Carlson, S. E. Fitzwater, E. T. Peltzer and L. M. Tupas. Analyses of dissolved organic carbon in seawater: the JGOFS EqPac methods comparison. Marine Chemistry 48, 91-108.

51. 1995 Thomas, F. I. M. and M. J. Atkinson. Field calibration of a microhole potentiostatic oxygen sensor for oceanic CTDs. Journal of Atmospheric and Oceanic Technology 12, 390-394.

52. 1995 Thomas, F. I. M., S. A. McCarthy, J. Bower, S. Krothapalli, M. J. Atkinson and P. Flament. Response characteristics of two oxygen sensors for oceanic CTDs. Journal of Atmospheric and Oceanic Technology 12, 687-690.

53. 1995 Tilbrook, B. D. and D. M. Karl. Methane sources, distributions and sinks from California coastal waters to the oligotrophic North Pacific gyre. Marine Chemistry 49, 51-64.

54. 1995 Winn, C. D., L. Campbell, J. Christian, R. M. Letelier, D. V. Hebel, J. E. Dore, L. Fujieki and D. M. Karl. Seasonal variability in the phytoplankton community of the North Pacific subtropical gyre. Global Biogeochemical Cycles 9, 605-620.

55. 1996 Anbar, A.D., G.J. Wasserburg, D.A. Papanastassiou and P.S. Andersson. Iridium in natural waters. Science 273, 1524-1528.

56. 1996 Andersen, R. A., R. R. Bidigare, M. D. Keller and M. Latasa. A comparison of HPLC pigment signatures and electron microscopic observations for oligotrophic waters of the North Atlantic and Pacific Oceans. Deep-Sea Research II 43, 517-537.

57. 1996 Atkinson, M. J., F. I. M. Thomas and N. Larson. Effects of pressure on oxygen sensors. Journal of Atmospheric and Oceanic Technology 13, 1267-1274.

58. 1996 Bingham, F. M. and R. Lukas Seasonal cycles of temperature, salinity and dissolved oxygen observed in the Hawaii Ocean Time-series. Deep-Sea Research II 43, 199-213.

59. 1996 Campos, M. L. A. M., A. M. Farrenkopf, T. D. Jickells and G. W. Luther III. A comparison of dissolved iodine cycling at the Bermuda Atlantic Time-series station and Hawaii Ocean Time-series station. Deep-Sea Research II 43, 455-466.

60. 1996 Chiswell, S. M. Intraseasonal oscillations at Station ALOHA, north of Oahu, Hawaii. Deep-Sea Research II 43, 305-319.

61. 1996 De La Rocha, C. L. and M. A. Brzezinski. Purification, recovery, and laser-driven fluorination of silicon from dissolved and particulate silica for the measurement of natural stable isotope abundances. Analytical Chemistry 68, 3746-3750.

62. 1996 Dore, J. E., T. Houlihan, D. V. Hebel, G. Tien, L. Tupas and D. M. Karl. Freezing as a method of sample preservation for the analysis of dissolved inorganic nutrients in seawater. Marine Chemistry 53, 173-185.

63. 1996 Dore, J. E. and D. M. Karl. Nitrification in the euphotic zone as a source for nitrite, nitrate and nitrous oxide at Station ALOHA. Limnology and Oceanography 41, 1619-1628.

64. 1996 Dore, J. E. and D. M. Karl. Nitrite distributions and dynamics at Station ALOHA. Deep-Sea Research II 43, 385-402.

65. 1996 Feller, R. J. and D. M. Karl. The National Association of Marine Laboratories: A connected web for studying long-term changes in U.S. coastal and marine waters. Biological Bulletin 190, 269-277.

66. 1996 Firing, E. Currents observed north of Oahu during the first five years of HOT. Deep-Sea Research II 43, 281-303.

67. 1996 Jones, D. R., D. M. Karl and E. A. Laws. Growth rates and production of heterotrophic bacteria and phytoplankton in the North Pacific subtropical gyre. Deep-Sea Research I 43, 1567-1580.

68. 1996 Karl, D. M., J. R. Christian, J. E. Dore, D. V. Hebel, R. M Letelier, L. M. Tupas and C. D. Winn. Seasonal and interannual variability in primary production and particle flux at Station ALOHA. Deep-Sea Research II 43, 539-568.

69. 1996 Karl, D. M. and R. Lukas. The Hawaii Ocean Time-series (HOT) program: Background, rationale and field implementation. Deep-Sea Research II 43, 129-156.

70. 1996 Karl, D. M. and A. F. Michaels. Preface: The Hawaiian Ocean Time-series (HOT) and Bermuda Atlantic Time-series Study (BATS). Deep-Sea Research II 43, 127-128.

71. 1996 Kennan, S. C. and R. Lukas. Saline intrusions in the intermediate waters north of Oahu, Hawaii. Deep-Sea Research II 43, 215-241.

72. 1996 Latasa, M., R. R. Bidigare, M. E. Ondrusek and M. C. Kennicutt II. HPLC analysis of algal pigments: a comparison exercise among laboratories and recommendations for improved analytical performance. Marine Chemistry 51, 315-324.

73. 1996 Lawson, L. M., E. E. Hofmann and Y. H. Spitz. Time series sampling and data assimilation in a simple marine ecosystem model. Deep-Sea Research II 43, 625-651.

74. 1996 Letelier, R. M., J. E. Dore, C. D. Winn and D. M. Karl. Seasonal and interannual variations in photosynthetic carbon assimilation at Station ALOHA. Deep-Sea Research II 43, 467-490.

75. 1996 Letelier, R. M. and D. M. Karl. Role of *Trichodesmium* spp. in the productivity of the subtropical North Pacific Ocean. Marine Ecology Progress Series 133, 263-273.

76. 1996 Lukas, R. and F. Santiago-Mandujano. Interannual variability of Pacific deep- and bottom-waters observed in the Hawaii Ocean Time-series. Deep-Sea Research II 43, 243-255.

77. 1996 Mitchum, G. T. On using satellite altimetric heights to provide a spatial context for the Hawaii Ocean Time-series measurements. Deep-Sea Research 43, 257-280.

78. 1996 Moyer, C. L., J. M. Tiedje, F. C. Dobbs and D. M. Karl. A computer-simulated restriction fragment length polymorphism analysis of bacterial small-subunit rRNA genes: Efficacy of selected tetrameric restriction enzymes for studies of microbial diversity in nature. Applied and Environmental Microbiology 62, 2501-2507.

79. 1996 Roy-Barman, M., J. H. Chen and G. J. Wasserburg. ^{230}Th-^{232}Th systematics in the central Pacific Ocean: The sources and the fates of thorium. Earth and Planetary Science Letters 139, 351-363.

80. 1996 Schudlich, R. and S. Emerson. Gas saturation in the surface ocean: The roles of heat flux, gas exchange and bubbles. Deep-Sea Research II 43, 569-589.

81. 1997 Benner, R., B. Biddanda, B. Black and M. McCarthy. Abundance, size distribution and stable carbon and nitrogen isotopic composition of marine organic matter isolated by tangential-flow ultrafiltration. Marine Chemistry 57, 243-263.

82. 1997 Campbell, L., H. Liu, H. A. Nolla and D. Vaulot. Annual variability of phytoplankton and bacteria in the subtropical North Pacific Ocean at Station ALOHA during the 1991-1994 ENSO event. Deep-Sea Research 44, 167-192.

83. 1997 Christian, J. R., M. R. Lewis and D. M. Karl. Vertical fluxes of carbon, nitrogen and phosphorus in the North Pacific subtropical gyre near Hawaii. Journal of Geophysical Research 102, 15,667-15,677.

84. 1997 Emerson, S., P. Quay, D. Karl, C. Winn, L. Tupas and M. Landry. Experimental determination of the organic carbon flux from open-ocean surface waters. Nature 389, 951-954.

85. 1997 Karl, D. M., R. Letelier, L. Tupas, J. Dore, J. Christian and D. Hebel. The role of nitrogen fixation in biogeochemical cycling in the subtropical North Pacific Ocean. Nature 388, 533-538.

86. 1997 Karl, D. M. and G. Tien. Temporal variability in dissolved phosphorus concentrations in the subtropical North Pacific Ocean. Marine Chemistry 56, 77-96.

87. 1997 Karl, D. M. and K. Yanagi. Partial characterization of the dissolved organic phosphorus pool in the oligotrophic North Pacific Ocean. Limnology and Oceanography 42, 1398-1405.

88. 1997 Karl, D. M. Oceanic carbon cycle and global environmental change: A microbiological perspective. In: M. T. Martins et al(eds.), Progress in Microbial Ecology. Proceedings of Seventh International Symposium on Microbial Ecology, Santos, Sao Paulo, Brazil, 1995. Sociedade Brasileira de Microbiologia / International Committee of Microbial Ecology, Brazil, pp. 163-172.

89. 1997 Lukas, R., F. Santiago-Mandujano and E. Firing. Long-term hydrographic variations observed in the Hawaii Ocean Time-series. in proceedings of the OOPC Ocean Climate Time-series Workshop, The Johns Hopkins University, Baltimore, Maryland, 18-20 March, 1997. GCOS Rept. No. 41, Annex XX.

90. 1997 Liu, H., L. Campbell and H. A. Nolla. Prochlorococcus growth rate and contribution to primary production in the equatorial and subtropical North Pacific Ocean. Aquatic Microbial Ecology 12, 39-42.

91. 1997 Sansone, F. J., B. N. Popp and T. M. Rust. Stable carbon isotopic analysis of low-level methane in water and gas. Analytical Chemistry 69, 40-44.

92. 1997 Troy, P. J., Y. H. Li and F. T. Mackenzie. Changes in surface morphology of calcite exposed to the oceanic water column. Aquatic Geochemistry 3, 1-20.

93. 1997 Venrick, E. L. Comparison of the phytoplankton species composition and structure in the Climax area (1973-1985) with that of Station ALOHA (1994). Limnology and Oceanography 42, 1643-1648.

94. 1998 Dore, J. E., B. N. Popp, D. M. Karl and F. J. Sansone. A large source of atmospheric nitrous oxide from subtropical North Pacific surface waters. Nature 396, 63-66.

95. 1998 Karl, D. M. and F. C. Dobbs. Molecular approaches to microbial biomass estimation in the sea. In: K. E. Cooksey (ed.), Molecular Approaches to the Study of the Ocean pp. 29-89. Chapman and Hall, London.

96. 1998 Karl, D. M., D. V. Hebel, K. Bjorkman and R. M. Letelier. The role of dissolved organic matter release in the productivity of the oligotrophic North Pacific Ocean. Limnology and Oceanography 43, 1270-1286.

97. 1998 Letelier, R. M. and D. M. Karl. *Trichodesmium* spp. physiology and nutrient fluxes in the North Pacific subtropical gyre. Aquatic Microbial Ecology 15, 265-276.

98. 1998 Loisel, H. and A. Morel. Light scattering and chlorophyll concentration in case 1 waters: A reexamination. Limnology and Oceanography 43, 847-858.

99. 1998 Lukas, R. A Freshening of the Upper Pycnocline in the North Pacific Subtropical Gyre. In Proceedings of The International Symposium TRIANGLE '98, September 29-October 2, 1998. Japan Marine Science and Technology Center, Yokosuka, Japan, 294-303.

100. 1998 Thomson-Bulldis, A. and D. Karl. Application of a novel method for phosphorus determinations in the oligotrophic North Pacific Ocean. Limnology and Oceanography 43, 1565-1577.

101. 1998 Winn, C. D., Y. H. Li, F. T. Mackenzie and D. M. Karl. Rising surface ocean dissolved inorganic carbon at the Hawaii Ocean Time-series site. Marine Chemistry 60, 33-47.

102. 1998 Zehr, J. P., M. T. Mellon and S. Zani. New nitrogen-fixing microorganisms detected in oligotrophic oceans by amplification of nitrogenase (nifH) genes. Applied and Environmental Microbiology 64, 3444-3450.

103. 1999 Calbet, A. and M. R. Landry. Mesozooplankton influences on the microbial food web: Direct and indirect trophic interactions in the oligotrophic open ocean. Limnology and Oceanography 44, 1370-1380.

104. 1999 Emerson, S. and D. M. Karl. The biological carbon pump in the subtropical Pacific Ocean: Nutrient limitations and CO_2 fluxes. In Y. Noriji (ed.), Proceedings of the 2nd International symposium on CO_2 in the Oceans, NIES, Tsukuba, Japan, pp. 317-323.

105. 1999 Firing, E., B. Qiu, and W. Miao. Time-dependent island rule and its application to the time-varying north Hawaiian ridge current. J. Physical Oceanography, 29, 2671-2688.

106. 1999 Karl, D. M. A sea of change: Biogeochemical variability in the North Pacific subtropical gyre. Ecosystems 2, 181-214.

107. 1999 Scharek, R., M. Latasa, D. M. Karl and R. R. Bidigare. Temporal variations in diatom abundance and downward vertical flux in the oligotrophic North Pacific gyre. Deep-Sea Research I 46, 1051-1075.

108. 1999 Scharek, R., L. Tupas and D. M. Karl. Diatom fluxes to the deep sea in the oligotrophic North Pacific gyre at Station ALOHA. Marine Ecology Progress Series 182, 55-67.

109. 2000 Björkman, K., A. L. Thomson-Bulldis and D. M. Karl. Phosphorus dynamics in the North Pacific subtropical gyre. Aquatic Microbial Ecology, 22: 185-198.

110. 2000 Karl, D. M. A new source of "new" nitrogen in the sea. Trends in Microbiology 8, 301.

111. 2000 Karl, D. M. Phosphorus, the staff of life. Nature 406, 31-32.

112. 2000 Letelier, R. M., D. M. Karl, M. R. Abbott, P. Flament, M. Freilich, R. Lukas and T. Strub. The role of late winter meso-scale events in the biogeochemical variability of the upper water column of the North Pacific Subtropical Gyre. Journal of Geophysical Research 105: 28,723-28,739.

113. 2000 Li, Y.-H., D. M. Karl, C. D. Winn, F. T. Mackenzie and K. Gans. Remineralization ratios in the subtropical North Pacific gyre. Aquatic Geochemistry 6, 65-86.

114. 2000 Michaels, A. F., D. M. Karl and A. H. Knap. Temporal studies of biogeochemical dynamics in oligotrophic oceans. In R. Hanson, H. Ducklow and J. Field (eds.), The Changing Ocean Carbon Cycle in the Sea, Cambridge Univ. Press, UK, pp. 392-413.

115. 2000 Ostrom, N. E., M. E. Russ, B. Popp, T. M. Rust and D. M. Karl. Mechanisms of nitrous oxide production in the subtropical North Pacific based on determinations of the isotopic abundances of nitrous oxide and di-oxygen. Chemosphere - Global Change Science 2: 281-290.

116. 2001 Al-Mutairi, H. and M.R. Landry. Active export of carbon and nitrogen at Station ALOHA by diel migrant zooplankton. Deep-Sea Res. II. 48: 2083-2104.

117. 2001 Benitez-Nelson, C., K. O. Buesseler, D. M. Karl and J. Andrews. A time-series study of particulate matter export in the North Pacific Subtropical Gyre based on ^{234}Th:^{238}U disequilibrium. Deep-Sea Research, 48: 2595-2611.

118. 2001 Calbet, A., M.R. Landry and S. Nunnery. Bacteria-flagellate interactions in the microbial food web of the oligotrophic subtropical North Pacific. Aquat. Microb. Ecol. 23: 283-292.

119. 2001 Cavender-Bares-K. K., D. M. Karl and S. W. Chisholm. Nutrient gradients in the western North Atlantic Ocean: Relationship to microbial community structure, and comparison to patterns in the Pacific Ocean. Deap-Sea Research 48: 2373-2395.

120. 2001 Donachie, S. P., J. R. Christian and D. M. Karl. Nutrient regulation of bacterial production and ectoenzyme activities in the subtropical North Pacific Ocean. Deep-Sea Research II, 48: 1719-1732.

121. 2001 Finnigan, T.D., D.S. Luther and R. Lukas. Observations of enhanced mixing near the Hawaiian Ridge. J. Phys. Oceanogr., accepted.

122. 2001 Hebel, D. V. and D. M. Karl. Seasonal, interannual and decadal variations in particulate matter concentrations and composition in the subtropical North Pacific Ocean. Deep-Sea Research II, 48: 1669-1696.

123. 2001 Karl, D. M., R. R. Bidigare and R. M. Letelier. Long-term changes in plankton community structure and productivity in the North Pacific subtropical Gyre: The domain shift hypothesis. Deep-Sea Research II, 48: 1449-1470.

124. 2001 Karl, D. M., K. M. Bjorkman, J. E. Dore, L. Fujieki, D. V. Hebel, T. Houlihan, R. M. Letelier and L. M. Tupas. Ecological nitrogen-to-phosphorus stoichiometry at Station ALOHA. Deep-Sea Research II, 48: 1529-1566.

125. 2001 Karl, D. M. and J. E. Dore. Microbial ecology at sea: Sampling, subsampling and incubation considerations. In: J. H. Paul (ed.), Methods in Microbiology, vol. 30, pp 13-39.

126. 2001 Karl, D. M. and A. F. Michaels. Nitrogen cycle. In: J. Steele, S. Thorpe and K. Turekian, Eds., Encyclopedia of Ocean Sciences, pp. 1876-1884.

127. 2001 Karl, D. M., J. E. Dore, R. Lukas, A. F. Michaels, N. R. Bates and A. Knap. Building the long-term picture: The U.S. JGOFS time-series programs. Oceanography, 14: 6-17.

128. 2001 Karner, M. B., E. F. Delong and D. M. Karl. Archaeal dominance in the mesopelagic zone of the Pacific Ocean, Nature, 409: 507-510.

129. 2001 Landry, M.R., H. Al-Mutairi, K.E. Selph, S. Christensen and S, Nunnery. Seasonal patterns of mesozooplankton abundance and biomass at Station ALOHA. Deep-Sea Res. II. 48: 2037-2062.

130. 2001 Landry, M. R. and D. L. Kirchman. Microbial community structure and variability in the tropical Pacific. Deep-Sea Res. II., in press.

131. 2001 Lukas, R. Freshening of the Upper Thermocline in the North Pacific Subtropical Gyre Associated With Decadal Changes of Rainfall. Geophys. Res.Lett., 28, 3485-3488.

132. 2001 Lukas, R. and F. Santiago-Mandujano. Extreme Water Mass Anomaly Observed in the Hawaii Ocean Time-series. Geophys. Res. Lett., 28, 2931-2934.

133. 2001 Lukas, R., F. Santiago-Mandujano, F. Bingham and A. Mantyla. Cold bottom water events observed in the Hawaii Ocean time-series: Implications for vertical mixing. Deep-Sea Res. I, 48 (4), 995-1021.

134. 2001 Ondrusek, M. E., R. R. Bidigare, K. Waters and D. M. Karl. A predictive model for estimating rates of primary production in the subtropical North Pacific Ocean. Deep-Sea Research II, 48: 1837-1863.

135. 2001 Roman, M.R., H.A. Adolf, M.R. Landry, L.P. Madin, D.K. Steinberg and X. Zhang. Estimates of oceanic mesozooplankton production: A comparison using the Bermuda and Hawaii time-series data. Deep-Sea Res. II., in press

136. 2001 Siegel, D. A., D. M. Karl and A. F. Michaels. Interpretations of biogeochemical processes from the US-JGOFS Bermuda and Hawaii time-series sites. Deep-Sea Research II 48: 1403-1404 (Editorial).

137. 2001 Zehr, J. P., P. J. Turner, E. Omoregie, A. Hansen, G. F. Steward, J. B. Waterbury, J. P. Montoya and D. M. Karl. Unicellular cyanobacteria fix N_2 in the North Pacific Ocean. Nature 412: 635-638.

138. 2002 Benitez-Nelson, C. R. and D. M. Karl. Phosphorus cycling in the North Pacific Subtropical Gyre using cosmogenic ^{32}P and ^{33}P. Limnology and Oceanography, 47: 762-770.

139. 2002 Church, M. J., H. W. Ducklow and D. M. Karl. Multi-year increases in dissolved organic matter inventories at Station ALOHA in the North Pacific Subtropical Gyre. Limnology and Oceanography, 47: 1-10.

140. 2002 Dore, J. E., J. R. Brum, L. Tupas and D. M. Karl. Seasonal and interannual variability in sources of nitrogen supporting export in the oligotrophic subtropical North Pacific Ocean. Limnology and Oceanography, in press.

141. 2002 Dore, J. E., C. J. Carrillo, D. V. Hebel and D. M. Karl. Carbon cycle observations at the Hawaii Ocean Time-series Station ALOHA. In Y. Noriji and R. Feely (eds.), Proceedings of the PICES North Pacific CO_2 Data Synthesis Symposium, Tsukuba, Japan, October 2000, in press.

142. 2002 Emerson, S., C. Stump, B. Johnson and D. M. Karl. In situ determination of oxygen and nitrogen concentrations in the upper ocean. Deep-Sea Research I, 49: 941-952.

143. 2002 Fennel, K. Y. H. Spitz, R. M. Letelier, M. R. Abbott and D. M. Karl. A deterministic model for N_2-fixation at Station ALOHA in the subtropical North Pacific Ocean. Deep-Sea Research II, 49: 149-174.

144. 2002 Karl, D. M. Nutrient dynamics in the deep blue sea. Trends in Microbiology, in press.

145. 2002 Karl, D. M., N. Bates, S. Emerson, P. J. Harrison, C. Jeandel, O. Llinas, K. K. Liu, J.-C. Marty, A. F. Michaels, J. C. Miquel, S. Neuer, Y. Noriji and C. S. Wong. Temporal studies of biogeochemical processes determined from ocean time-series obsevations during the JGOFS era. In: M Fasham et al., Eds., A JGOFS Synthesis, in press.

146. 2002 Karl, D. M., R. R. Bidigare and R. M. Letelier. Sustained and aperiodic variability in organic matter production and phototrophic microbial community structure in the North Pacific Subtropical Gyre. In: P. J. le B. Williams, D. R. Thomas and C. S. Reynolds, Eds.,

Phytoplankton Productivity and Carbon Assimilation in Marine and Freshwater Ecosystems, Blackwell Publishers, London, pp. 222-264.

147. 2002 Karl, D. M. and K. M. BjÖrkman. Dynamics of DOP. In: D. Hansell and C. Carlson, Eds., Biogeochemistry of Marine Dissolved Organic Matter, pp. 246-366, Elsevier Science.

148. 2002 Karl, D. M., A. Michaels, B. Bergman, D. Capone, E. Carpenter, R. Letelier, F. Lipschultz, H. Paerl, D. Sigman and L. Stal. Dinitrogen fixation in the world's oceans. Biogeochemistry, 57/58: 47-98.

149. 2002 Lee, K., D. M. Karl, J. Z. Zhang and R. Wanninkhof. Carbon export in the nitrate-depleted tropical and subtropical oceans: Implications for marine nitrogen fixation, Geophysical Research Letters, in press.

150. 2002 Smith, K.L., JR., R. J. Baldwin, D. M. Karl and A. Boetius. Benthic community responses to pulses in pelagic food supply: North Pacific subtropical gyre. Deep-Sea Research I 49:971-990.

7.3 Submitted Papers

1. Johnson, K. S., V. A. Elrod, S. E. Fitzwater, J. N. Plant, F. P. Chavez, S. J. Tanner, R. M. Gordon, D. L. Westphal, K. D. Perry and D. M. Karl. Iron and ecosystem response to surface ocean-lower atmosphere interactions in the North Pacific Ocean gyre. Submitted to Nature.
2. Gedeon, M. L., P. H. Ostrom, N. E. Ostrom, H. Gandhi and D. M. Karl. ^{15}N isotopic analysis of dissolved organic nitrogen from the North Pacific Subtropical Gyre: Implications for nitrogen biogeochemical cycling. Submitted to Geochimica et Cosmochimica Acta.
3. Neuer, S., R. Davenport, T. Freudenthal, G. Wefer, O. Llinas, M.-J Rueda, D. K. Steinberg and D. M. Karl. Differences in the biological carbon pump at three subtropical ocean sites. Submitted to Nature.
4. Bjorkman, K. M. and D. M. Karl. Bioavailability of dissolved organic phosphorus in the euphotic zone at Station ALOHA, North Pacific Subtropical Gyre. Submitted to Limnology and Oceanography.

7.4 Theses and Dissertations

1. 1992 Sabine, C. L. Geochemistry of particulate and dissolved inorganic carbon in the central North Pacific. Ph.D. Dissertation, May 1992.
2. 1993 Kennan, S. Variability of the intermediate water north of Oahu. M.S. Thesis, December 1993.
3. 1994 Letelier, R. M. Studies on the ecology of *Trichodesmium* spp. (Cyanophyceae) in the central North Pacific gyre. Ph.D. Dissertation, April 1994.
4. 1994 Liu, H. B. Growth and mortality rates of *Prochlorococcus* and *Synechococcus* measured by a selective inhibitor technique. M.S. Thesis, May 1994.

5. 1995 Dore, J. E. Microbial nitrification in the marine euphotic zone: Rates and relationships with nitrite distributions, recycled production and nitrous oxide generation. Ph.D. Dissertation, May 1995.
6. 1995 Christian, J. R. Biochemical mechanisms of bacterial utilization of dissolved and particulate organic matter in the upper ocean. Ph.D. Dissertation, December 1995.
7. 1995 Troy, P.J. Surface chemistry of solids in the upper ocean. Ph.D. Dissertation, University of Hawaii at Manoa, August 1995.
8. 1997 Thomson-Bulldis, A. A Novel Method for the determination of phosphate and dissolved organic phosphorus concentrations in seawater. M.S. Thesis, University of Hawaii, December 1997.
9. 1999 Al-Mutari, H.A. Active export of carbon and nitrogen by diel-migrant zooplankton at Station ALOHA. M.S. Thesis, University of Hawaii at Manoa, May 1998.
10. 1999 Cavender-Bares, K.K. Size distributions, population dynamics, and single-cell properties of marine plankton in diverse nutrient environments. Ph.D. Dissertation, Massachusetts Institute of Technology, June 1999.
11. 1999 Björkman, K.M. Nutrient dynamics in the North Pacific subtropical gyre: phosphorus fluxes in the upper oligotrophic ocean. Ph.D. Dissertation, Stockholm University, December 1999.

7.5 Data Reports and Manuals

1. 1990 Karl, D. M., C. D. Winn, D. V. W. Hebel and R. Letelier. Hawaii Ocean Time- series Program Field and Laboratory Protocols, September 1990. School of Ocean and Earth Science and Technology, Univ. of Hawaii, Honolulu, HI, 72 pp.
2. 1990 Collins, D. J., W. J. Rhea and A. van Tran. Bio-optical profile data report: HOT- 3. National Aeronautics and Space Administration JPL Publ. #90-36.
3. 1990 Chiswell, S., E. Firing, D. Karl, R. Lukas and C. Winn. Hawaii Ocean Time- series Program Data Report 1, 1988-1989. SOEST Tech. Rept. #1, School of Ocean and Earth Science and Technology, Univ. of Hawaii, Honolulu, HI, 269 pp.
4. 1992 Winn, C., S. Chiswell, E. Firing, D. Karl and R. Lukas. Hawaii Ocean Time- series Program Data Report 2, 1990. SOEST Tech. Rept. 92-1, School of Ocean and Earth Science and Technology, Univ. of Hawaii, Honolulu, HI, 175 pp.
5. 1993 Winn, C., R. Lukas, D. Karl and E. Firing. Hawaii Ocean Time-series Program Data Report 3, 1991. SOEST Tech. Report 93-3, School of Ocean and Earth Science and Technology, Univ. of Hawaii, Honolulu, HI, 228 pp.
6. 1993 Tupas, L., F. Santiago-Mandujano, D. Hebel, R. Lukas, D. Karl and E. Firing. Hawaii Ocean Time-series Program Data Report 4, 1992. SOEST Tech. Report 93-14, School of Ocean and Earth Science and Technology, Univ. of Hawaii, Honolulu, HI, 248 pp.

7. 1994 Tupas, L., F. Santiago-Mandujano, D. Hebel, E. Firing, F. Bingham, R. Lukas and D. Karl. Hawaii Ocean Time-series Program Data Report 5, 1993. SOEST Tech. Report 94-5, School of Ocean and Earth Science and Technology, Univ. of Hawaii, Honolulu, HI, 156 pp.
8. 1994 Voss, C. I. and W. W. Wood Synthesis of geochemical, isotopic and groundwater modelling analysis to explain regional flow in a coastal aquifer of Southern Oahu, Hawaii. In: Mathematical Models and Their Applications to Isotope Studies in Groundwater Hydrology, pp. 147-178, International Atomic Energy Agency, Vienna, Austria.
9. 1995 Tupas, L., F. Santiago-Mandujano, D. Hebel, E. Firing, R. Lukas and D. Karl. Hawaii Ocean Time-series Program Data Report 6, 1994. SOEST Tech. Report 95-6, School of Ocean and Earth Science and Technology, Univ. of Hawaii, Honolulu, HI, 199 pp.
10. 1996 Karl, D., L. Tupas, F. Santiago-Mandujano, C. Nosse, D. Hebel, E. Firing and R. Lukas. Hawaii Ocean Time-series Program Data Report 7: 1995. SOEST Tech. Report 96-9, School of Ocean and Earth Science and Technology, Univ. of Hawaii, Honolulu, HI, 228 pp.
11. 1997 Tupas, L., F. Santiago-Mandujano, D. Hebel, C. Nosse, L. Fujieki, E. Firing, R. Lukas and D. Karl. Hawaii Ocean Time-series Program Data Report 8: 1996. SOEST Tech. Report 97-7, School of Ocean and Earth Science and Technology, Univ. of Hawaii, Honolulu, HI, 296 pp.
12. 1998 Tupas, L., F. Santiago-Mandujano, D. Hebel, C. Nosse, L. Fujieki, R. Lukas and D. Karl. Hawaii Ocean Time-series Program Data Report 9: 1997. SOEST Tech. Report 98-9, School of Ocean and Earth Science and Technology, Univ. of Hawaii, Honolulu, HI, 159 pp.
13. 1999 Tupas, L., F. Santiago-Mandujano, C. Nosse, D. Hebel, L. Fujieki, R. Lukas and D. Karl. Hawaii Ocean Time-series Program Data Report 10: 1998. SOEST Tech. Report 99-5, School of Ocean and Earth Science and Technology, Univ. of Hawaii, Honolulu, HI, 246 pp.
14. 2000 Santiago-Mandujano, F., J. Dore, L. Tupas, D. Hebel, L. Fujieki, R. Lukas and D. Karl. Hawaii Ocean Time-series Program Data Report 11: 1999.

7.6 Newsletters

1. 1989 Karl, D. M. Hawaiian Ocean Time-series program: It's HOT. GOFS Newsletter 1(2), 1-3.
2. 1990 Karl, D. M. HOT Stuff: An update on the Hawaiian Ocean Time-series program. U.S. JGOFS Newsletter 2(1), 6,9.
3. 1990 Karl, David M. HOT Stuff: Rescue at sea. U.S. JGOFS Newsletter 2(2), 8.
4. 1991 Karl, D. M. HOT Stuff: Retrospect and prospect. U.S. JGOFS Newsletter 2(3), 10.
5. 1991 Karl, D. M. HOT Stuff: Hectic spring schedule keeps HOT team hustling. U.S. JGOFS Newsletter 2(4), 9-10.
6. 1991 Lukas, R. and S. Chiswell. Submesoscale water mass variations in the salinity minimum of the North Pacific. WOCE Notes, 3(1), 6-8.
7. 1992 Karl, D. M. Hawaii Time-series program: Progress and prospects. U.S. JGOFS Newsletter 3(4), 1,15.

8. 1992 Michaels, A. F. Time-series programs compare results, methods and plans for future. U.S. JGOFS Newsletter 4(1), 7,9.
9. 1992 Winn, C. W. HOT program builds time-series set of carbon measurements for central Pacific. U.S. JGOFS Newsletter 4(2), 7.
10. 1992 Dickey, T. D. Oversight committee reviews time-series programs, issues recommendations. U.S. JGOFS Newsletter 4(2), 14-15.
11. 1992 Firing, E. and P. Hacker. ADCP results from WHP P16/P17. WOCE Notes, 4(3), 6- 12.
12. 1992 Chiswell, S. Inverted echo sounders at the WOCE deep-water station. WOCE Notes, 4(4), 1, 3-6.
13. 1993 Karl, D. M. HOT Stuff: The five-year perspective. U.S. JGOFS Newsletter 5(1), 6,15.
14. 1994 Karl, D. M. HOT Stuff: Surprises emerging from five years' worth of data. U.S. JGOFS Newsletter 5(4), 9-10.
15. 1994 Tupas, L. M. Euphotic zone nitrate variability in the central North Pacific gyre at the Hawaii Ocean Time-series Station ALOHA. International WOCE Newsletter 17, 21-23.
16. 1994 Lukas, R. HOT results show interannual variability of Pacific Deep and Bottom waters. WOCE Notes 6(2), 1, 3, 14-15.
17. 1995 Karl, D. M. HOT and COLD: A trapper's tale of two oceans. U.S. JGOFS Newsletter 6(2): 7, 15.
18. 1995 Karl, D. M. HOT Stuff: New hypotheses and projects evolve from growing data set. U.S. JGOFS Newsletter 7(1): 11.
19. 1996 Winn, C.D. and P. G. Driscoll. Hawaii Time-series data reveal rising ocean CO2 levels. U.S. JGOFS Newsletter 7(4): 7-8.
20. 1996 Karl, D. M. The Hawaii Ocean Time-series study: Still HOT at 75. U.S. JGOFS Newsletter 7(4): 8-9.
21. 1997 Karl, D.M. HOT scientists deploy mooring at Station ALOHA. US JGOFS Newsletter 8(2): 4.
22. 1997 Karl, D.M. Ocean time-series meetings explore new collaboration for future. US JGOFS Newsletter 8(3): 15.
23. 1998 Karl, D.M. The changing sea: Long-term biogeochemical variability in the subtropical North pacific. US JGOFS Newsletter 9(3): 7-9.
24. 1999 Karl, D.M. Wave goodbye: HOT flagship retires from UNOLS fleet. US JGOFS Newsletter 10(1): 6.

7.7 Symposia

1) Presentations from the "HOT Program: Progress and Prospectus" symposium, 3-4 June 1992, East-West Center, Honolulu, HI
   a) Campbell, L. Bacterial numbers by flow cytometry: A new approach
   b) Chiswell, S. Results from the inverted echo sounder network

c) Christian, J. Biomass closure in the epipelagic zone
d) Christian, J. Exoenzymatic hydrolysis of high molecular weight organic matter
e) Dore, J. Annual and short-term variability in the distribution of nitrite at the US-JGOFS time-series station ALOHA
f) Dore, J. and D. Hebel. Low-level nitrate and nitrite above the nutricline at Station ALOHA
g) Firing, E. Ocean currents near ALOHA
h) Hebel, D., R. Letelier and J. Dore. Evaluation of the depth dependence and temporal variability of primary production at Station ALOHA
i) Hebel, D., R. Letelier and J. Dore. Past and present dissolved oxygen trends, methodology, and quality control during the Hawaii Ocean Time series
j) Hebel, D. and U. Magaard. Structure and temporal variability in biomass estimates at Station ALOHA
k) Houlihan, T. and D. Hebel. Organic and inorganic nutrients: Water column structure and usefulness in time-series analysis
l) Karl, D. Carbon utilization in the mesopelagic zone: AOU-DOC relationships
m) Karl, D. HOT/JGOFS program objectives: A brief overview
n) Karl, D. P-control of N2 fixation: An ecosystem model
o) Karl, D. Primary production and particle flux
p) Karl, D. et al. Review and re-assessment of core measurements: Suggestions for refinement and improvement
q) Karl, D. and G. Tien. Low-level SRP above the nutricline at Station ALOHA
r) Karl, D., L. Tupas, G. Tien and B. Popp. "High-temperature" DOC: Pools and implications
s) Karl, D., K. Yanagi and K. Bjorkman. Composition and turnover of oceanic DOP
t) Letelier, R. Temporal variability of algal accessory pigments at Station ALOHA: What does it tell about the phytoplankton community structure at the DCML?
u) Letelier, R. and D. Hebel. Evaluation of fluorometric and HPLC chlorophyll a measurements at Station ALOHA
v) Letelier, R. and F. Santiago-Mandujano. Wind, sea surface temperature and significant wave height records from NDBC buoy #51001 compared to ship observations at Station ALOHA
w) Lukas, R. Water mass variability observed in the Hawaii Ocean Time-series
x) Sadler, D., C. Winn and C. Carrillo. Time-series measurements of pH: A new approach for HOT
y) Schudlich, R. Upper ocean gas modelling at Station ALOHA
z) Winn, C. DIC variability
aa) Winn, C. and C. Carrillo. DIC and alkalinity profiles and elemental ratios

2) Presentations from the "HOT Golden Anniversary Science Symposium," 16 November 1993, East-West Center, Honolulu, HI
a) Bingham, F. M. The oceanographic context of HOT
b) Campbell, L., H. Nolla, H. Liu and D. Vaulot. Phytoplankton population dynamics at the Hawaii Ocean Time series Station ALOHA
c) Campbell, L., H. Nolla and D. Vaulot. The importance of Prochlorococcus to community structure in the central North Pacific Ocean
d) Christian, J. Vertical fluxes of carbon and nitrogen at Station ALOHA

e) Dore, J. Nitrate diffusive flux cannot support new production during quiescent periods at Station ALOHA
f) Dore, J. Nitrification in lower euphotic zone at Station ALOHA: Patterns and significance
g) Firing, E. The north Hawaiian ridge current and other flows near ALOHA
h) Hebel, D. Temporal distribution, abundance and variability of suspended particualte matter (particulate carbon, nitrogen and phosphorus) at Station ALOHA -- Observations of a seasonal cycle
i) Karl, D., D. Hebel, L. Tupas, J. Dore and C. Winn. Station ALOHA particle fluxes and estimates of export production
j) Karl, D. M., R. Letelier, L. Tupas, J. Dore, D. Hebel and C. Winn. N2 fixation as a contributor to new production at Station ALOHA
k) Karl, D. M., G. Tien and K. Yanagi. Phosphorus dynamics at Station ALOHA
l) Kennan, S. C. Possibilities for stirring along the Hawaiian ridge
m) Krothapalli, S., Y. H. Li and F. T. Mackenzie. What controls the temporal variability of carbon flux at Station ALOHA?
n) Letelier, R. M. Inorganic carbon assimilation at Station ALOHA: Possible evidence of a change in carbon fluxes
o) Letelier, R. M. Spatial and temporal distribution of Trichodesmium sp. at Station ALOHA: How important are they?
p) Liu, H. and L. Campbell. Measurement of growth and mortality rates of *Prochlorococcus* and *Synechococcus* at Station ALOHA using a new selective inhibitor technique
q) Lukas, R. and F. Bingham. Annual and interannual variations of hydrographic properties observed in the Hawaii Ocean Time-series (HOT)
r) Lukas, R., F. M. Bingham and A. Mantyla An anomalous cold event in the bottom water observed at Station ALOHA
s) Moyer, C. L., L. Campbell, D. M. Karl and J. Wilcox. Restriction fragment length polymorphism (RFLP) and DNA sequence analysis of PCR-generated clones to assess diversity of picoeukaryotic algae in the subtropical central North Pacific Ocean (Station ALOHA)
t) Polovina, J. J. and D. R. Kobayashi. HOT and Hawaii's fisheries landings: Complementary or independent time-series?
u) Sadler, D. Time series measurement of pH at Station ALOHA
v) Smith, C. R., D. J. DeMaster, R. H. Pope, S. P. Garner, D. J. Hoover and S. E. Doan. Seabed radionuclides, bioturbation and benthic community structure at the Hawaii Ocean Time-series Station ALOHA
w) Tupas, L. M., B. N. Popp and D. M. Karl. Dissolved organic carbon in oligotrophic waters: Experiments on sample preservation, storage and analysis
x) Winn, C. D. Air-sea carbon dioxide exchange at Station ALOHA
y) Yuan, J.and C. I. Measures. Sampling and analysis of dissolved iron

3) Presentations from the "HOT-75 Commemorative Science Symposium," 9 September 1996, East-West Center, Honolulu, HI
a) Atkinson, M. A Potentiostatic, Solid-state Oxygen Sensor for Oceanic CTDs
b) Bidigare, R., M. Latasa, R. Andersen and M. Keller. A Comparison of HPLC Pigment Signatures and Electron Microscopic Observations for Oligotrophic Waters of the North Atlantic and North Pacific Oceans

c) Campbell, L., H. Liu, H. Nolla and D. Vaulot. Annual Variability of Phytoplankton and Bacteria in the Subtropical North Pacific Ocean at Station ALOHA during the 1991- 1994 ENSO Event
d) Christian, J., M. Lewis and D. Karl. Vertical Fluxes of Carbon, Nitrogen and Phosphorus at the US-JGOFS Time-Series Station ALOHA
e) Dore, J. and D. Karl. Nitrification, New Production and Nitrous Oxide at Station ALOHA
f) Ducklow, H. Joint Global Ocean Flux Study -- Vision and Progress
g) Emerson, S., C. Stump and D. Wilber. Inert Gases as Tracers of Diapycnal Mixing in the Upper Ocean
h) Firing, E. Currents in the Vicinity of Station ALOHA: An Update
i) Fujieki, L. HOT-DOGS: A New Tool for HOT Program Data Base Analysis and Presentation
j) Hebel, D., L. Tupas and D. Karl. The Importance of Organic Exudates in the Measurement of Oligotrophic Ocean Primary Productivity
k) Karl, D., D. Hebel and L. Tupas. Regionalization of Station ALOHA
l) Karl, D., G. Tien, K. Bjrkman, K. Yanagi, R.Letelier, A. Colman and A. Thomson. The "Forgotten" Open Ocean P-Cycle
m) Karl, D., L. Tupas, D. Hebel, R. Letelier, J. Christian and J. Dore. Station ALOHA N-Cycle: The Case for N_2 Fixation
n) Landry, M., K. Selph and H. Al-Mutairi. Seasonal and Diurnal Variability of the Mesozooplankton Community at Ocean Station ALOHA
o) Letelier, R. and M. Abbott. Effects of a Subsurface *Trichodesmium* spp. Bloom on the Optical Reflectance Measured in the Upper 150 m of the Water Column in the North Pacific Subtropical Gyre
p) Liu, H., L. Campbell and H. Nolla. Prochlorococcus Growth Rate and Daily Variability at Station ALOHA
q) Lopez, M. and M. Huntley. Particle Concentrations at the Hawaii Ocean Time-series Station (Station ALOHA) Measured with an Optical Plankton Counter
r) Michaels, A. and A. Knap. The Bermuda Atlantic Time-Series Study (BATS): A View from the "Other" Ocean
s) Nolla, H., J. Kirshtein, M. Landry, D. Karl, L. Campbell and D. Pence. Flow Cytometry Correction Factors for Enumeration of Heterotrophic Bacteria and Phytoplankton
t) Quay, P. and H. Anderson. A Dissolved Inorganic Carbon Budget at Station ALOHA
u) Santiago-Mandujano, F. and R. Lukas. Cold Bottom Water Events Observed in the Hawaii Ocean Time-Series: Modelling and Implications for Vertical Mixing
v) Scharek, R., M. Latasa, D. Karl and R. Bidigare. Vertical Flux of Diatoms at the JGOFS/WOCE Station ALOHA
w) Smith, C., R. Miller, R. Pope and D. DeMaster. Seafloor Inventories of Pb-210, Th-234 and Benthic Biomass as Proxies for Deep POC Flux: Placing Export Production at the HOT Station in a General Oceanic Context
x) Tien, G., D. Pence and D. Karl. Hydrogen Peroxide Measurements at Station ALOHA
y) Tupas, L., G. Tien, D. Hebel and D. Karl. Dissolved Organic Carbon Dynamics in the Upper Water Column at Station ALOHA
z) Vink, S., K. Falkner, V. Tersol, J. Yuan and C. Measures. Variations in Iron, Aluminum, Beryllium and Barium Concentrations in Surface Waters at Station ALOHA
aa) Winn, C. Secular Changes in Inorganic Carbon Parameters at HOT and BATS

8.0 DATA AVAILABILITY AND DISTRIBUTION

Data collected by HOT program scientists are made available to the oceanographic community in various ways as soon after processing as possible. The complete data set, containing data collected since year 1 of the HOT program (1988-89), as well as 2 dbar averaged CTD data, are available from a pair of workstations at the University of Hawaii, and may be accessed using anonymous File Transer Protocol (FTP) or the World Wide Web (WWW).

8.1 File Transfer Protocol

In order to maximize ease of access, the data are in ASCII files. File names are chosen so that they may be copied to DOS machines without ambiguity. (DOS users should be aware that Unix is case-sensitive, and Unix extensions may be longer than 3 characters.)

The data are in a subdirectory called ***/pub/hot***. More information about the data base is given in several files called ***Readme.**** at this level. The file ***Readme.first*** gives general information on the data base; we encourage users to read it first.

The following is an example of how to use FTP to obtain HOT data. The user's command are denoted by bold italicized text. The workstation's Internet address is ***mana.soest.hawaii.edu***, or ***128.171.154.9*** (either address should work). All hydrographic information reside at this address. Biogeochemical and optical data are stored at ***hahana.soest.hawaii.edu***, or ***128. 171. 153. 101***.

1. At the Prompt >, type ***ftp 128.171.154.9*** or ***ftp mana.soest.hawaii.edu.***

2. When asked for your login name, type ***anonymous***.

3. When asked for a password, type in your email address.

4. To change to the HOT database, type ***cd /pub/hot***. To view files type **ls**. A directory of files and subdirectories will appear.

5a. To obtain information about the database type ***get Readme.first***. This will transfer an ASCII file to your system. Use any text editor to view it.

5b. To obtain a list of publications, type ***cd publication-list*** then ***get hotpub.lis***.

5c. To obtain the HOT Field and Laboratory Protocols manual, type ***cd protocols*** then ***get 1142.asc***.

5d. To obtain CTD data, type ***cd ctd/hot-#***, where # is the HOT cruise of interest, then type ***mget *.ctd*** to transfer all the cruise CTD files to your system.

5e. To obtain water column data, type ***cd water***, then ***get <filename>*** where the filename is hot#.gof (JGOFS data) or hot#.sea (WOCE data) and # is the HOT cruise of interest.

6. To exit type ***bye***.

7. Optical parameters are located on another server. To obtain light data, at the prompt type ***ftp 128.171.153.101*** or ***ftp hahana.soest.hawaii.edu*** then follow steps 2 to 4.

To access data from recent cruises (data preliminarily calibrated and quality controlled), the user is required to submit a simple registration form available at www.soest.hawaii.edu/HOT_WOCE/regis-form.html. After submitting the registration form, an e-mail will be sent to the user with further instructions on how to access the data.

8.2 World Wide Web

The Hawaii Ocean Time-series Program maintains a site on the World Wide Web where data and information about the program and its activities can easily be accessed over the Internet. The address is http://hahana.soest.hawaii.edu/hot/hot.html. This web page is the springboard from which the homepages of the Physical Oceanographic and JGOFS components are accessible. The first half of the most recent year's hydrographic data is usually available by July and the second half by January the following year with certain quality control caveats. All data are quality controlled by around June of the following year. Downloading of data is through FTP but the web pages provide a more detailed means of access.

8.3 HOT-DOGS©

HOT-DOGS is the acronym for the HOT Data Organization and Graphical System. It's address is http://hahana.soest.hawaii.edu/hot/hot-dogs/interface.html. HOT-DOGS is a Matlab™ based program that displays HOT data in a graphical format as depth profiles or time-series plots. In addition to its graphical capabilities, HOT-DOGS provides a means of downloading selected data parameters during specific years of the program. The user may perform the following:

- **Data Extraction**
  - Bottle (Rosette)
  - Microzooplankton (Nets)
  - Particle Flux
  - Primary Production

- **Display**
  - Bottle (Rosette)
  - CTD
  - HPLC Pigments
  - Particle Flux
  - Primary Production
  - Solar Irradiance
  - Underway Measurments
  - User Defined

- **Standard Depths** (vertical Water-Column)
  - Bottle (Rosette)
  - HPLC Pigments
  - Primary Production
  - User Defined

- **Time-series**
  - Bottle (Rosette)
  - HPLC Pigments
  - Particle Flux
  - Primary Production
  - User Defined

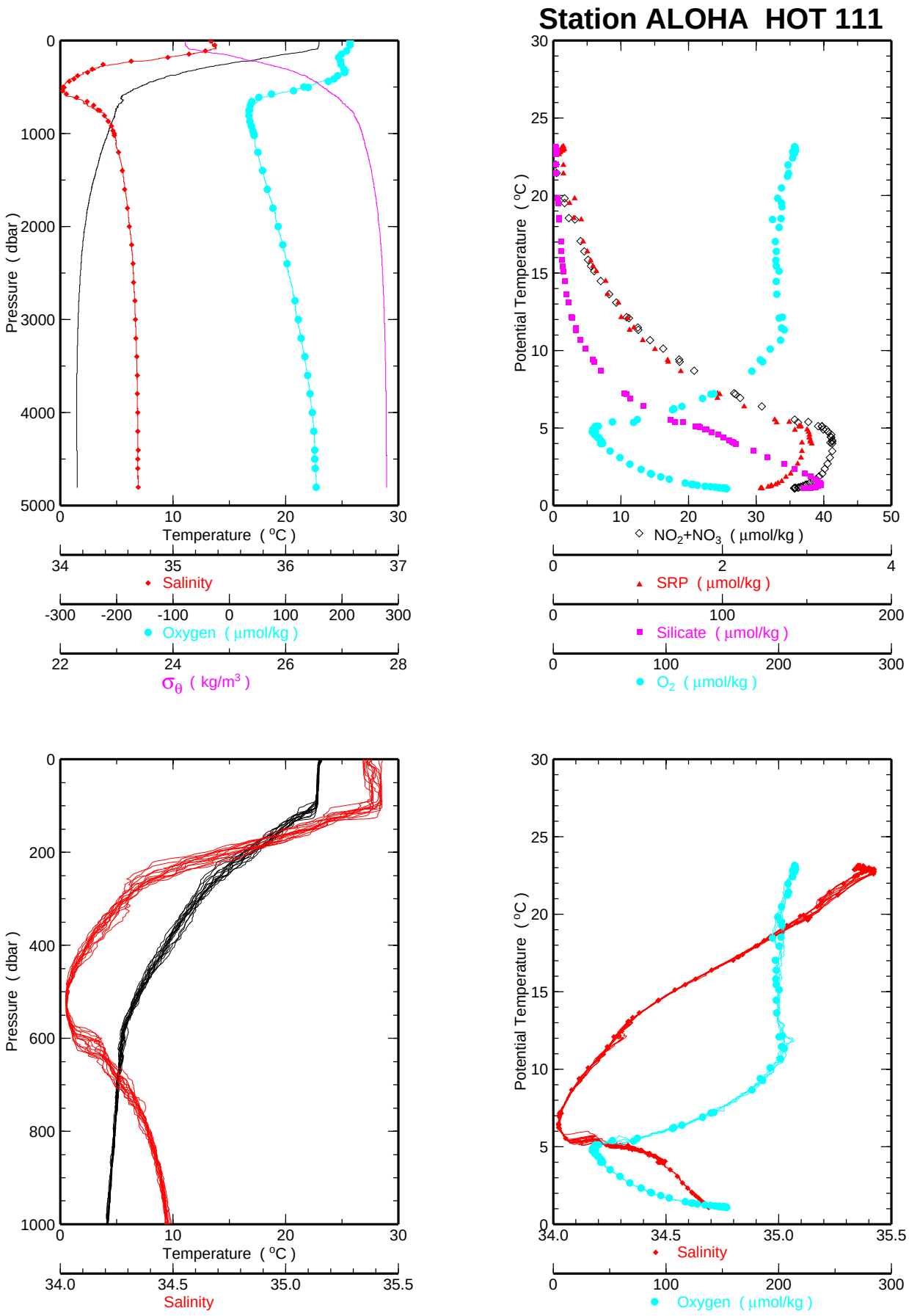
Station ALOHA HOT 111
Pressure (dbar)
Temperature (°C)
Salinity
Oxygen (µmol/kg)
σθ (kg/m3)
Potential Temperature (°C)
NO2+NO3 (µmol/kg)
SRP (µmol/kg)
Silicate (µmol/kg)
O2 (µmol/kg)

Figure 6.1.1a

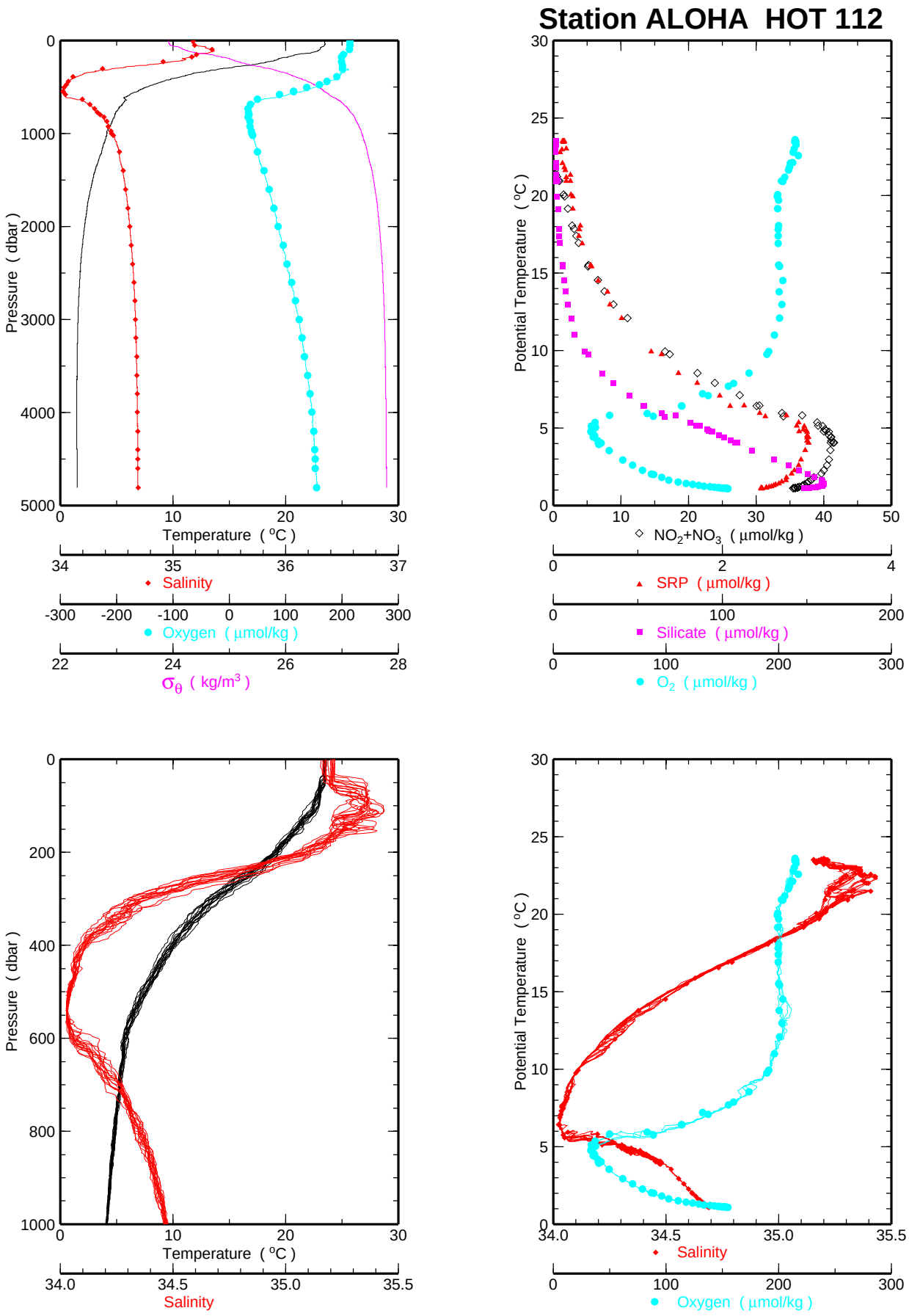
Station ALOHA HOT 112
Pressure (dbar)
Temperature (°C)
Salinity
Oxygen (µmol/kg)
σθ (kg/m3)
Potential Temperature (°C)
NO2+NO3 (µmol/kg)
SRP (µmol/kg)
Silicate (µmol/kg)
O2 (µmol/kg)

Figure 6.1.1b

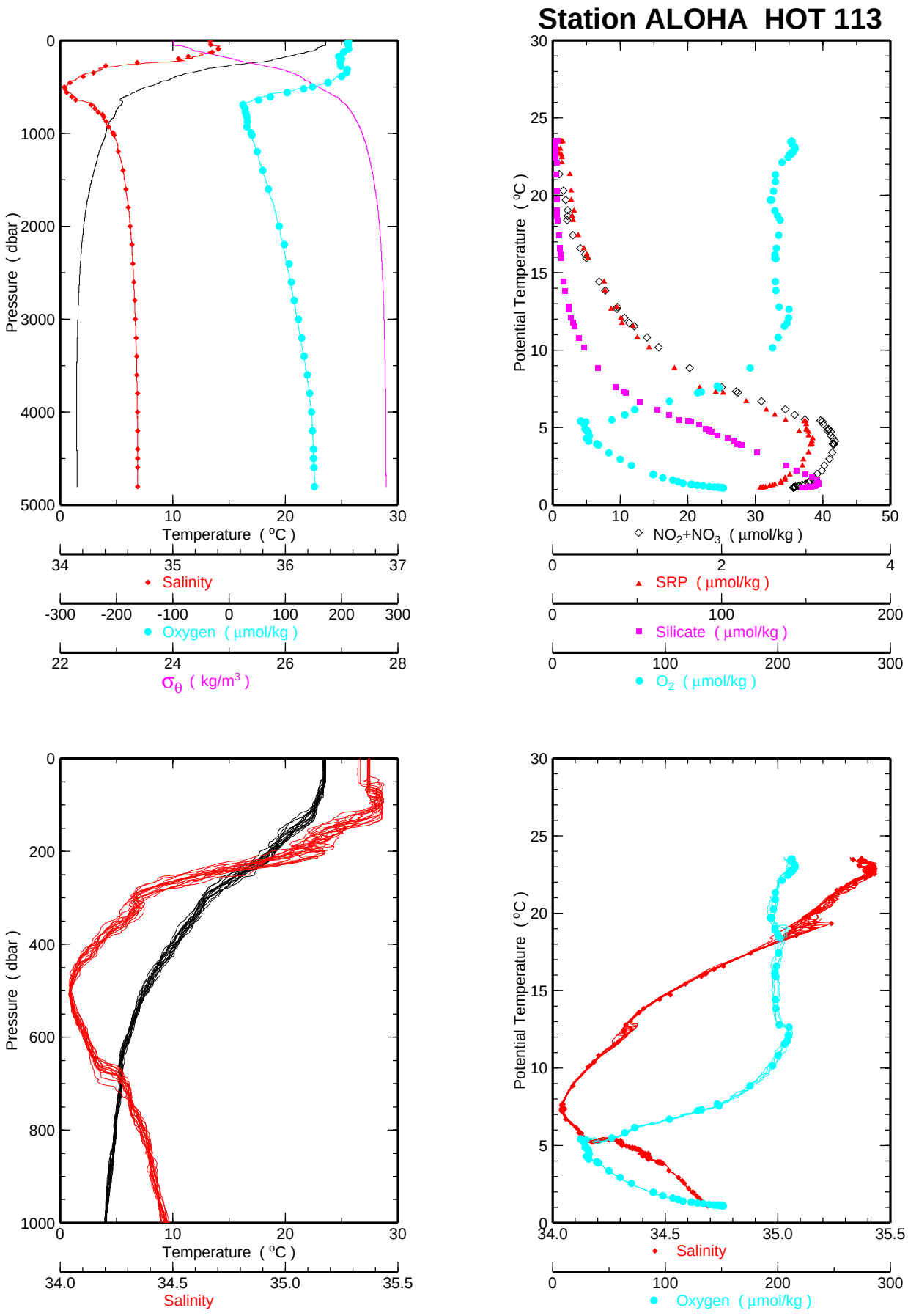
Station ALOHA HOT 113
Pressure (dbar)
Temperature (°C)
Salinity
Oxygen (µmol/kg)
σθ (kg/m3)
Potential Temperature (°C)
NO2+NO3 (µmol/kg)
SRP (µmol/kg)
Silicate (µmol/kg)
O2 (µmol/kg)

Figure 6.1.1c

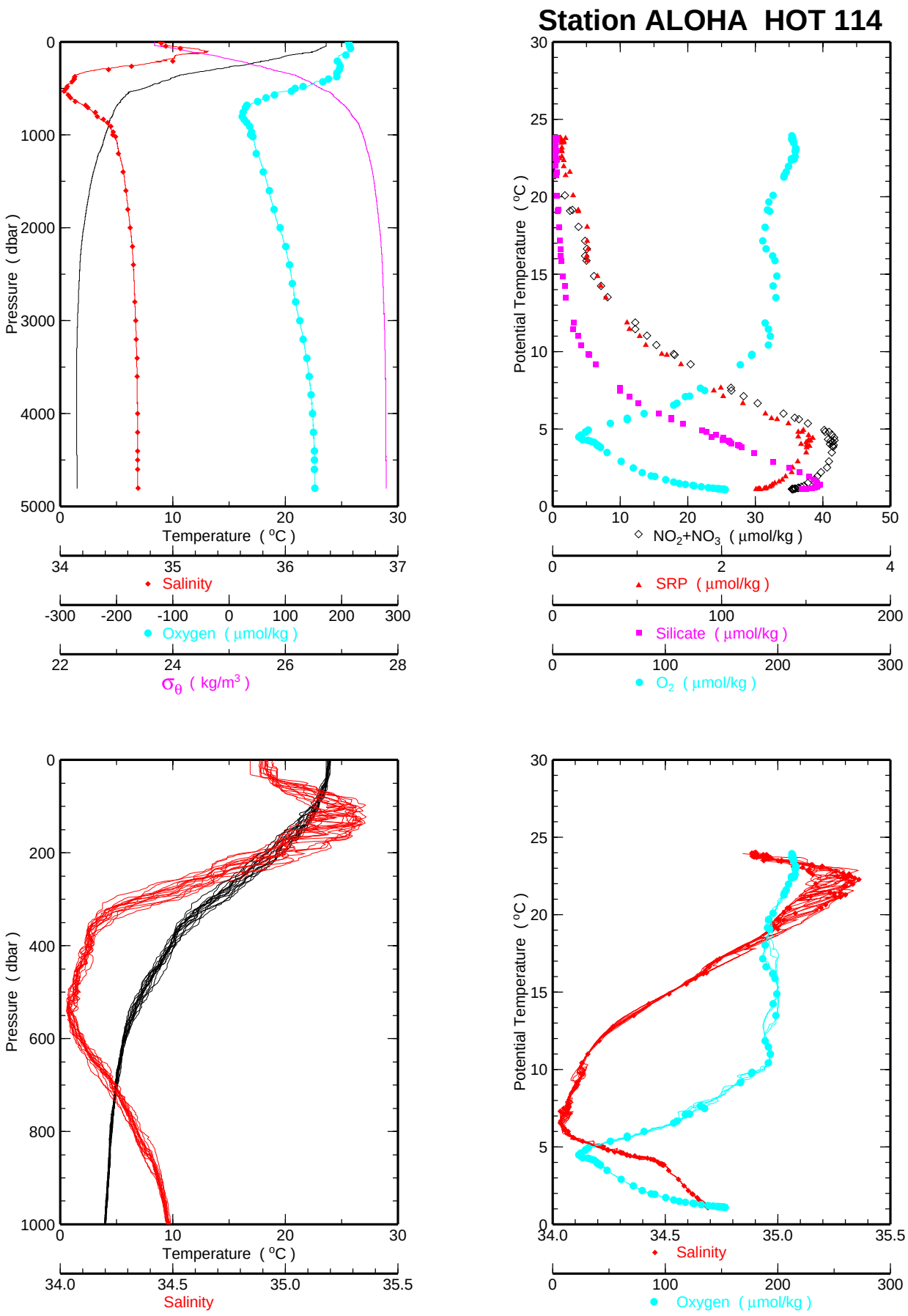
Station ALOHA HOT 114
Pressure (dbar)
Temperature (°C)
Salinity
Oxygen (µmol/kg)
σθ (kg/m3)
Potential Temperature (°C)
NO2+NO3 (µmol/kg)
SRP (µmol/kg)
Silicate (µmol/kg)
O2 (µmol/kg)

Figure 6.1.1d

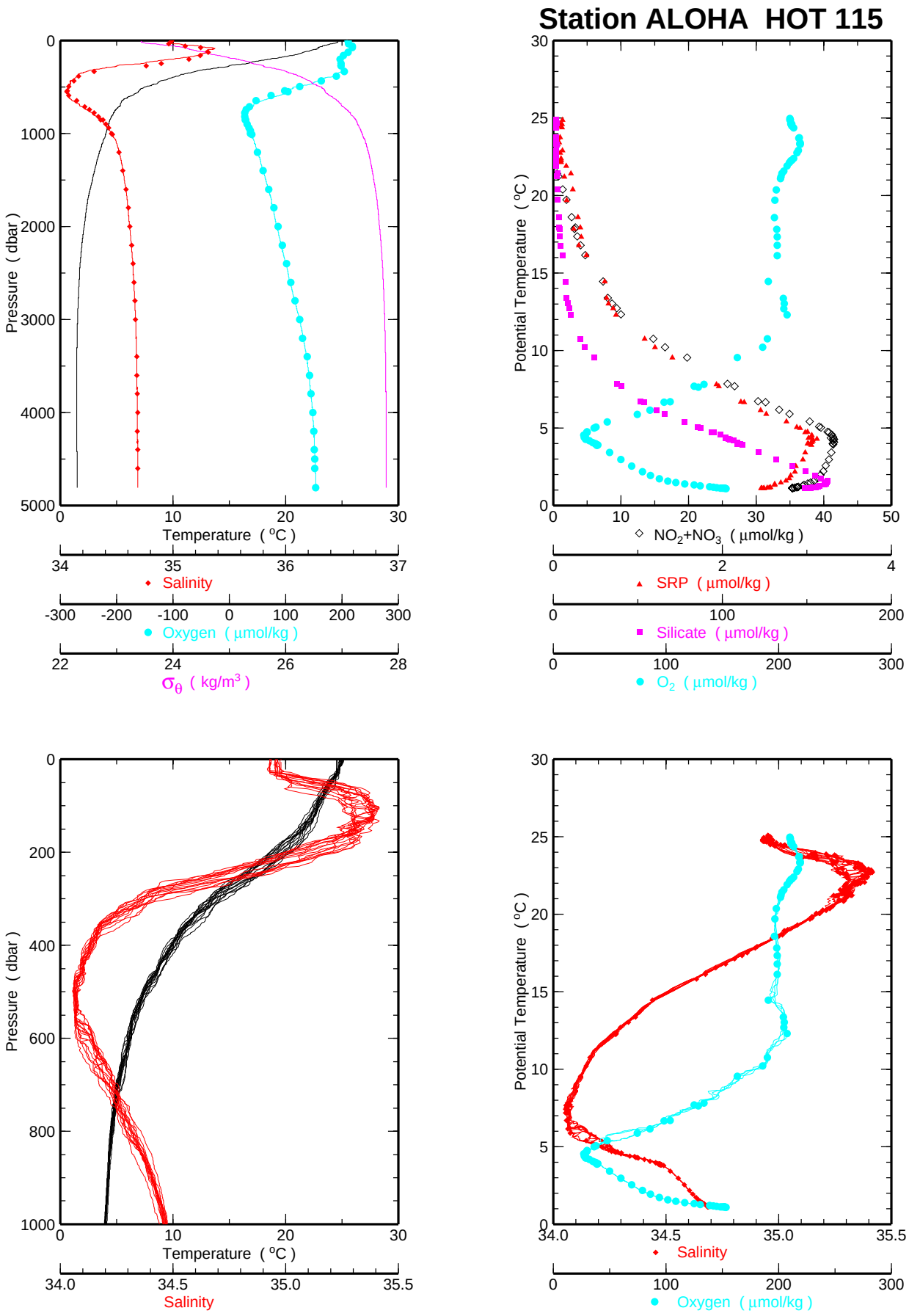
Station ALOHA HOT 115
Pressure (dbar)
Temperature (°C)
Salinity
Oxygen (µmol/kg)
σθ (kg/m3)
Potential Temperature (°C)
NO2+NO3 (µmol/kg)
SRP (µmol/kg)
Silicate (µmol/kg)
O2 (µmol/kg)

Figure 6.1.1e

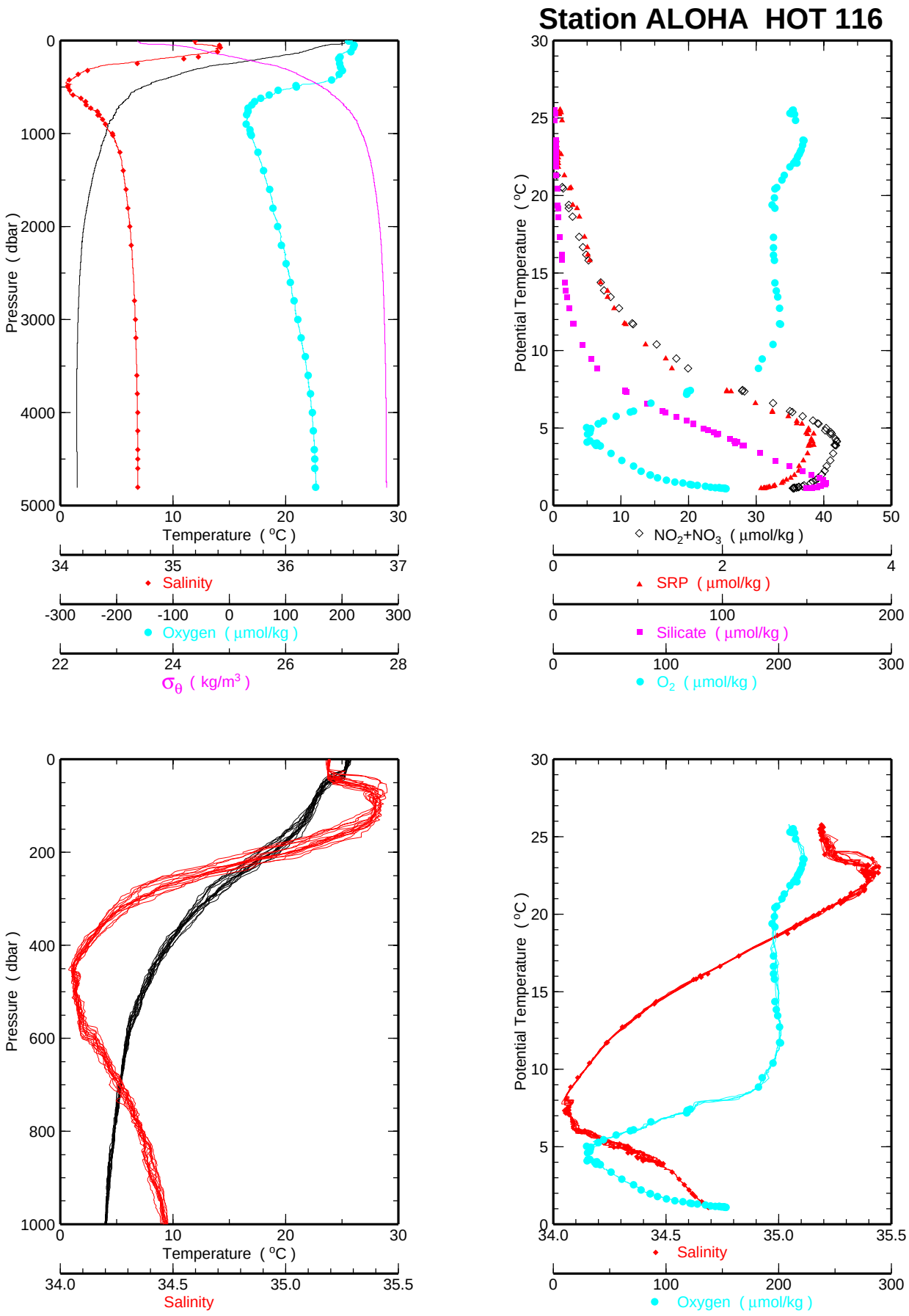
Station ALOHA HOT 116
Pressure (dbar)
Temperature (°C)
Salinity
Oxygen (µmol/kg)
σθ (kg/m3)
Potential Temperature (°C)
NO2+NO3 (µmol/kg)
SRP (µmol/kg)
Silicate (µmol/kg)
O2 (µmol/kg)

Figure 6.1.1f

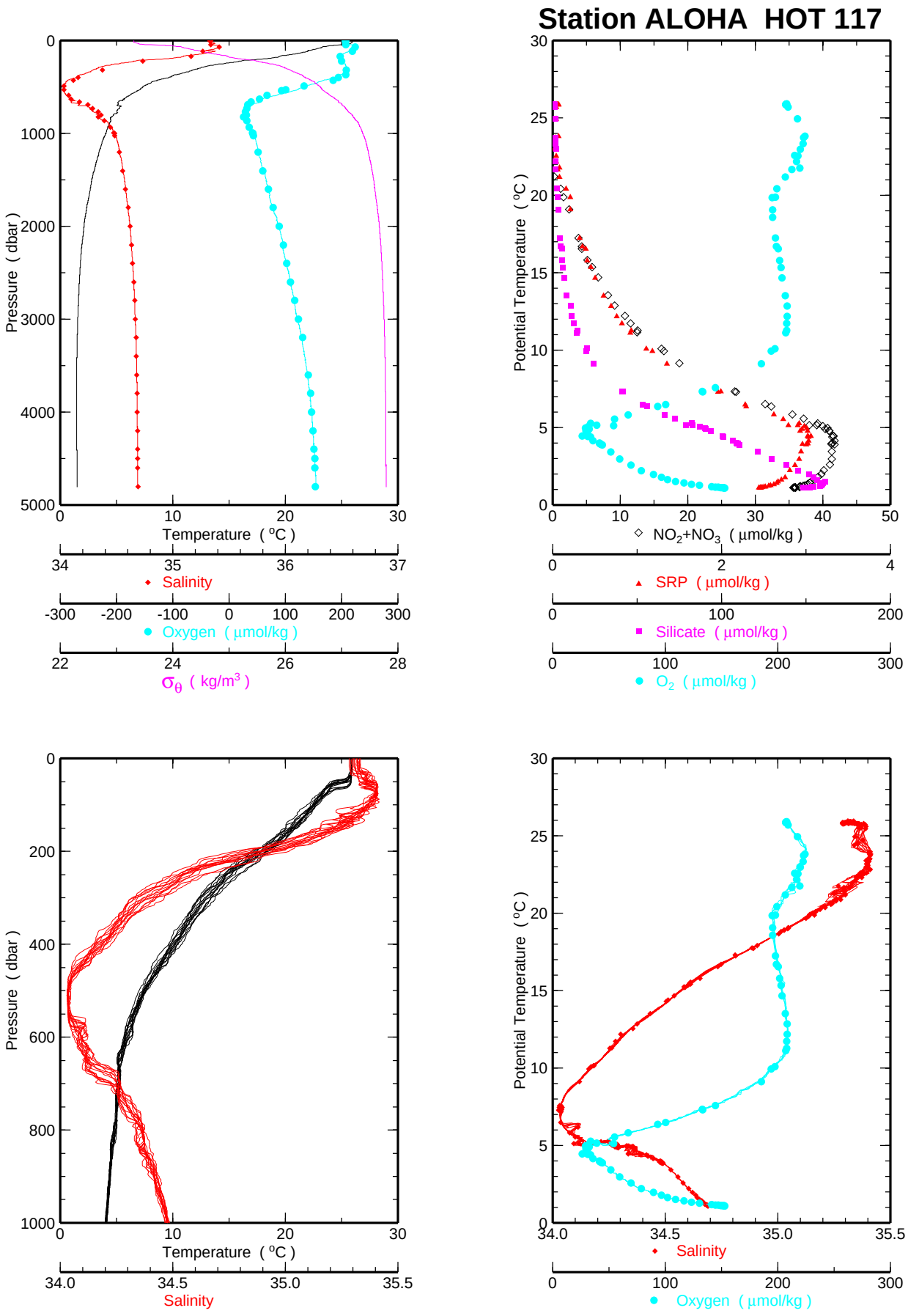
Station ALOHA HOT 117
Pressure (dbar)
Temperature (°C)
Salinity
Oxygen (µmol/kg)
σθ (kg/m3)
Potential Temperature (°C)
NO2+NO3 (µmol/kg)
SRP (µmol/kg)
Silicate (µmol/kg)
O2 (µmol/kg)

Figure 6.1.1g

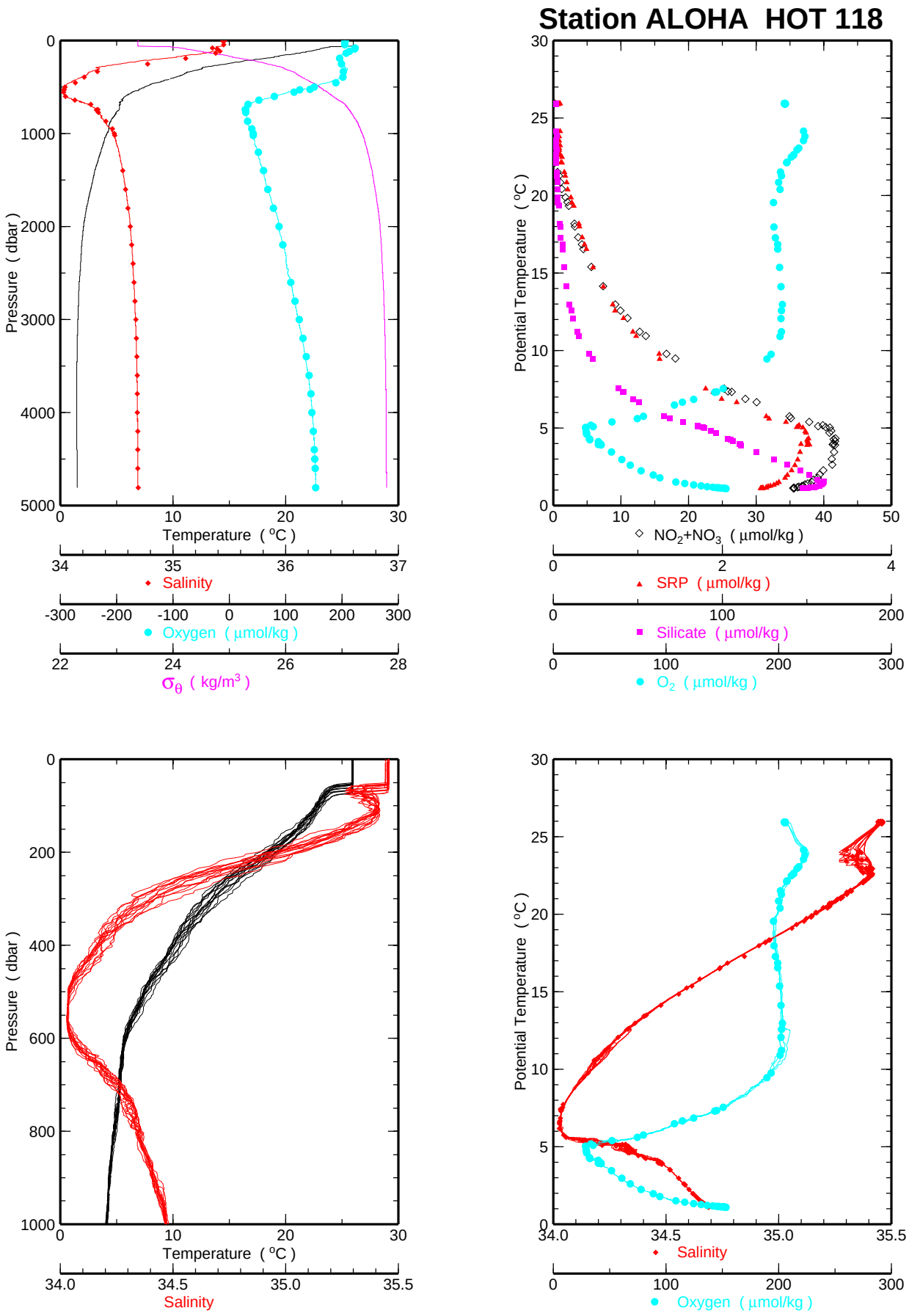
Station ALOHA HOT 118
Pressure (dbar)
Temperature (°C)
Salinity
Oxygen (µmol/kg)
σθ (kg/m3)
Potential Temperature (°C)
NO2+NO3 (µmol/kg)
SRP (µmol/kg)
Silicate (µmol/kg)
O2 (µmol/kg)

Figure 6.1.1h

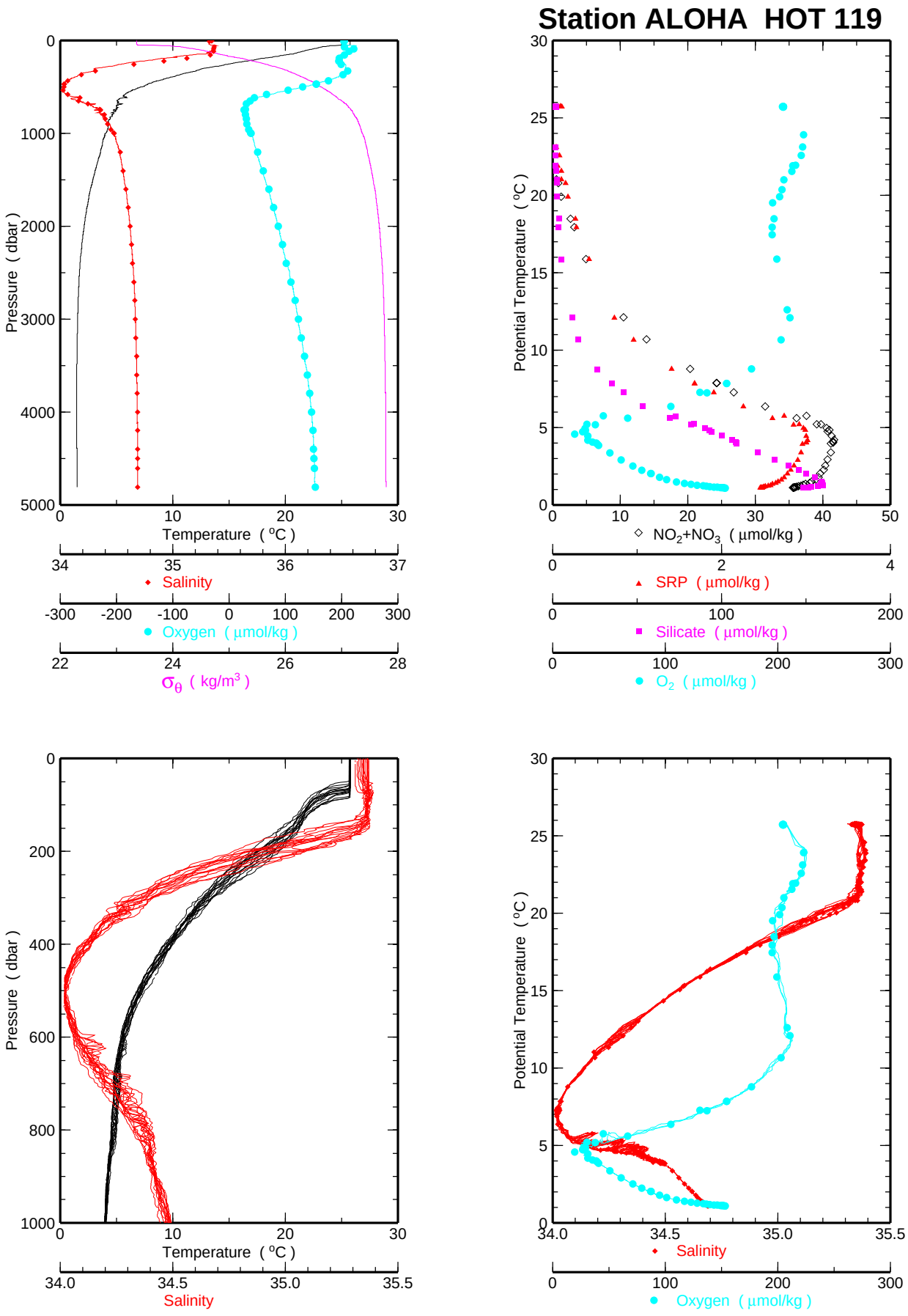
Station ALOHA HOT 119
Pressure (dbar)
Temperature (°C)
Salinity
Oxygen (µmol/kg)
σθ (kg/m3)
Potential Temperature (°C)
NO2+NO3 (µmol/kg)
SRP (µmol/kg)
Silicate (µmol/kg)
O2 (µmol/kg)

Figure 6.1.1i

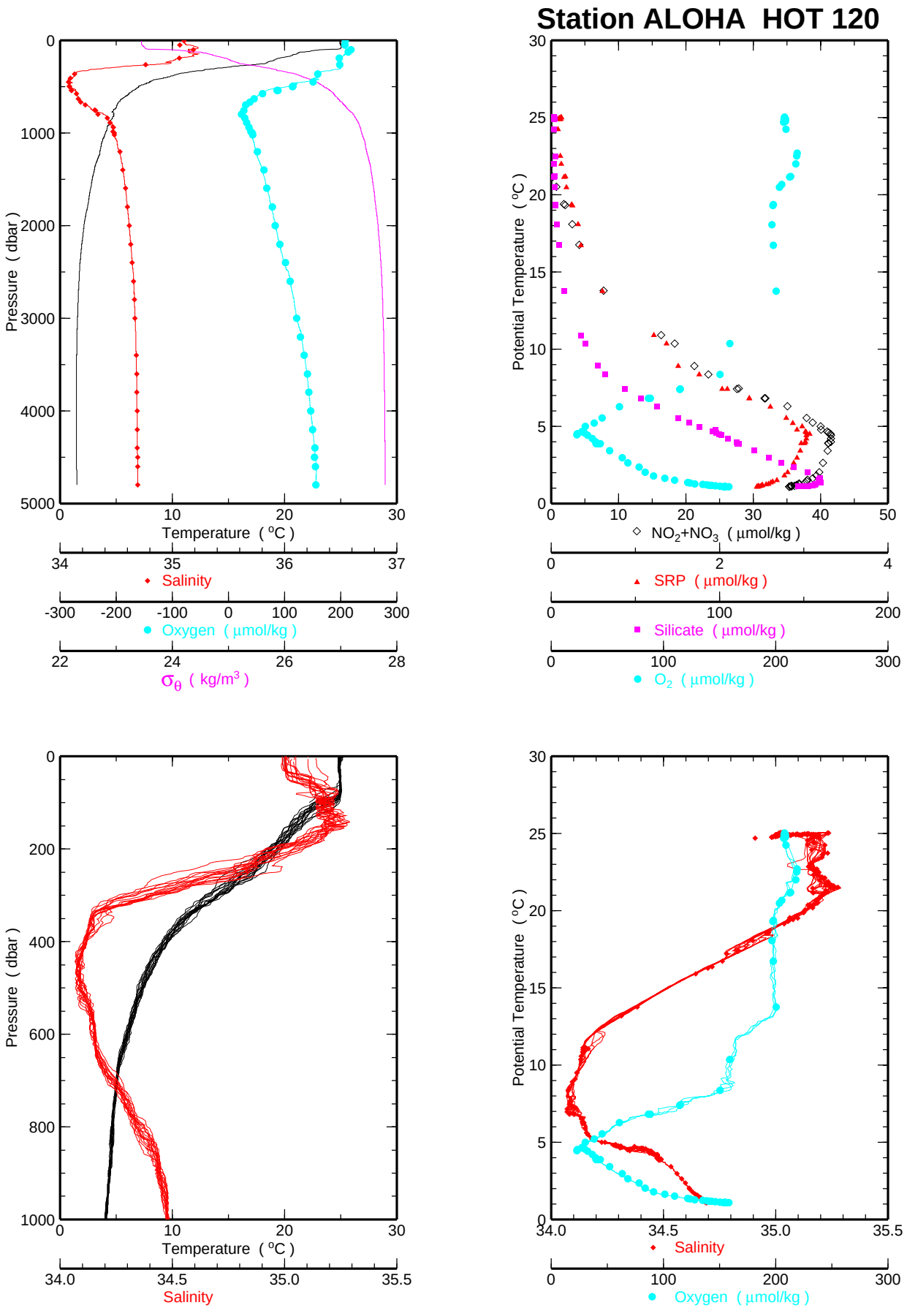
Station ALOHA HOT 120
Pressure (dbar)
Temperature (°C)
Salinity
Oxygen (µmol/kg)
σθ (kg/m3)
Potential Temperature (°C)
NO2+NO3 (µmol/kg)
SRP (µmol/kg)
Silicate (µmol/kg)
O2 (µmol/kg)

Figure 6.1.1j

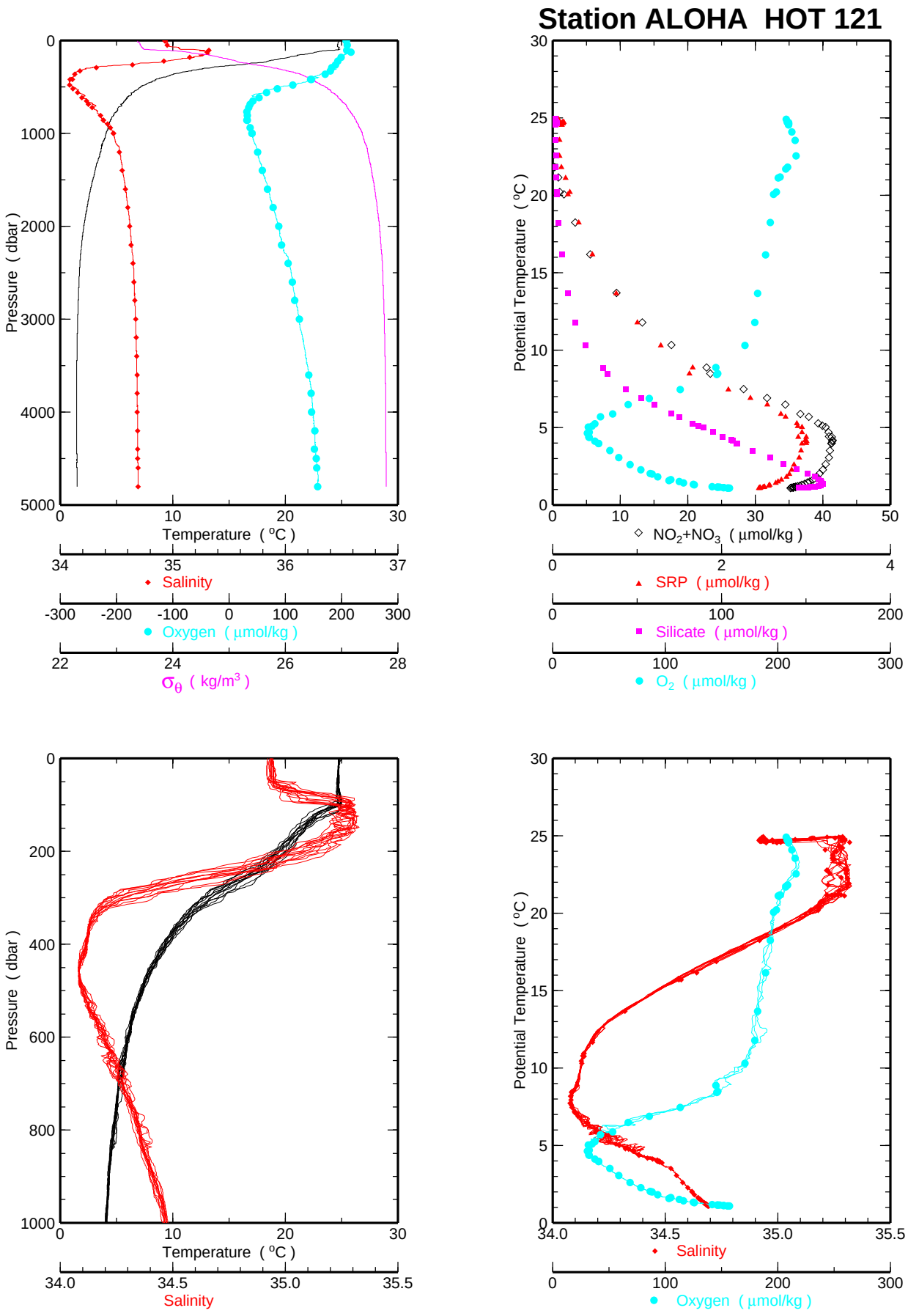
Station ALOHA HOT 121
Pressure (dbar)
Temperature (°C)
Salinity
Oxygen (µmol/kg)
σθ (kg/m3)
Potential Temperature (°C)
NO2+NO3 (µmol/kg)
SRP (µmol/kg)
Silicate (µmol/kg)
O2 (µmol/kg)

Figure 6.1.1k

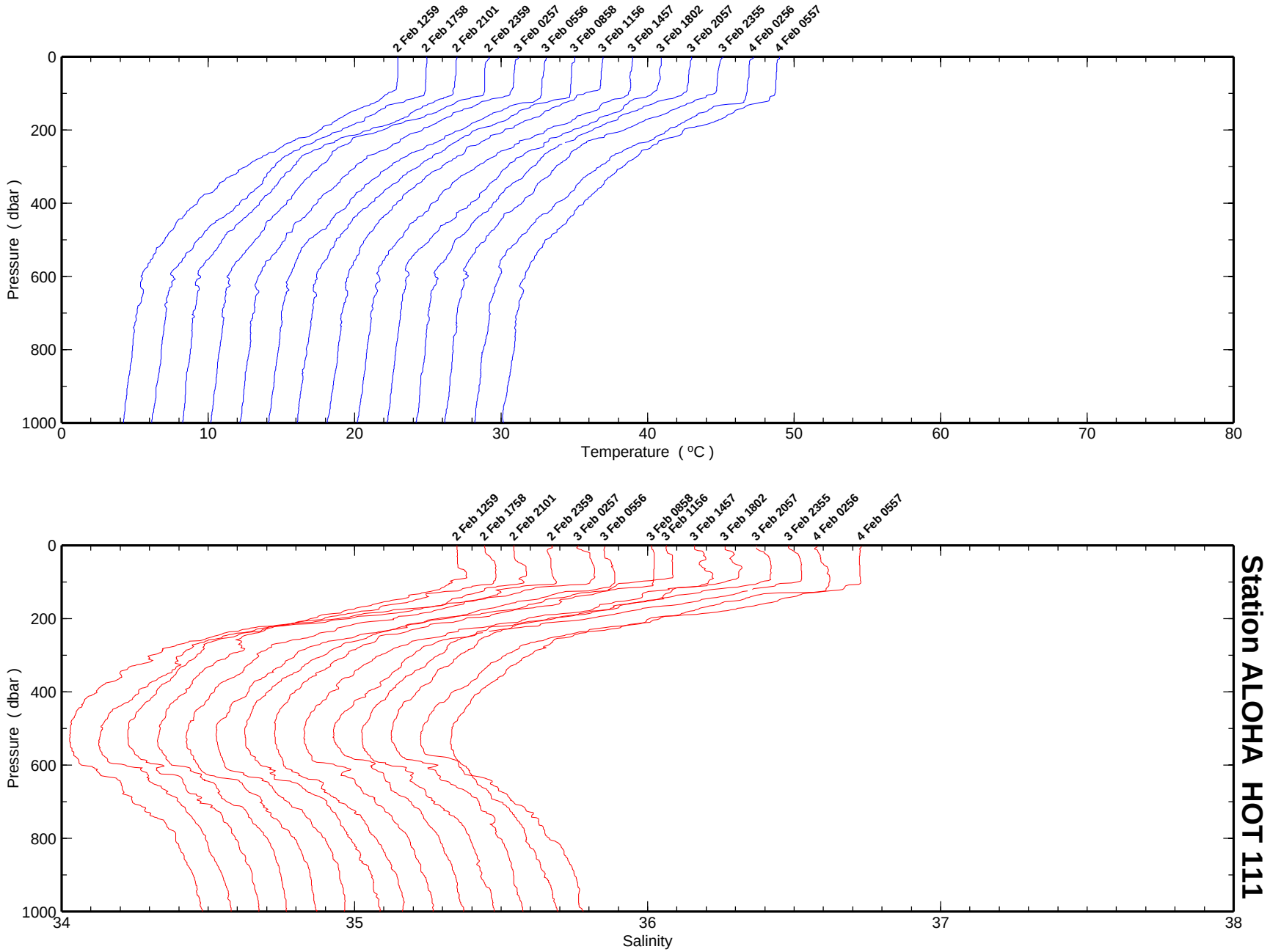
2 Feb 1259
2 Feb 1758
2 Feb 2101
2 Feb 2359
3 Feb 0257
3 Feb 0556
3 Feb 0858
3 Feb 1156
3 Feb 1457
3 Feb 1802
3 Feb 2057
3 Feb 2355
4 Feb 0256
4 Feb 0557
Pressure (dbar)
Temperature (°C)
Salinity
Station ALOHA HOT 111

Figure 6.1.2a

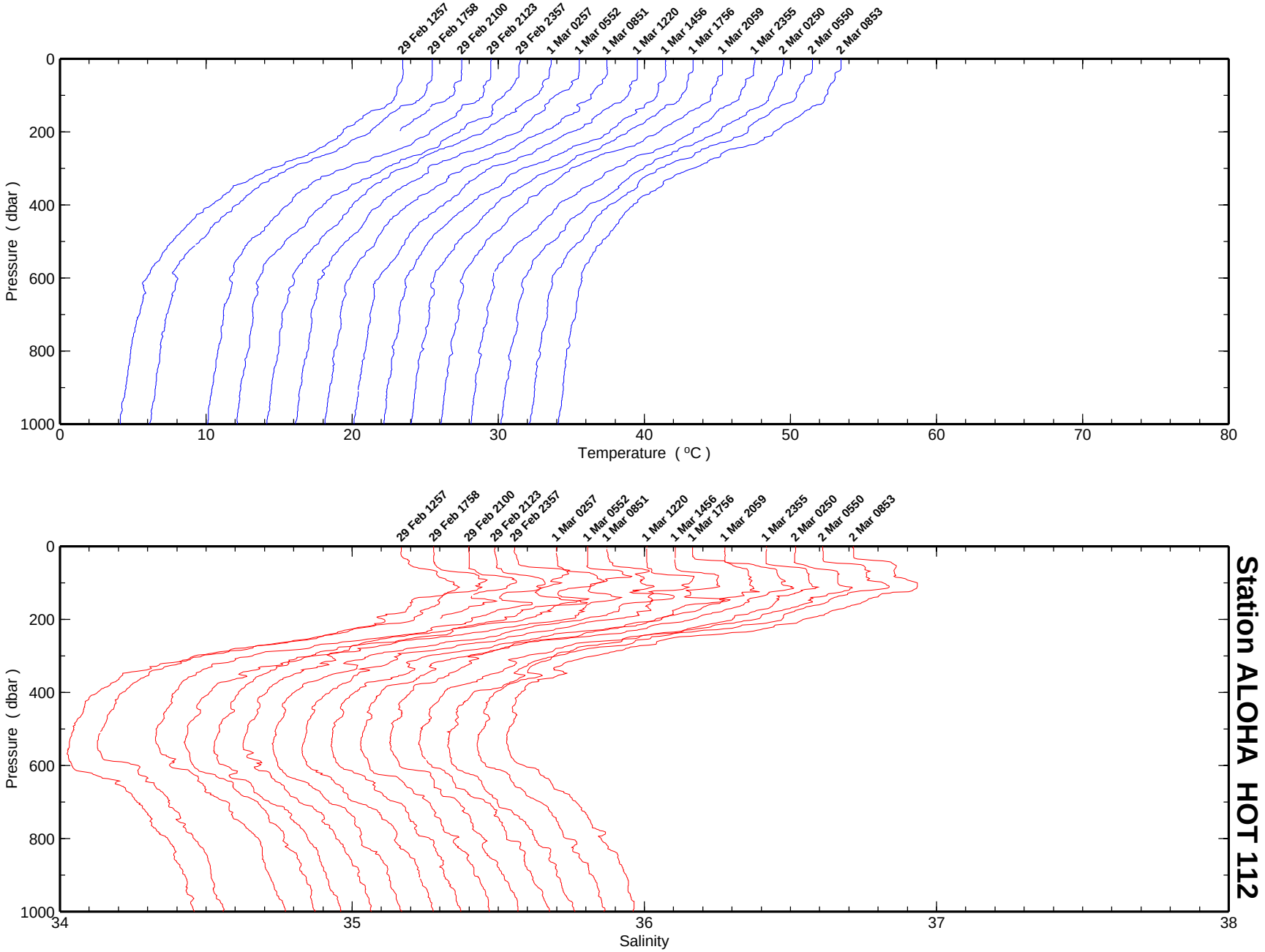
29 Feb 1257
29 Feb 1758
29 Feb 2100
29 Feb 2123
29 Feb 2357
1 Mar 0257
1 Mar 0552
1 Mar 0851
1 Mar 1220
1 Mar 1456
1 Mar 1756
1 Mar 2059
1 Mar 2355
2 Mar 0250
2 Mar 0550
2 Mar 0853
Pressure (dbar)
Temperature (°C)
Salinity
Station ALOHA HOT 112

Figure 6.1.2b

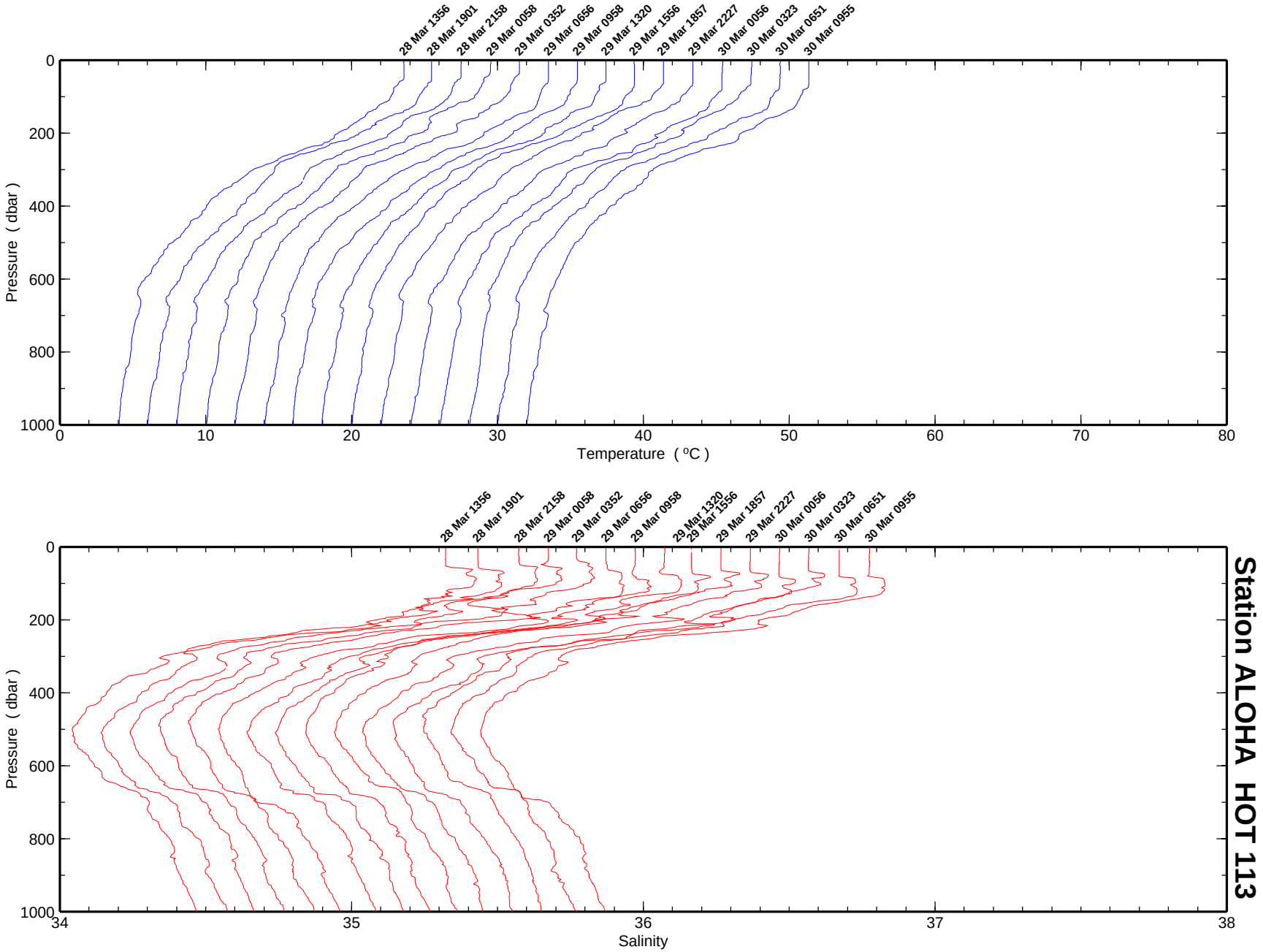
28 Mar 1356
28 Mar 1901
28 Mar 2158
29 Mar 0058
29 Mar 0352
29 Mar 0656
29 Mar 0958
29 Mar 1320
29 Mar 1556
29 Mar 1857
29 Mar 2227
30 Mar 0056
30 Mar 0323
30 Mar 0651
30 Mar 0955
Pressure (dbar)
Temperature (°C)
Salinity
Station ALOHA HOT 113

Figure 6.1.2c

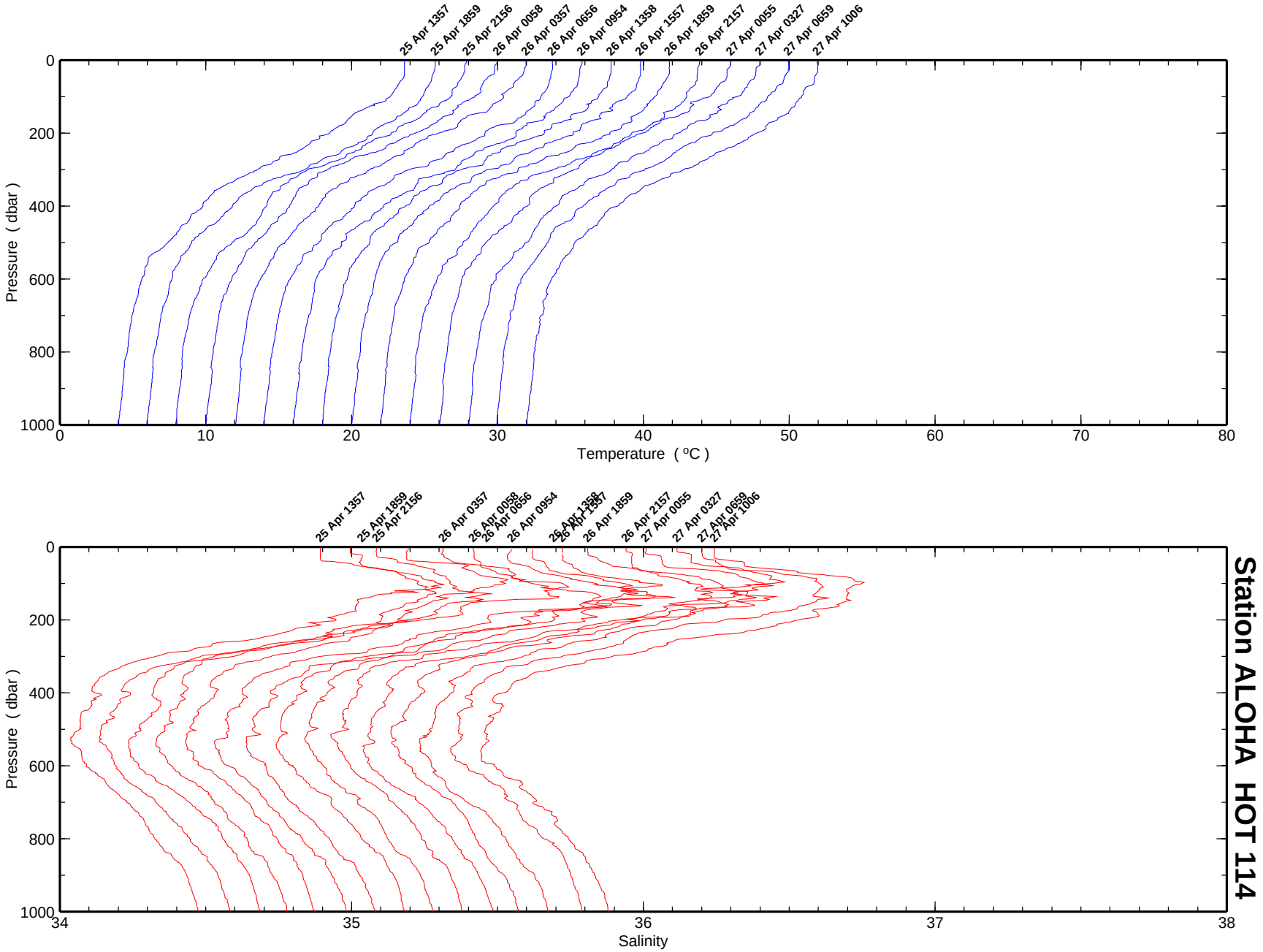
25 Apr 1357
25 Apr 1859
25 Apr 2156
26 Apr 0058
26 Apr 0357
26 Apr 0656
26 Apr 0954
26 Apr 1358
26 Apr 1557
26 Apr 1859
26 Apr 2157
27 Apr 0055
27 Apr 0327
27 Apr 0659
27 Apr 1006
Pressure (dbar)
Temperature (ºC)
Salinity
Station ALOHA HOT 114

Figure 6.1.2d

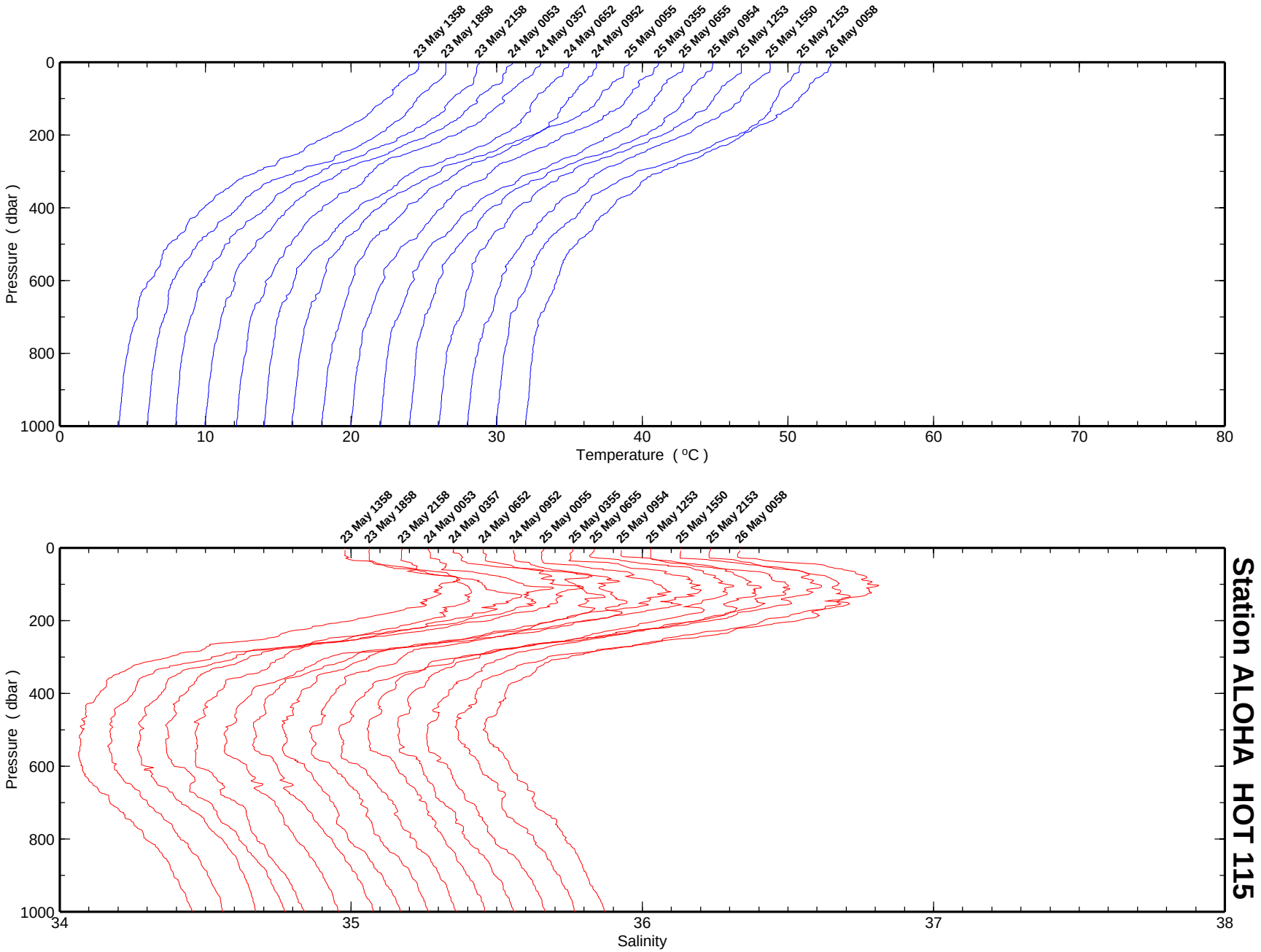
23 May 1358
23 May 1858
23 May 2158
24 May 0053
24 May 0357
24 May 0652
24 May 0952
25 May 0055
25 May 0355
25 May 0655
25 May 0954
25 May 1253
25 May 1550
25 May 2153
26 May 0058
Pressure (dbar)
Temperature (°C)
Salinity
Station ALOHA HOT 115

Figure 6.1.2e

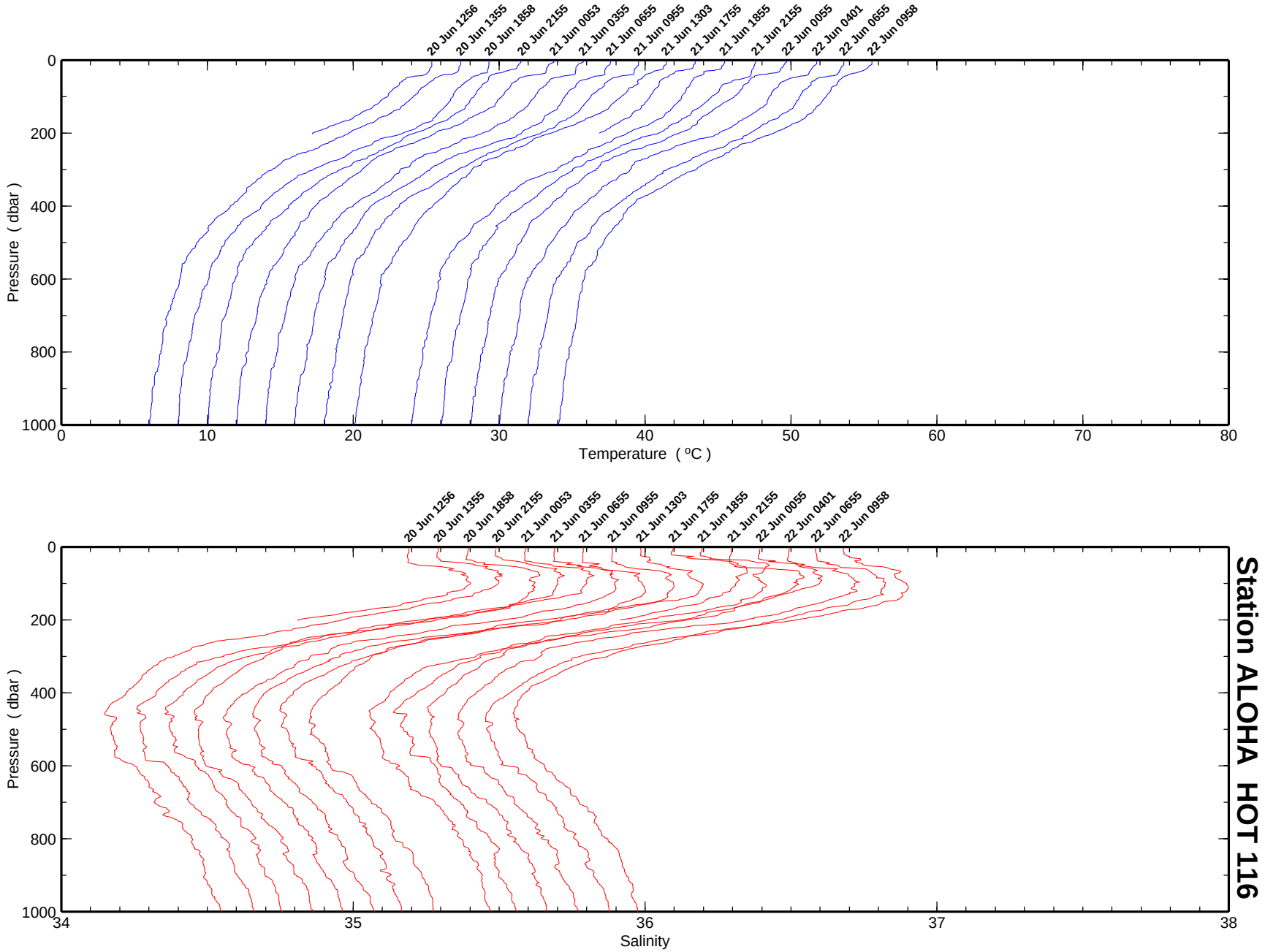
20 Jun 1256
20 Jun 1355
20 Jun 1858
20 Jun 2155
21 Jun 0053
21 Jun 0355
21 Jun 0655
21 Jun 0955
21 Jun 1303
21 Jun 1755
21 Jun 1855
21 Jun 2155
22 Jun 0055
22 Jun 0401
22 Jun 0655
22 Jun 0958
Pressure (dbar)
Temperature (ºC)
Salinity
Station ALOHA HOT 116

Figure 6.1.2f

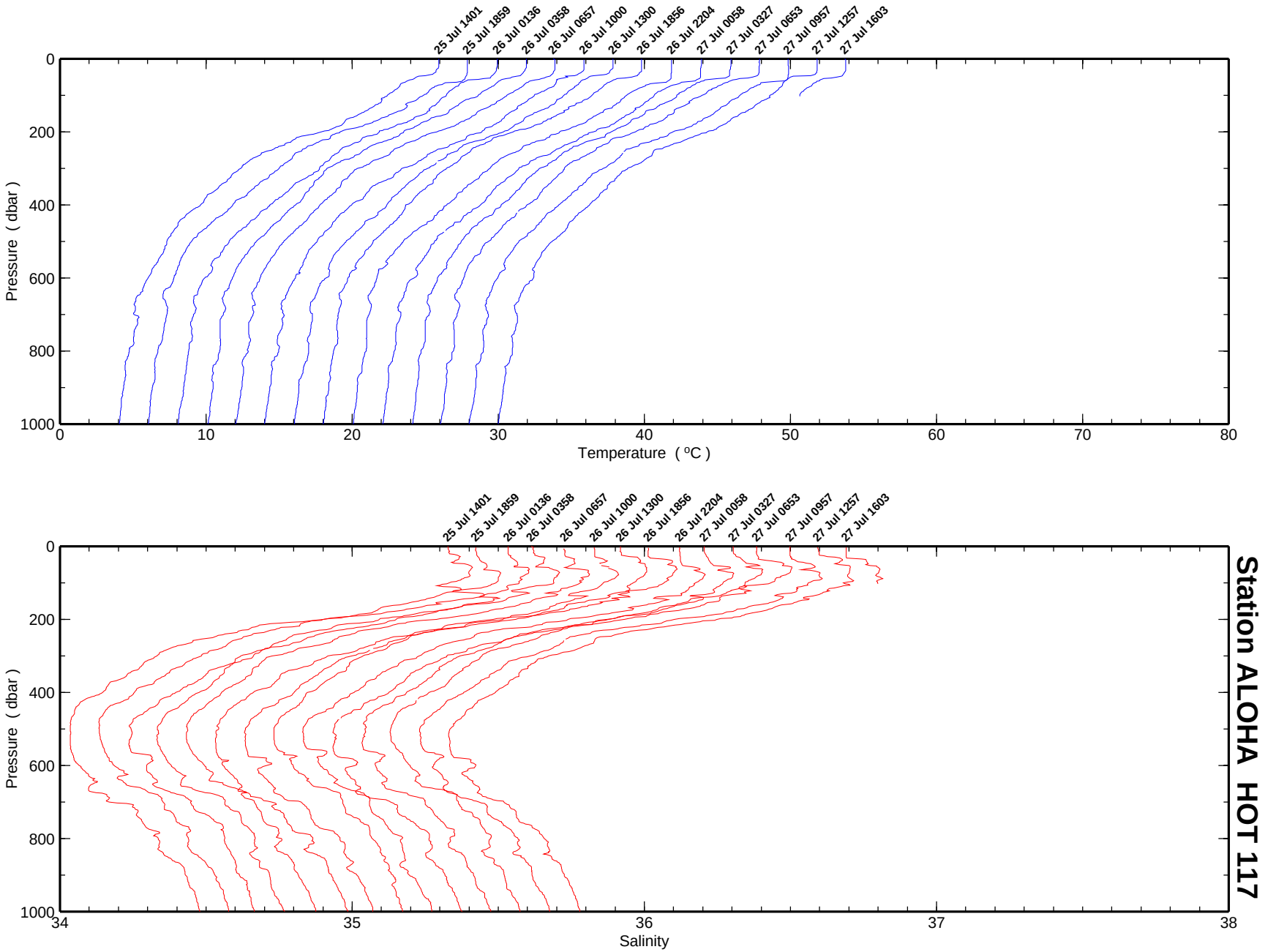
25 Jul 1401
25 Jul 1859
26 Jul 0136
26 Jul 0358
26 Jul 0657
26 Jul 1000
26 Jul 1300
26 Jul 1856
26 Jul 2204
27 Jul 0058
27 Jul 0327
27 Jul 0653
27 Jul 0957
27 Jul 1257
27 Jul 1603
Pressure (dbar)
Temperature (°C)
Salinity
Station ALOHA HOT 117

Figure 6.1.2g

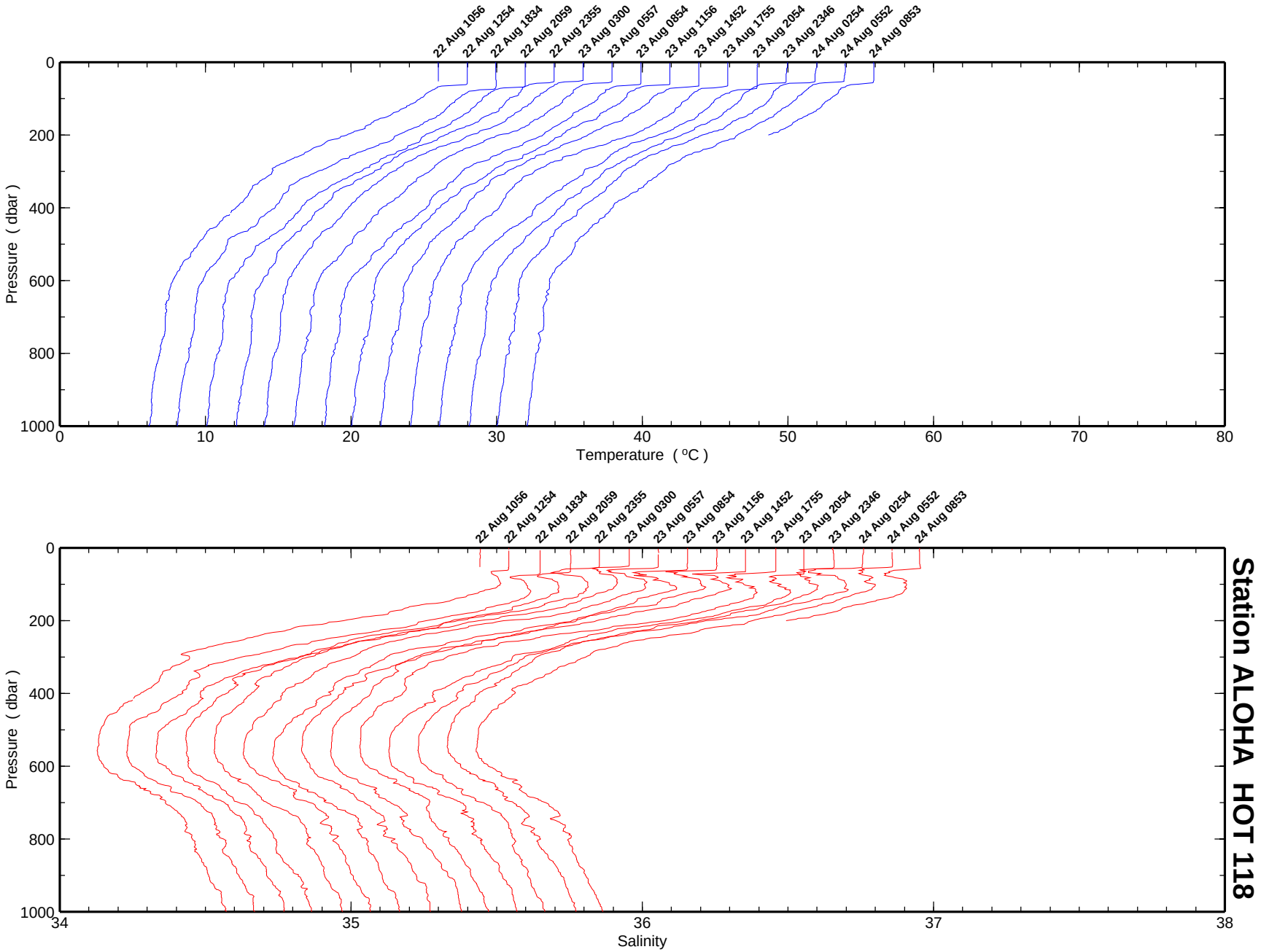
22 Aug 1056
22 Aug 1254
22 Aug 1834
22 Aug 2059
22 Aug 2355
23 Aug 0300
23 Aug 0557
23 Aug 0854
23 Aug 1156
23 Aug 1452
23 Aug 1755
23 Aug 2054
23 Aug 2346
24 Aug 0254
24 Aug 0552
24 Aug 0853
Pressure (dbar)
Temperature (°C)
Salinity
Station ALOHA HOT 118

Figure 6.1.2h

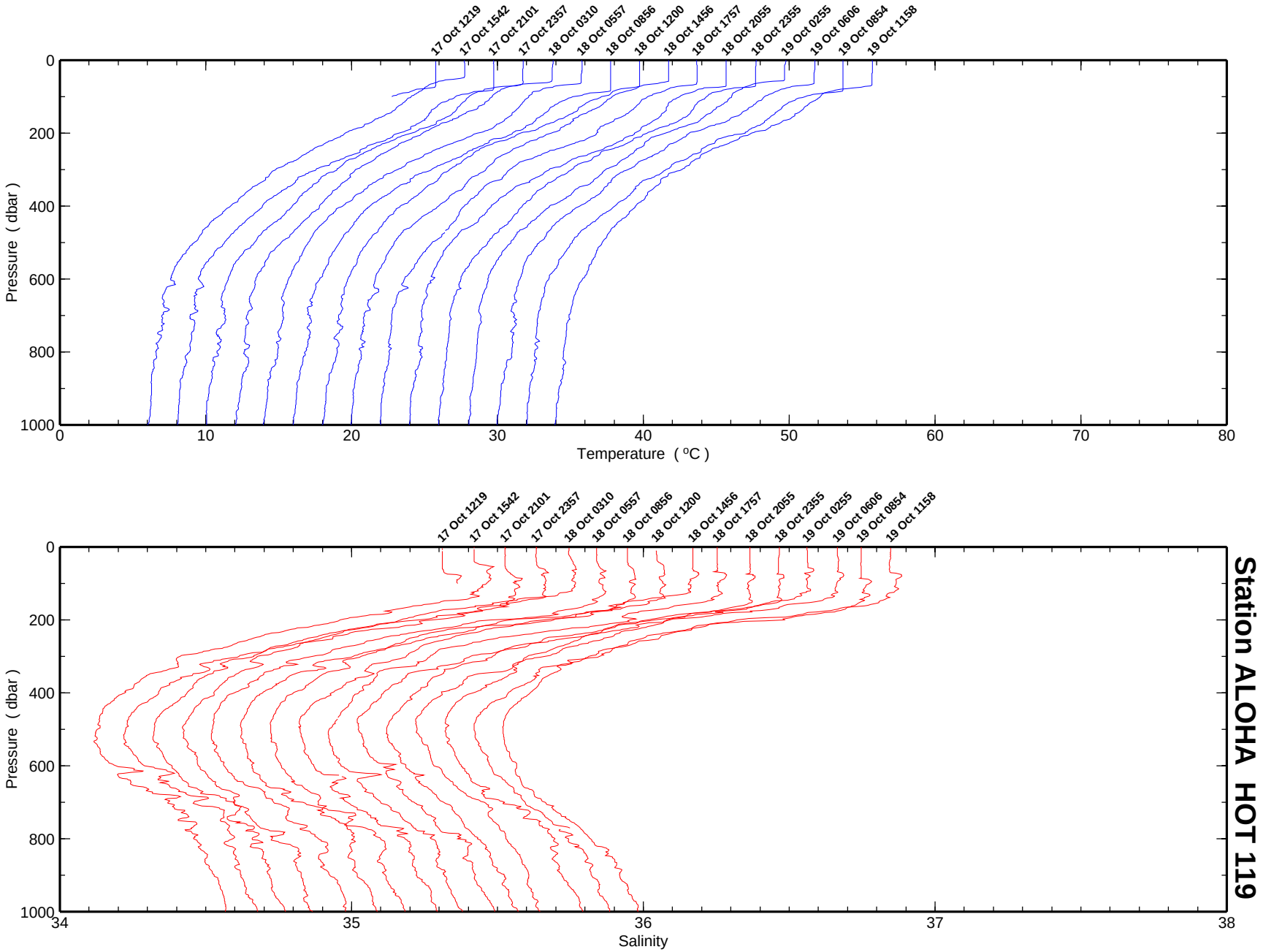
17 Oct 1219
17 Oct 1542
17 Oct 2101
17 Oct 2357
18 Oct 0310
18 Oct 0557
18 Oct 0856
18 Oct 1200
18 Oct 1456
18 Oct 1757
18 Oct 2055
18 Oct 2355
19 Oct 0255
19 Oct 0606
19 Oct 0854
19 Oct 1158
Pressure (dbar)
Temperature (°C)
Salinity
Station ALOHA HOT 119

Figure 6.1.2i

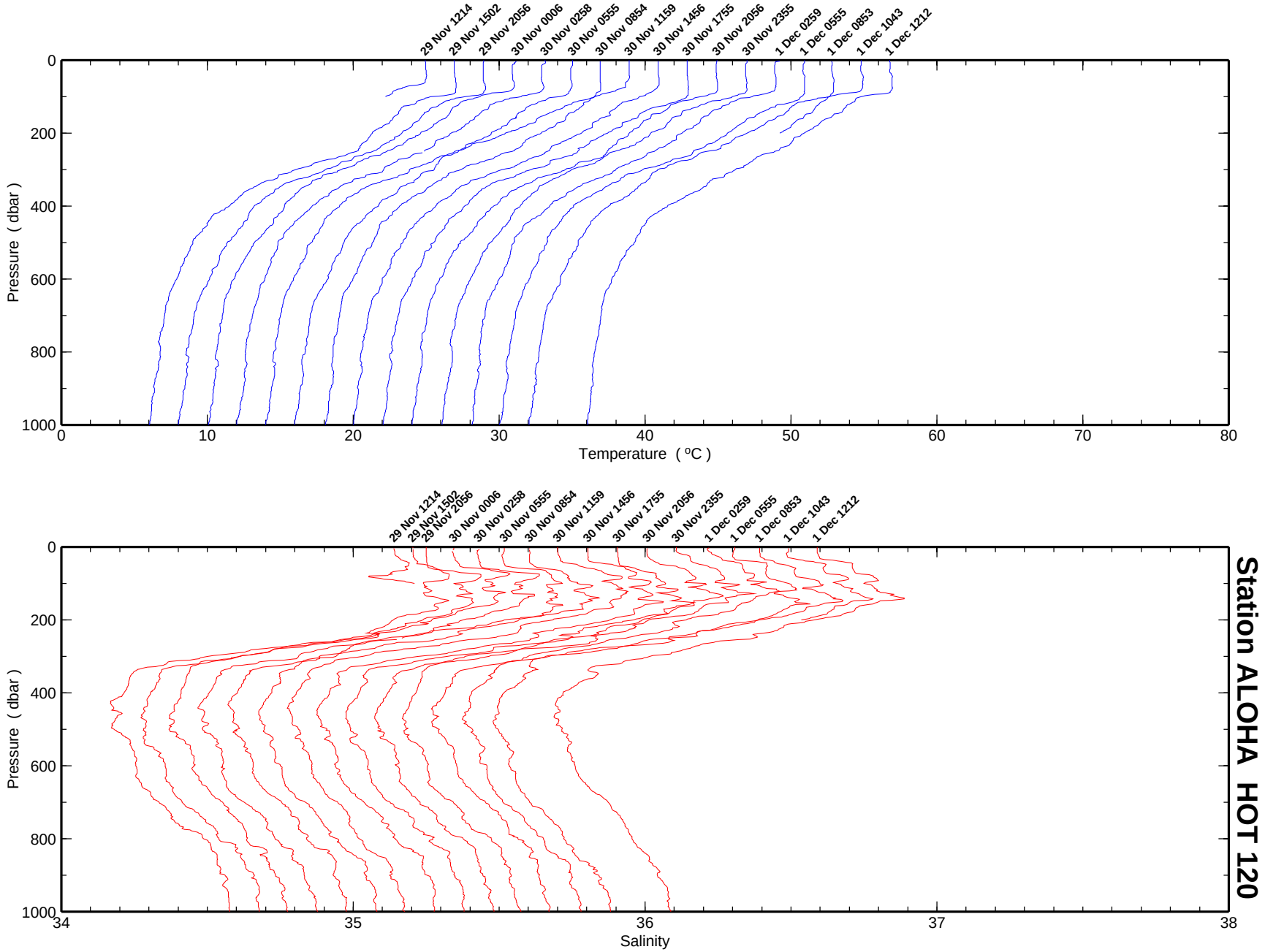
29 Nov 1214
29 Nov 1502
29 Nov 2056
30 Nov 0006
30 Nov 0258
30 Nov 0555
30 Nov 0854
30 Nov 1159
30 Nov 1456
30 Nov 1755
30 Nov 2056
30 Nov 2355
1 Dec 0259
1 Dec 0555
1 Dec 0853
1 Dec 1043
1 Dec 1212
Pressure (dbar)
Temperature (ºC)
Salinity
Station ALOHA HOT 120

Figure 6.1.2j

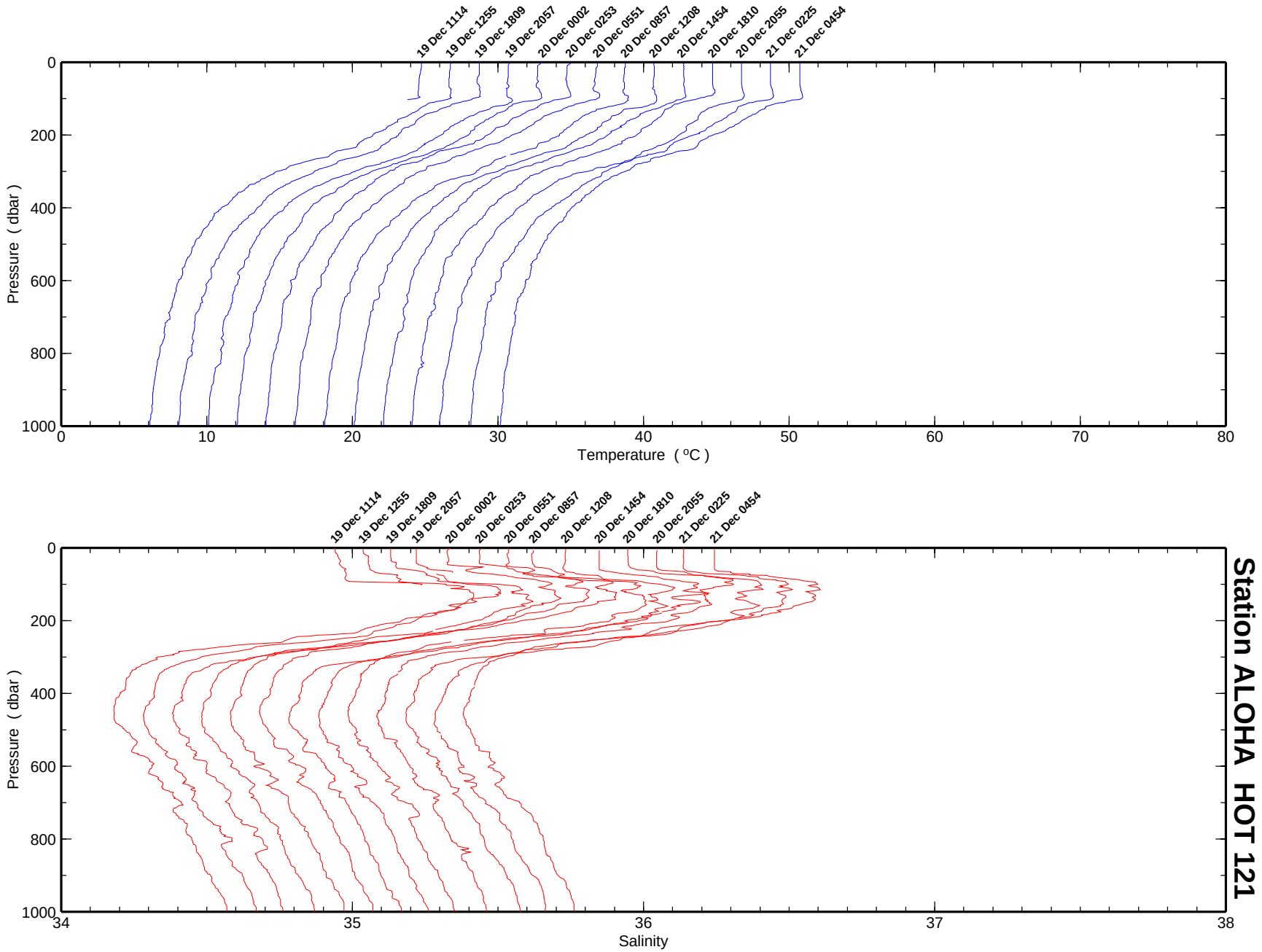
19 Dec 1114
19 Dec 1255
19 Dec 1809
19 Dec 2057
20 Dec 0002
20 Dec 0253
20 Dec 0551
20 Dec 0857
20 Dec 1208
20 Dec 1454
20 Dec 1810
20 Dec 2055
21 Dec 0225
21 Dec 0454
Pressure (dbar)
Temperature (ºC)
Salinity
Station ALOHA HOT 121

Figure 6.1.2k

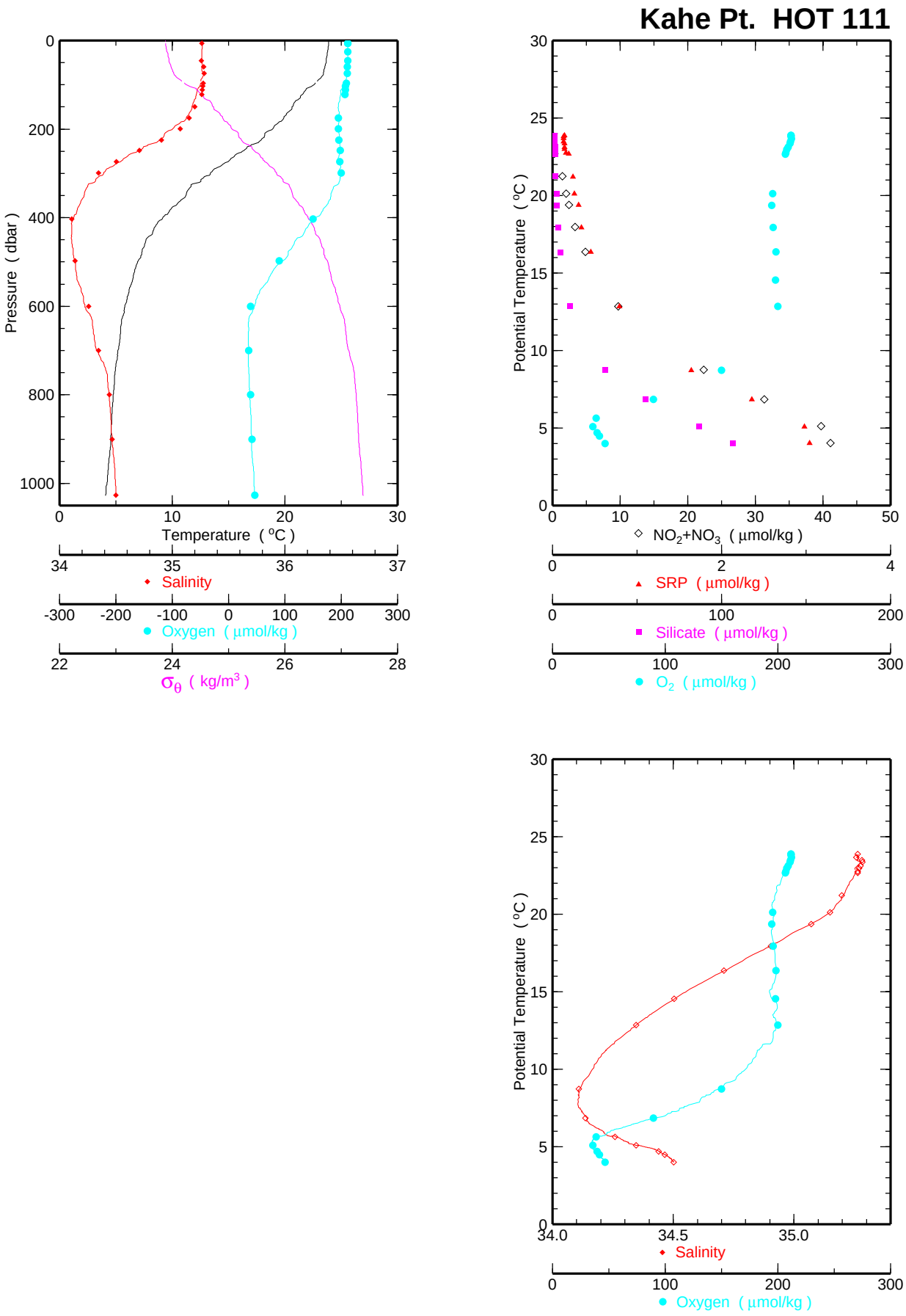
Kahe Pt. HOT 111
Pressure (dbar)
Temperature (°C)
Salinity
Oxygen (µmol/kg)
σθ (kg/m3)
Potential Temperature (°C)
NO2+NO3 (µmol/kg)
SRP (µmol/kg)
Silicate (µmol/kg)
O2 (µmol/kg)
Potential Temperature (°C)
Salinity
Oxygen (µmol/kg)

Figure 6.1.3a

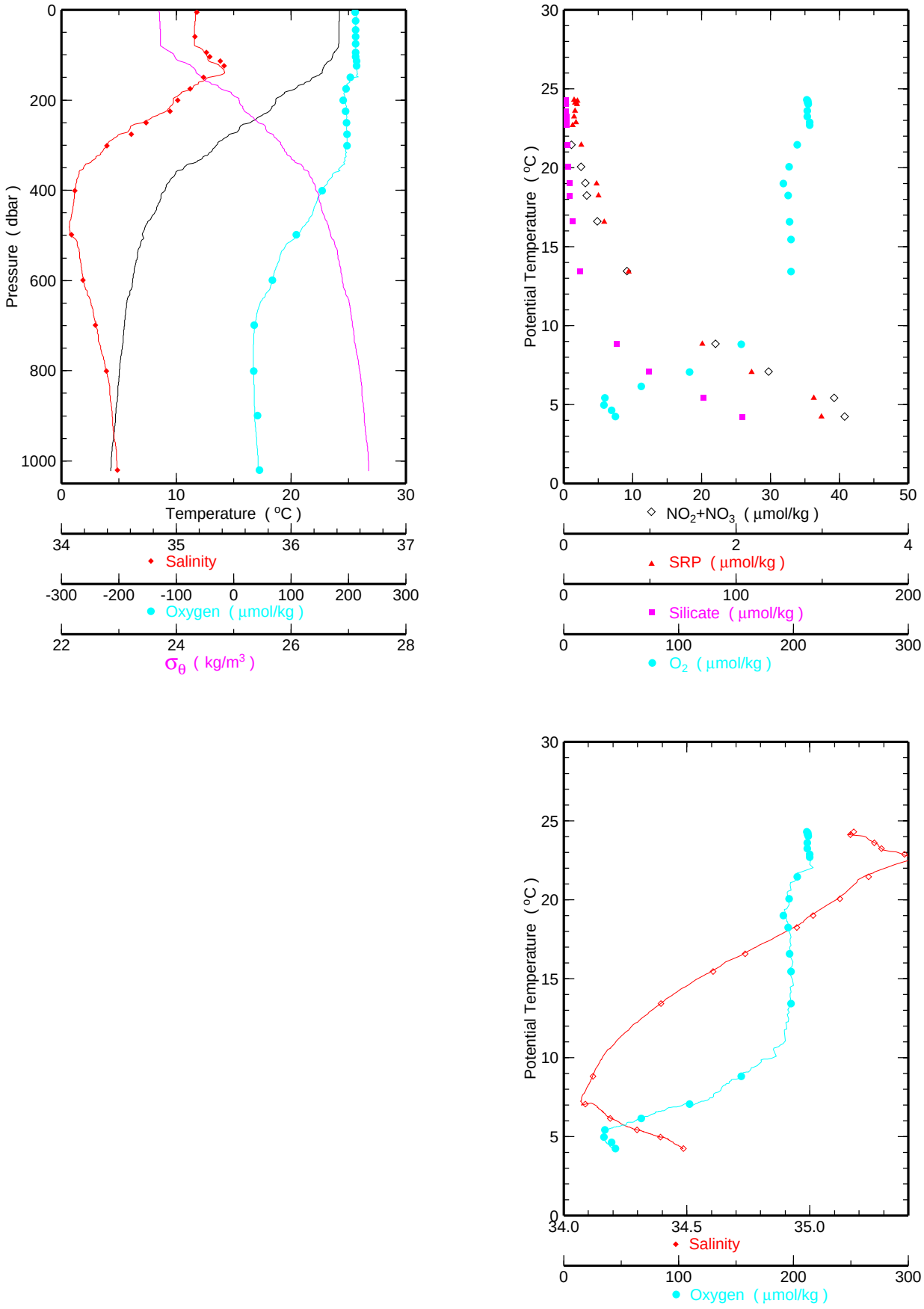
Kahe Pt. HOT 112
Pressure (dbar)
Temperature (°C)
Salinity
Oxygen (µmol/kg)
σθ (kg/m3)
Potential Temperature (°C)
NO2+NO3 (µmol/kg)
SRP (µmol/kg)
Silicate (µmol/kg)
O2 (µmol/kg)
Potential Temperature (°C)
Salinity
Oxygen (µmol/kg)

Figure 6.1.3b

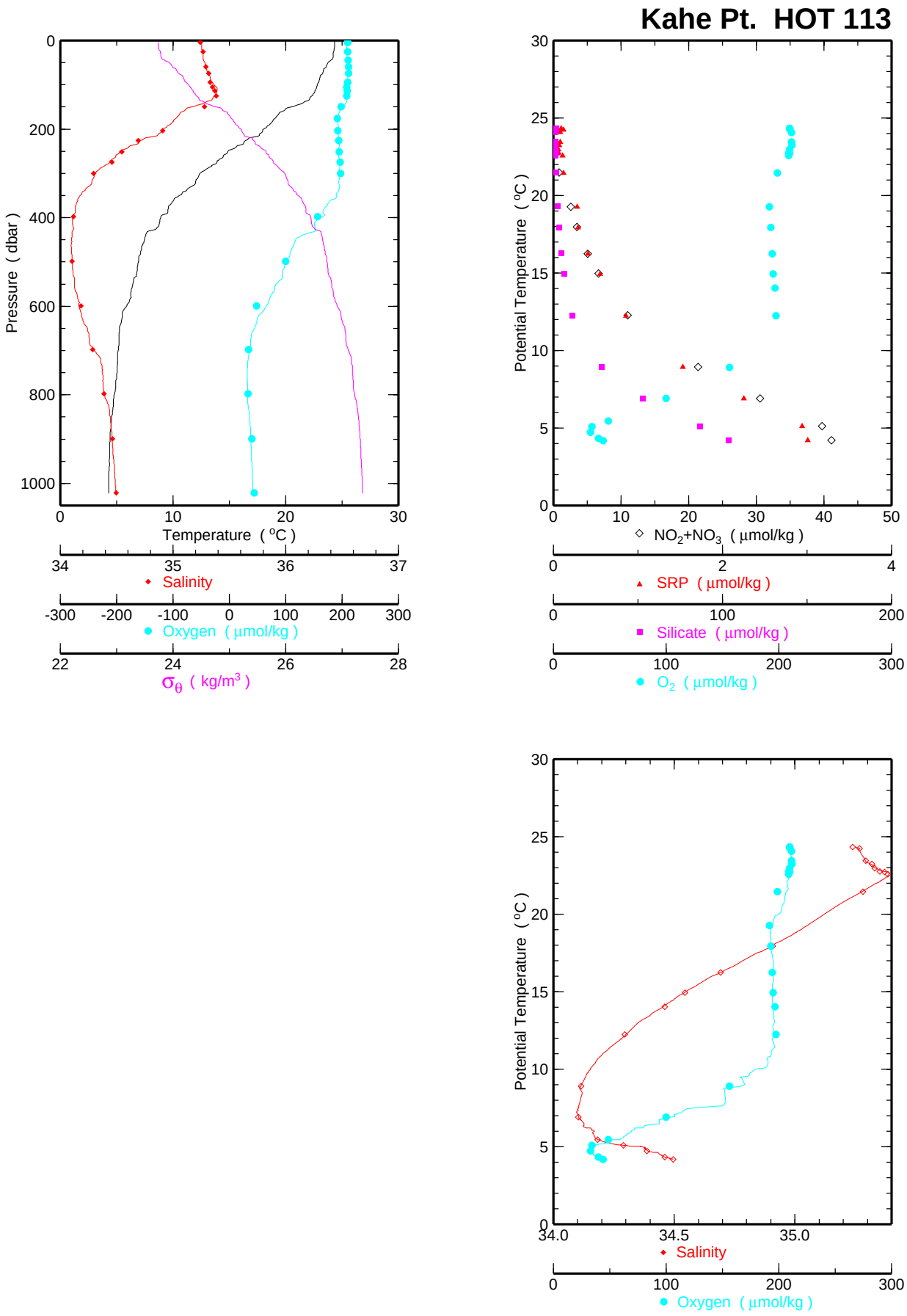
Kahe Pt. HOT 113
Pressure (dbar)
Temperature (°C)
Salinity
Oxygen (µmol/kg)
σθ (kg/m3)
Potential Temperature (°C)
NO2+NO3 (µmol/kg)
SRP (µmol/kg)
Silicate (µmol/kg)
O2 (µmol/kg)
Potential Temperature (°C)
Salinity
Oxygen (µmol/kg)

Figure 6.1.3c

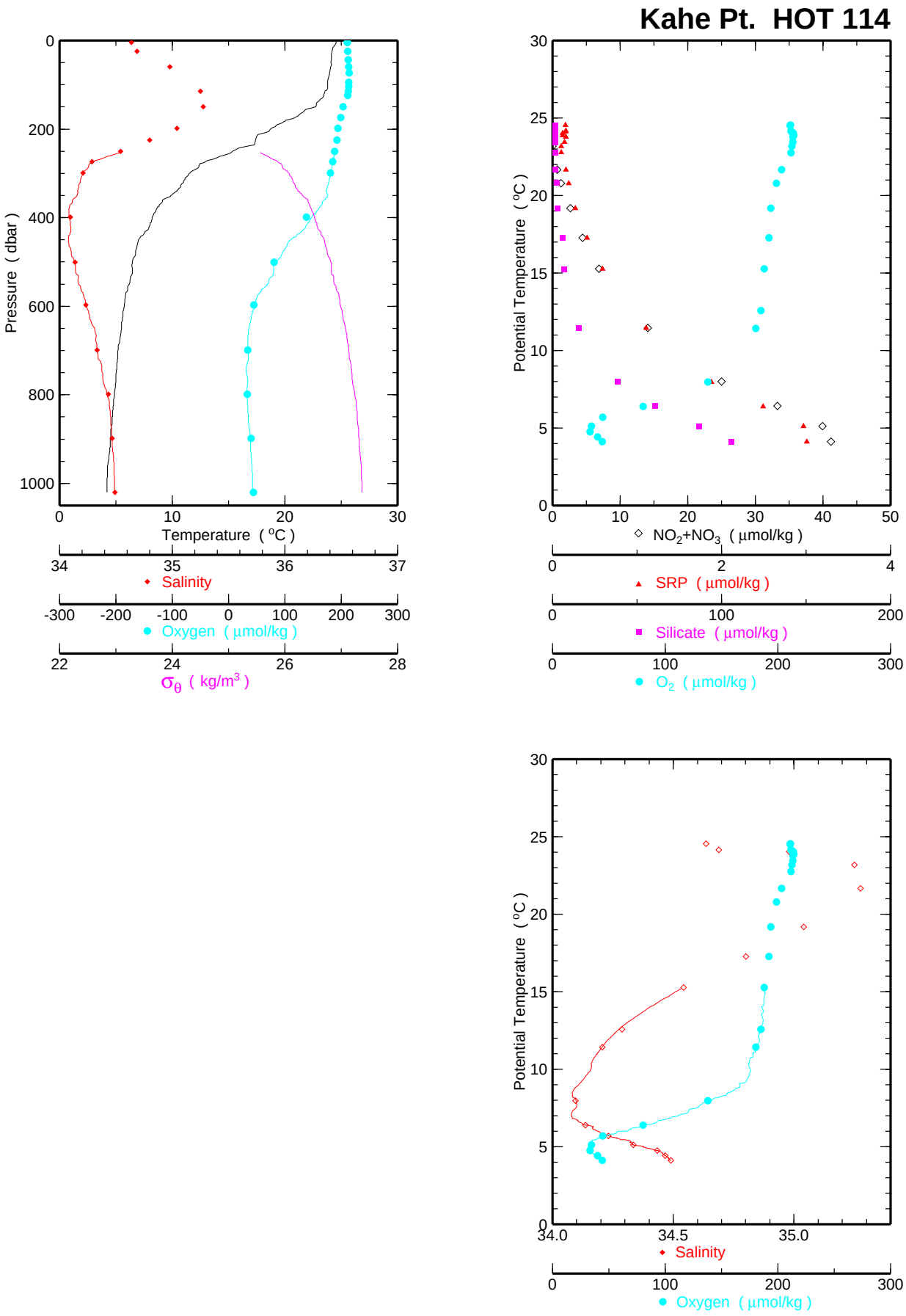
Kahe Pt. HOT 114
Pressure (dbar)
Temperature (°C)
Salinity
Oxygen (µmol/kg)
σθ (kg/m3)
Potential Temperature (°C)
NO2+NO3 (µmol/kg)
SRP (µmol/kg)
Silicate (µmol/kg)
O2 (µmol/kg)
Potential Temperature (°C)
Salinity
Oxygen (µmol/kg)

Figure 6.1.3d

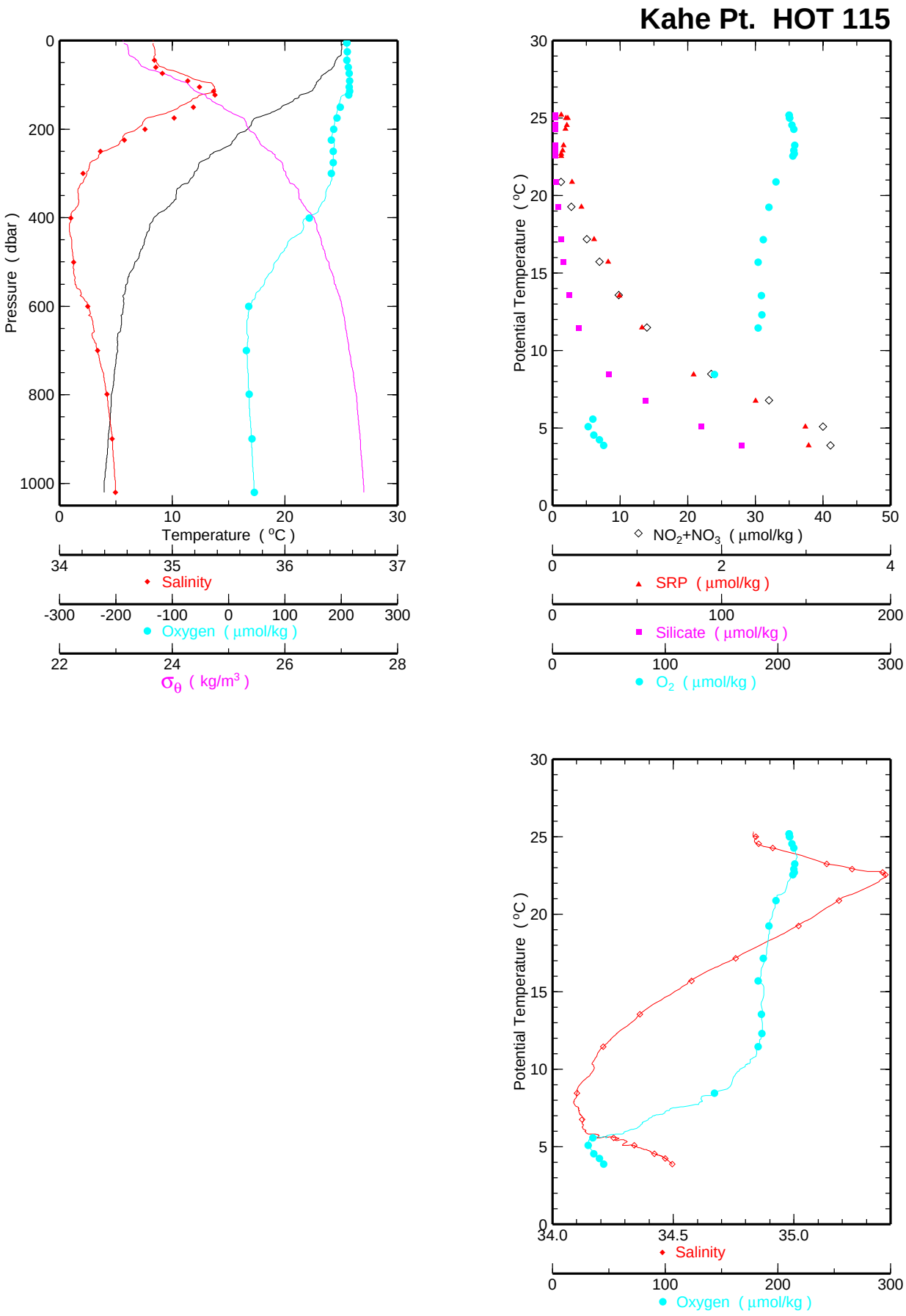
Kahe Pt. HOT 115
Pressure (dbar)
Temperature (°C)
Salinity
Oxygen (µmol/kg)
σθ (kg/m3)
Potential Temperature (°C)
NO2+NO3 (µmol/kg)
SRP (µmol/kg)
Silicate (µmol/kg)
O2 (µmol/kg)
Potential Temperature (°C)
Salinity
Oxygen (µmol/kg)

Figure 6.1.3e

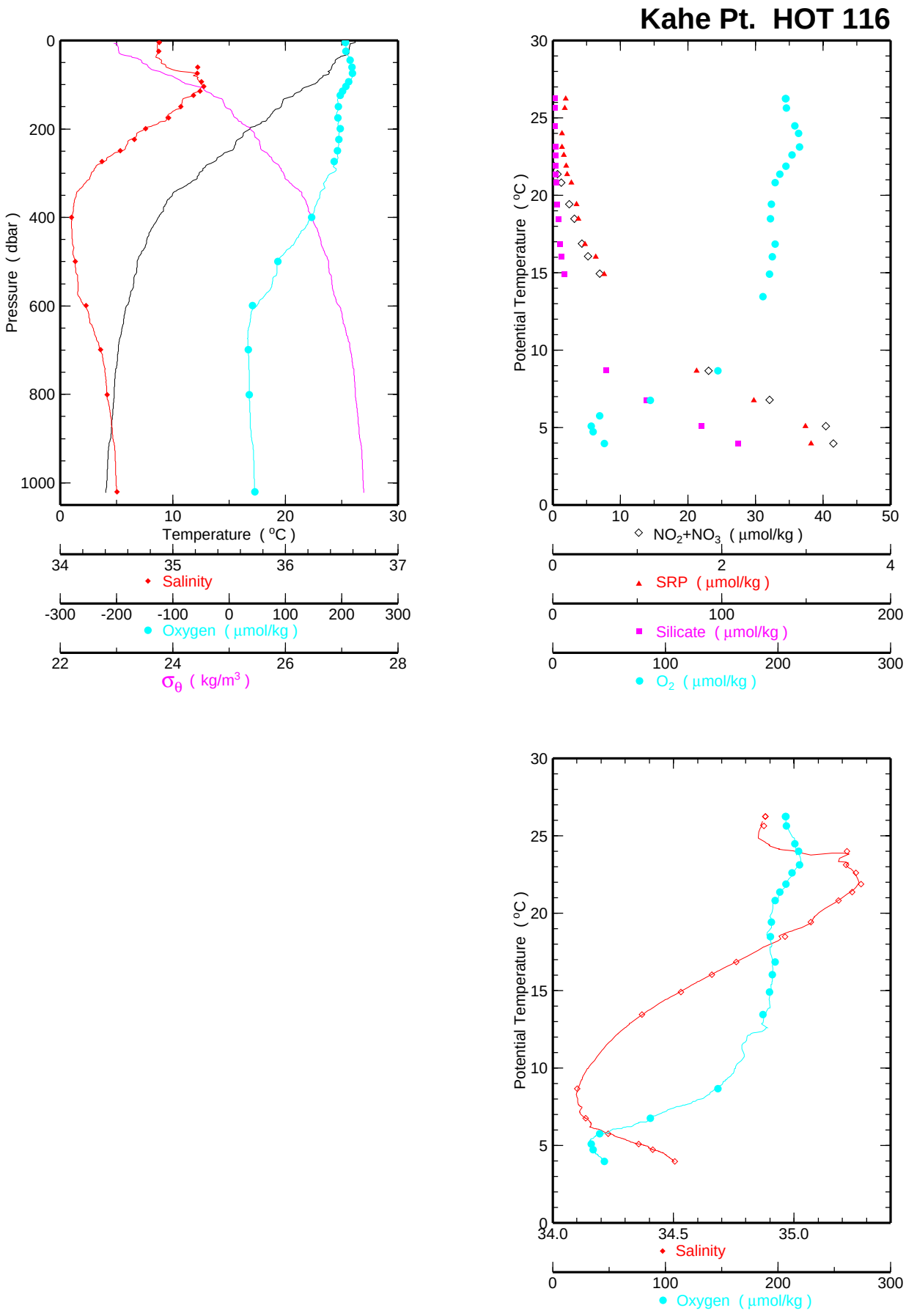
Kahe Pt. HOT 116
Pressure (dbar)
Temperature (°C)
Salinity
Oxygen (µmol/kg)
σθ (kg/m3)
Potential Temperature (°C)
NO2+NO3 (µmol/kg)
SRP (µmol/kg)
Silicate (µmol/kg)
O2 (µmol/kg)
Potential Temperature (°C)
Salinity
Oxygen (µmol/kg)

Figure 6.1.3f

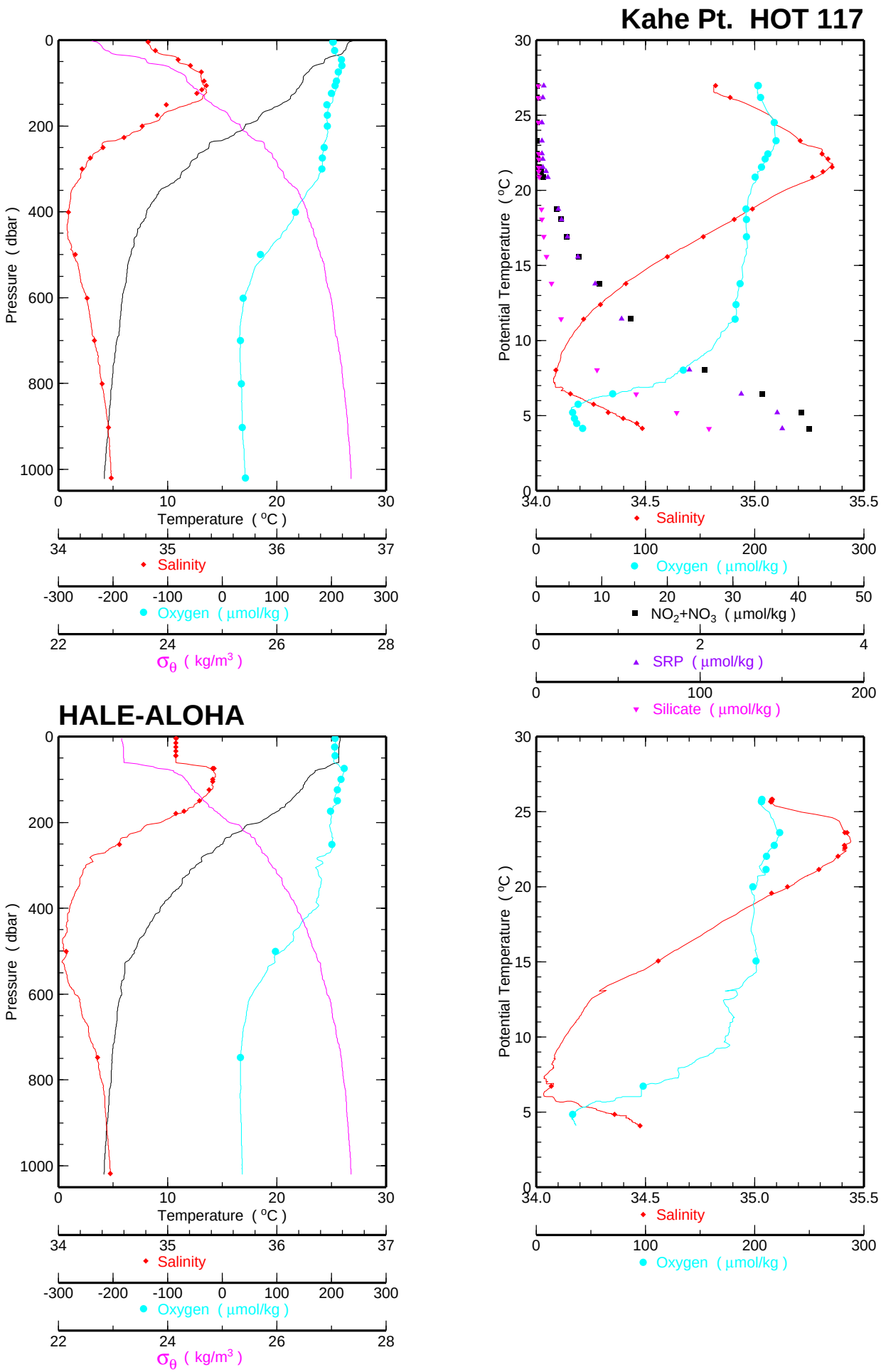
Kahe Pt. HOT 117
HALE-ALOHA
Pressure (dbar)
Temperature (°C)
Salinity
Oxygen (µmol/kg)
σθ (kg/m3)
Potential Temperature (°C)
NO2+NO3 (µmol/kg)
SRP (µmol/kg)
Silicate (µmol/kg)

Figure 6.1.3g

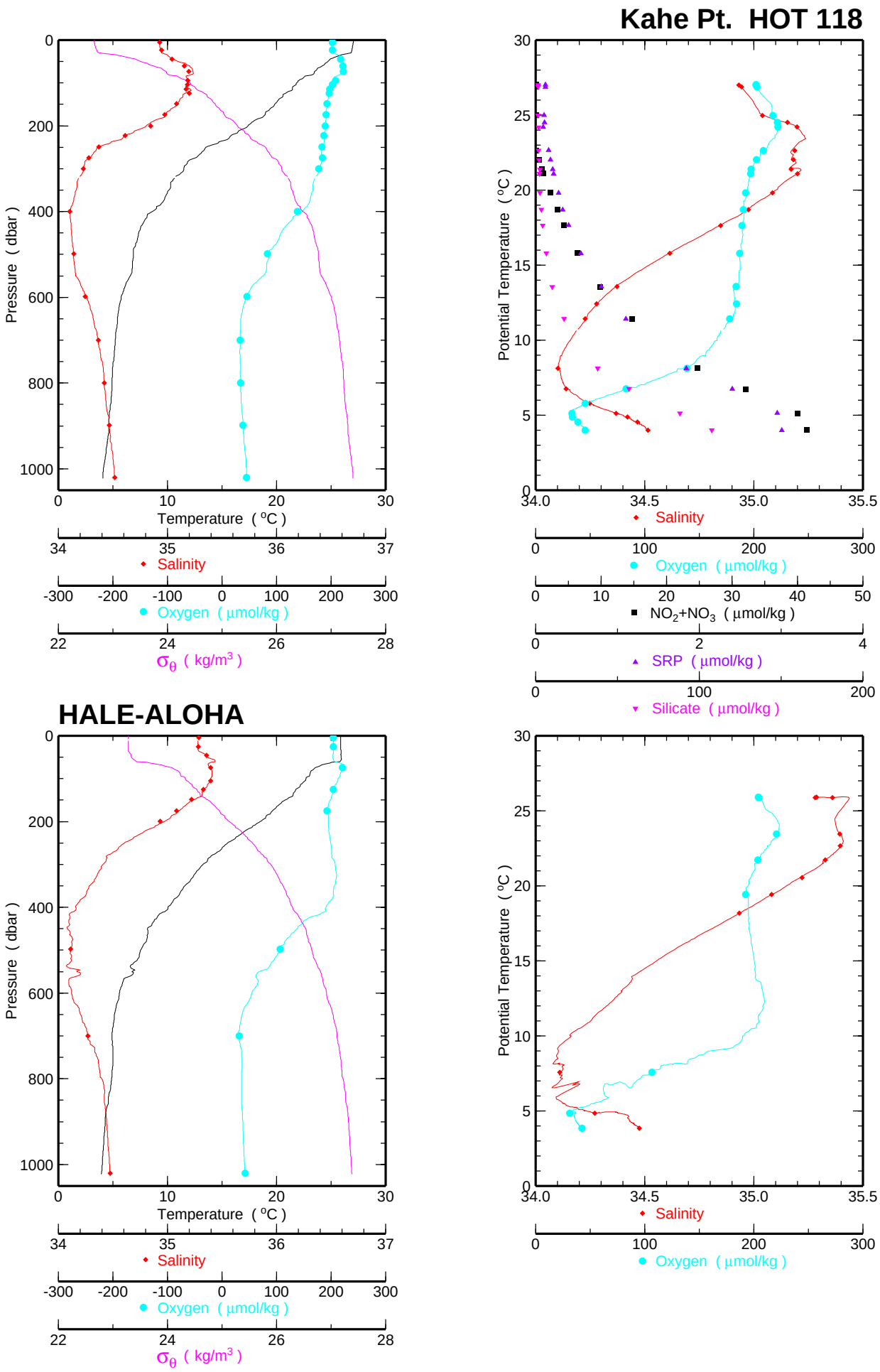
Kahe Pt. HOT 118
HALE-ALOHA
Pressure (dbar)
Potential Temperature (°C)
Temperature (°C)
Salinity
Oxygen (µmol/kg)
σθ (kg/m3)
NO2+NO3 (µmol/kg)
SRP (µmol/kg)
Silicate (µmol/kg)

Figure 6.1.3h

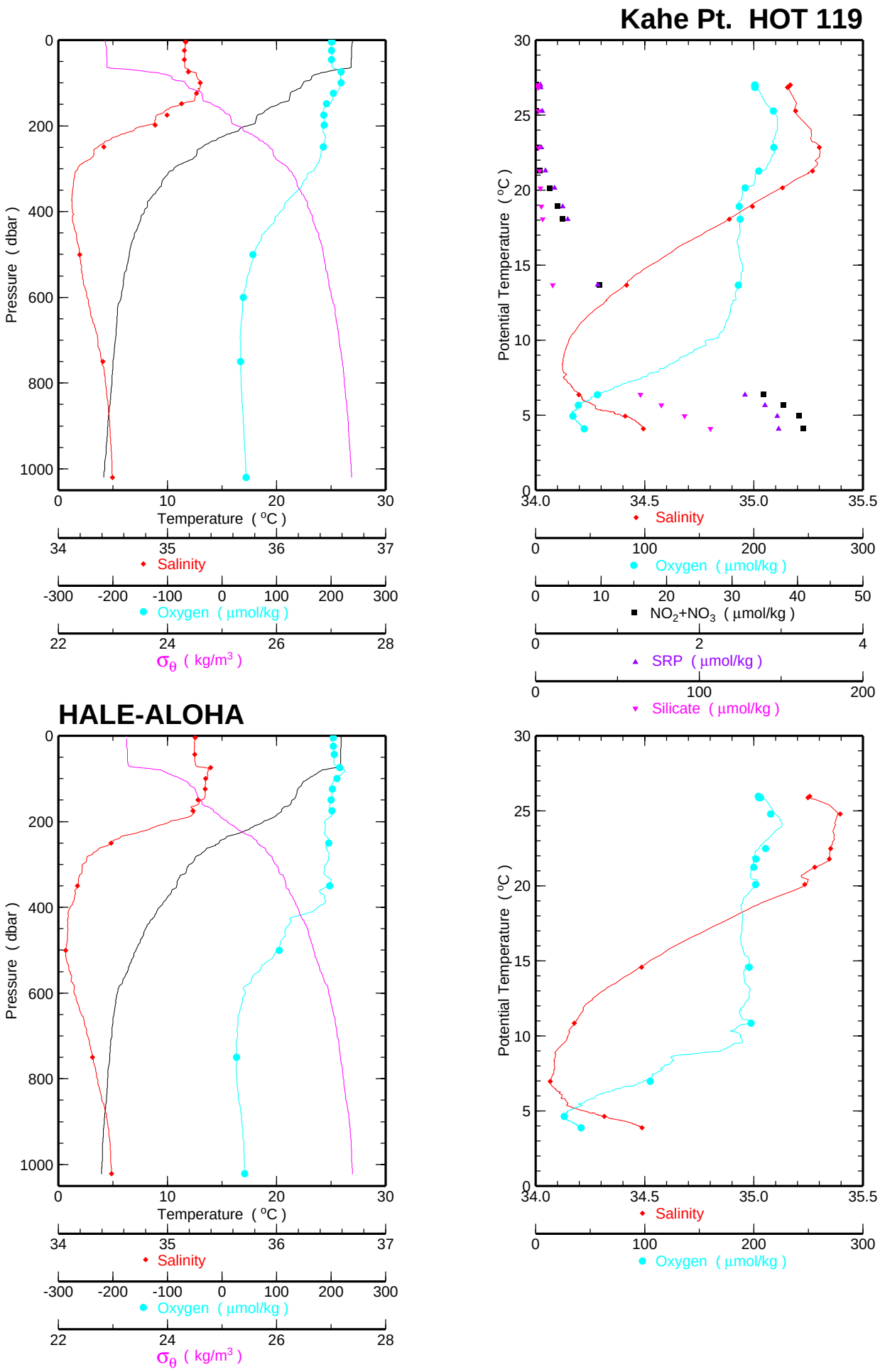
Kahe Pt. HOT 119
HALE-ALOHA
Pressure (dbar)
Temperature (°C)
Salinity
Oxygen (µmol/kg)
σθ (kg/m3)
Potential Temperature (°C)
NO2+NO3 (µmol/kg)
SRP (µmol/kg)
Silicate (µmol/kg)

Figure 6.1.3i

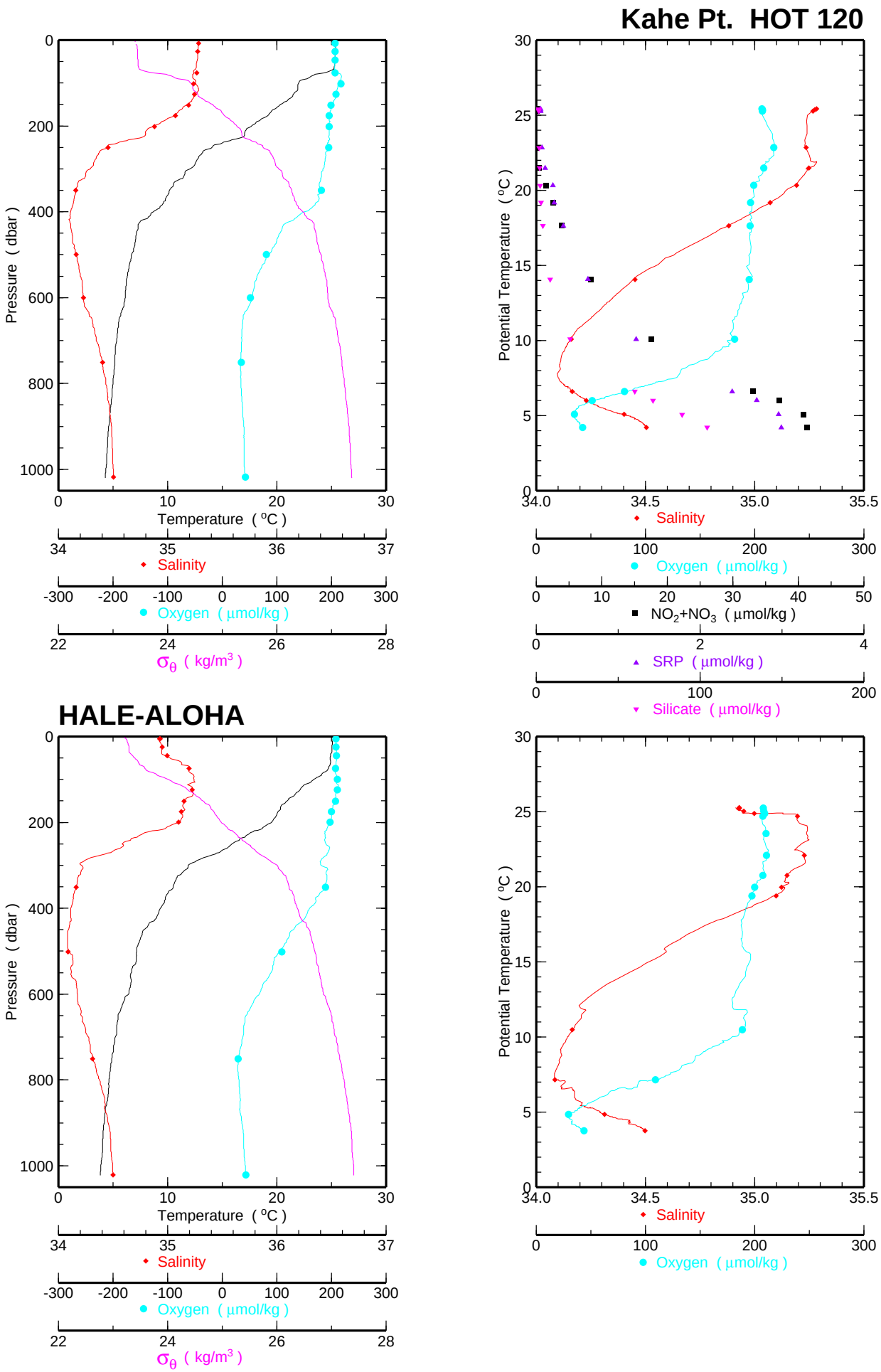
Kahe Pt. HOT 120
HALE-ALOHA
Pressure (dbar)
Temperature (°C)
Salinity
Oxygen (µmol/kg)
σθ (kg/m³)
Potential Temperature (°C)
NO2+NO3 (µmol/kg)
SRP (µmol/kg)
Silicate (µmol/kg)

Figure 6.1.3j

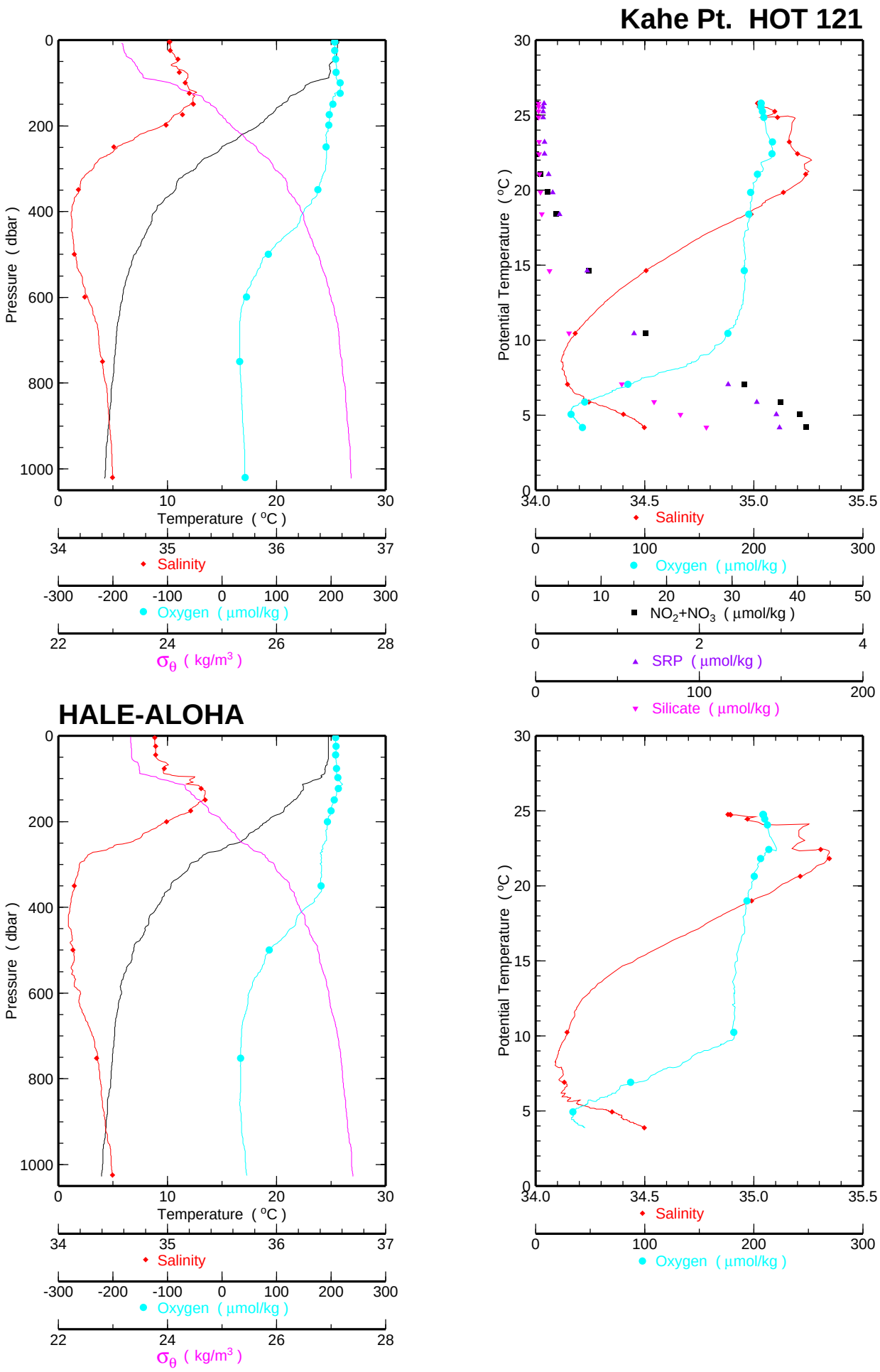
Kahe Pt. HOT 121
HALE-ALOHA
Pressure (dbar)
Temperature (°C)
Salinity
Oxygen (µmol/kg)
σθ (kg/m3)
Potential Temperature (°C)
NO2+NO3 (µmol/kg)
SRP (µmol/kg)
Silicate (µmol/kg)

Figure 6.1.3k

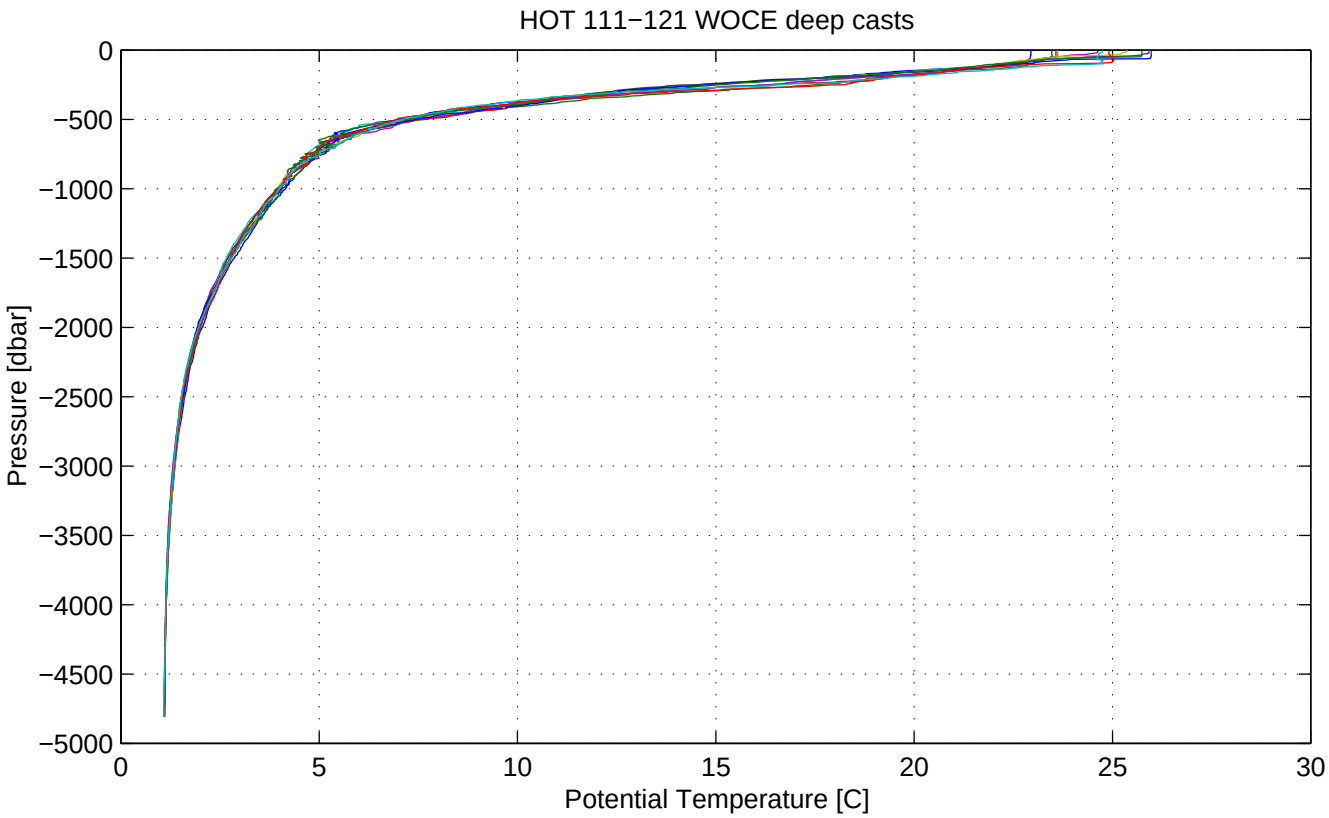
HOT 111−121 WOCE deep casts
Pressure [dbar]
Potential Temperature [C]
0
−500
−1000
−1500
−2000
−2500
−3000
−3500
−4000
−4500
−5000
0
5
10
15
20
25
30

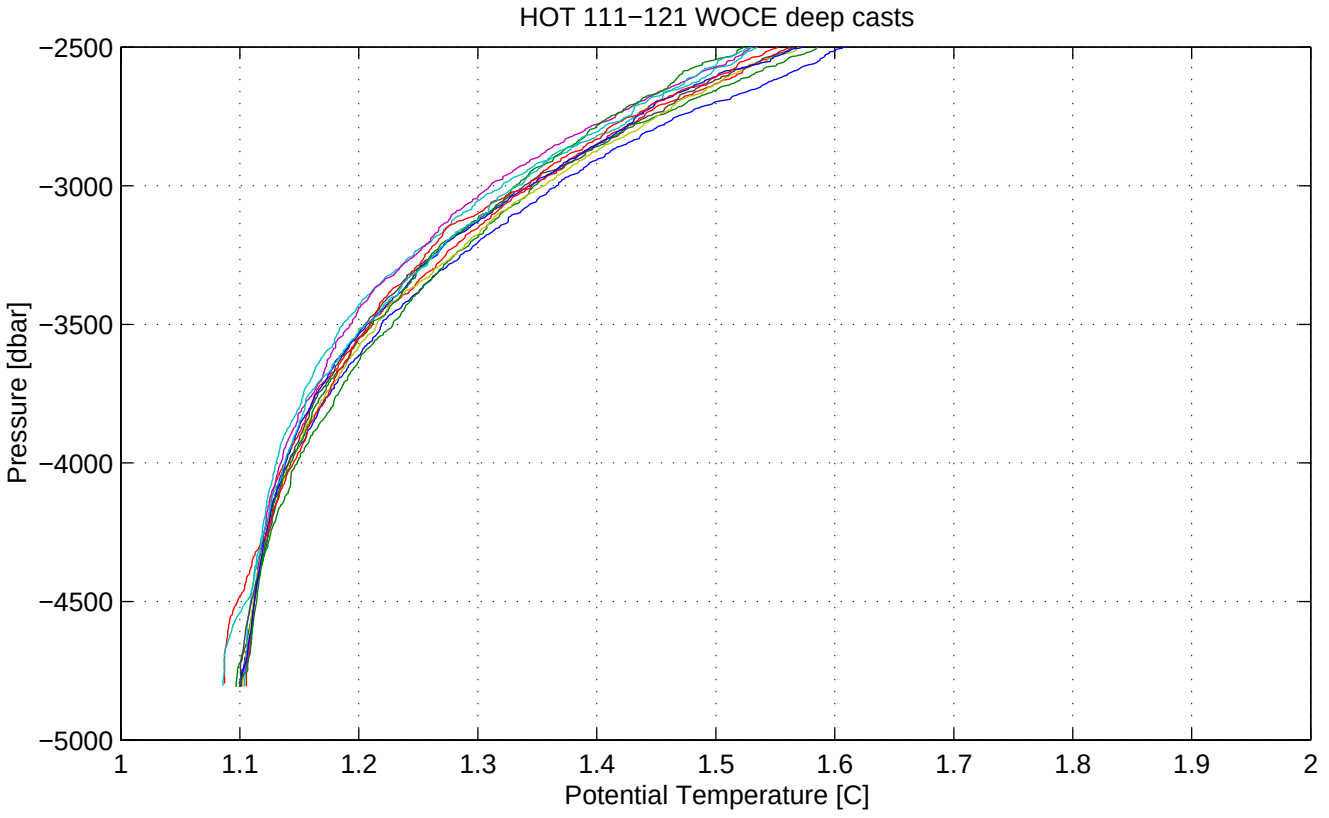
HOT 111−121 WOCE deep casts
Pressure [dbar]
Potential Temperature [C]
−2500
−3000
−3500
−4000
−4500
−5000
1
1.1
1.2
1.3
1.4
1.5
1.6
1.7
1.8
1.9
2

Figure 6.1.4

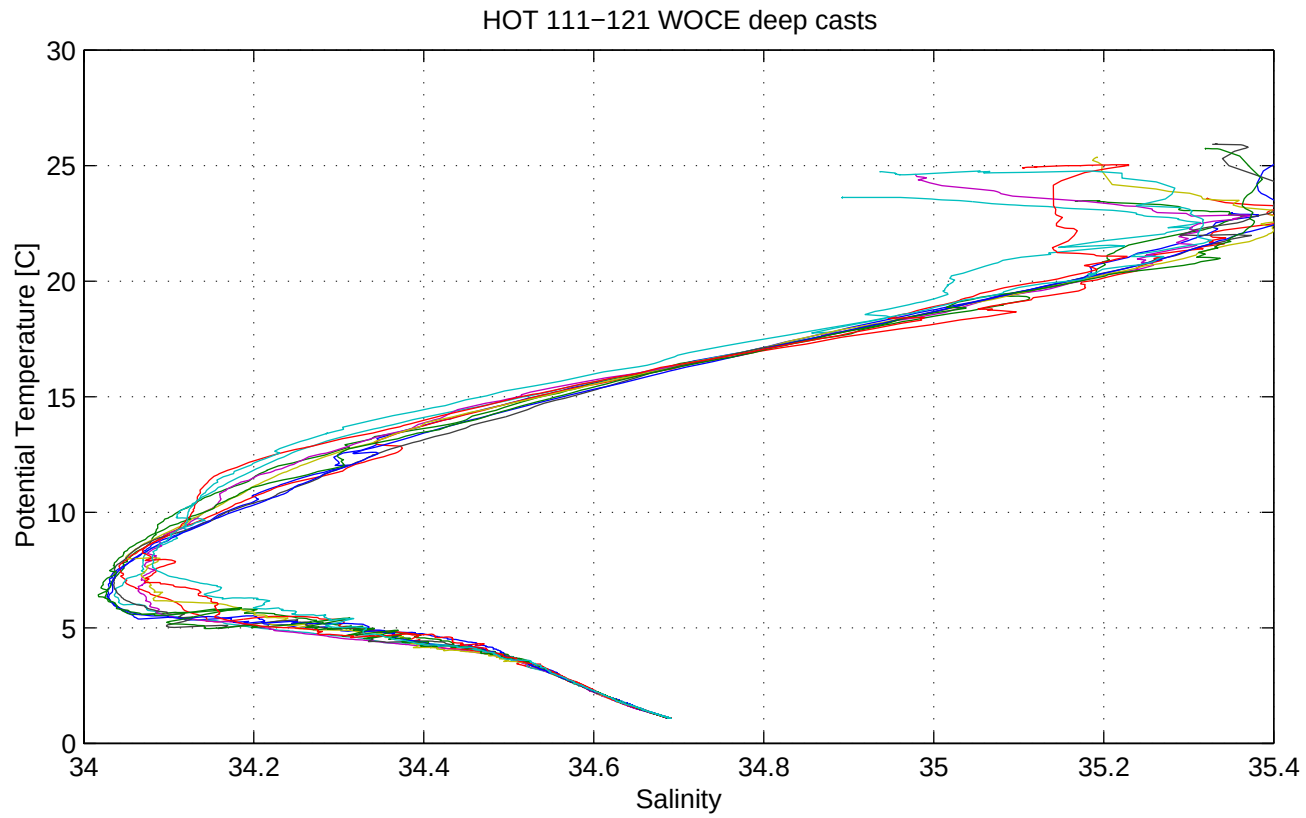
HOT 111−121 WOCE deep casts
Potential Temperature [C]
Salinity
30
25
20
15
10
5
0
34
34.2
34.4
34.6
34.8
35
35.2
35.4

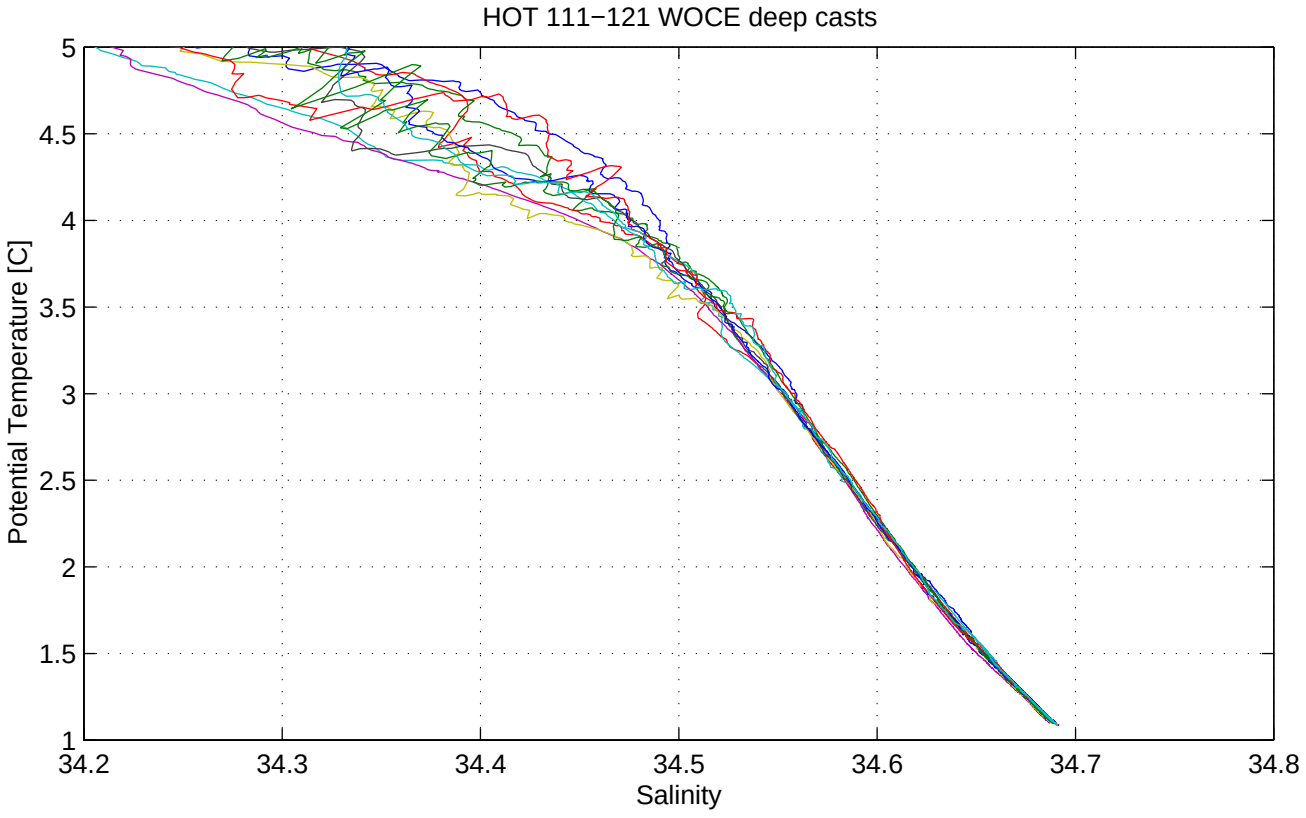
HOT 111−121 WOCE deep casts
Potential Temperature [C]
Salinity
5
4.5
4
3.5
3
2.5
2
1.5
1
34.2
34.3
34.4
34.5
34.6
34.7
34.8

Figure 6.1.5

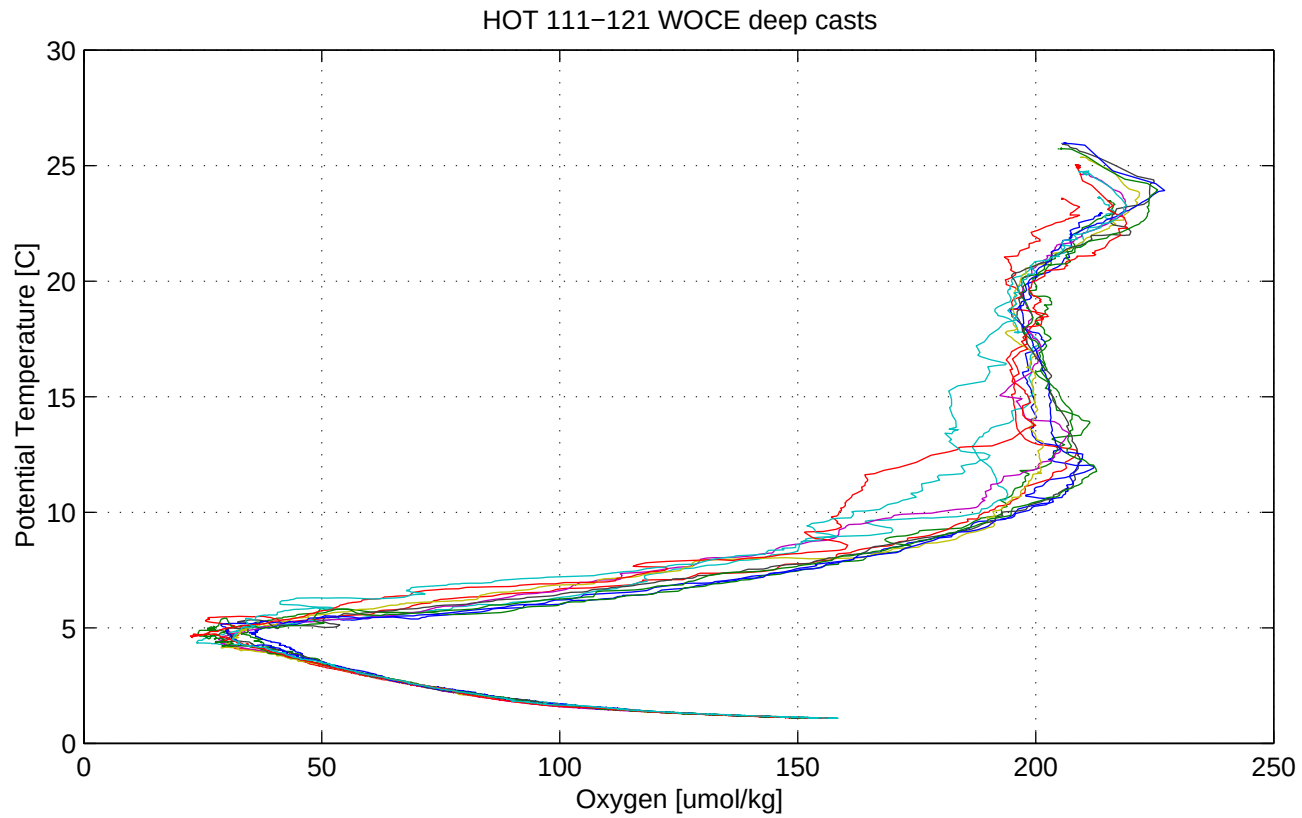
HOT 111−121 WOCE deep casts
Potential Temperature [C]
Oxygen [umol/kg]
0
5
10
15
20
25
30
0
50
100
150
200
250

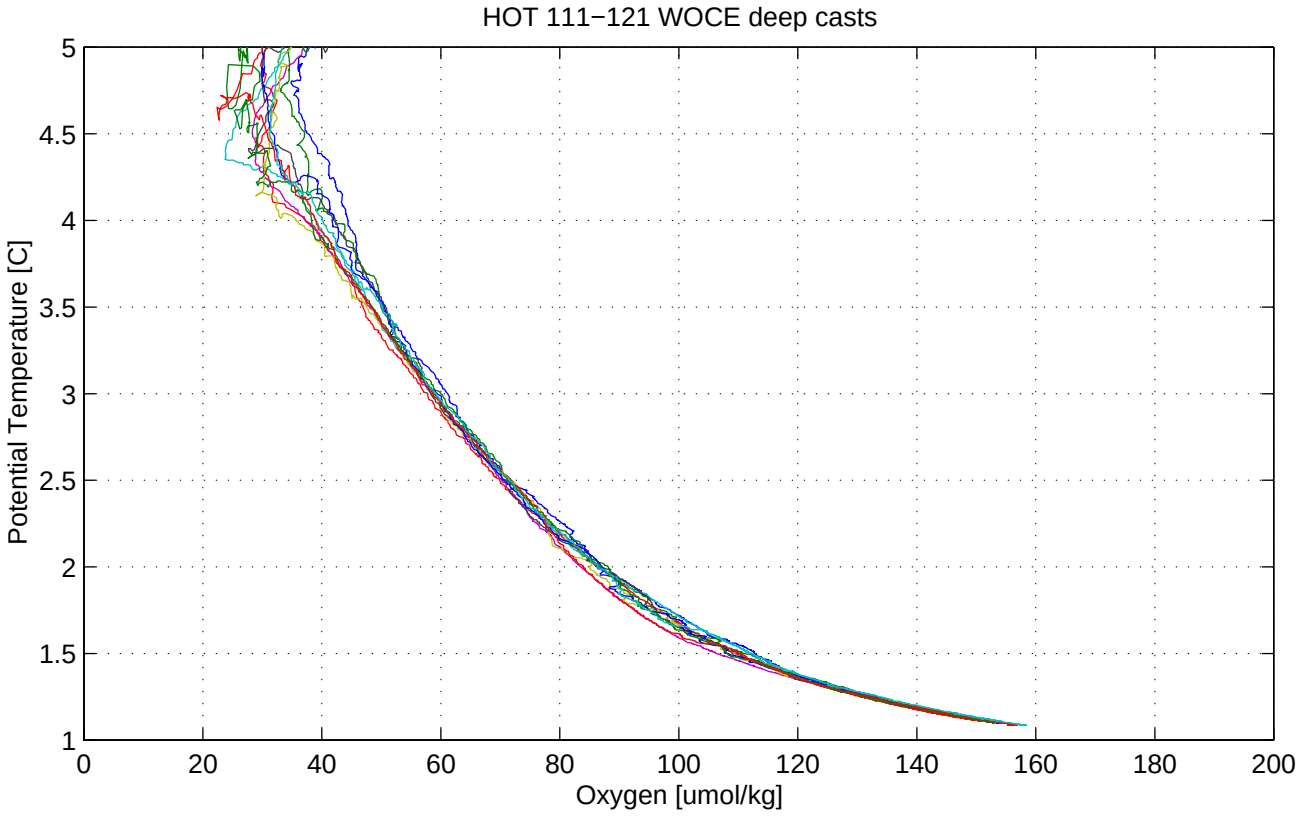
HOT 111−121 WOCE deep casts
Potential Temperature [C]
Oxygen [umol/kg]
1
1.5
2
2.5
3
3.5
4
4.5
5
0
20
40
60
80
100
120
140
160
180
200

Figure 6.1.6

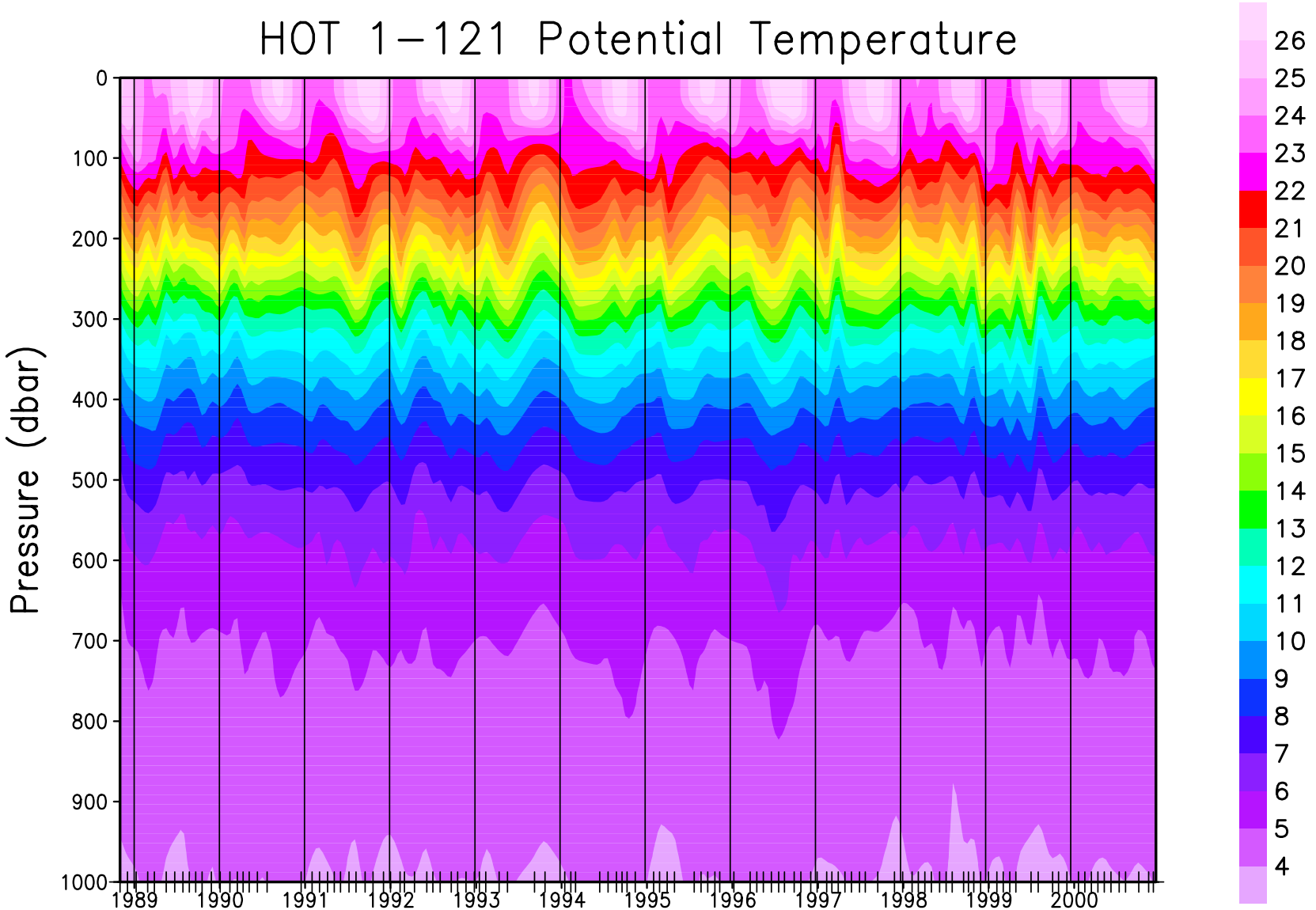
HOT 1–121 Potential Temperature
Pressure (dbar)
0
100
200
300
400
500
600
700
800
900
1000
1989
1990
1991
1992
1993
1994
1995
1996
1997
1998
1999
2000
26
25
24
23
22
21
20
19
18
17
16
15
14
13
12
11
10
9
8
7
6
5
4

Figure 6.1.7

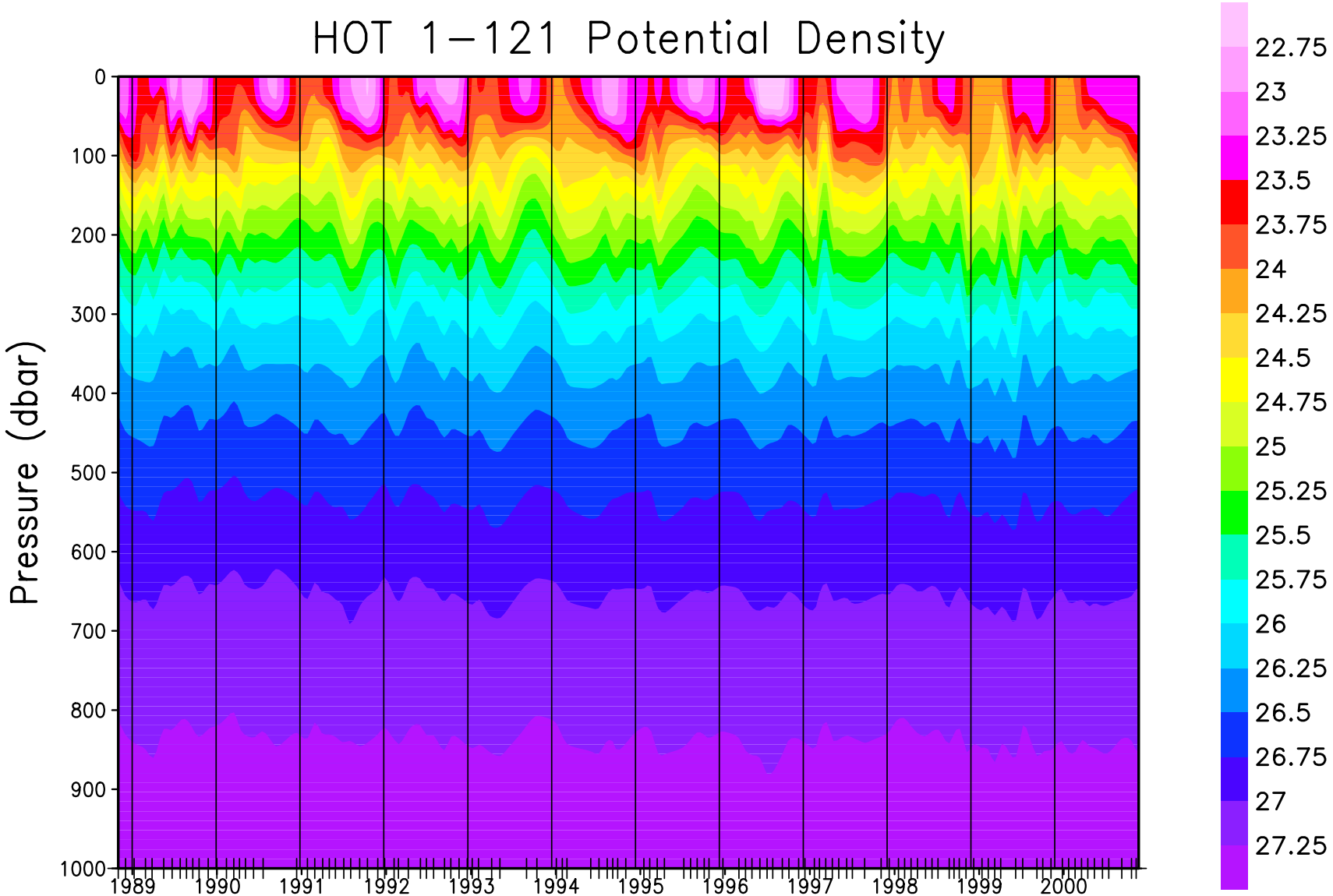
HOT 1–121 Potential Density
Pressure (dbar)
0
100
200
300
400
500
600
700
800
900
1000
1989
1990
1991
1992
1993
1994
1995
1996
1997
1998
1999
2000
22.75
23
23.25
23.5
23.75
24
24.25
24.5
24.75
25
25.25
25.5
25.75
26
26.25
26.5
26.75
27
27.25

Figure 6.1.8

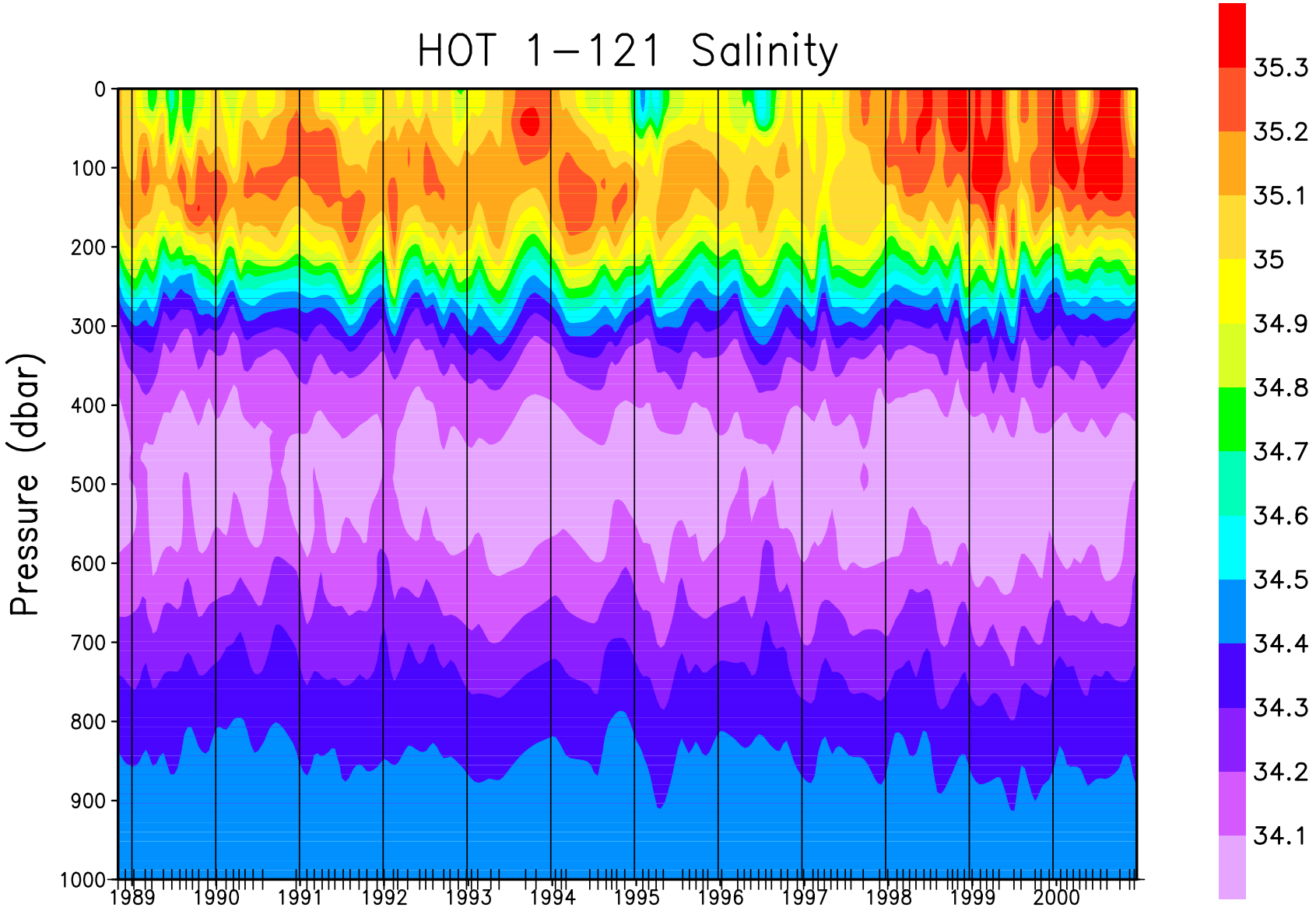
HOT 1–121 Salinity
Pressure (dbar)
0
100
200
300
400
500
600
700
800
900
1000
1989
1990
1991
1992
1993
1994
1995
1996
1997
1998
1999
2000
35.3
35.2
35.1
35
34.9
34.8
34.7
34.6
34.5
34.4
34.3
34.2
34.1

Figure 6.1.9

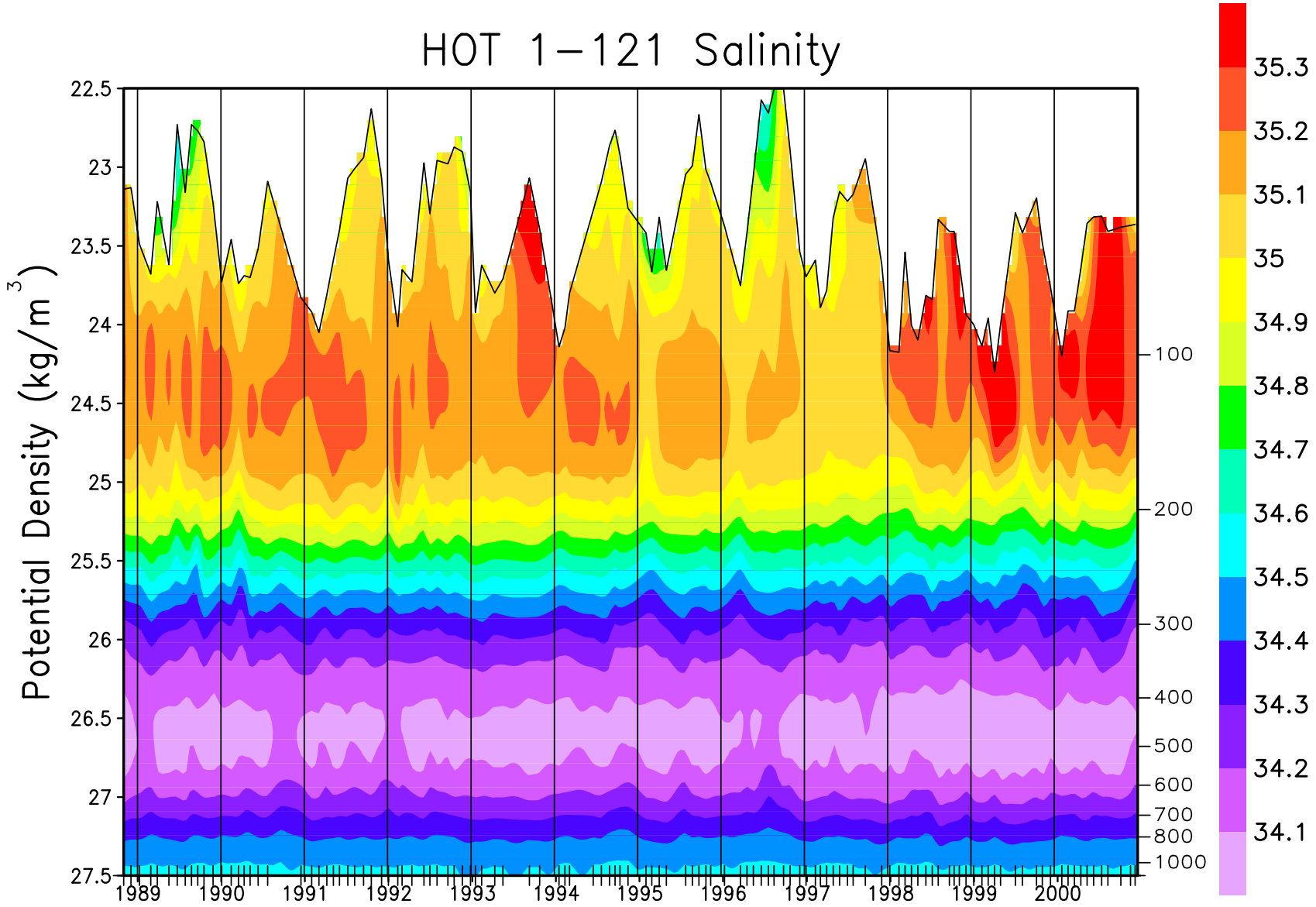
HOT 1–121 Salinity
Potential Density (kg/m3)
22.5
23
23.5
24
24.5
25
25.5
26
26.5
27
27.5
1989
1990
1991
1992
1993
1994
1995
1996
1997
1998
1999
2000
100
200
300
400
500
600
700
800
1000
35.3
35.2
35.1
35
34.9
34.8
34.7
34.6
34.5
34.4
34.3
34.2
34.1

Figure 6.1.10

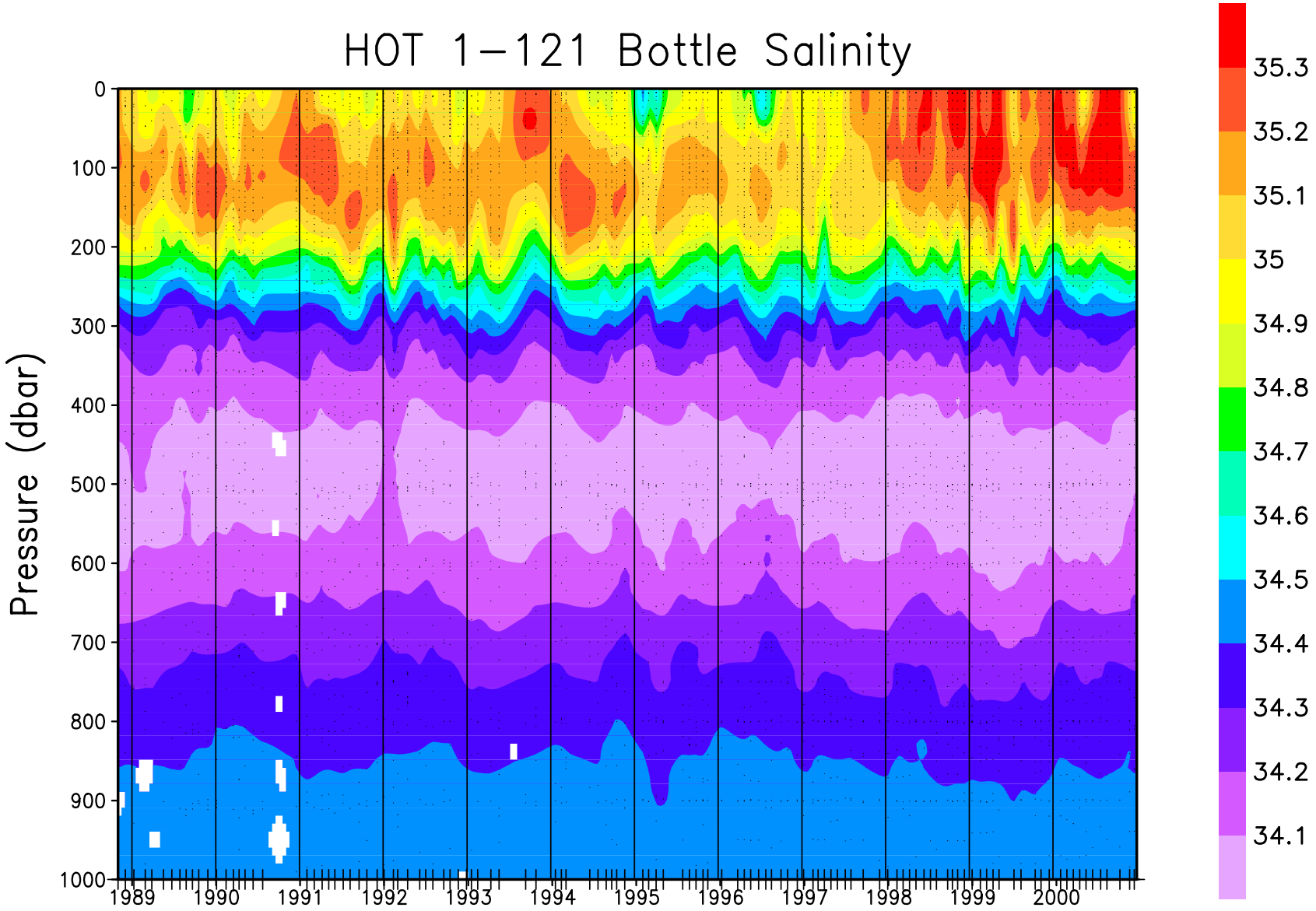
HOT 1–121 Bottle Salinity
Pressure (dbar)
0
100
200
300
400
500
600
700
800
900
1000
1989
1990
1991
1992
1993
1994
1995
1996
1997
1998
1999
2000
35.3
35.2
35.1
35
34.9
34.8
34.7
34.6
34.5
34.4
34.3
34.2
34.1

Figure 6.1.11

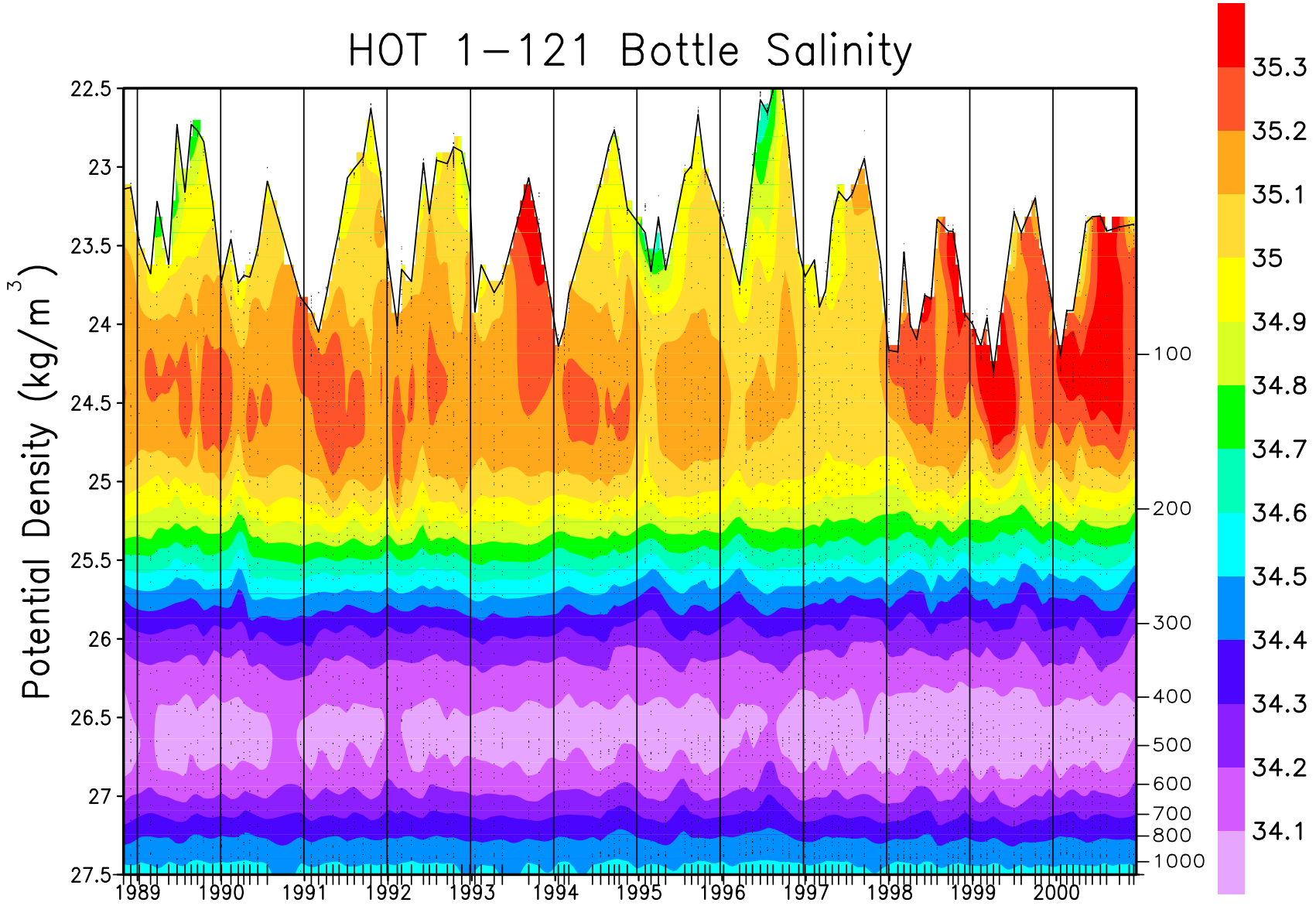
HOT 1–121 Bottle Salinity
Potential Density (kg/m3)
22.5
23
23.5
24
24.5
25
25.5
26
26.5
27
27.5
1989
1990
1991
1992
1993
1994
1995
1996
1997
1998
1999
2000
100
200
300
400
500
600
700
800
1000
35.3
35.2
35.1
35
34.9
34.8
34.7
34.6
34.5
34.4
34.3
34.2
34.1

Figure 6.1.12

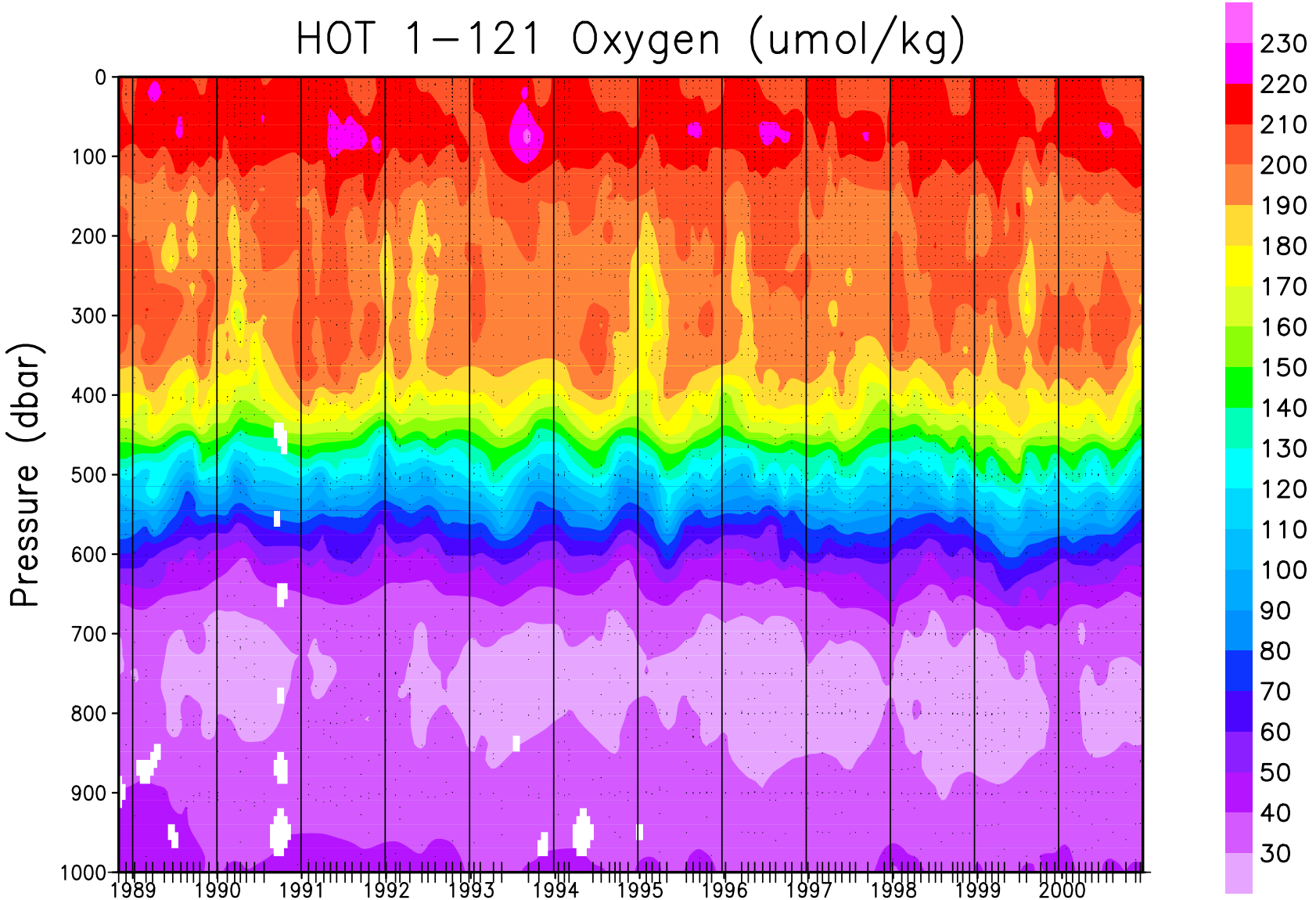
HOT 1–121 Oxygen (umol/kg)
Pressure (dbar)
0
100
200
300
400
500
600
700
800
900
1000
1989
1990
1991
1992
1993
1994
1995
1996
1997
1998
1999
2000
230
220
210
200
190
180
170
160
150
140
130
120
110
100
90
80
70
60
50
40
30

Figure 6.1.13

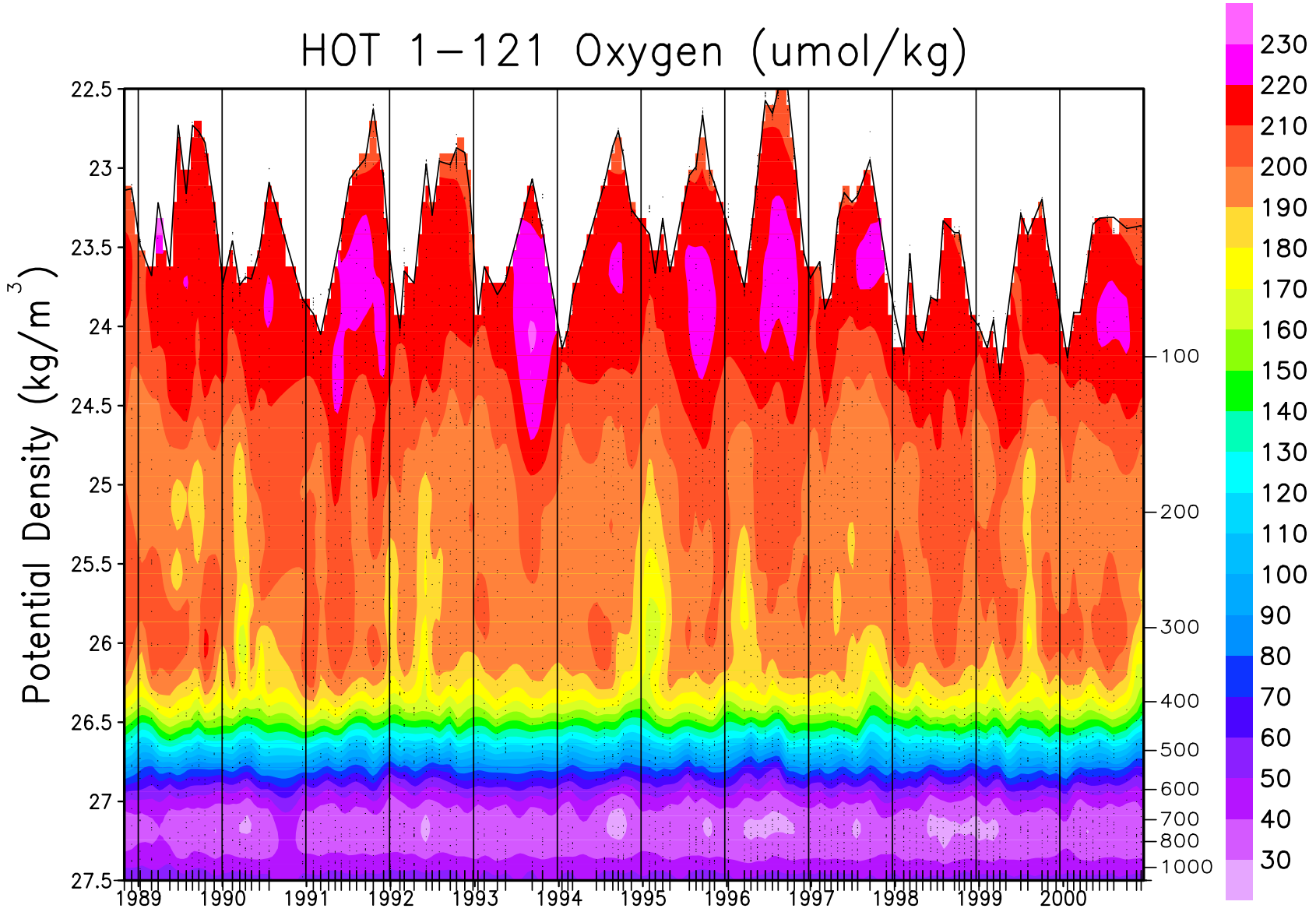
HOT 1–121 Oxygen (umol/kg)
Potential Density (kg/m3)
22.5
23
23.5
24
24.5
25
25.5
26
26.5
27
27.5
1989
1990
1991
1992
1993
1994
1995
1996
1997
1998
1999
2000
100
200
300
400
500
600
700
800
1000
230
220
210
200
190
180
170
160
150
140
130
120
110
100
90
80
70
60
50
40
30

Figure 6.1.14

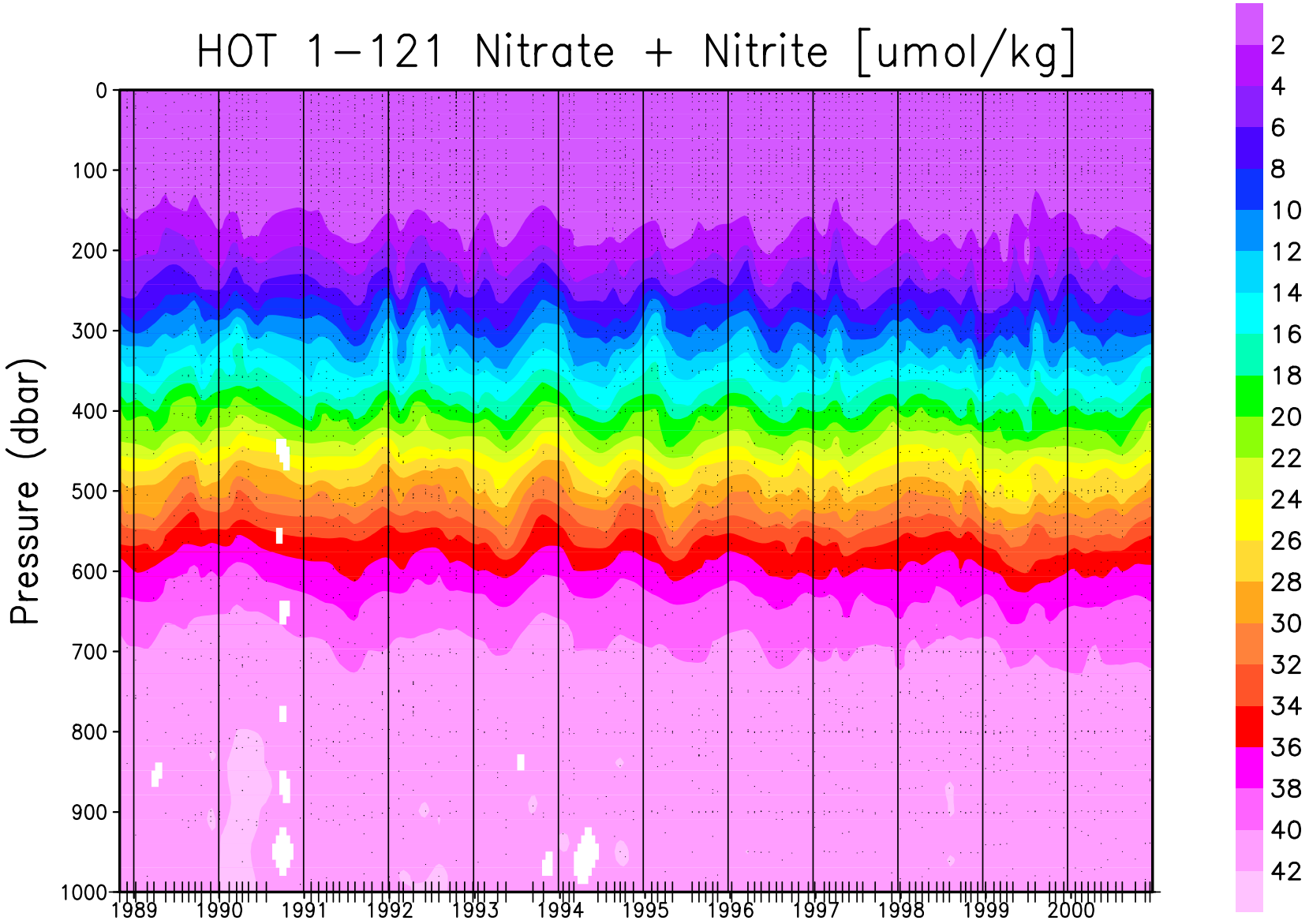
HOT 1–121 Nitrate + Nitrite [umol/kg]
Pressure (dbar)
0
100
200
300
400
500
600
700
800
900
1000
1989
1990
1991
1992
1993
1994
1995
1996
1997
1998
1999
2000
2
4
6
8
10
12
14
16
18
20
22
24
26
28
30
32
34
36
38
40
42

Figure 6.1.15

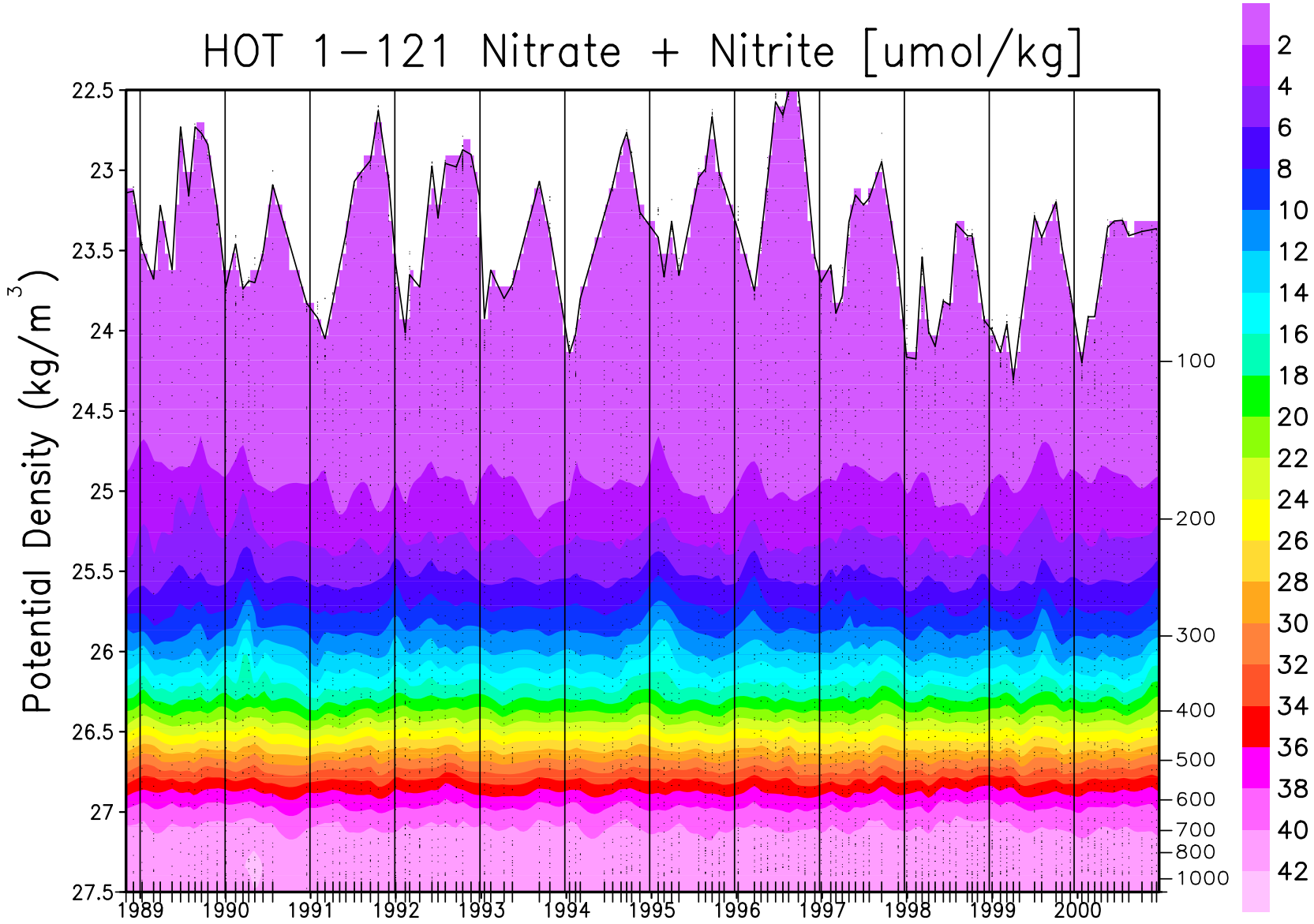
HOT 1–121 Nitrate + Nitrite [umol/kg]
Potential Density (kg/m3)
22.5
23
23.5
24
24.5
25
25.5
26
26.5
27
27.5
1989
1990
1991
1992
1993
1994
1995
1996
1997
1998
1999
2000
100
200
300
400
500
600
700
800
1000
2
4
6
8
10
12
14
16
18
20
22
24
26
28
30
32
34
36
38
40
42

Figure 6.1.16

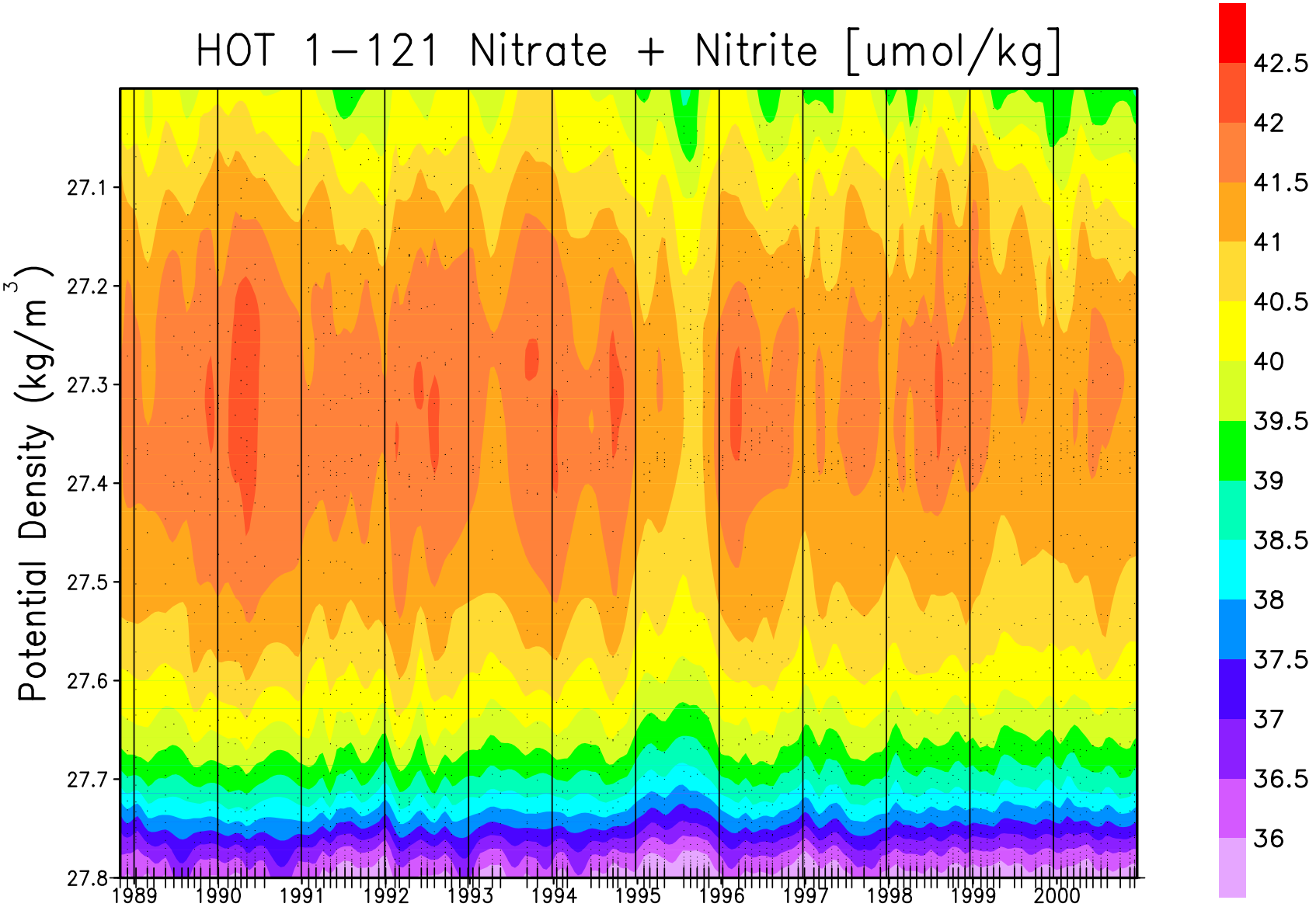
HOT 1−121 Nitrate + Nitrite [umol/kg]
Potential Density (kg/m3)
27.1
27.2
27.3
27.4
27.5
27.6
27.7
27.8
1989
1990
1991
1992
1993
1994
1995
1996
1997
1998
1999
2000
42.5
42
41.5
41
40.5
40
39.5
39
38.5
38
37.5
37
36.5
36

Figure 6.1.17

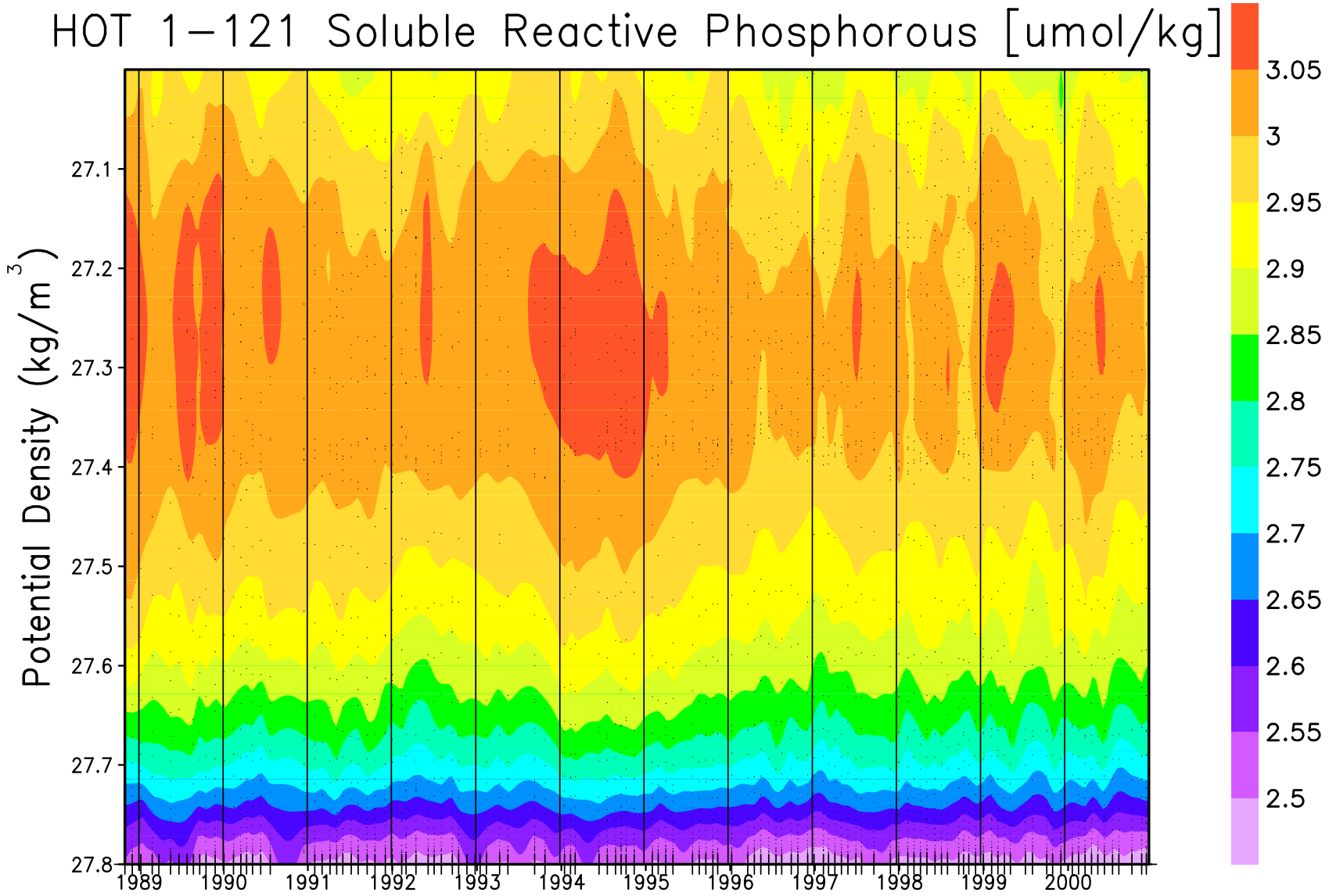
HOT 1–121 Soluble Reactive Phosphorous [umol/kg]
Potential Density (kg/m3)
27.1
27.2
27.3
27.4
27.5
27.6
27.7
27.8
1989
1990
1991
1992
1993
1994
1995
1996
1997
1998
1999
2000
3.05
3
2.95
2.9
2.85
2.8
2.75
2.7
2.65
2.6
2.55
2.5

Figure 6.1.18

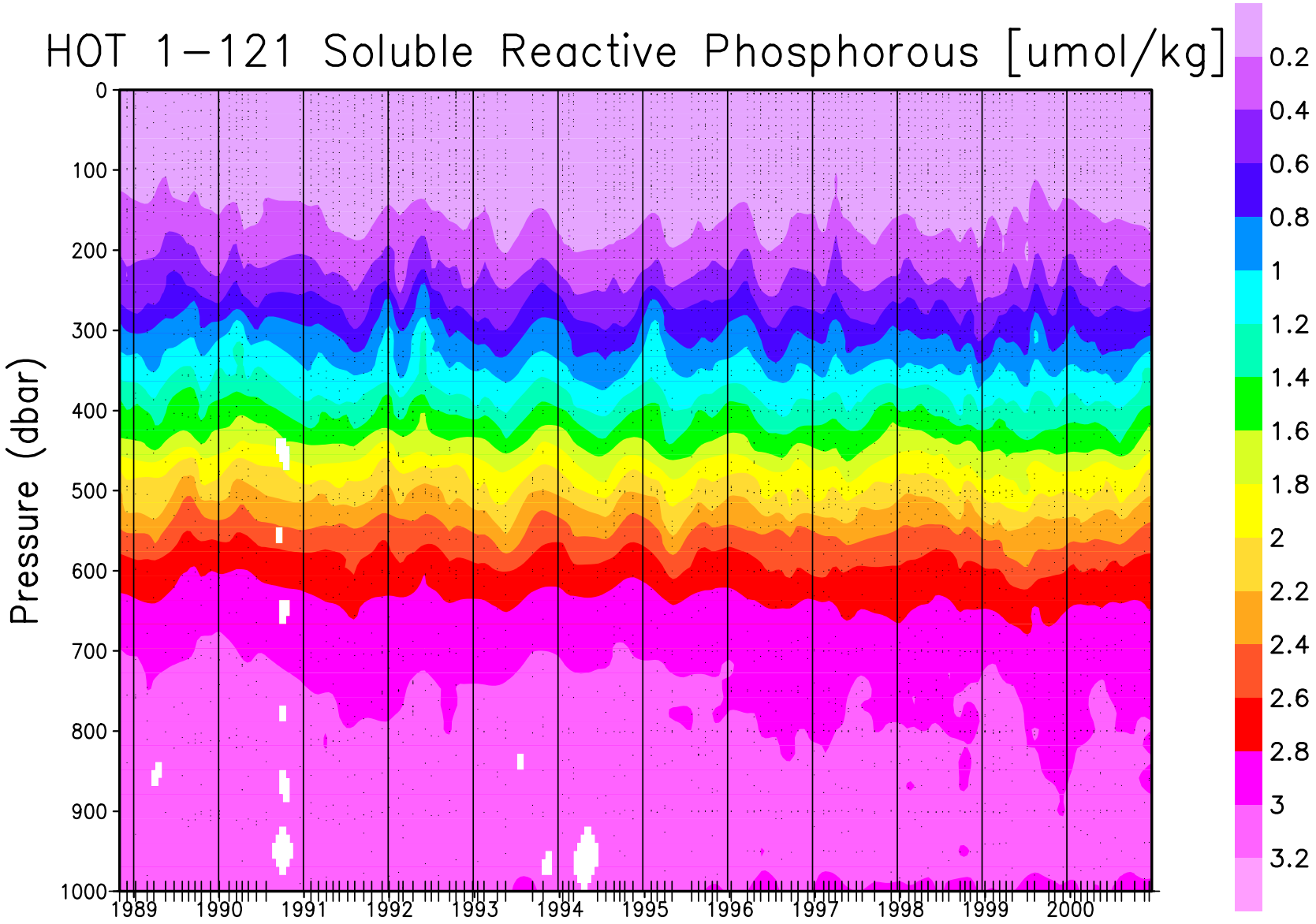
HOT 1–121 Soluble Reactive Phosphorous [umol/kg]
Pressure (dbar)
0
100
200
300
400
500
600
700
800
900
1000
1989
1990
1991
1992
1993
1994
1995
1996
1997
1998
1999
2000
0.2
0.4
0.6
0.8
1
1.2
1.4
1.6
1.8
2
2.2
2.4
2.6
2.8
3
3.2

Figure 6.1.19

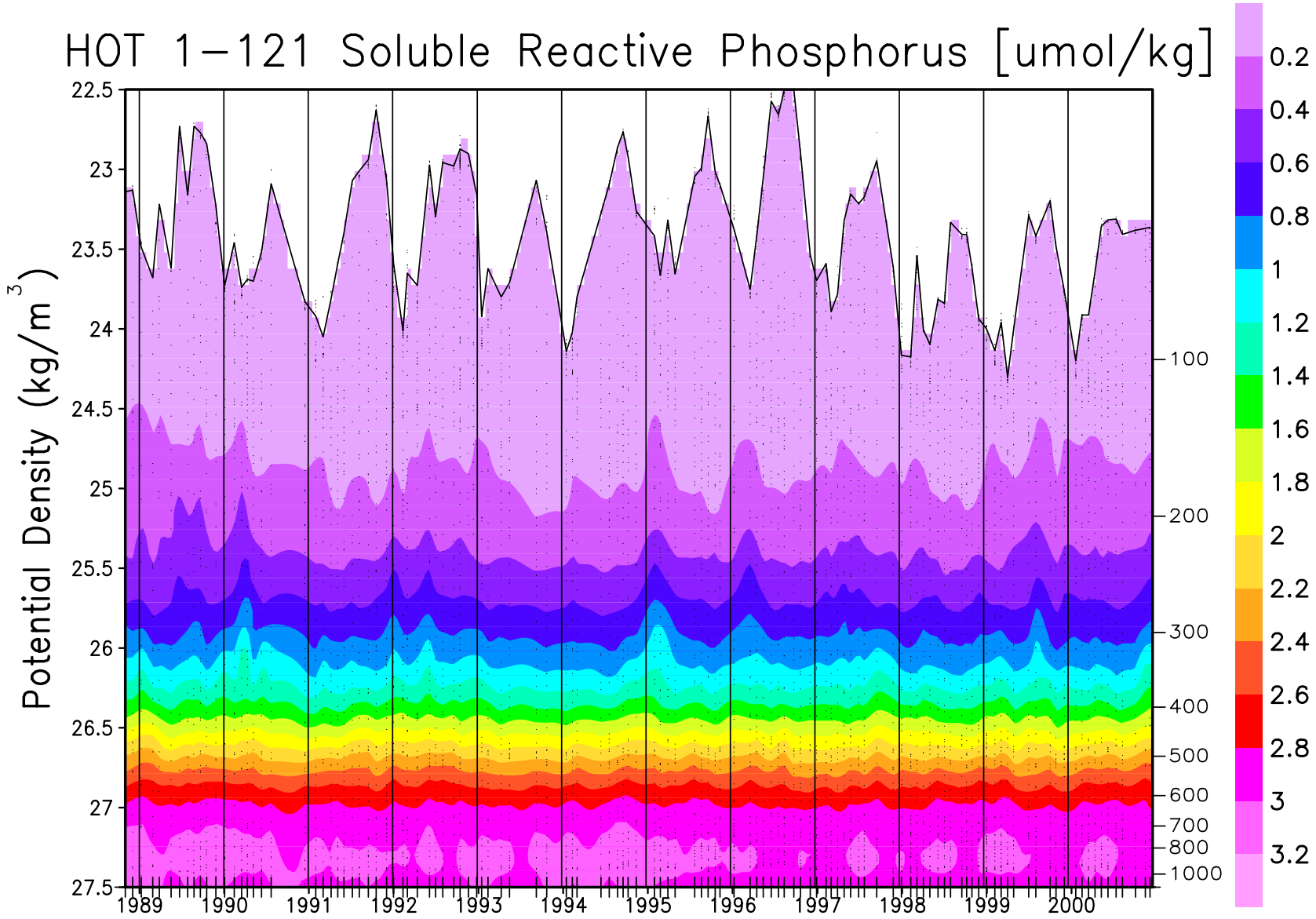
HOT 1–121 Soluble Reactive Phosphorus [umol/kg]
Potential Density (kg/m3)
22.5
23
23.5
24
24.5
25
25.5
26
26.5
27
27.5
1989
1990
1991
1992
1993
1994
1995
1996
1997
1998
1999
2000
100
200
300
400
500
600
700
800
1000
0.2
0.4
0.6
0.8
1
1.2
1.4
1.6
1.8
2
2.2
2.4
2.6
2.8
3
3.2

Figure 6.1.20

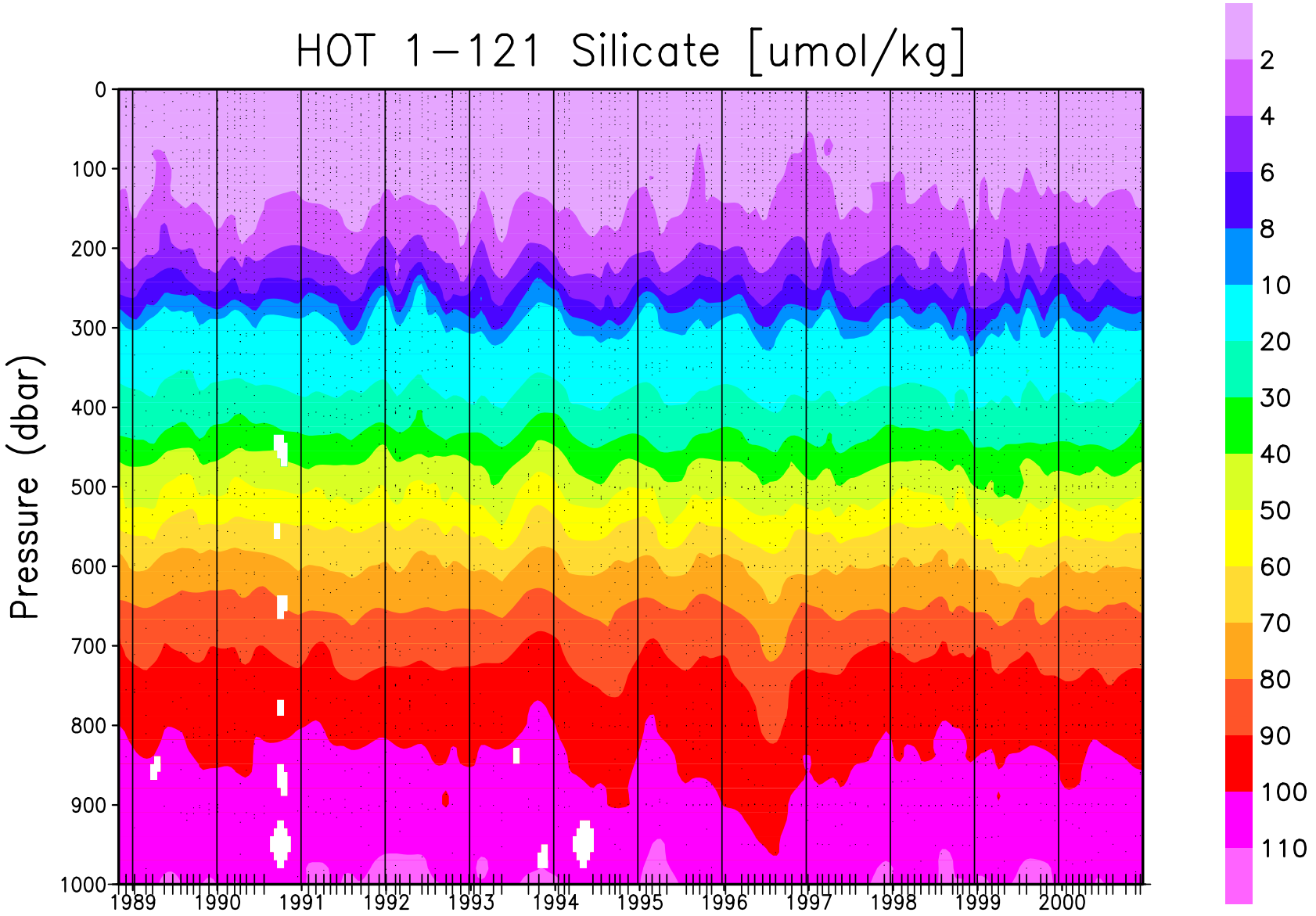
HOT 1–121 Silicate [umol/kg]
Pressure (dbar)
0
100
200
300
400
500
600
700
800
900
1000
1989
1990
1991
1992
1993
1994
1995
1996
1997
1998
1999
2000
2
4
6
8
10
20
30
40
50
60
70
80
90
100
110

Figure 6.1.21

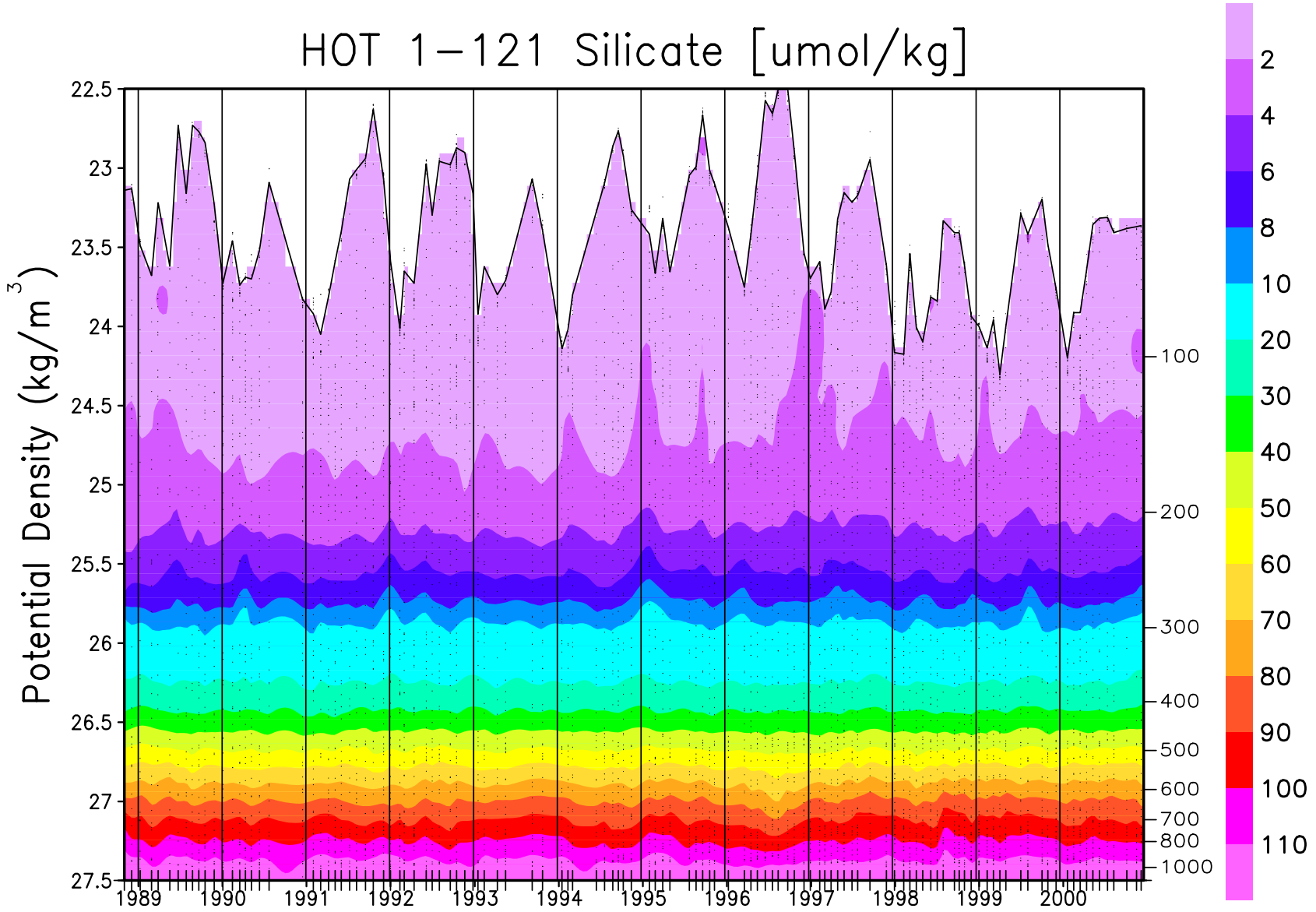
HOT 1–121 Silicate [umol/kg]
Potential Density (kg/m3)
22.5
23
23.5
24
24.5
25
25.5
26
26.5
27
27.5
1989
1990
1991
1992
1993
1994
1995
1996
1997
1998
1999
2000
100
200
300
400
500
600
700
800
1000
2
4
6
8
10
20
30
40
50
60
70
80
90
100
110

Figure 6.1.22

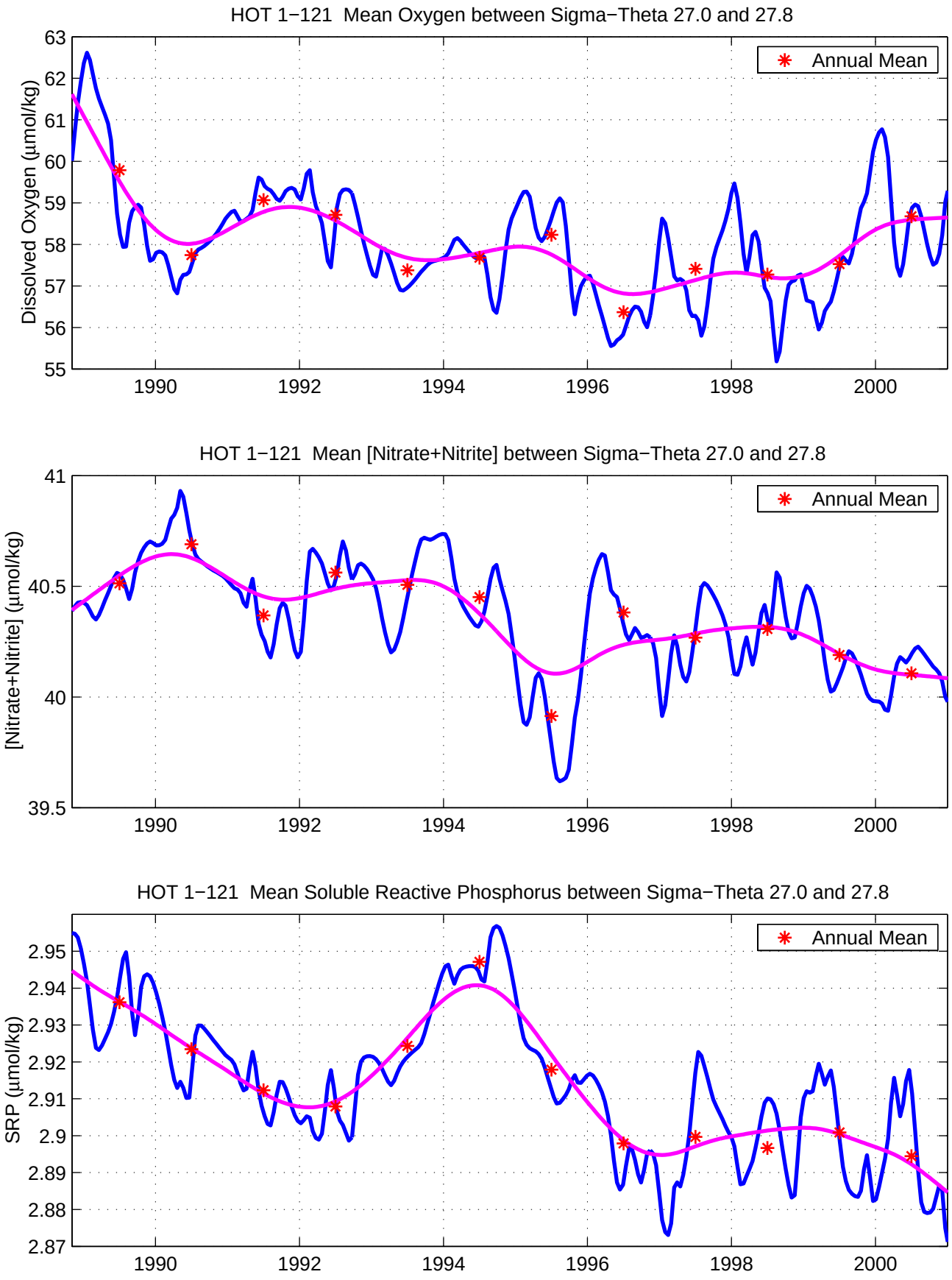
HOT 1−121 Mean Oxygen between Sigma−Theta 27.0 and 27.8
Dissolved Oxygen (µmol/kg)
Annual Mean
HOT 1−121 Mean [Nitrate+Nitrite] between Sigma−Theta 27.0 and 27.8
[Nitrate+Nitrite] (µmol/kg)
Annual Mean
HOT 1−121 Mean Soluble Reactive Phosphorus between Sigma−Theta 27.0 and 27.8
SRP (µmol/kg)
Annual Mean
1990
1992
1994
1996
1998
2000

Figure 6.1.23

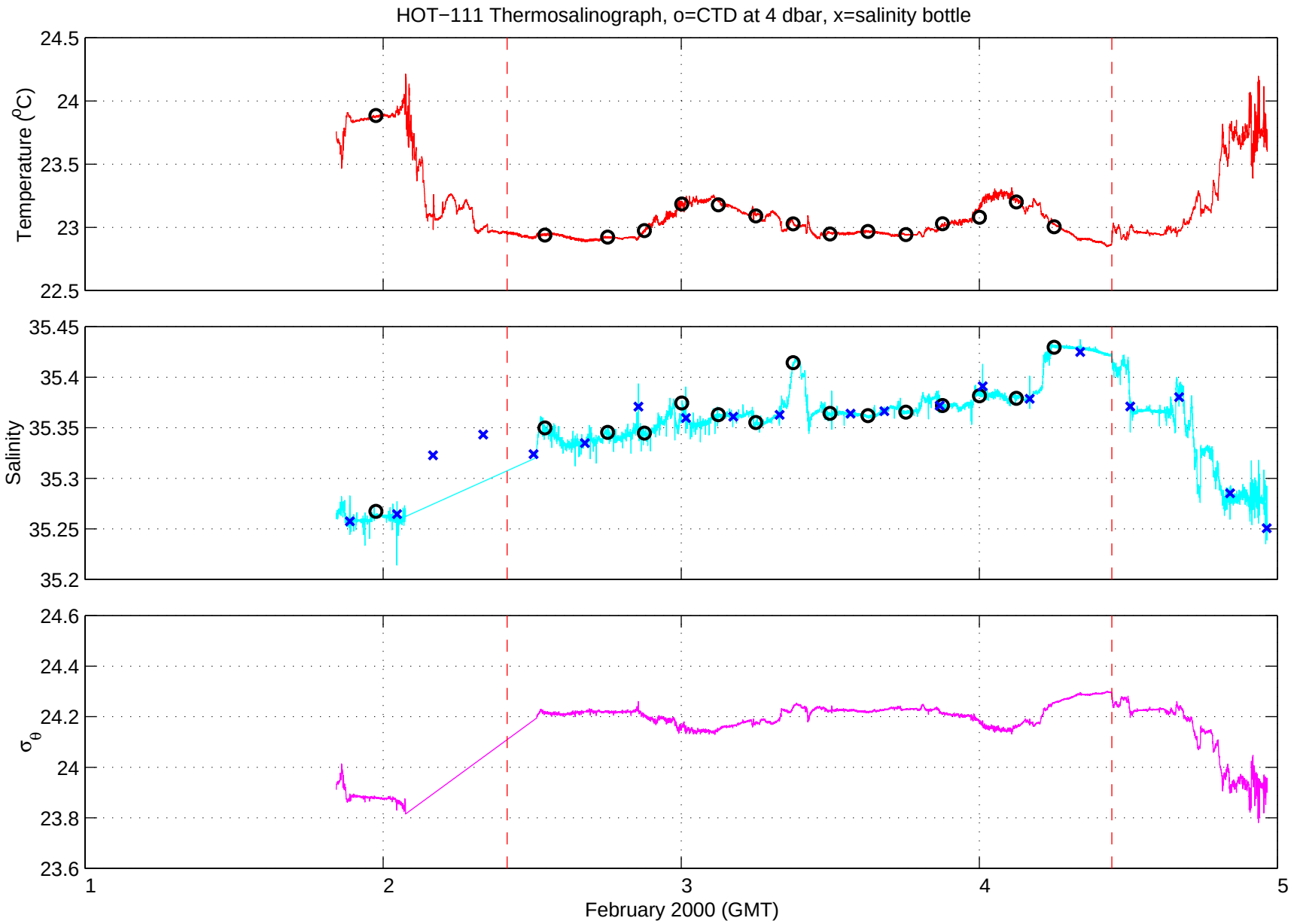
HOT−111 Thermosalinograph, o=CTD at 4 dbar, x=salinity bottle
Temperature (°C)
24.5
24
23.5
23
22.5
Salinity
35.45
35.4
35.35
35.3
35.25
35.2
σθ
24.6
24.4
24.2
24
23.8
23.6
1
2
3
4
5
February 2000 (GMT)

Figure 6.2.1a

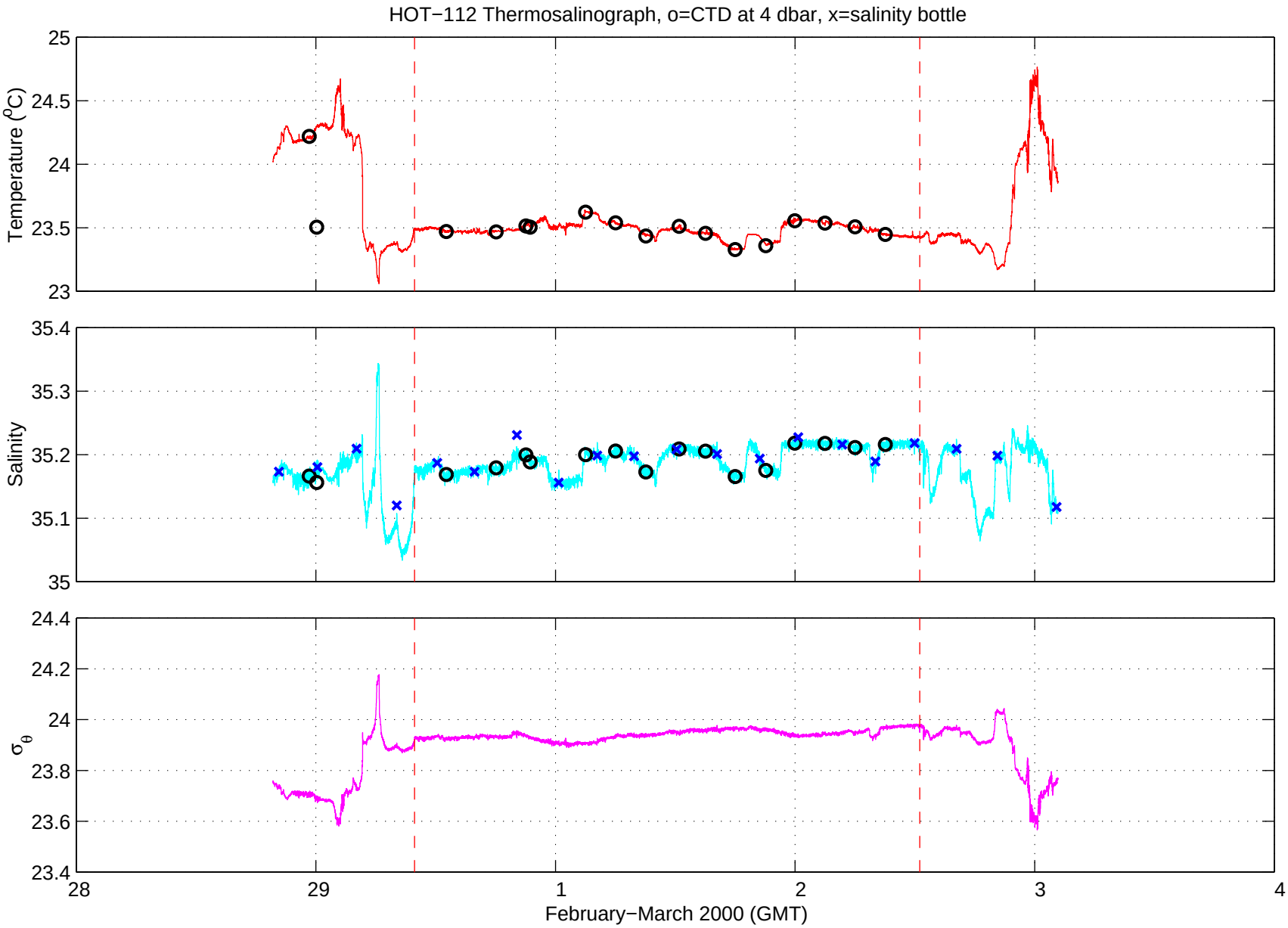
HOT−112 Thermosalinograph, o=CTD at 4 dbar, x=salinity bottle
Temperature (°C)
25
24.5
24
23.5
23
Salinity
35.4
35.3
35.2
35.1
35
σθ
24.4
24.2
24
23.8
23.6
23.4
28
29
1
2
3
4
February−March 2000 (GMT)

Figure 6.2.1b

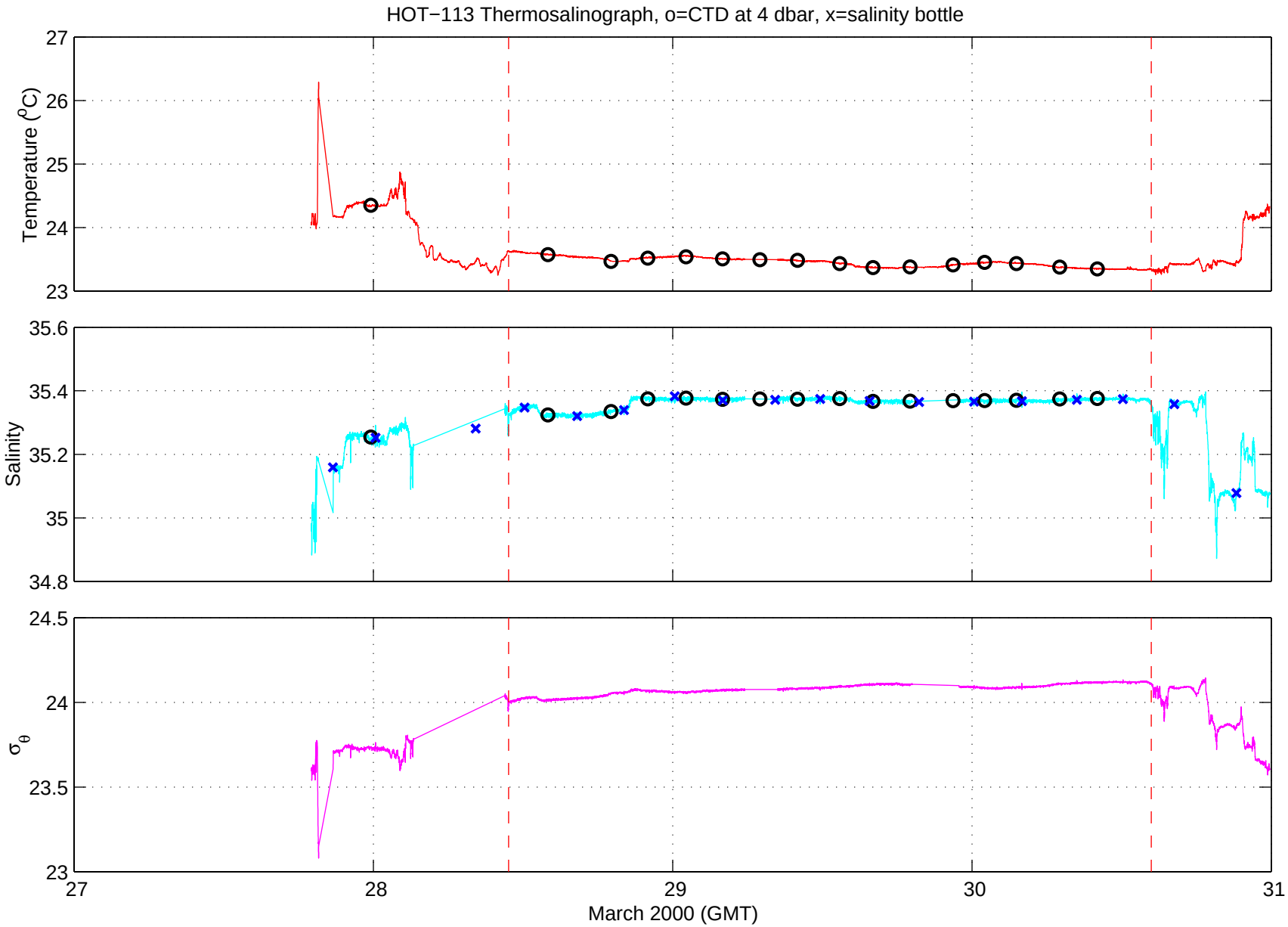
HOT−113 Thermosalinograph, o=CTD at 4 dbar, x=salinity bottle
Temperature (°C)
27
26
25
24
23
Salinity
35.6
35.4
35.2
35
34.8
σθ
24.5
24
23.5
23
27
28
29
30
31
March 2000 (GMT)

Figure 6.2.1c

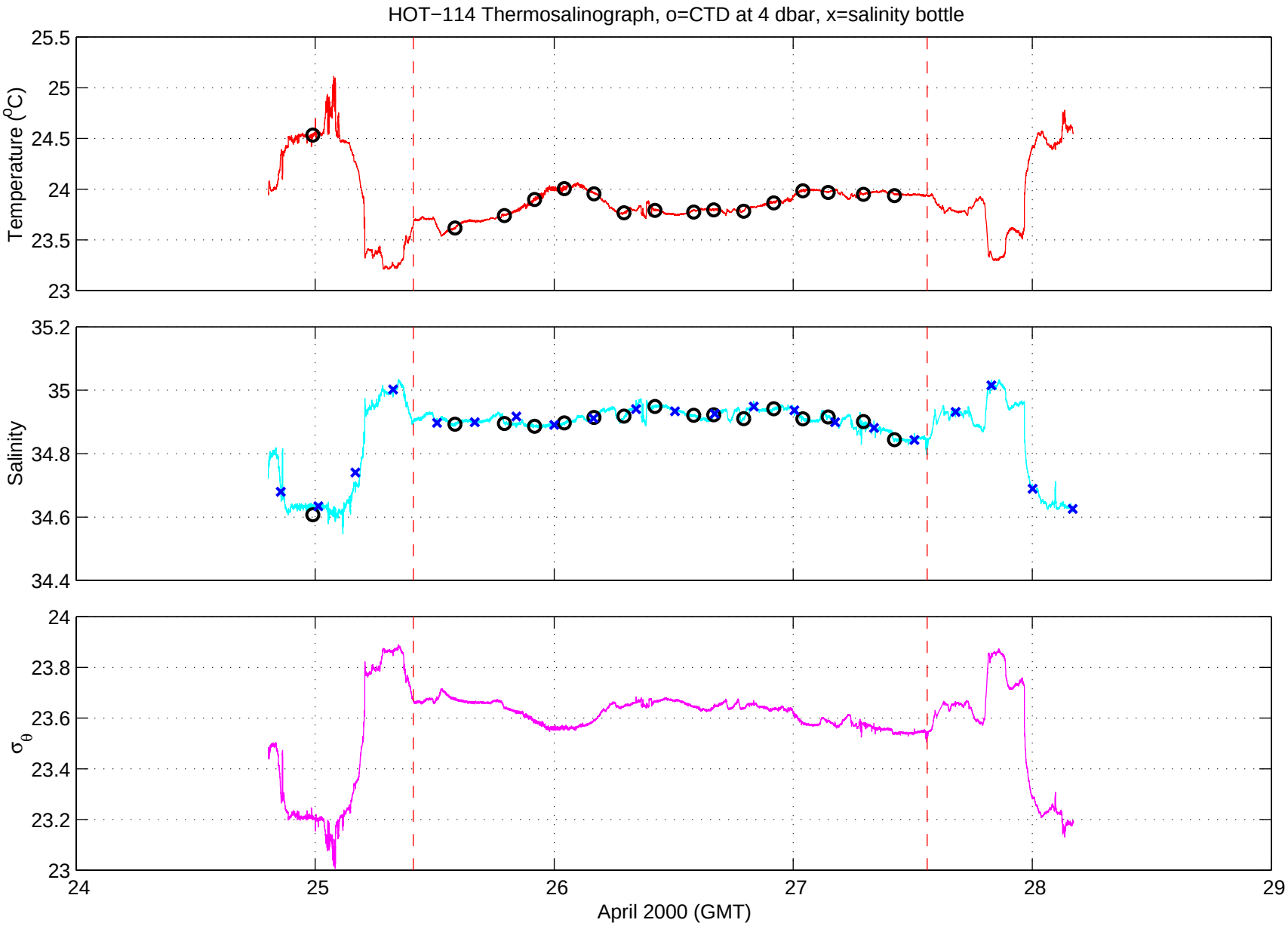
HOT−114 Thermosalinograph, o=CTD at 4 dbar, x=salinity bottle
Temperature (°C)
25.5
25
24.5
24
23.5
23
Salinity
35.2
35
34.8
34.6
34.4
σθ
24
23.8
23.6
23.4
23.2
23
24
25
26
27
28
29
April 2000 (GMT)

Figure 6.2.1d

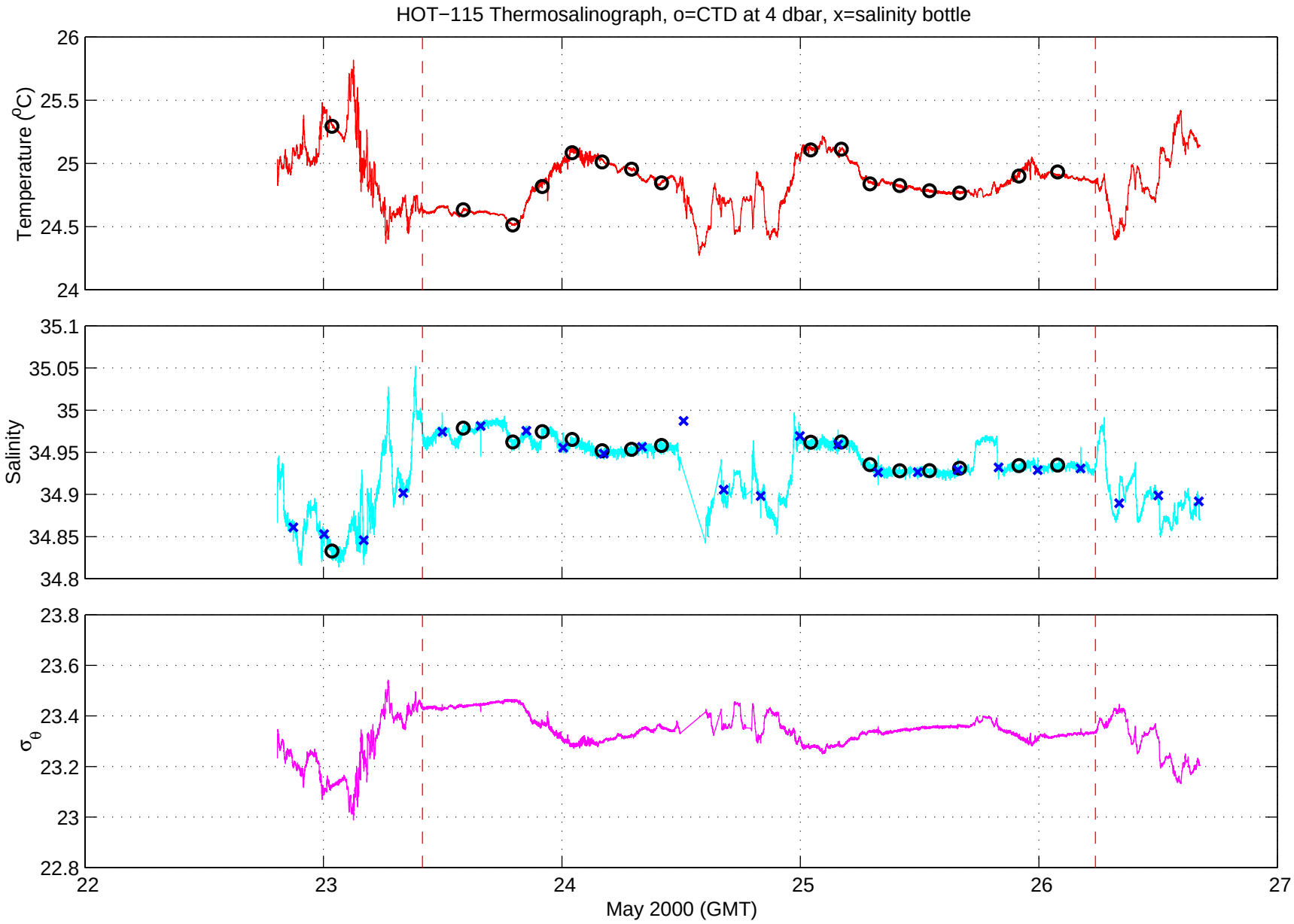
HOT−115 Thermosalinograph, o=CTD at 4 dbar, x=salinity bottle
Temperature (°C)
26
25.5
25
24.5
24
Salinity
35.1
35.05
35
34.95
34.9
34.85
34.8
σθ
23.8
23.6
23.4
23.2
23
22.8
22
23
24
25
26
27
May 2000 (GMT)

Figure 6.2.1e

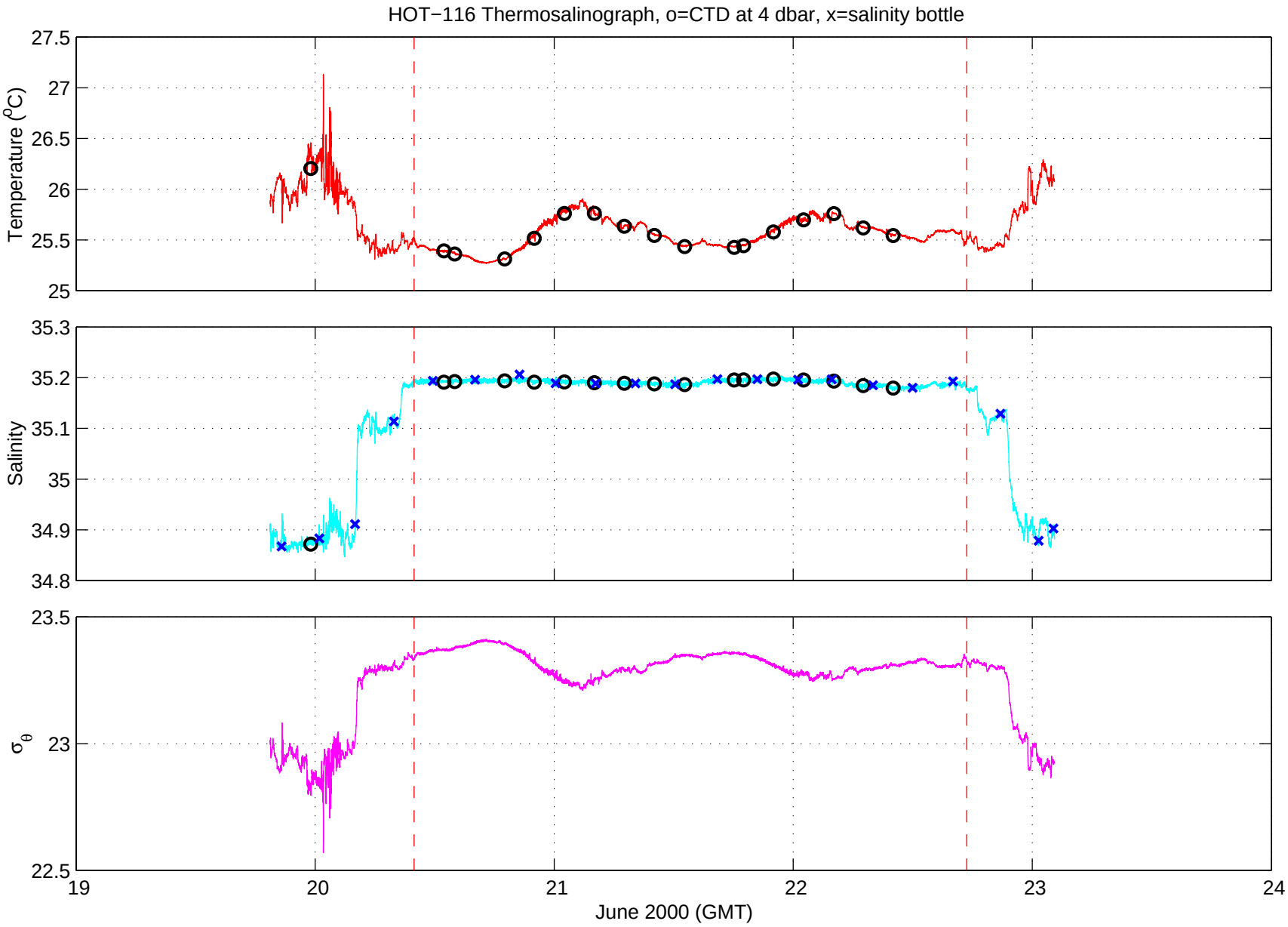
HOT−116 Thermosalinograph, o=CTD at 4 dbar, x=salinity bottle
Temperature (°C)
27.5
27
26.5
26
25.5
25
Salinity
35.3
35.2
35.1
35
34.9
34.8
σθ
23.5
23
22.5
19
20
21
22
23
24
June 2000 (GMT)

Figure 6.2.1f

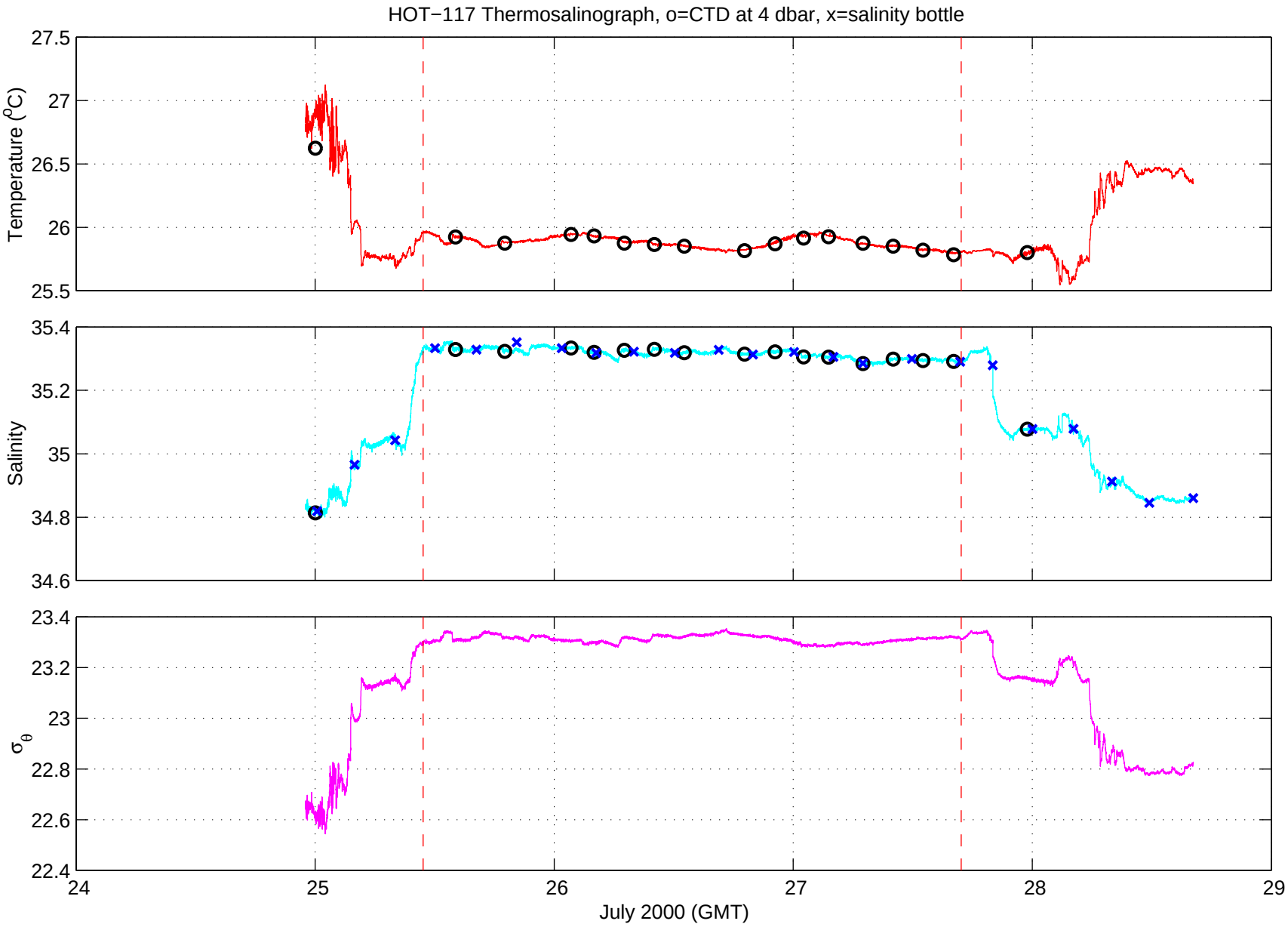
HOT−117 Thermosalinograph, o=CTD at 4 dbar, x=salinity bottle
Temperature (°C)
27.5
27
26.5
26
25.5
Salinity
35.4
35.2
35
34.8
34.6
σθ
23.4
23.2
23
22.8
22.6
22.4
24
25
26
27
28
29
July 2000 (GMT)

Figure 6.2.1g

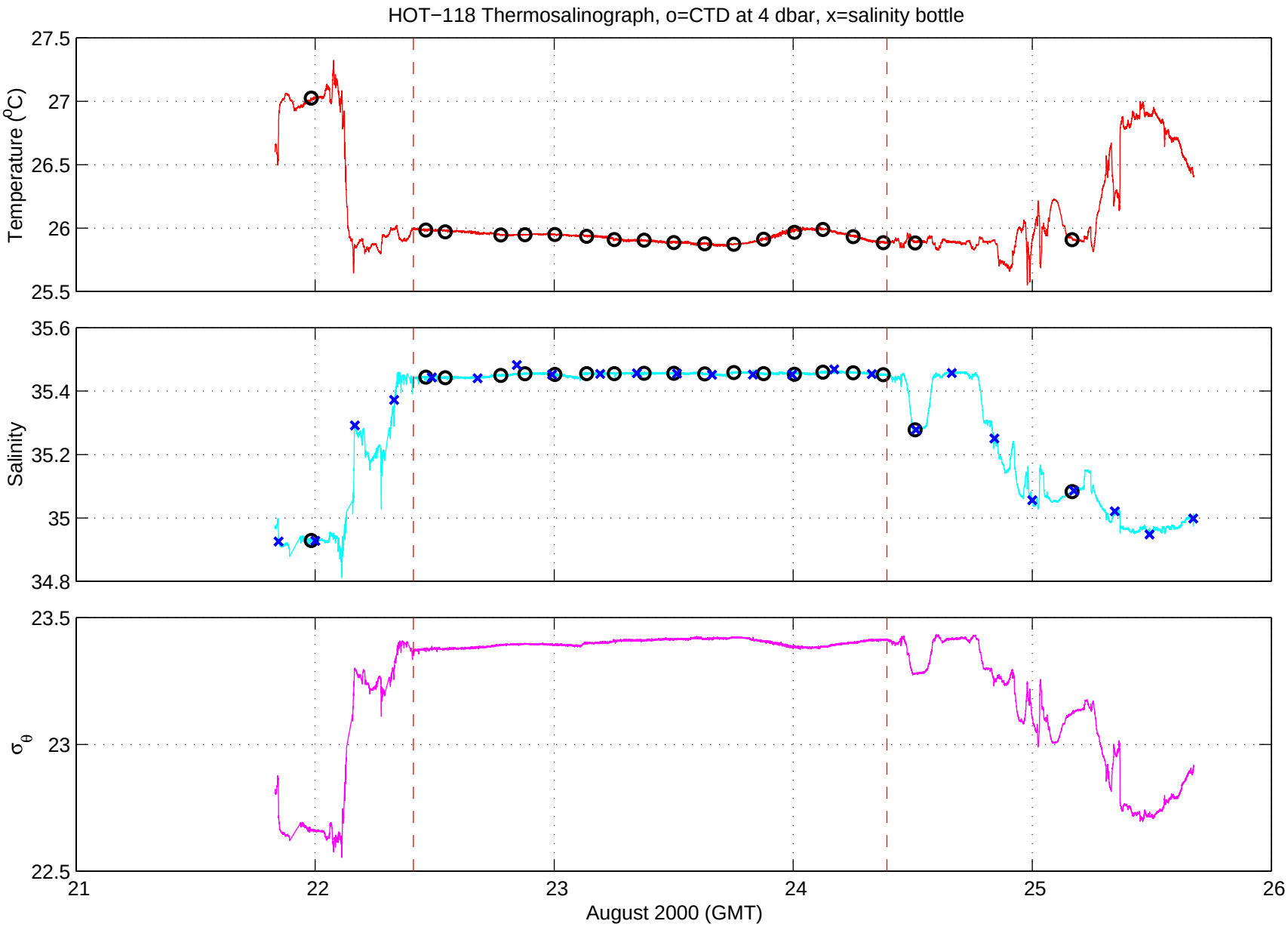
HOT−118 Thermosalinograph, o=CTD at 4 dbar, x=salinity bottle
Temperature (°C)
27.5
27
26.5
26
25.5
Salinity
35.6
35.4
35.2
35
34.8
σθ
23.5
23
22.5
21
22
23
24
25
26
August 2000 (GMT)

Figure 6.2.1h

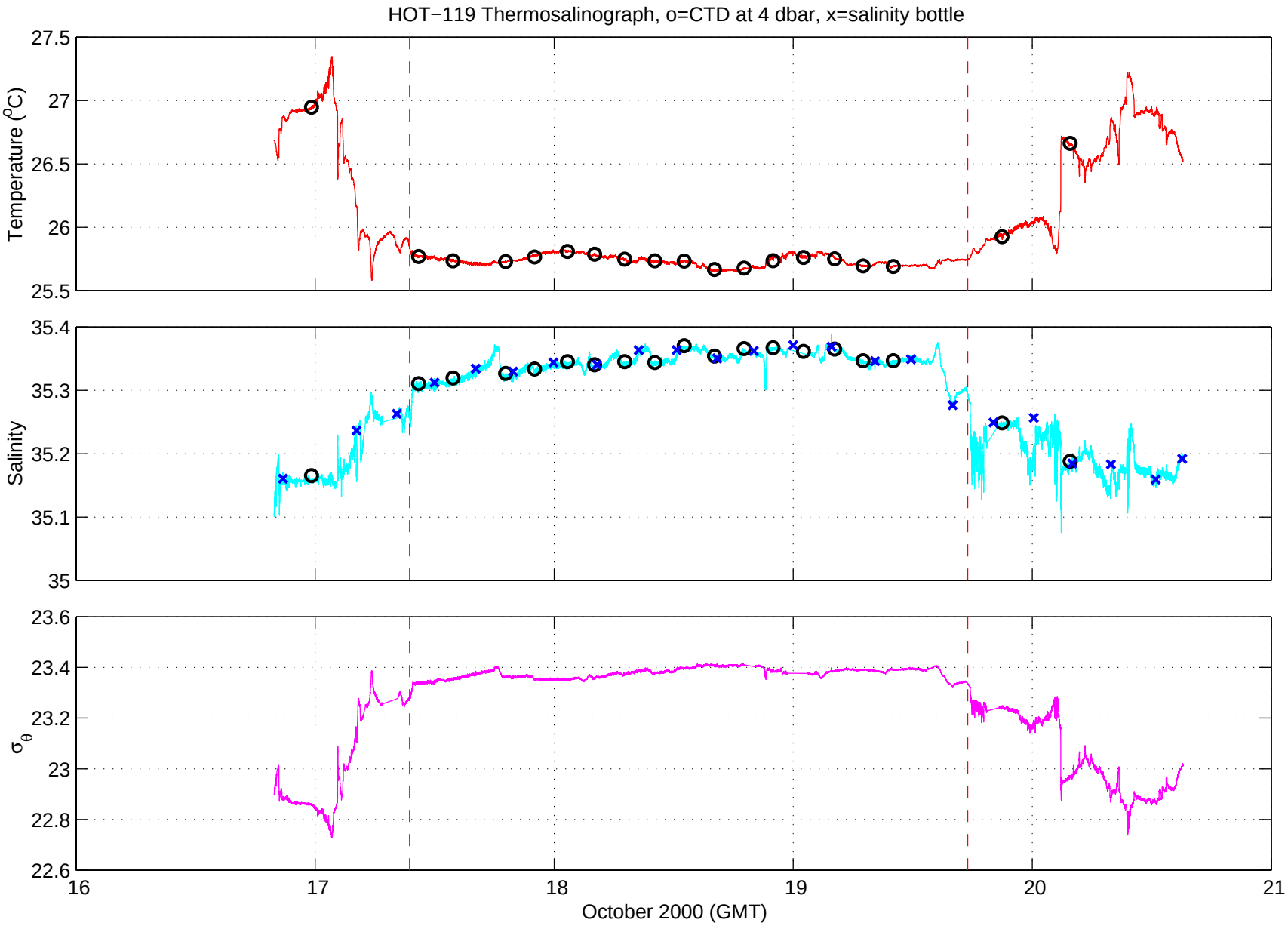
HOT−119 Thermosalinograph, o=CTD at 4 dbar, x=salinity bottle
Temperature (°C)
27.5
27
26.5
26
25.5
Salinity
35.4
35.3
35.2
35.1
35
σθ
23.6
23.4
23.2
23
22.8
22.6
16
17
18
19
20
21
October 2000 (GMT)

Figure 6.2.1i

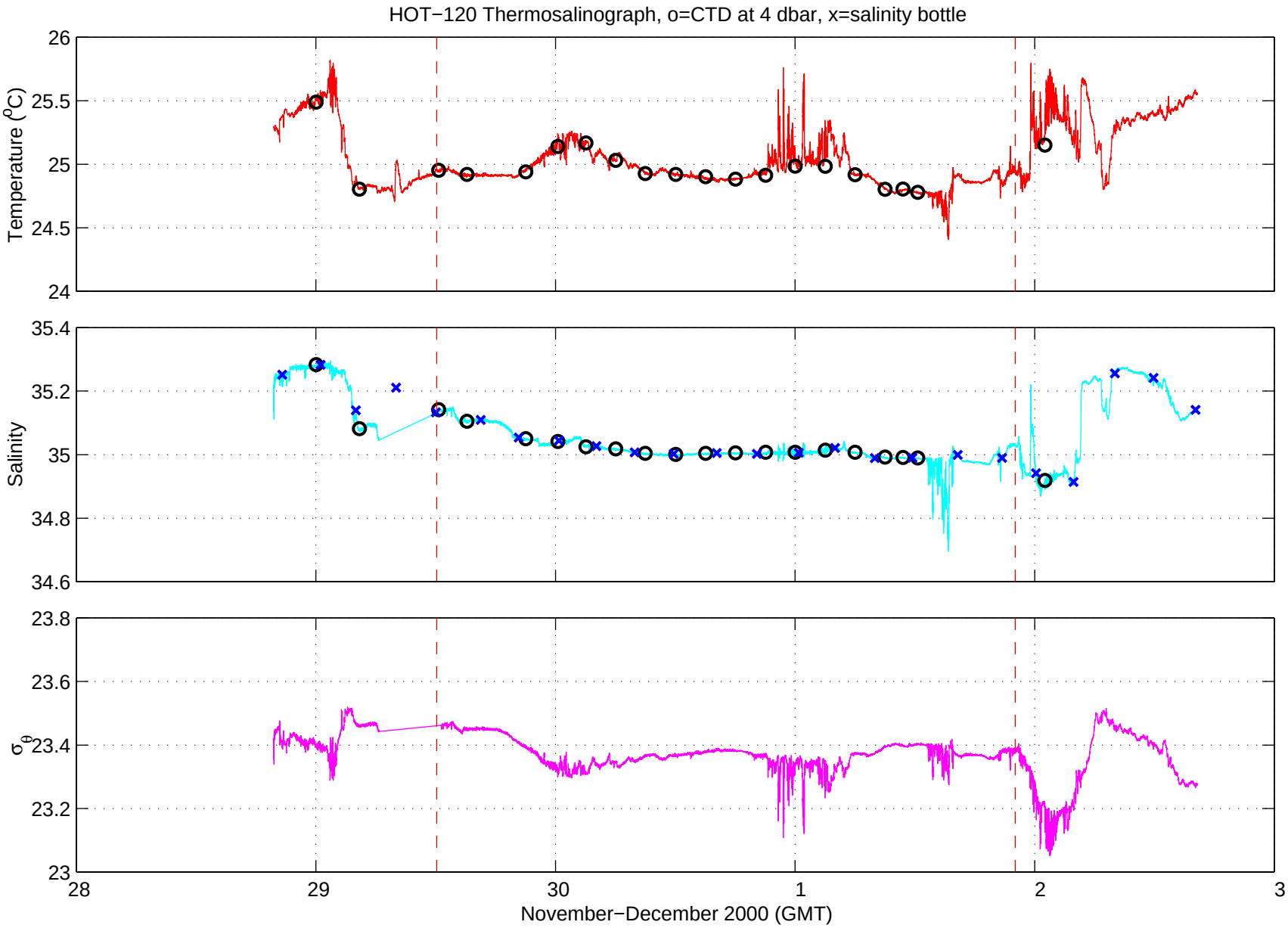
HOT−120 Thermosalinograph, o=CTD at 4 dbar, x=salinity bottle
Temperature (°C)
26
25.5
25
24.5
24
Salinity
35.4
35.2
35
34.8
34.6
σθ
23.8
23.6
23.4
23.2
23
28
29
30
1
2
3
November−December 2000 (GMT)

Figure 6.2.1j

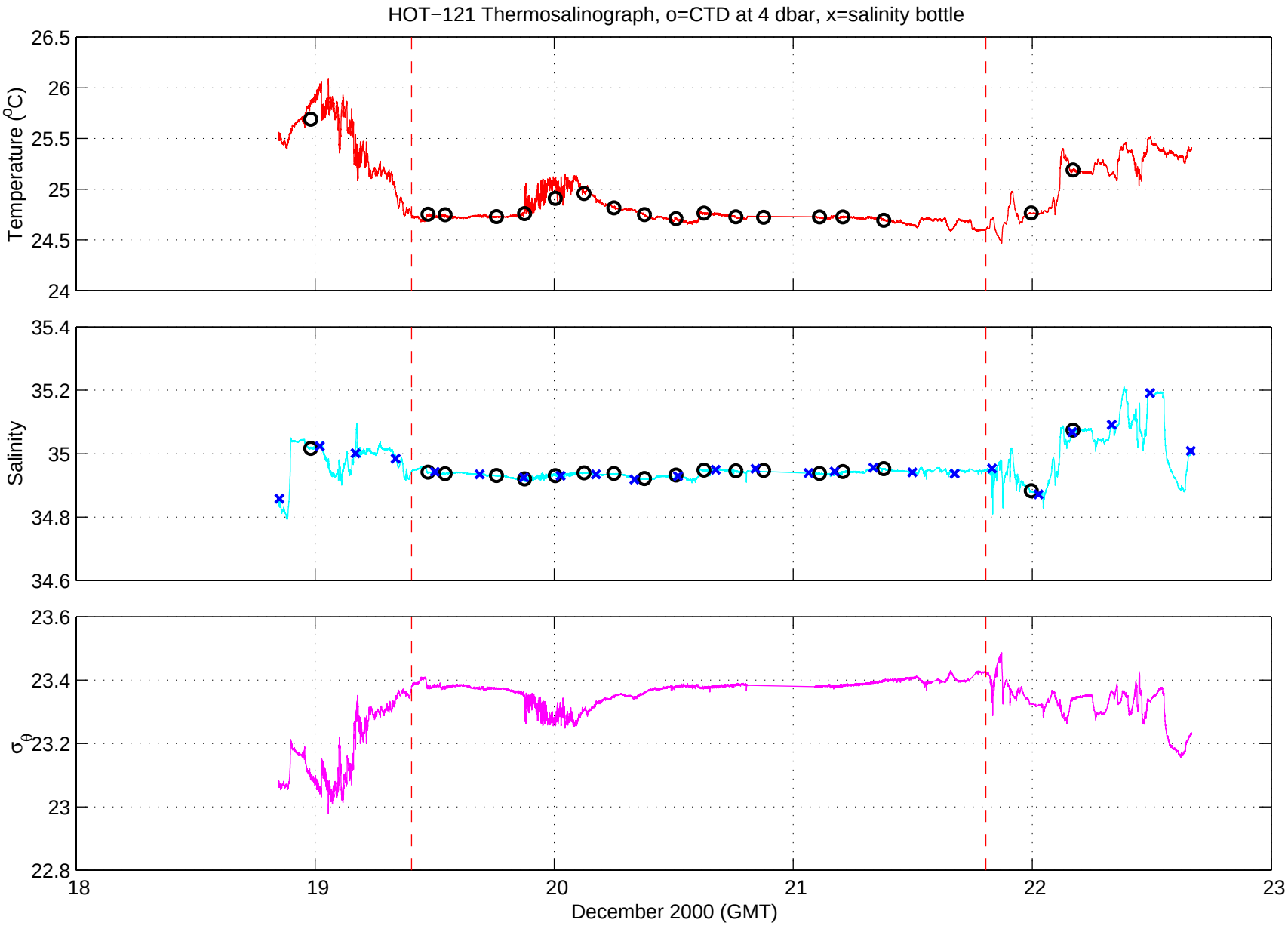
HOT−121 Thermosalinograph, o=CTD at 4 dbar, x=salinity bottle
Temperature (°C)
26.5
26
25.5
25
24.5
24
Salinity
35.4
35.2
35
34.8
34.6
σθ
23.6
23.4
23.2
23
22.8
18
19
20
21
22
23
December 2000 (GMT)

Figure 6.2.1k

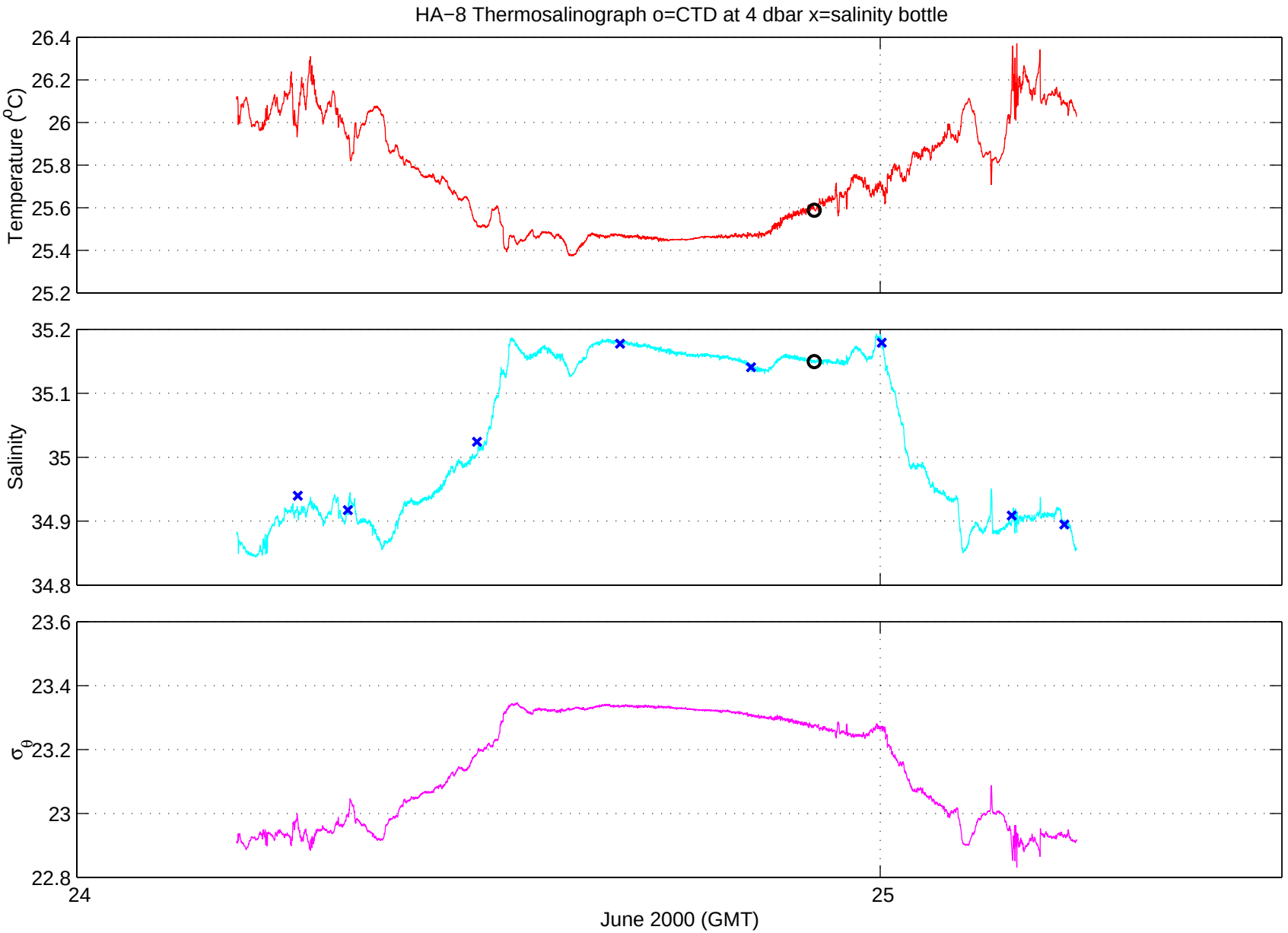
HA−8 Thermosalinograph o=CTD at 4 dbar x=salinity bottle
Temperature (°C)
26.4
26.2
26
25.8
25.6
25.4
25.2
Salinity
35.2
35.1
35
34.9
34.8
σθ
23.6
23.4
23.2
23
22.8
24
25
June 2000 (GMT)

Figure 6.2.1l

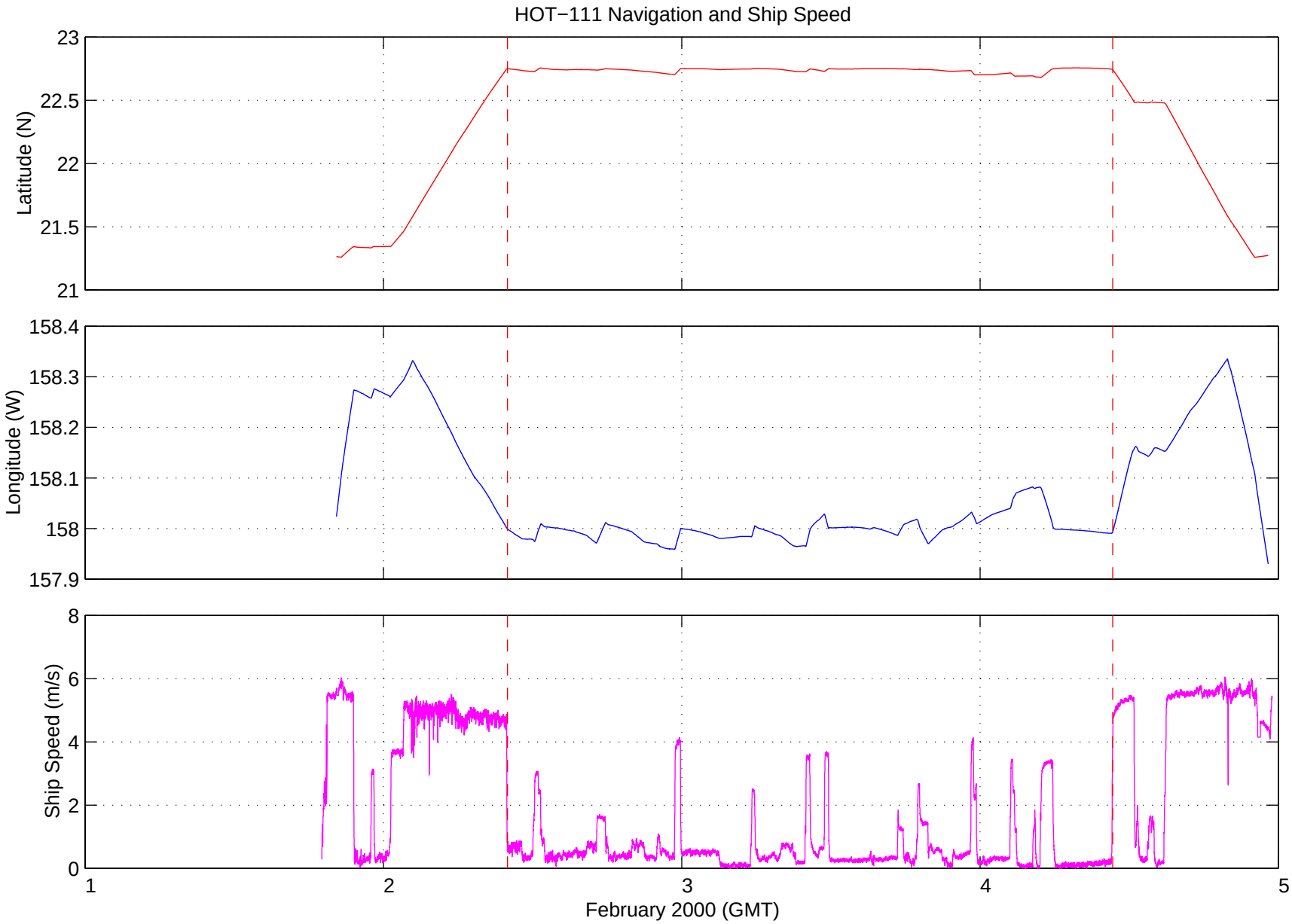
HOT−111 Navigation and Ship Speed
Latitude (N)
23
22.5
22
21.5
21
Longitude (W)
158.4
158.3
158.2
158.1
158
157.9
Ship Speed (m/s)
8
6
4
2
0
1
2
3
4
5
February 2000 (GMT)

Figure 6.2.2a

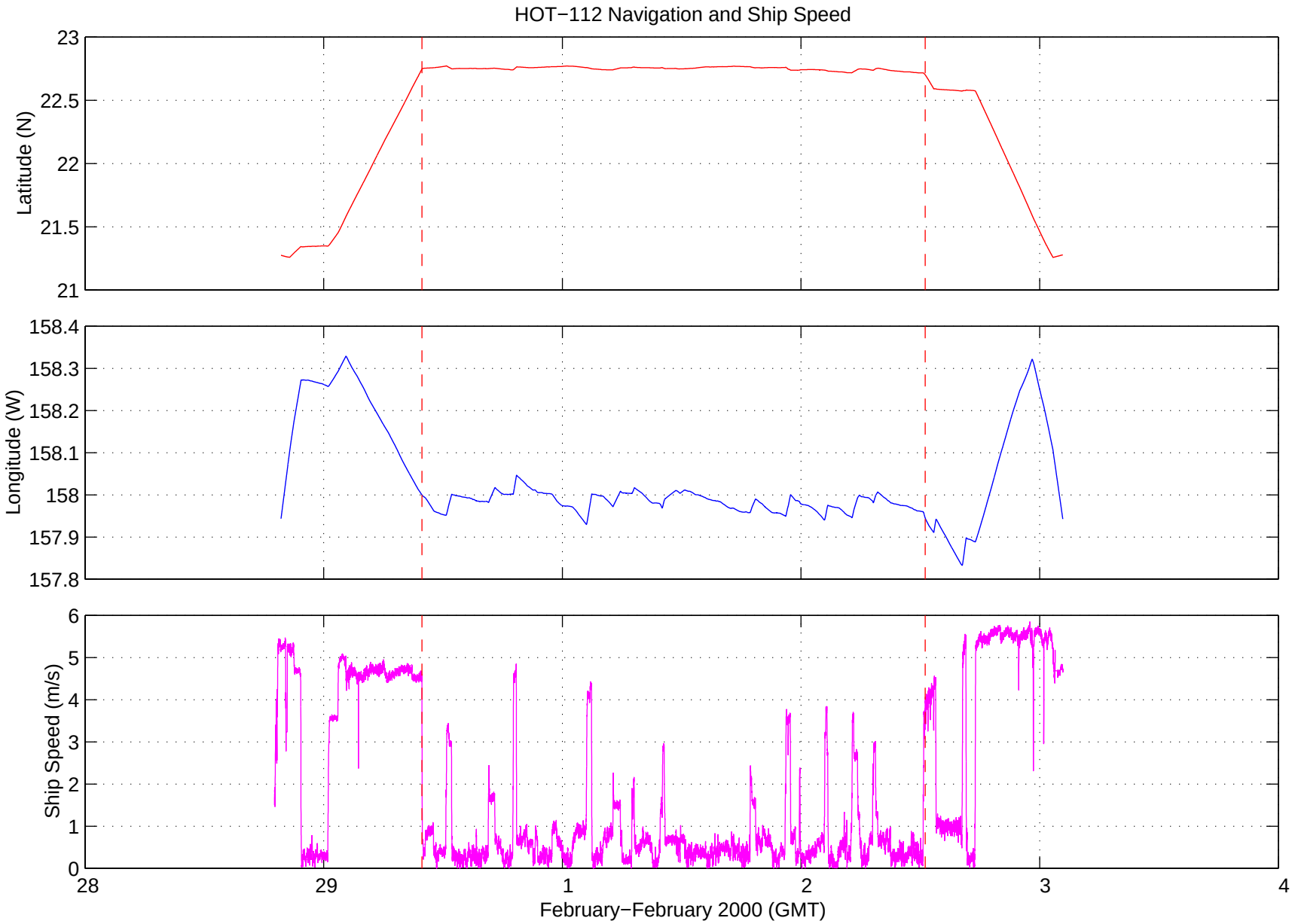
HOT−112 Navigation and Ship Speed
Latitude (N)
23
22.5
22
21.5
21
Longitude (W)
158.4
158.3
158.2
158.1
158
157.9
157.8
Ship Speed (m/s)
6
5
4
3
2
1
0
28
29
1
2
3
4
February−February 2000 (GMT)

Figure 6.2.2b


HOT−113 Navigation and Ship Speed
Latitude (N)
23
22.5
22
21.5
21
Longitude (W)
158.4
158.3
158.2
158.1
158
157.9
157.8
Ship Speed (m/s)
6
5
4
3
2
1
0
27
28
29
30
31
March 2000 (GMT)

Figure 6.2.2c

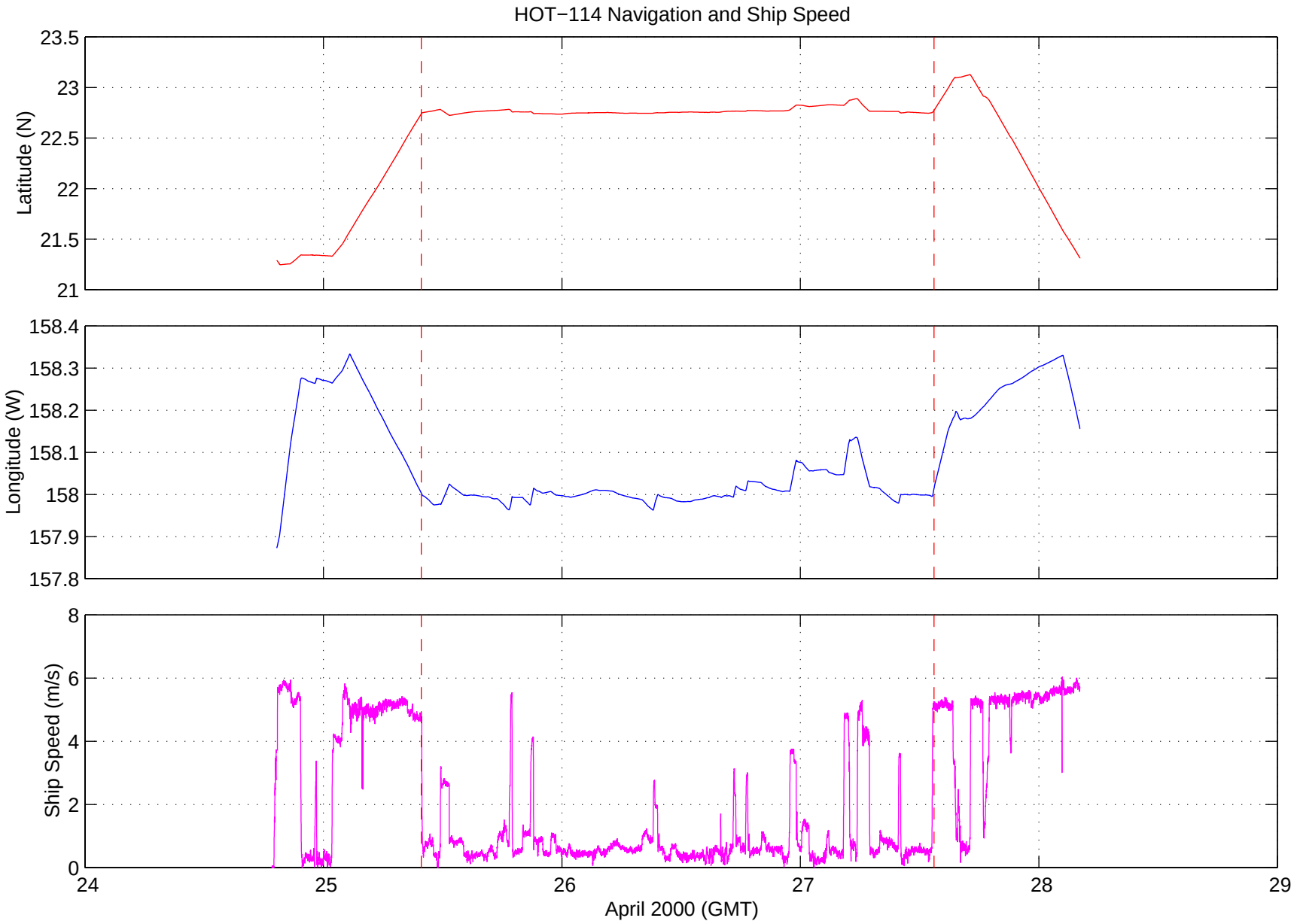
HOT−114 Navigation and Ship Speed
Latitude (N)
23.5
23
22.5
22
21.5
21
Longitude (W)
158.4
158.3
158.2
158.1
158
157.9
157.8
Ship Speed (m/s)
8
6
4
2
0
24
25
26
27
28
29
April 2000 (GMT)

Figure 6.2.2d

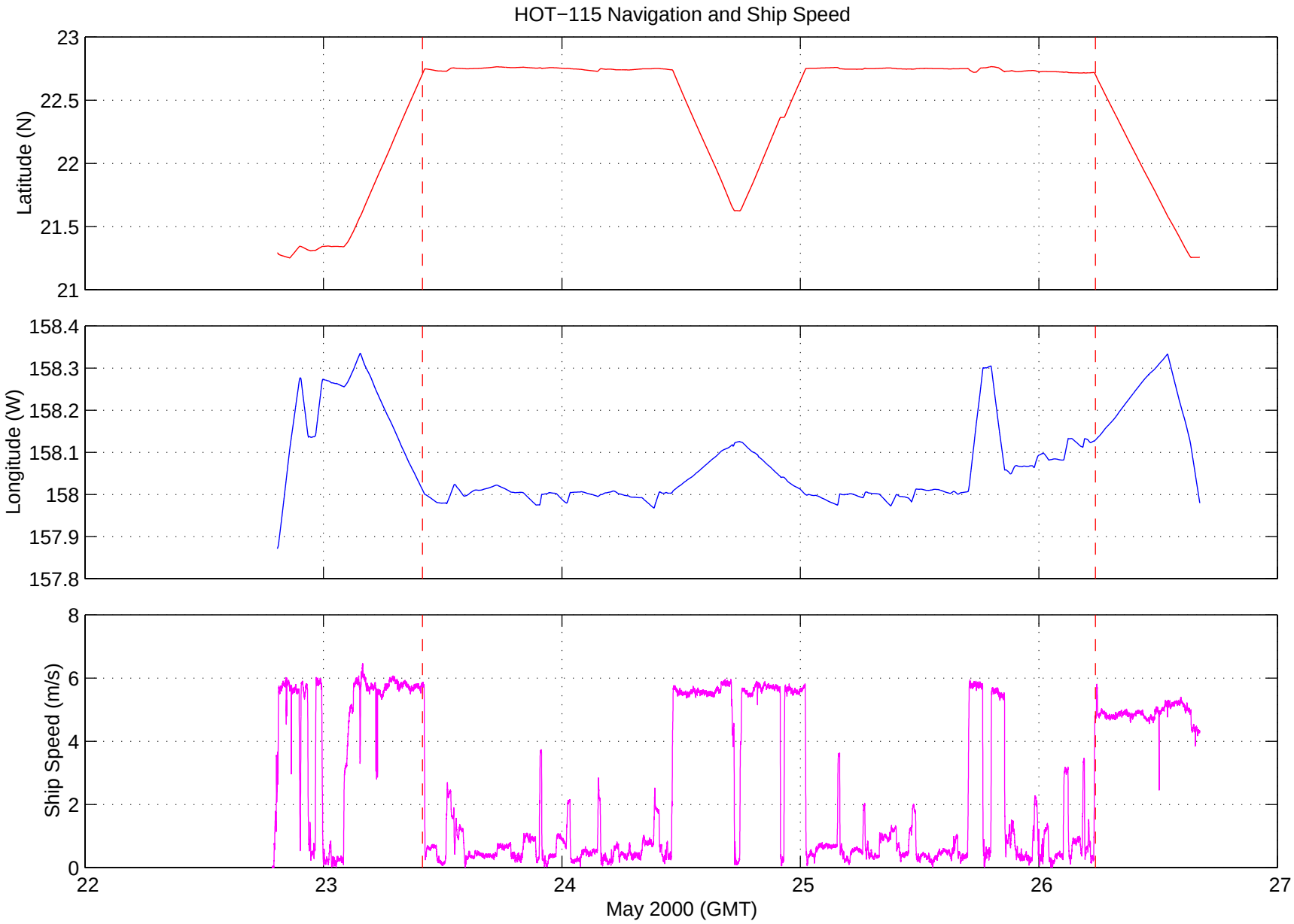
HOT−115 Navigation and Ship Speed
Latitude (N)
23
22.5
22
21.5
21
Longitude (W)
158.4
158.3
158.2
158.1
158
157.9
157.8
Ship Speed (m/s)
8
6
4
2
0
22
23
24
25
26
27
May 2000 (GMT)

Figure 6.2.2e

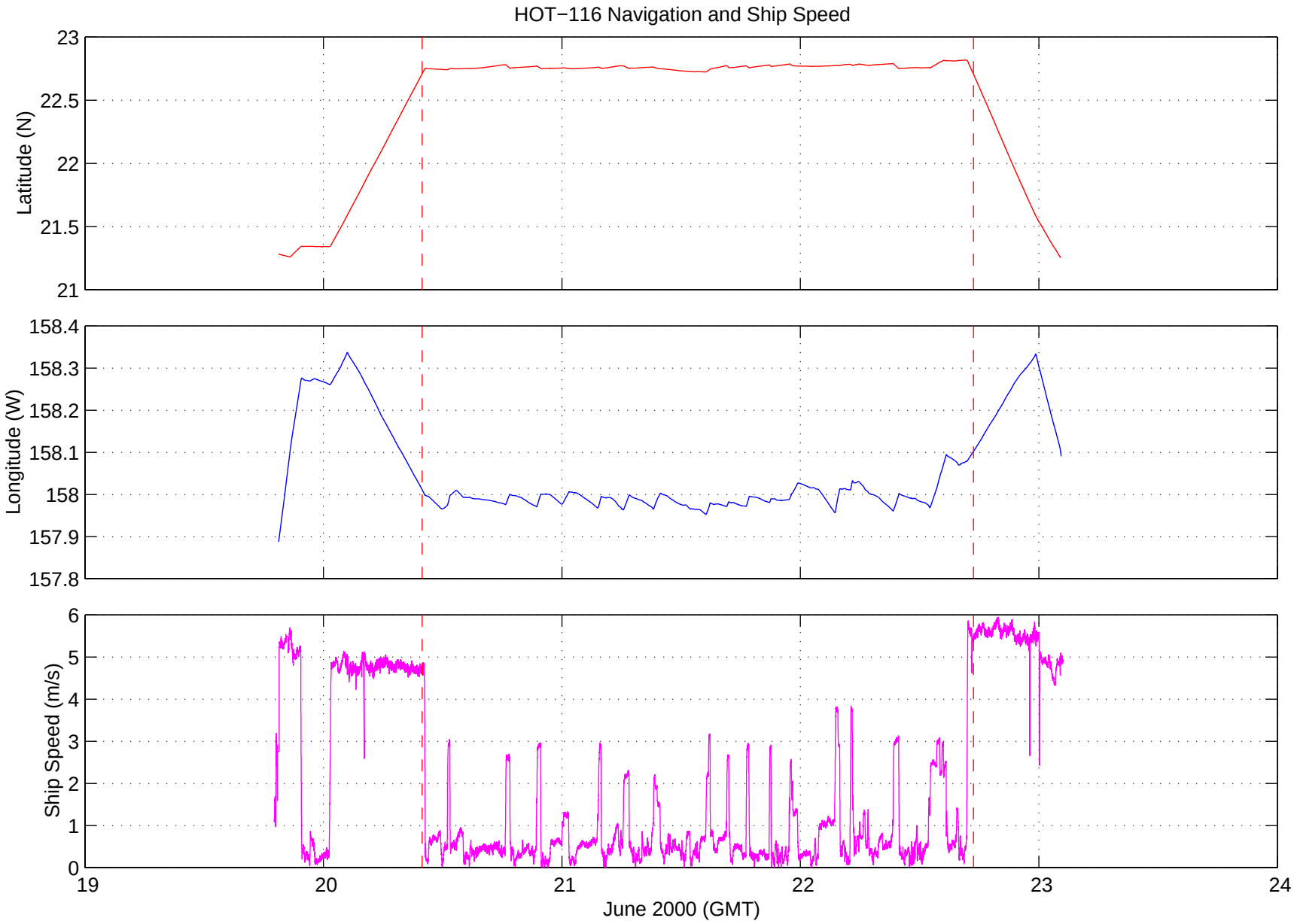
HOT−116 Navigation and Ship Speed
Latitude (N)
23
22.5
22
21.5
21
Longitude (W)
158.4
158.3
158.2
158.1
158
157.9
157.8
Ship Speed (m/s)
6
5
4
3
2
1
0
19
20
21
22
23
24
June 2000 (GMT)

Figure 6.2.2f

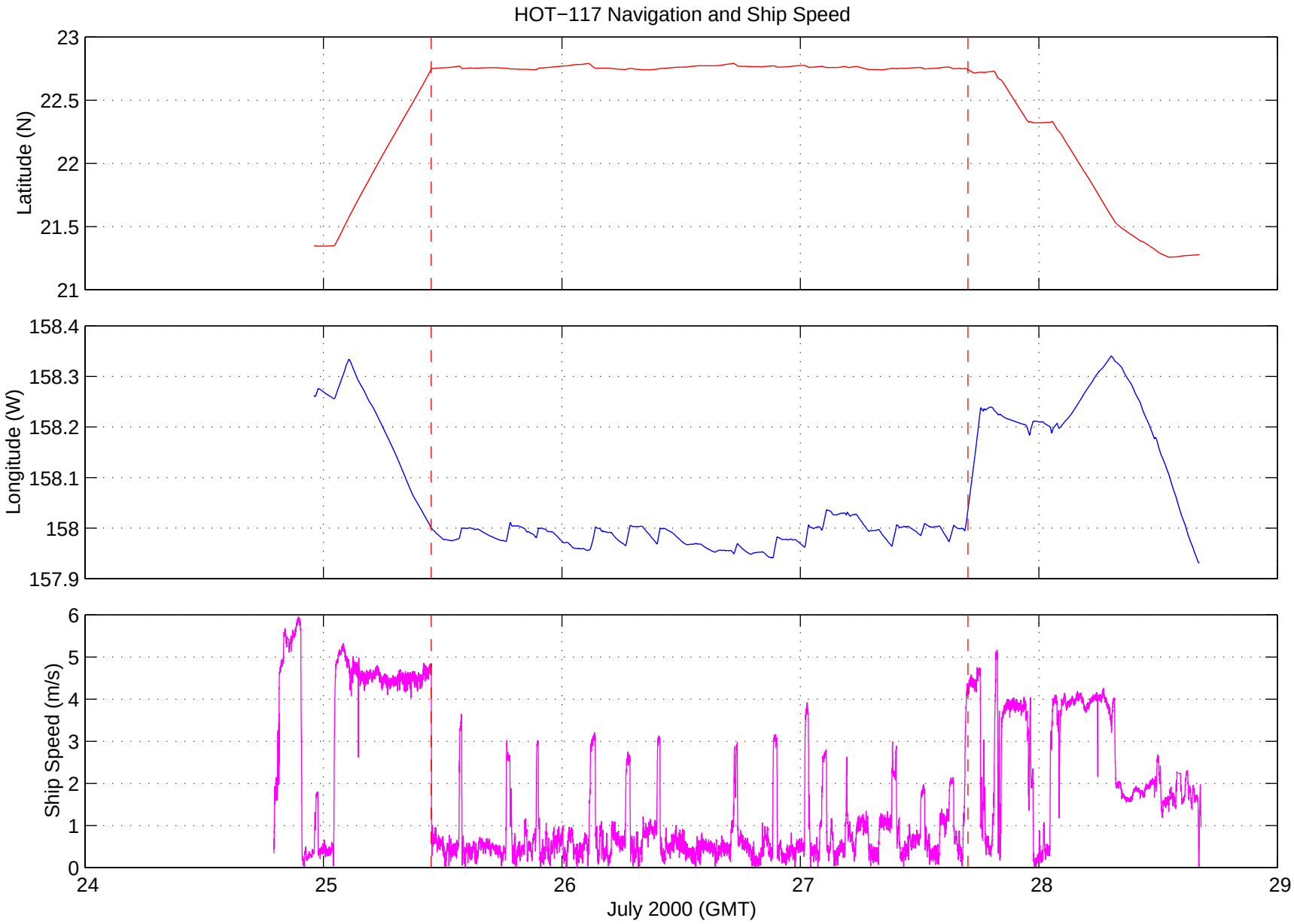
HOT−117 Navigation and Ship Speed
Latitude (N)
23
22.5
22
21.5
21
Longitude (W)
158.4
158.3
158.2
158.1
158
157.9
Ship Speed (m/s)
6
5
4
3
2
1
0
24
25
26
27
28
29
July 2000 (GMT)

Figure 6.2.2g

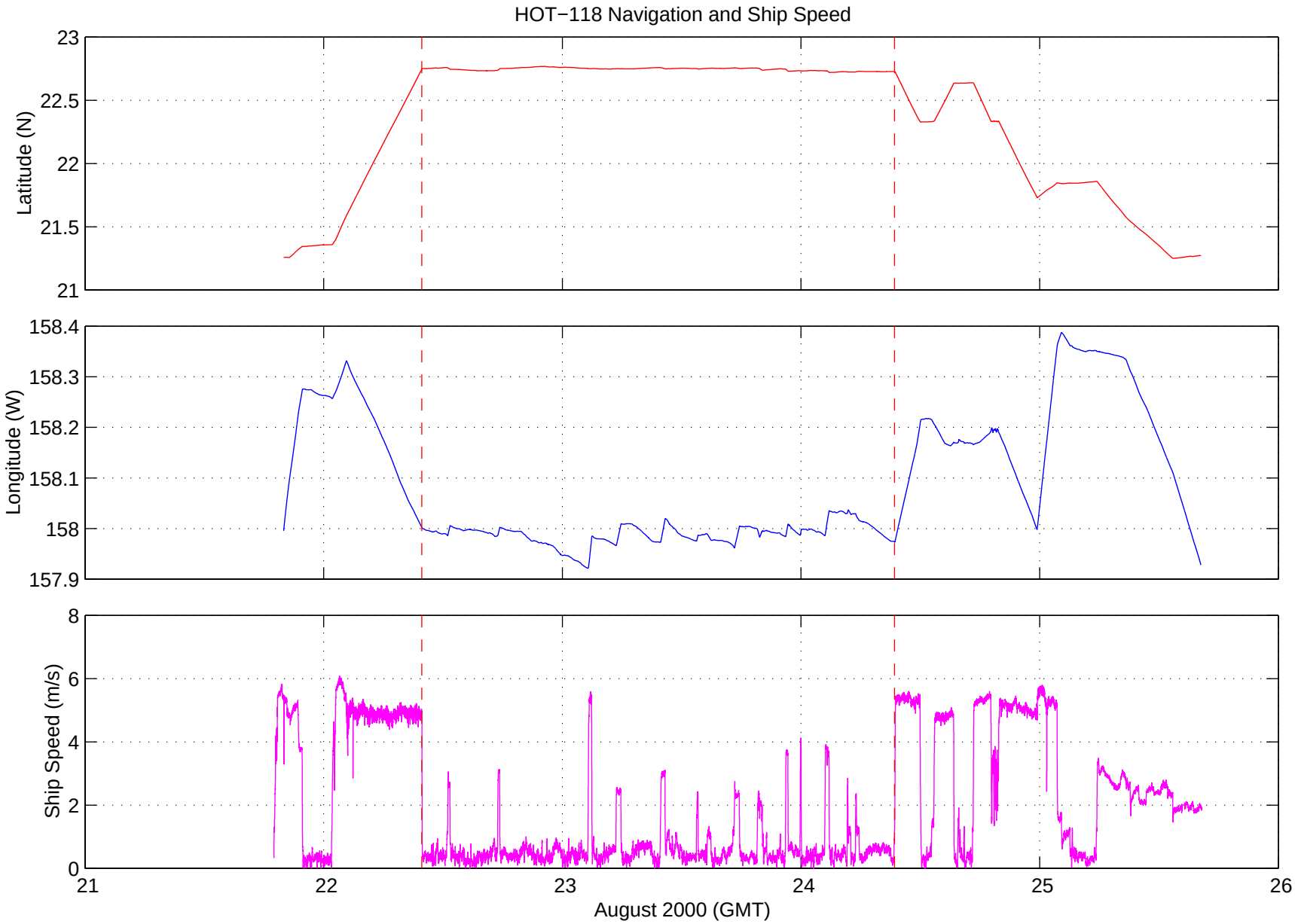
HOT−118 Navigation and Ship Speed
Latitude (N)
23
22.5
22
21.5
21
Longitude (W)
158.4
158.3
158.2
158.1
158
157.9
Ship Speed (m/s)
8
6
4
2
0
21
22
23
24
25
26
August 2000 (GMT)

Figure 6.2.2h

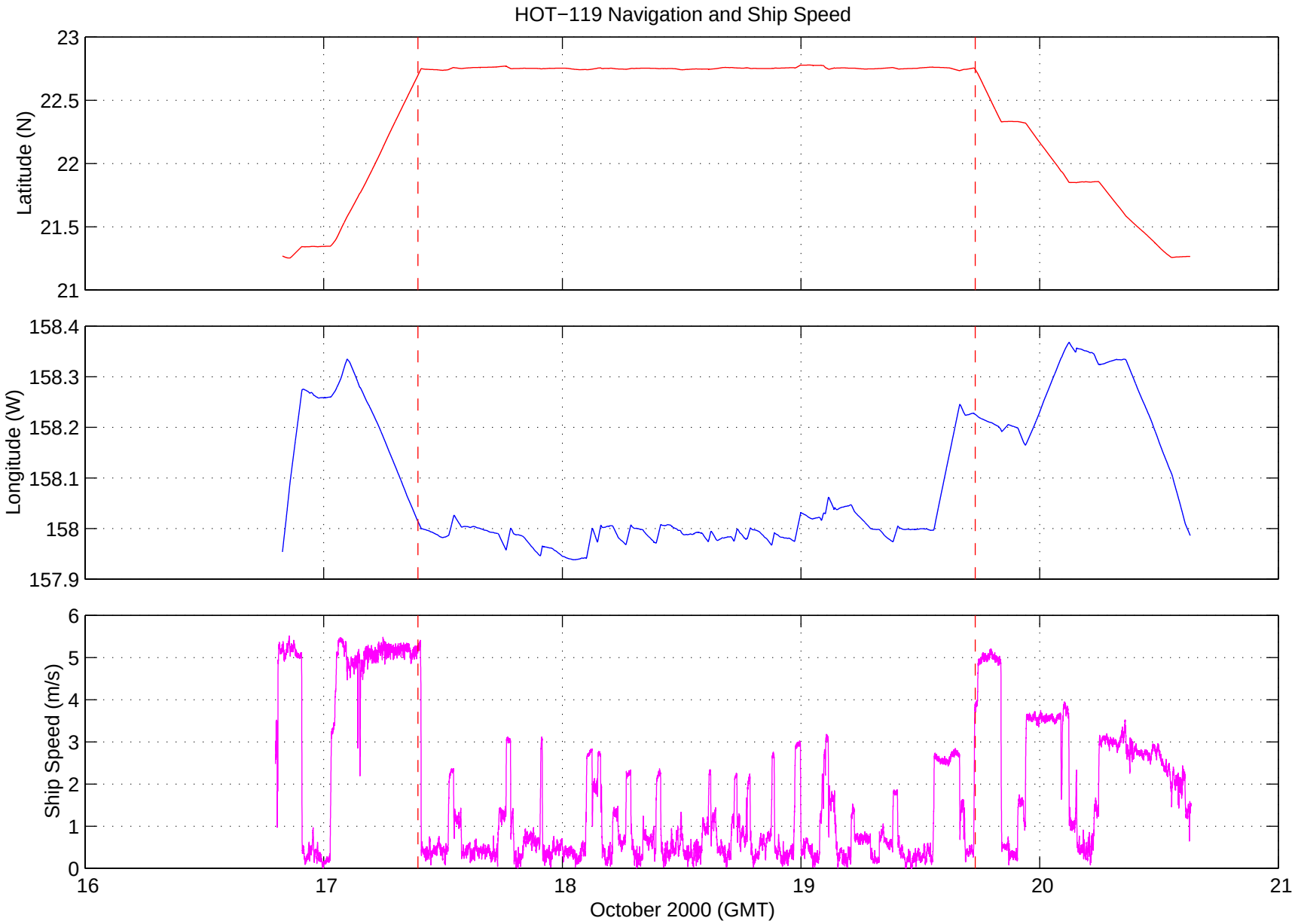
HOT−119 Navigation and Ship Speed
Latitude (N)
23
22.5
22
21.5
21
Longitude (W)
158.4
158.3
158.2
158.1
158
157.9
Ship Speed (m/s)
6
5
4
3
2
1
0
16
17
18
19
20
21
October 2000 (GMT)

Figure 6.2.2i

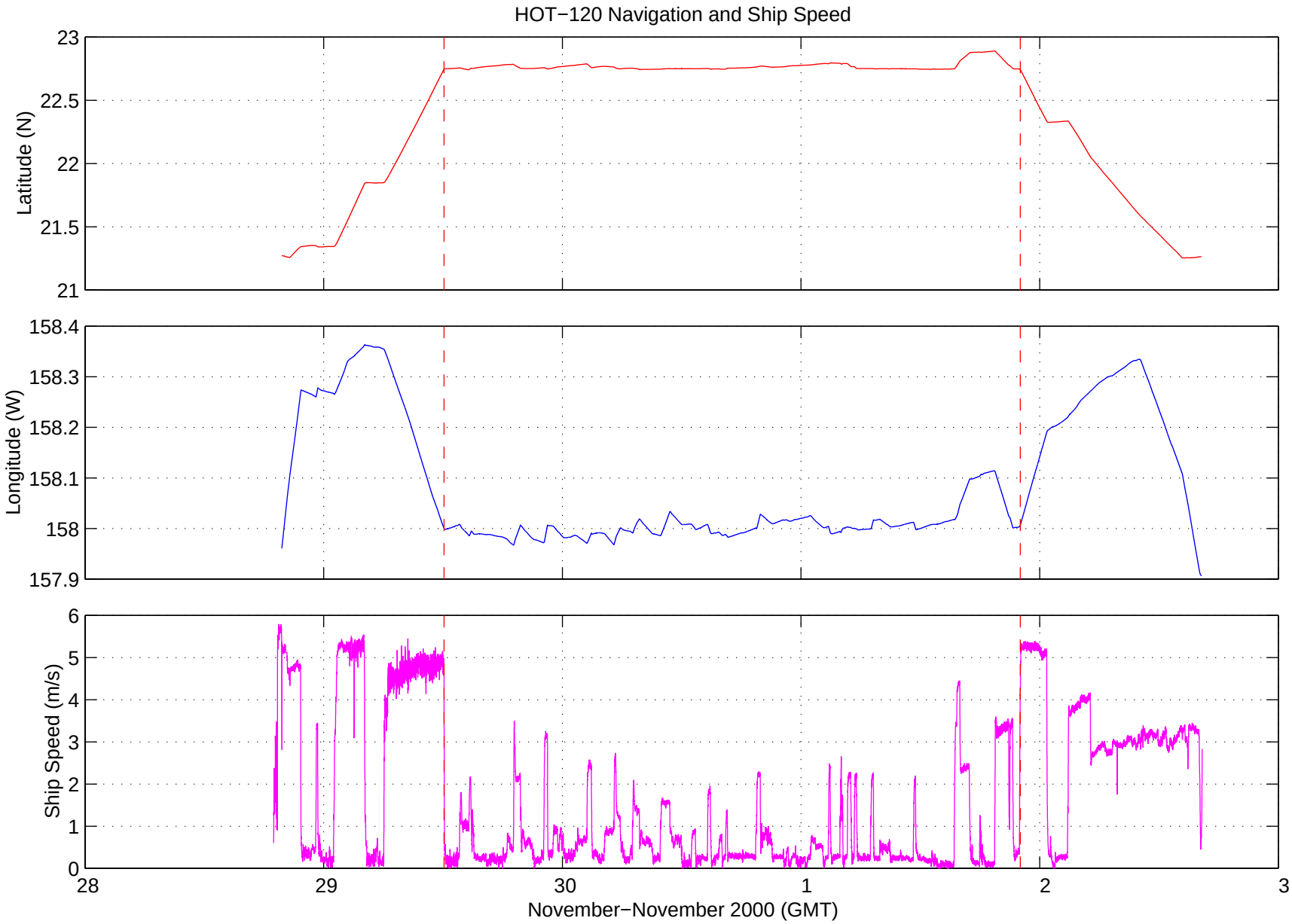
HOT−120 Navigation and Ship Speed
Latitude (N)
23
22.5
22
21.5
21
Longitude (W)
158.4
158.3
158.2
158.1
158
157.9
Ship Speed (m/s)
6
5
4
3
2
1
0
28
29
30
1
2
3
November−November 2000 (GMT)

Figure 6.2.2j

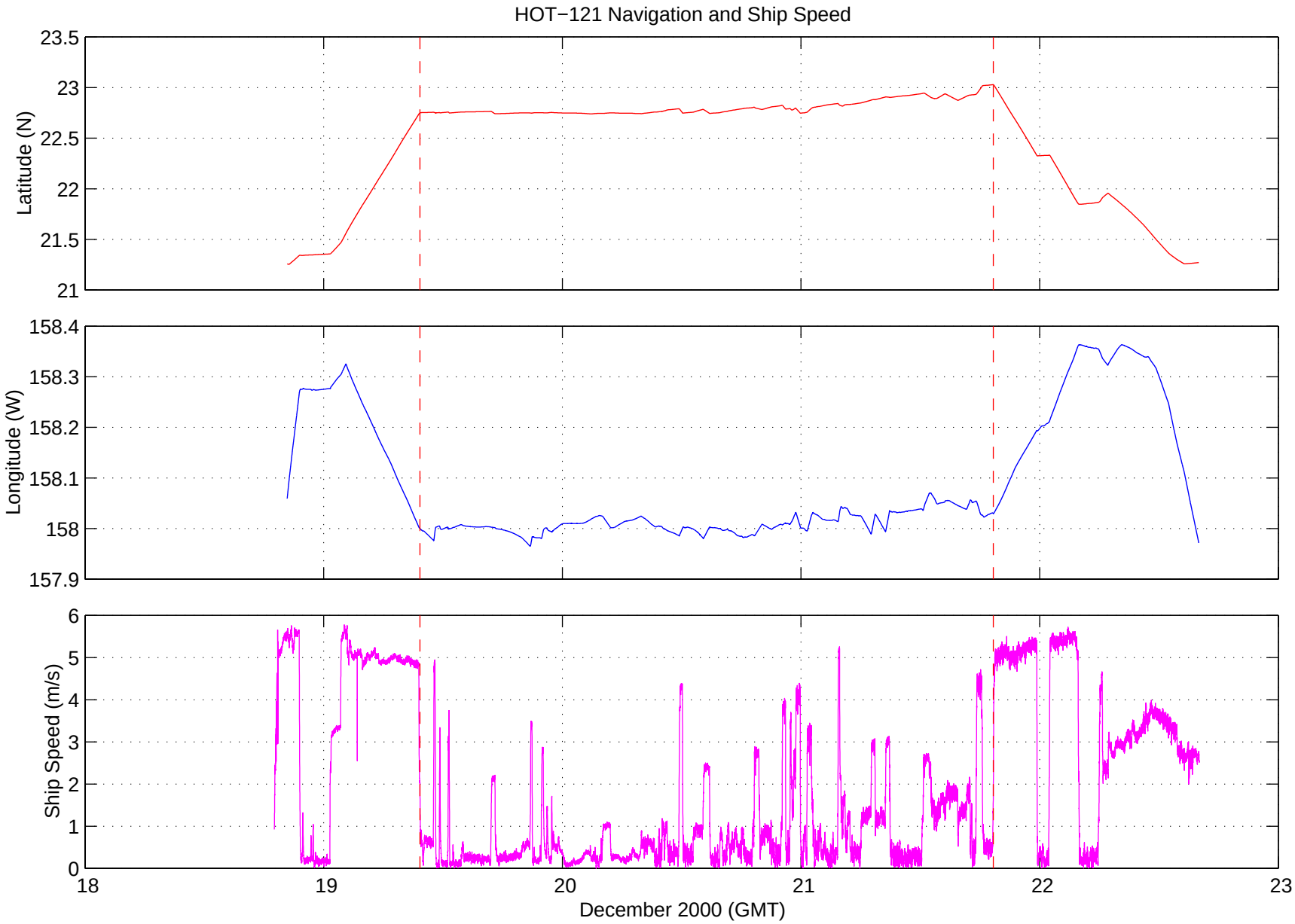
HOT−121 Navigation and Ship Speed
Latitude (N)
23.5
23
22.5
22
21.5
21
Longitude (W)
158.4
158.3
158.2
158.1
158
157.9
Ship Speed (m/s)
6
5
4
3
2
1
0
18
19
20
21
22
23
December 2000 (GMT)

Figure 6.2.2k

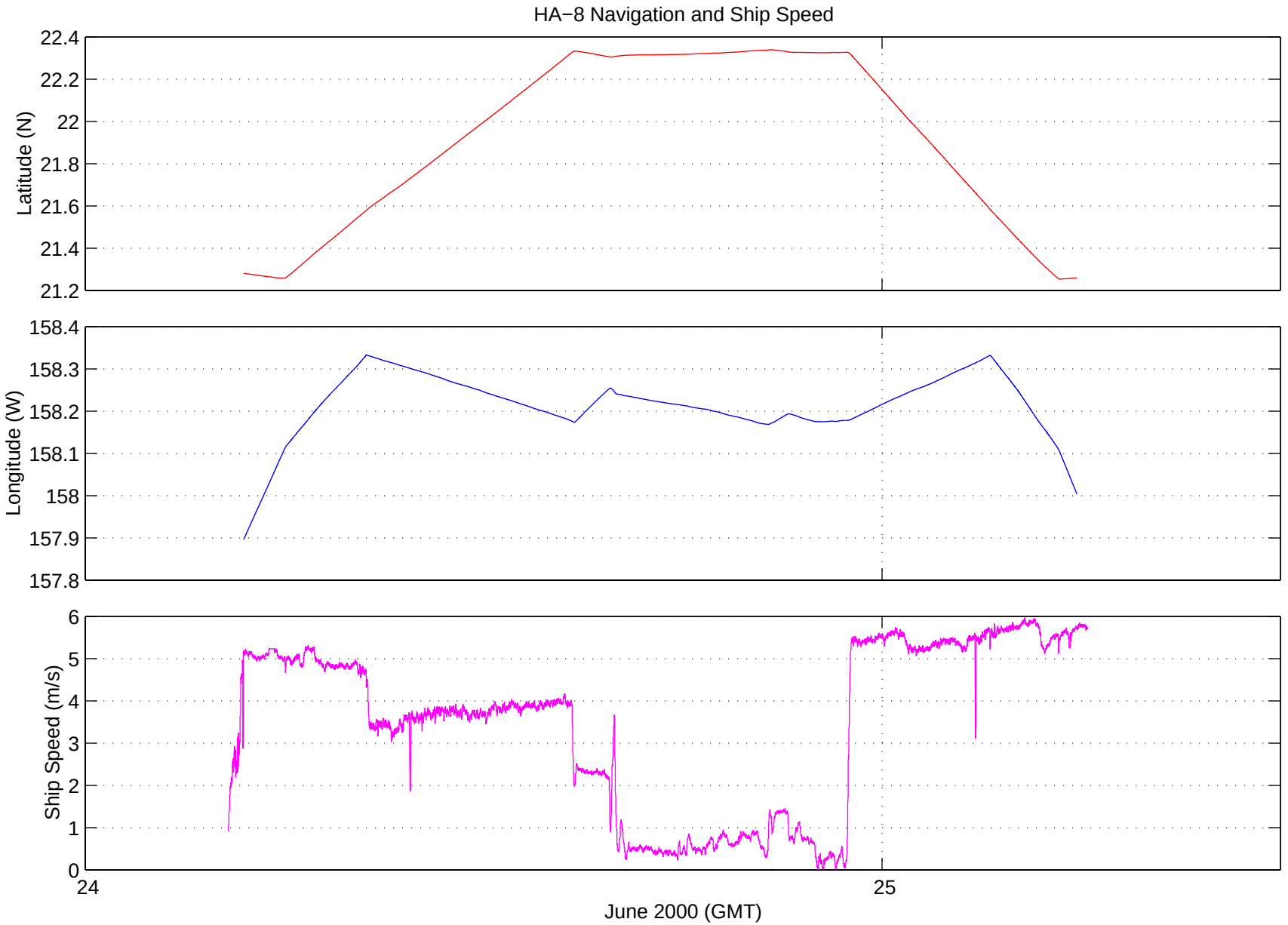
HA−8 Navigation and Ship Speed
Latitude (N)
22.4
22.2
22
21.8
21.6
21.4
21.2
Longitude (W)
158.4
158.3
158.2
158.1
158
157.9
157.8
Ship Speed (m/s)
6
5
4
3
2
1
0
24
25
June 2000 (GMT)

Figure 6.2.2l

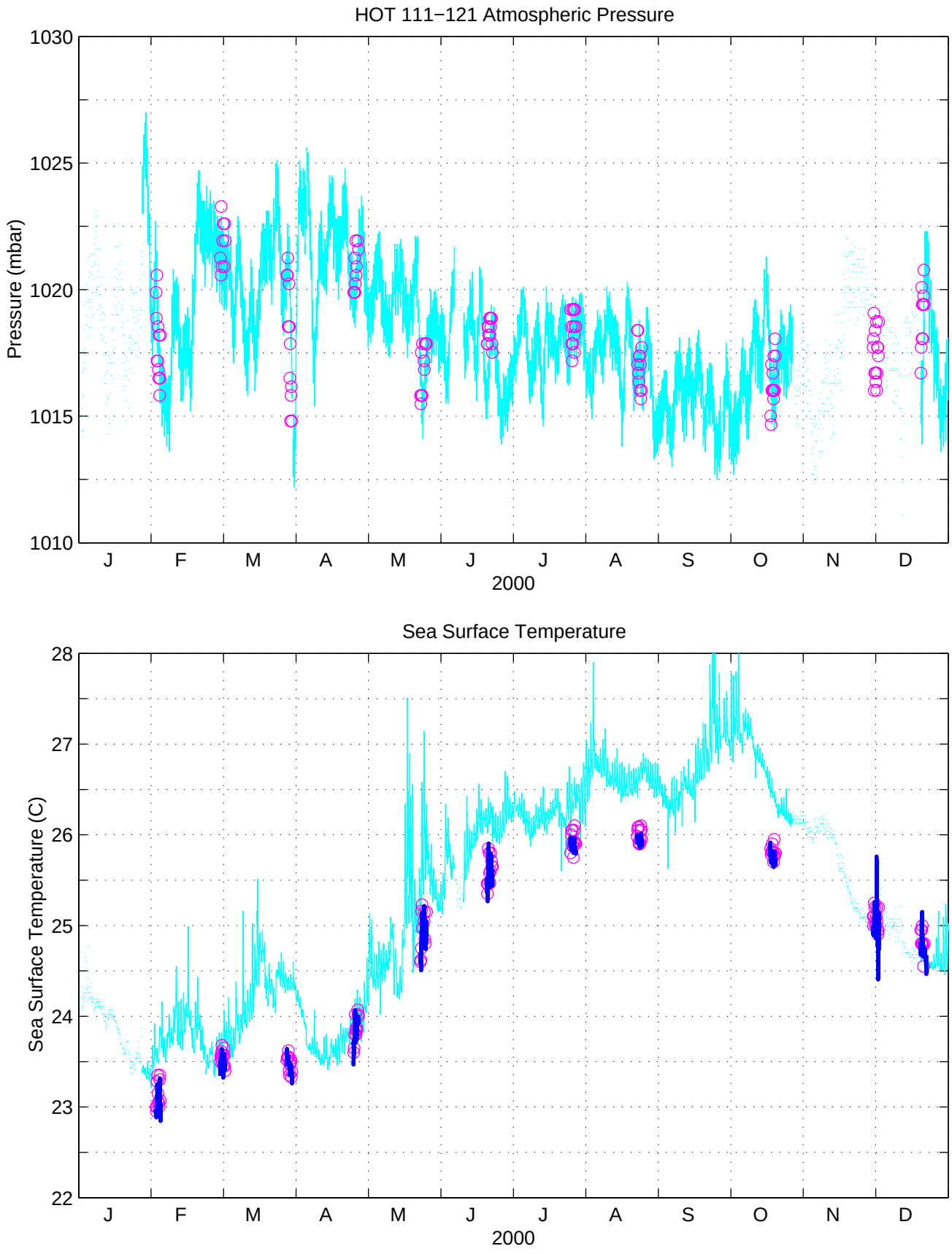
HOT 111−121 Atmospheric Pressure
Pressure (mbar)
1030
1025
1020
1015
1010
J
F
M
A
M
J
J
A
S
O
N
D
2000
Sea Surface Temperature
Sea Surface Temperature (C)
28
27
26
25
24
23
22
J
F
M
A
M
J
J
A
S
O
N
D
2000

Figure 6.3.1

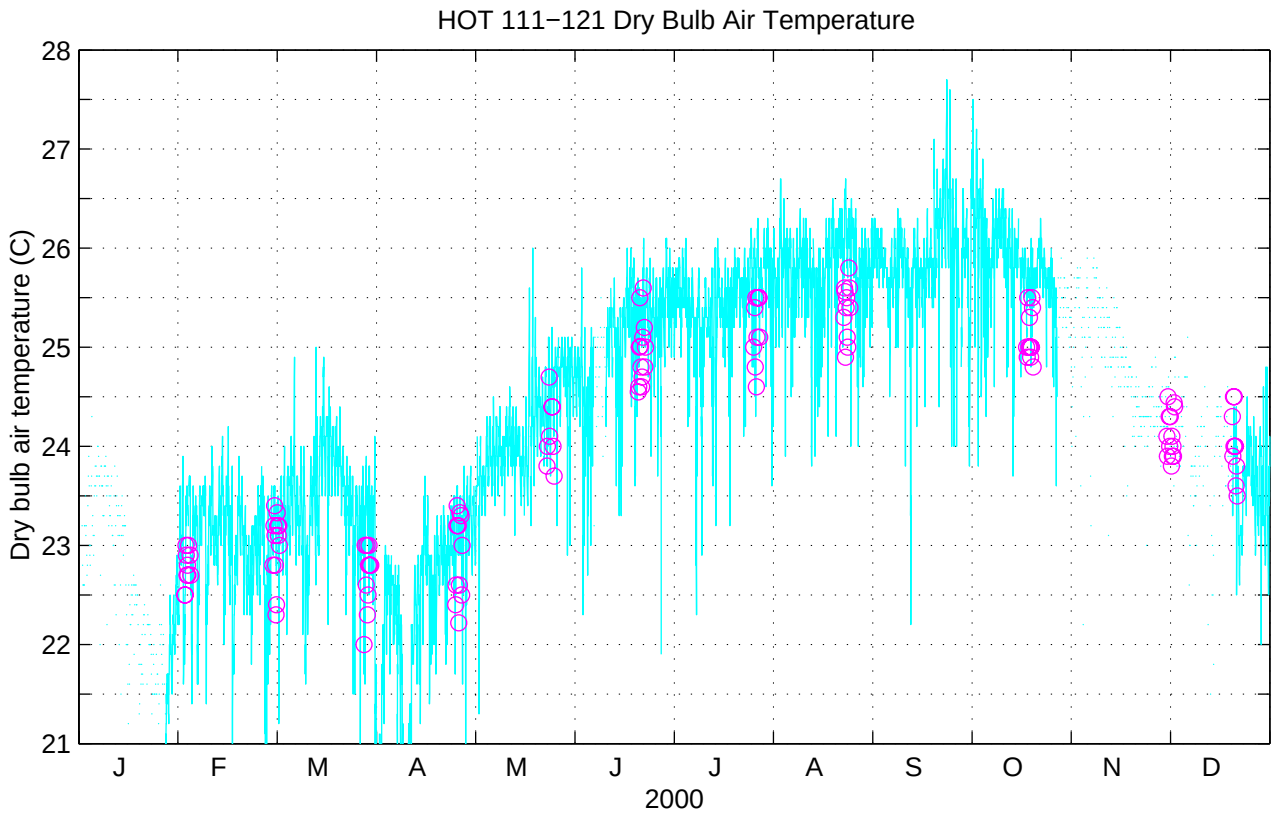
HOT 111−121 Dry Bulb Air Temperature
Dry bulb air temperature (C)
28
27
26
25
24
23
22
21
J
F
M
A
M
J
J
A
S
O
N
D
2000

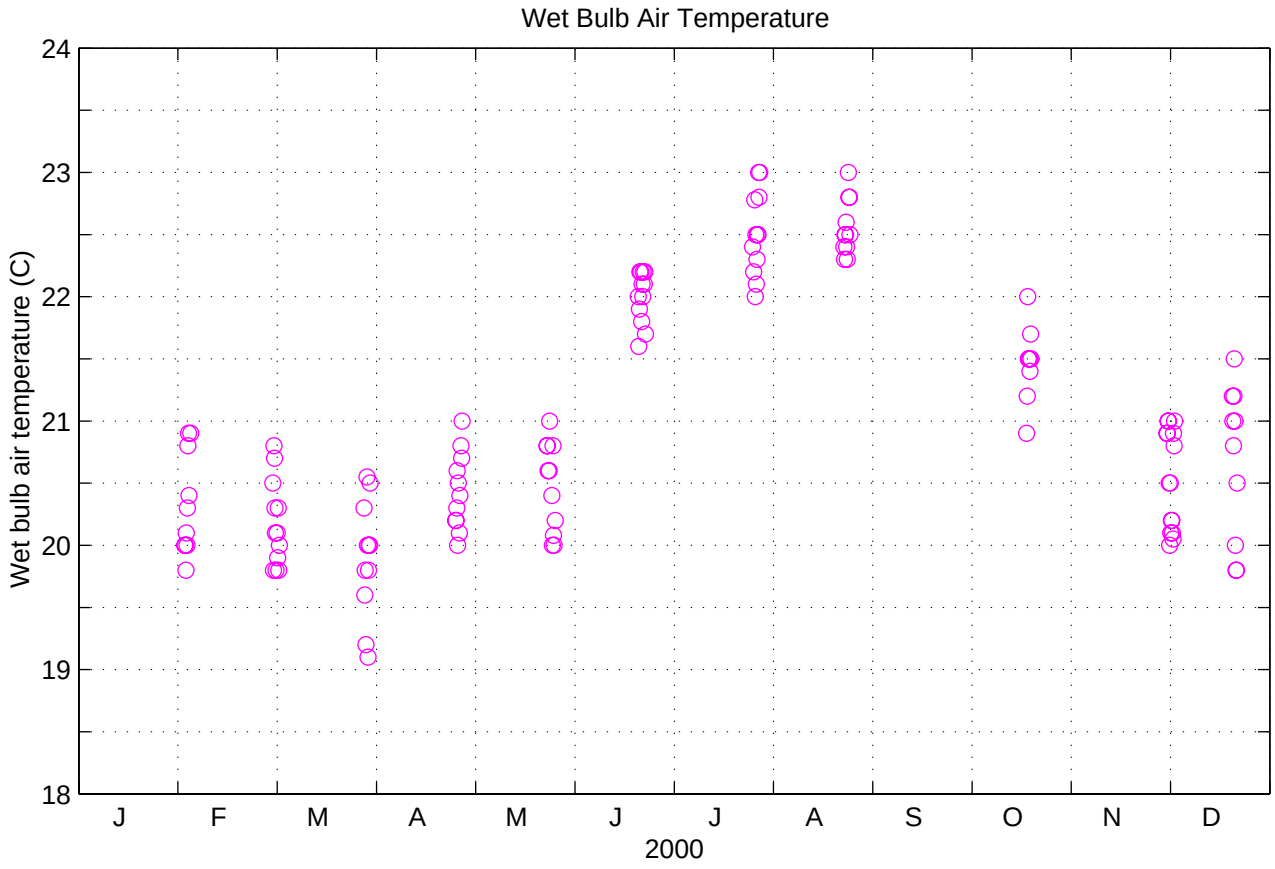
Wet Bulb Air Temperature
Wet bulb air temperature (C)
24
23
22
21
20
19
18
J
F
M
A
M
J
J
A
S
O
N
D
2000

Figure 6.3.2

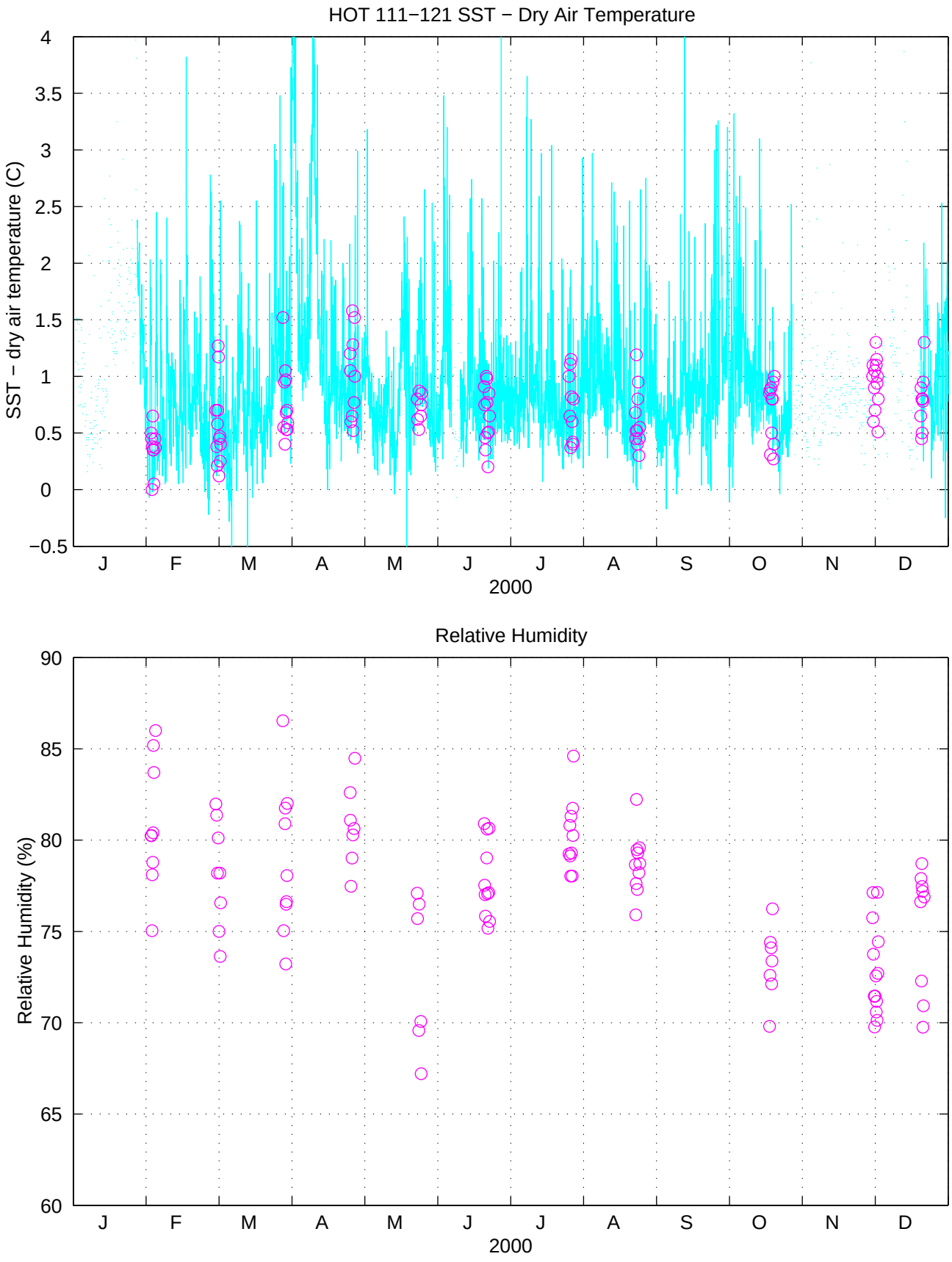
HOT 111−121 SST − Dry Air Temperature
SST − dry air temperature (C)
4
3.5
3
2.5
2
1.5
1
0.5
0
−0.5
J
F
M
A
M
J
J
A
S
O
N
D
2000
Relative Humidity
Relative Humidity (%)
90
85
80
75
70
65
60
J
F
M
A
M
J
J
A
S
O
N
D
2000

Figure 6.3.3

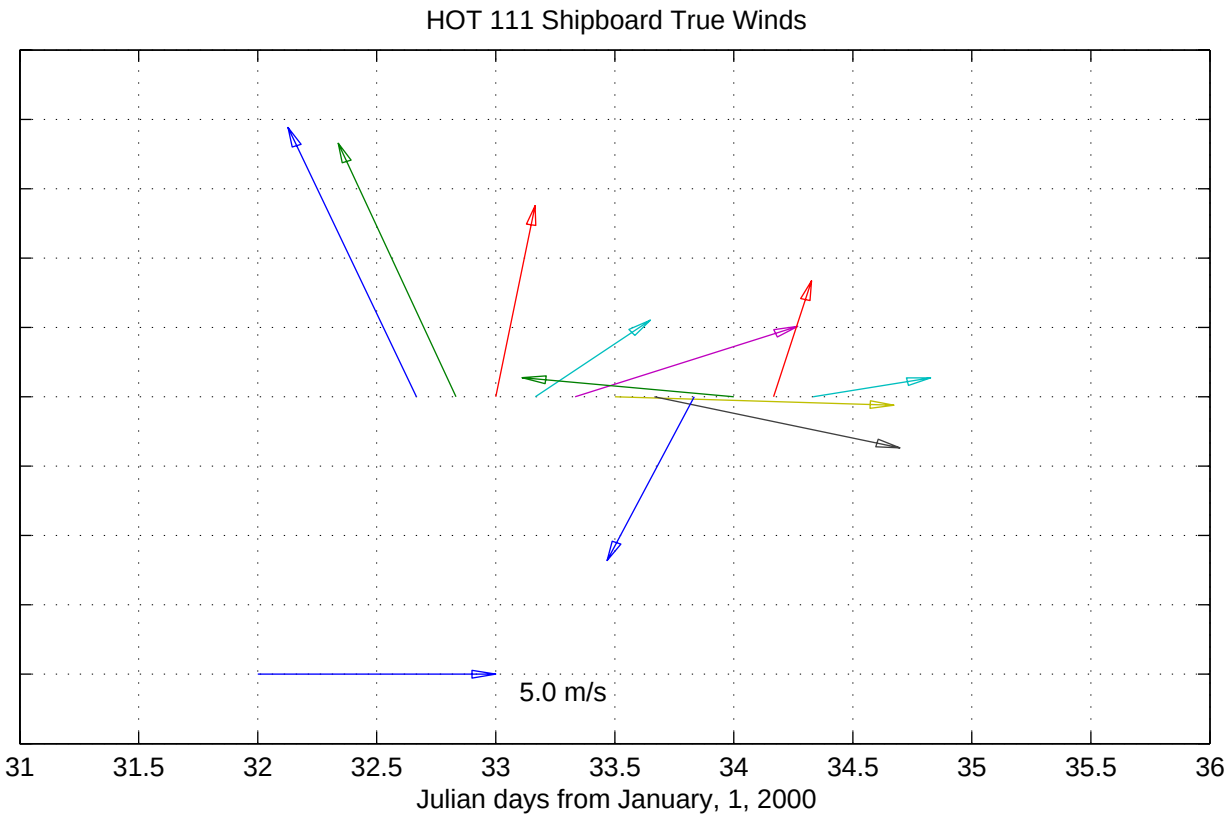
HOT 111 Shipboard True Winds
5.0 m/s
31
31.5
32
32.5
33
33.5
34
34.5
35
35.5
36
Julian days from January, 1, 2000

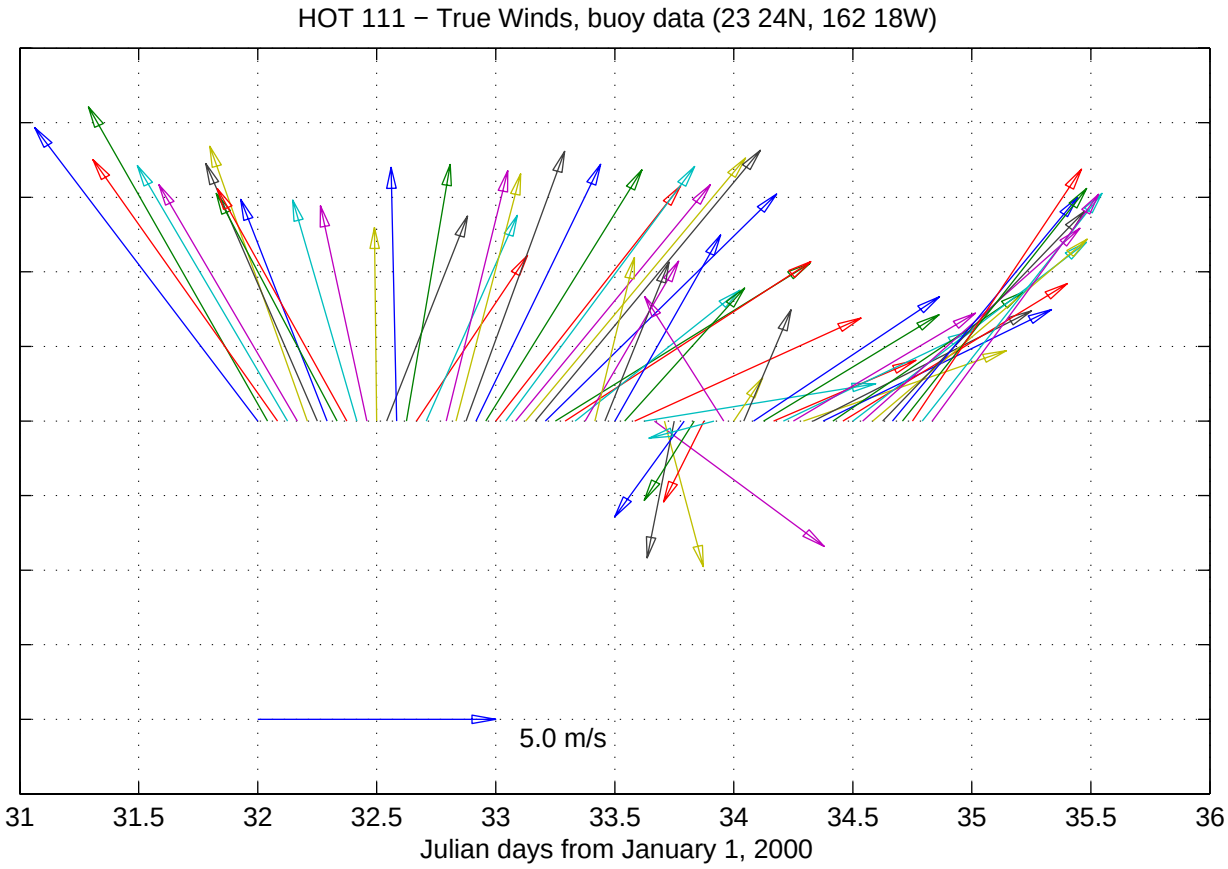
HOT 111 − True Winds, buoy data (23 24N, 162 18W)
5.0 m/s
31
31.5
32
32.5
33
33.5
34
34.5
35
35.5
36
Julian days from January 1, 2000

Figure 6.3.4a

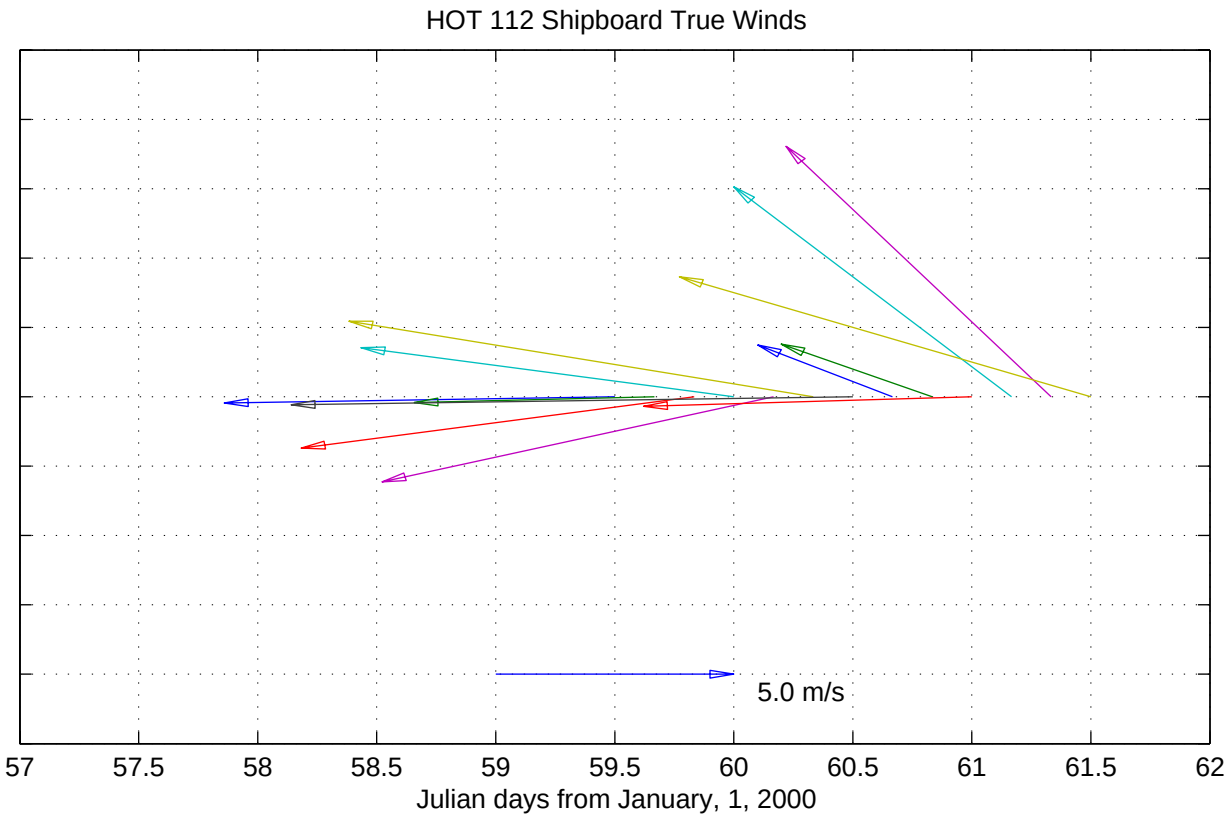
HOT 112 Shipboard True Winds
5.0 m/s
57
57.5
58
58.5
59
59.5
60
60.5
61
61.5
62
Julian days from January, 1, 2000

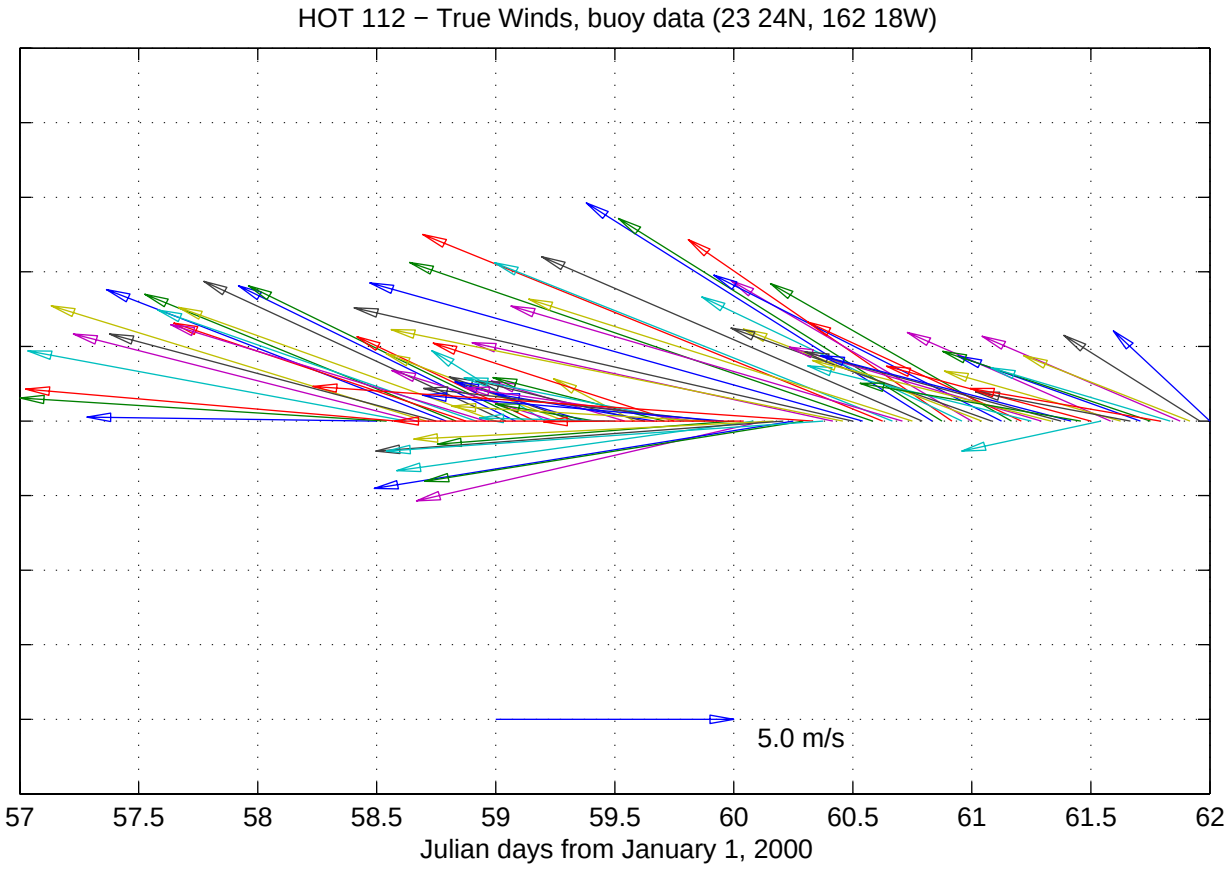
HOT 112 − True Winds, buoy data (23 24N, 162 18W)
5.0 m/s
57
57.5
58
58.5
59
59.5
60
60.5
61
61.5
62
Julian days from January 1, 2000

Figure 6.3.4b

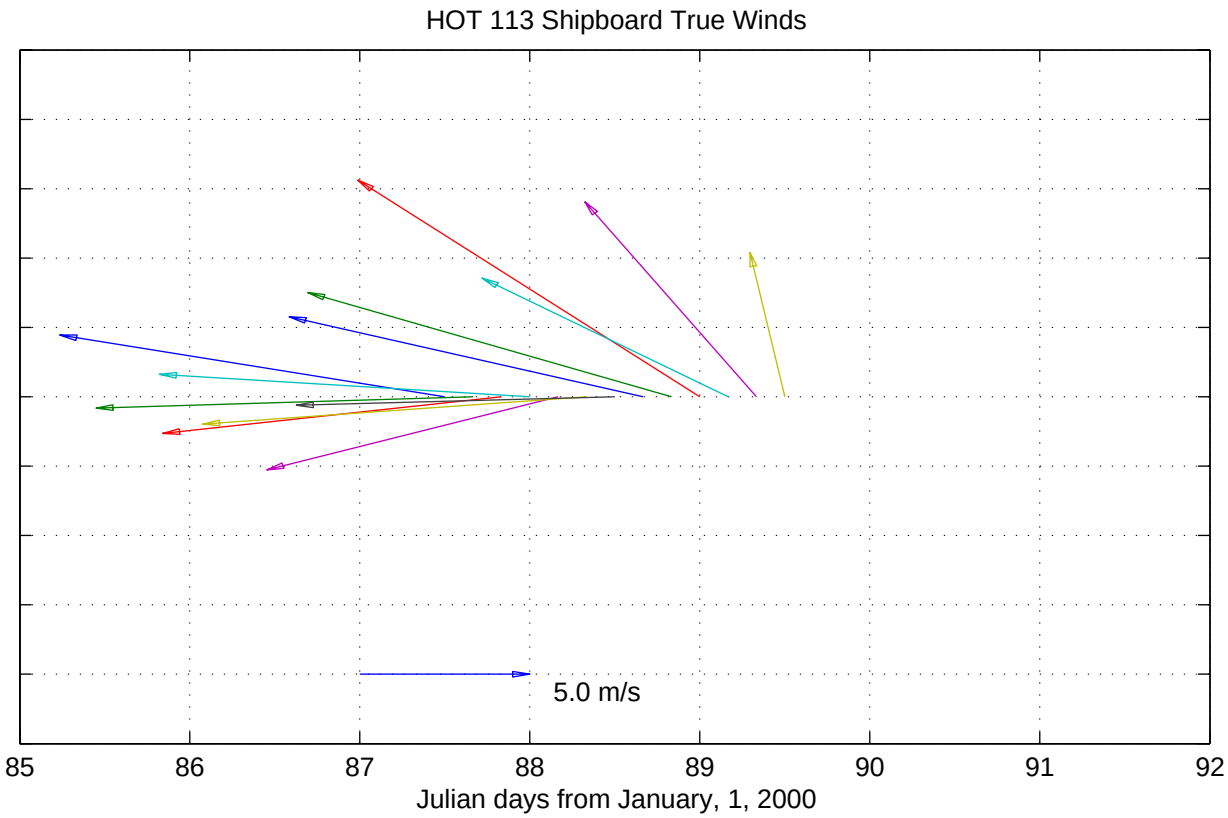
HOT 113 Shipboard True Winds
5.0 m/s
85
86
87
88
89
90
91
92
Julian days from January, 1, 2000

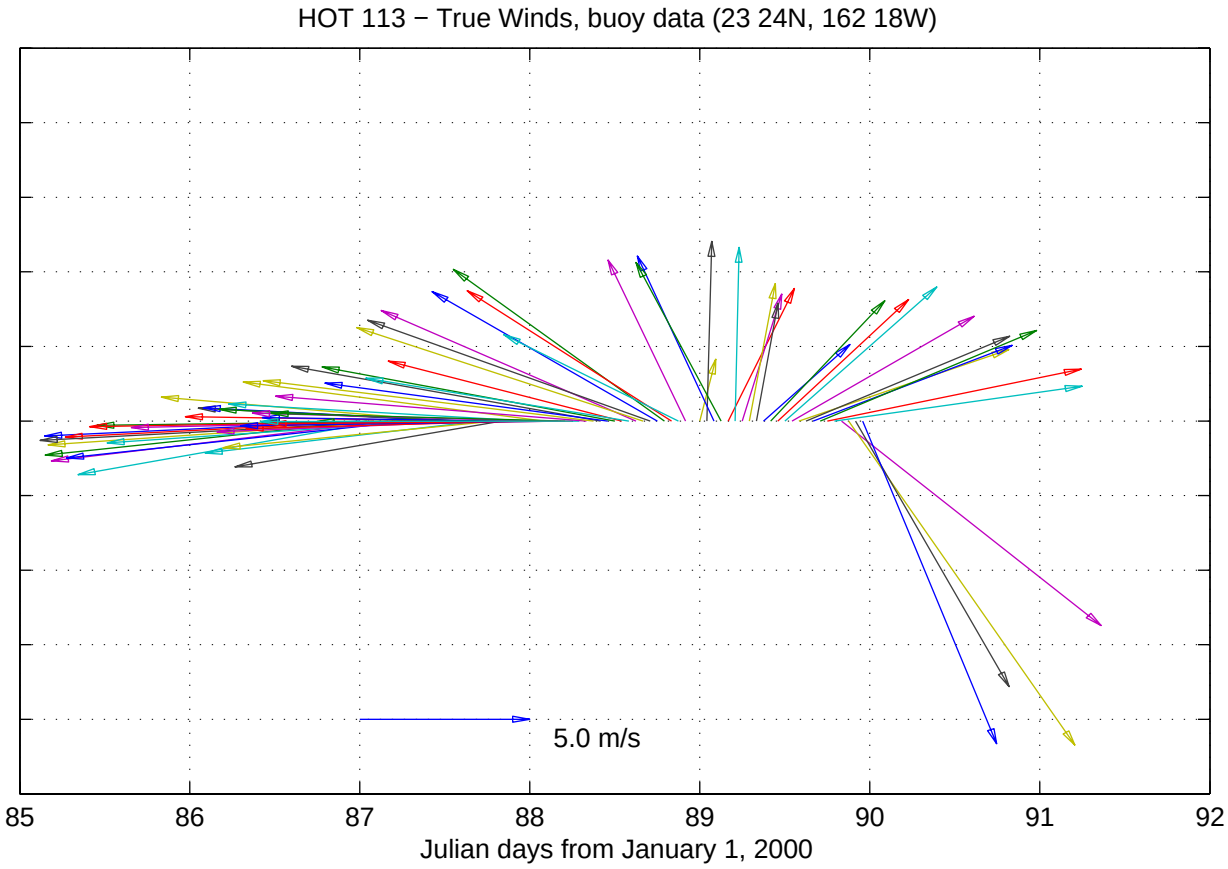
HOT 113 − True Winds, buoy data (23 24N, 162 18W)
5.0 m/s
85
86
87
88
89
90
91
92
Julian days from January 1, 2000

Figure 6.3.4c

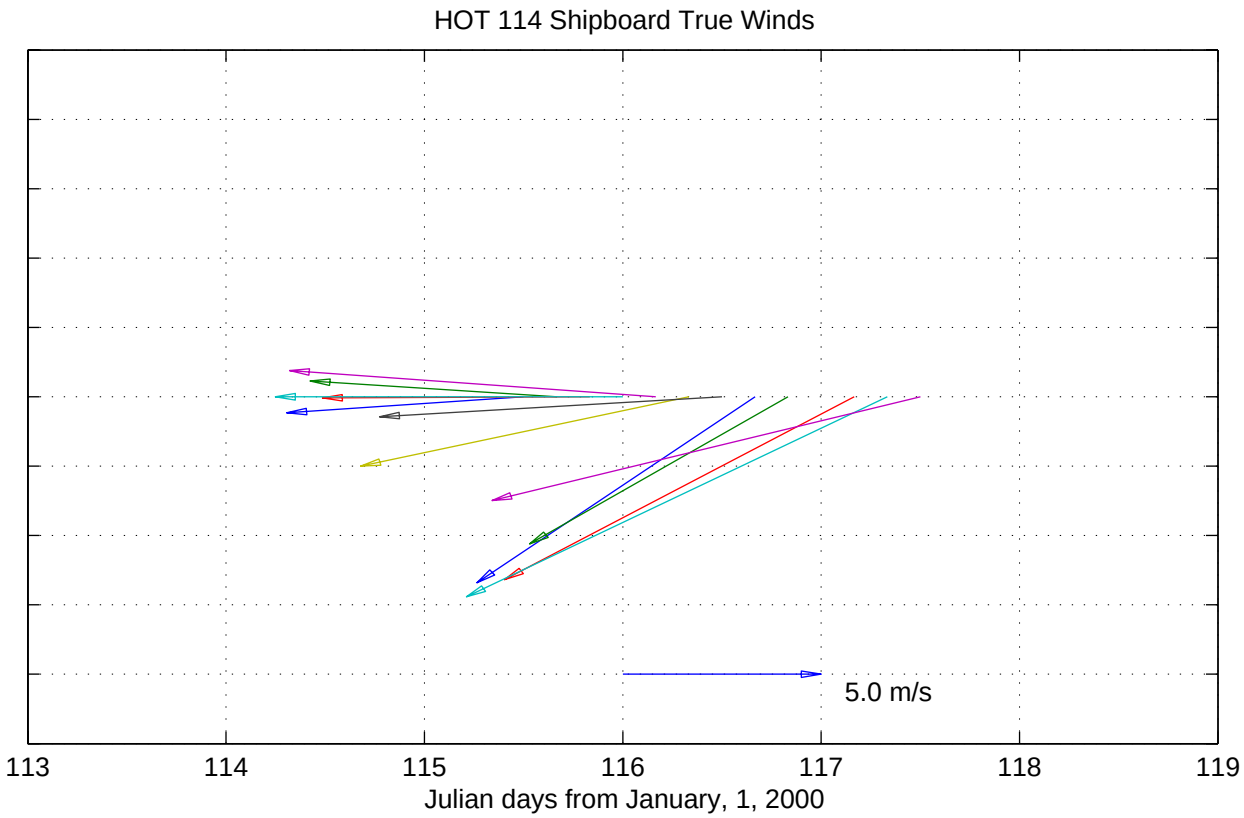
HOT 114 Shipboard True Winds
5.0 m/s
113
114
115
116
117
118
119
Julian days from January, 1, 2000

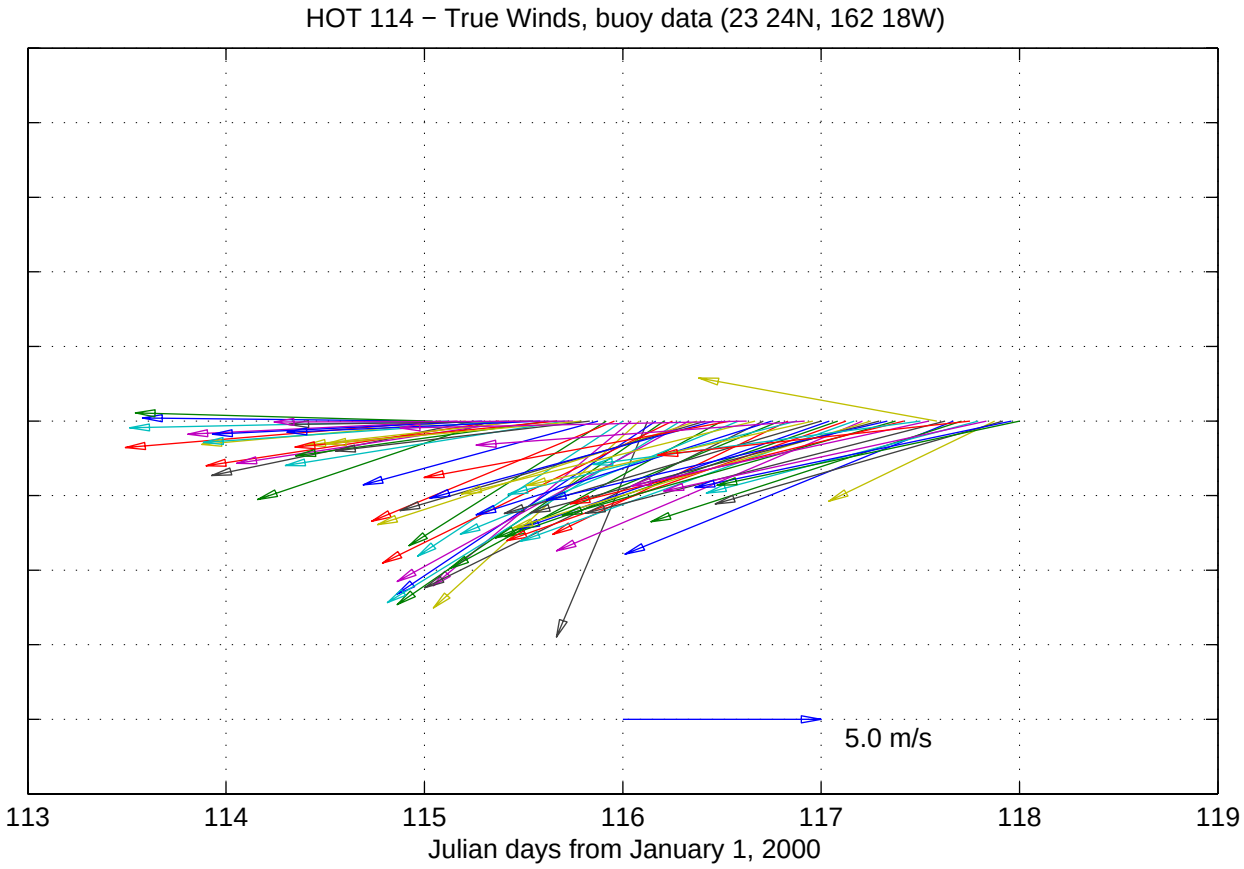
HOT 114 − True Winds, buoy data (23 24N, 162 18W)
5.0 m/s
113
114
115
116
117
118
119
Julian days from January 1, 2000

Figure 6.3.4d

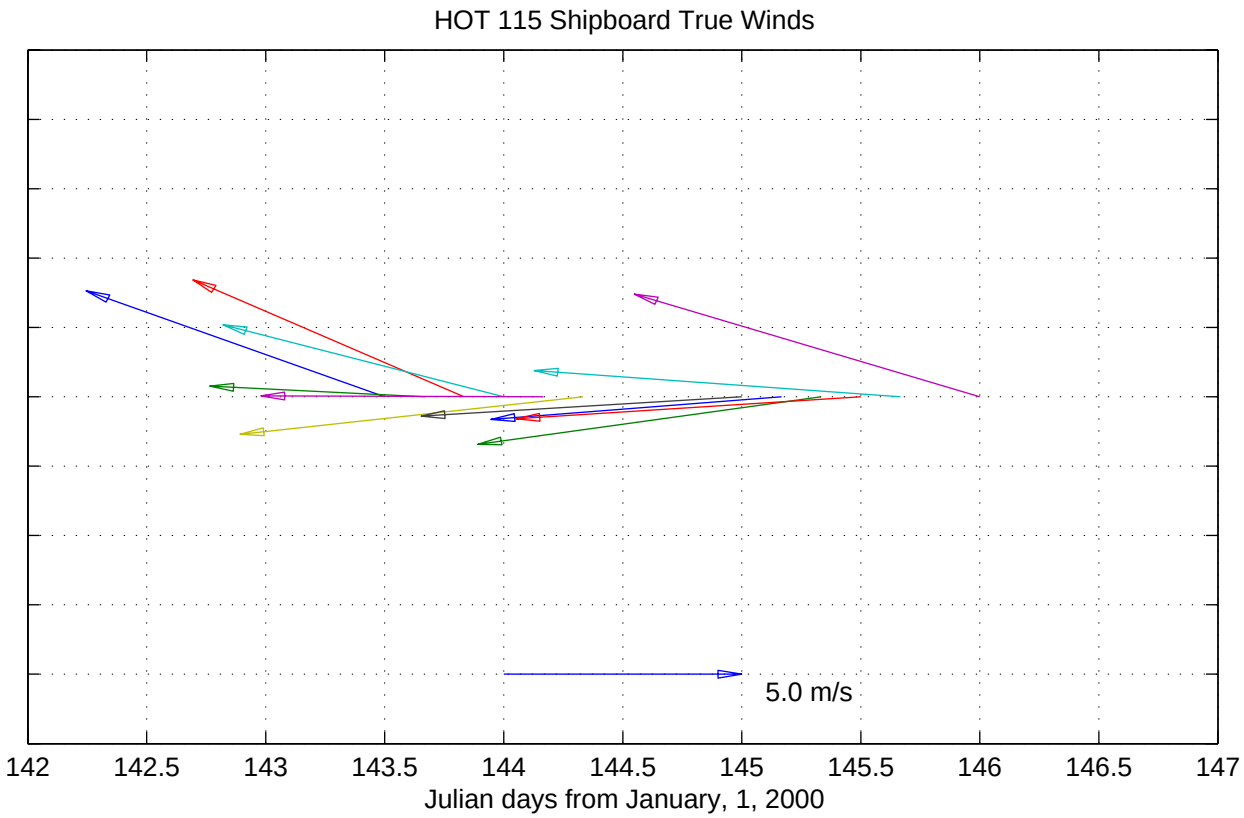
HOT 115 Shipboard True Winds
5.0 m/s
142
142.5
143
143.5
144
144.5
145
145.5
146
146.5
147
Julian days from January, 1, 2000

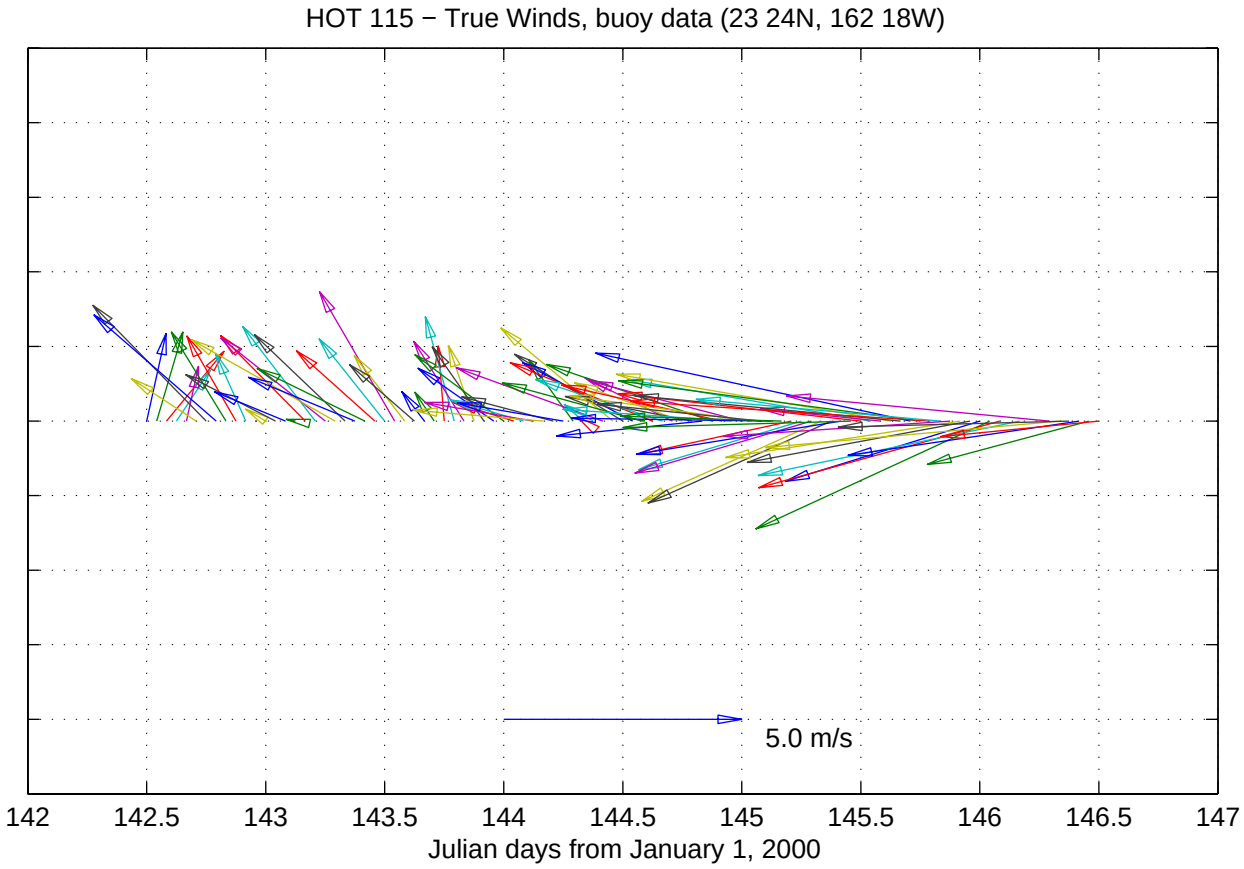
HOT 115 − True Winds, buoy data (23 24N, 162 18W)
5.0 m/s
142
142.5
143
143.5
144
144.5
145
145.5
146
146.5
147
Julian days from January 1, 2000

Figure 6.3.4e

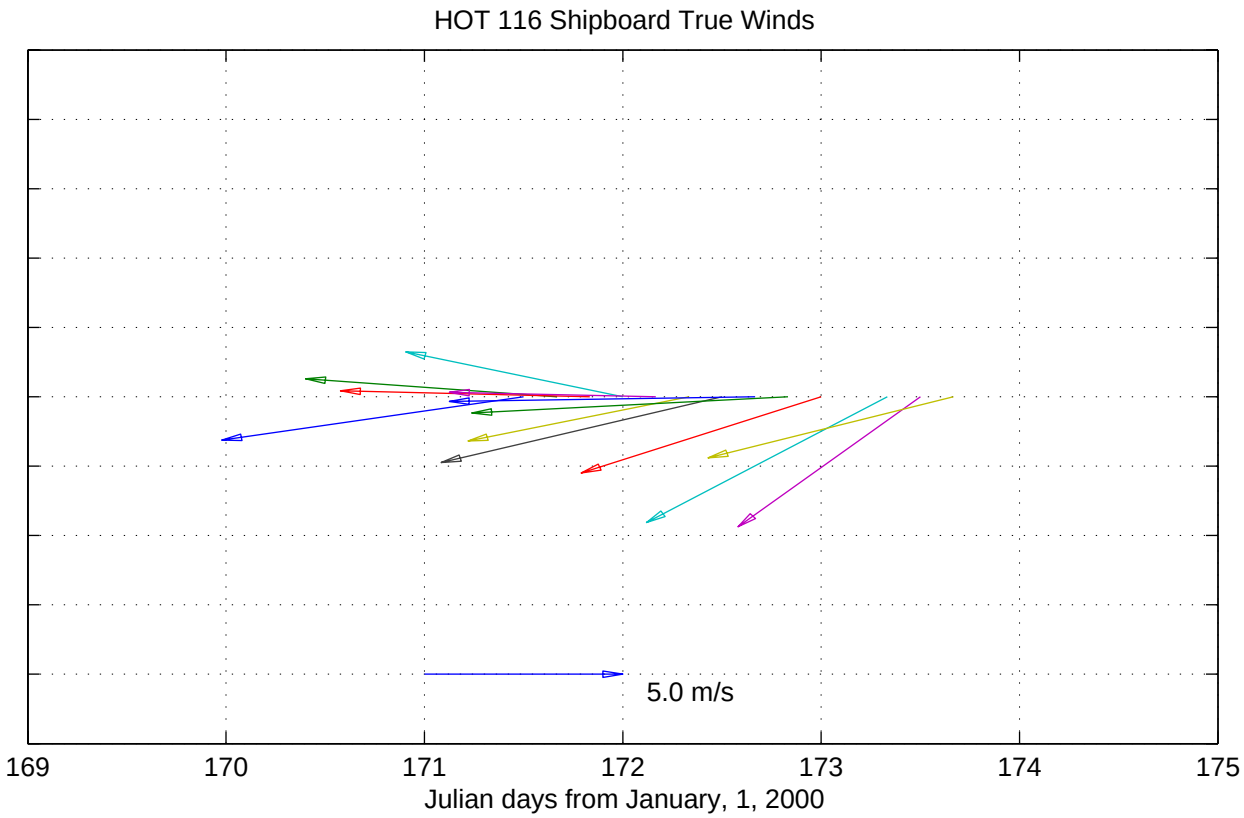
HOT 116 Shipboard True Winds
5.0 m/s
169
170
171
172
173
174
175
Julian days from January, 1, 2000

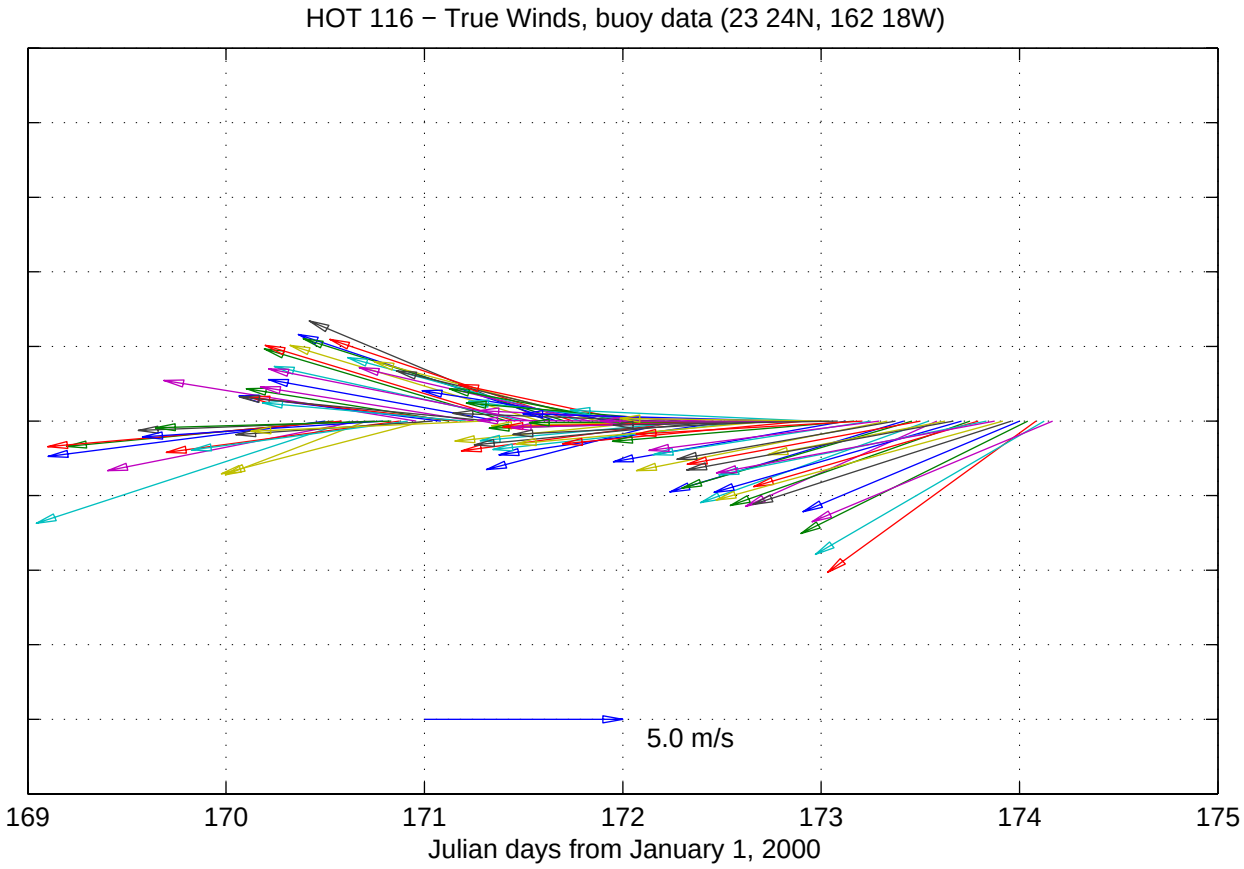
HOT 116 − True Winds, buoy data (23 24N, 162 18W)
5.0 m/s
169
170
171
172
173
174
175
Julian days from January 1, 2000

Figure 6.3.4f

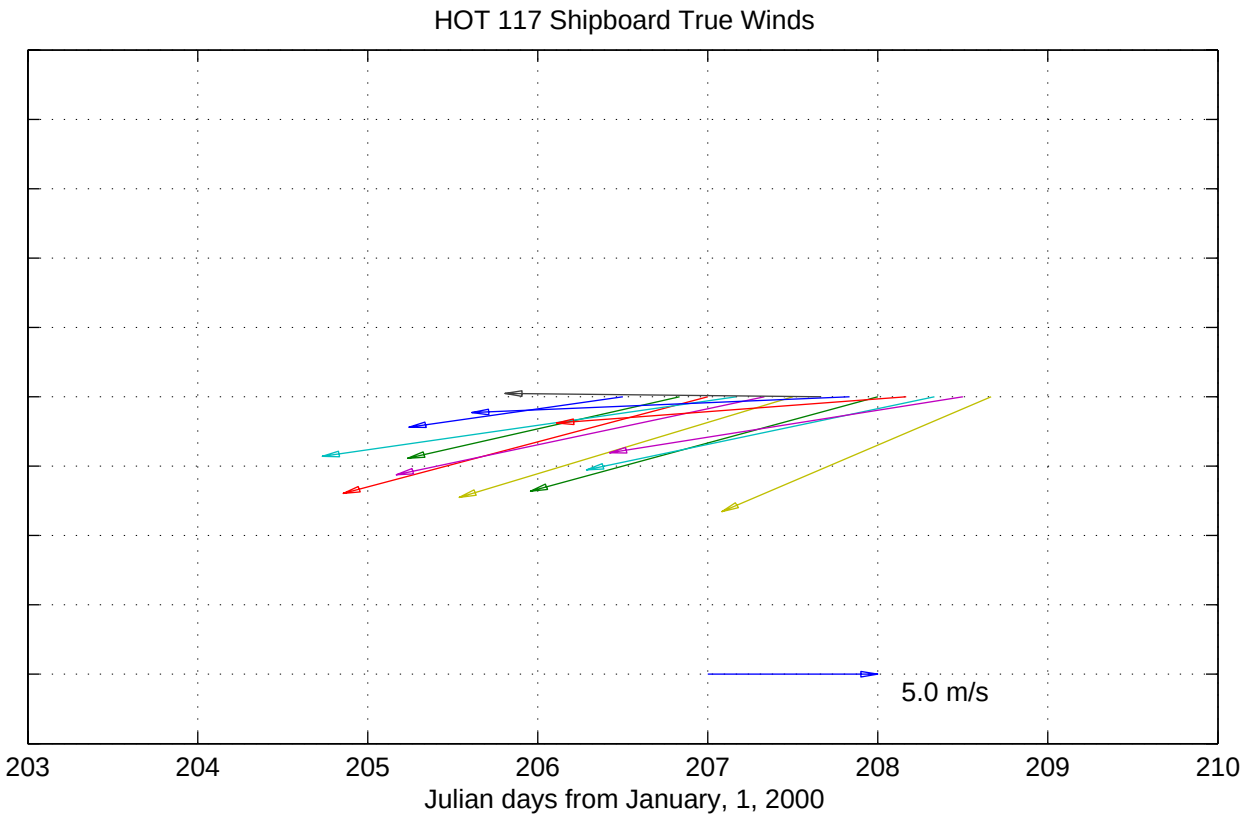
HOT 117 Shipboard True Winds
5.0 m/s
203
204
205
206
207
208
209
210
Julian days from January, 1, 2000

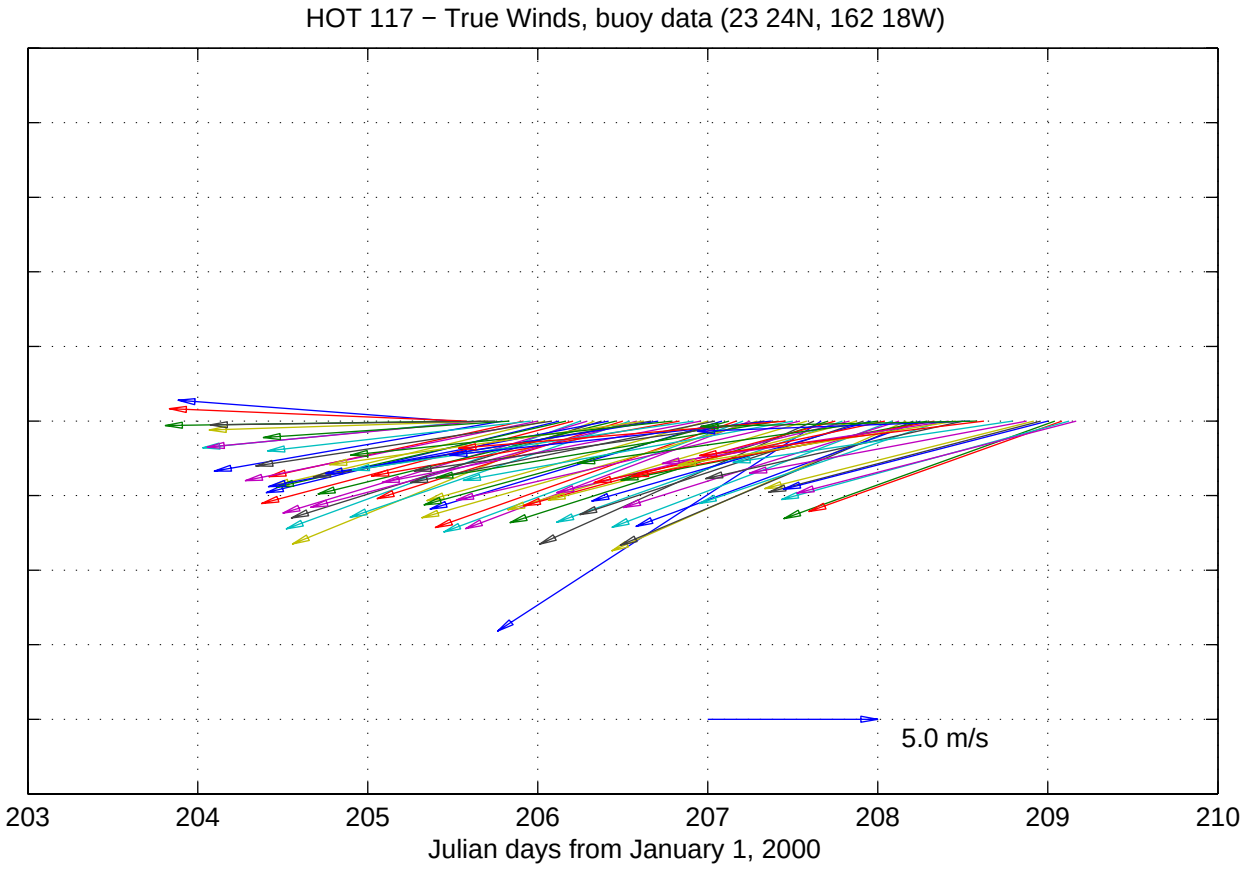
HOT 117 − True Winds, buoy data (23 24N, 162 18W)
5.0 m/s
203
204
205
206
207
208
209
210
Julian days from January 1, 2000

Figure 6.3.4g

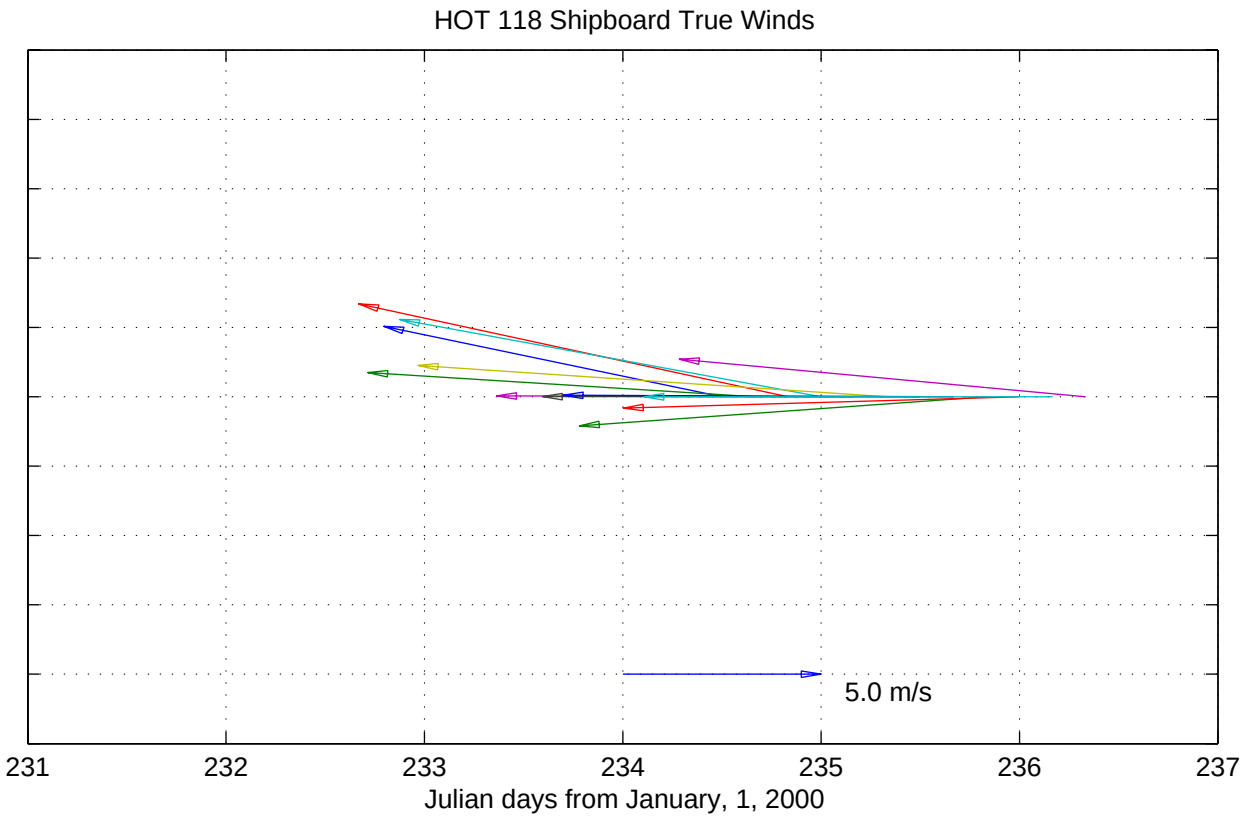
HOT 118 Shipboard True Winds
5.0 m/s
231
232
233
234
235
236
237
Julian days from January, 1, 2000

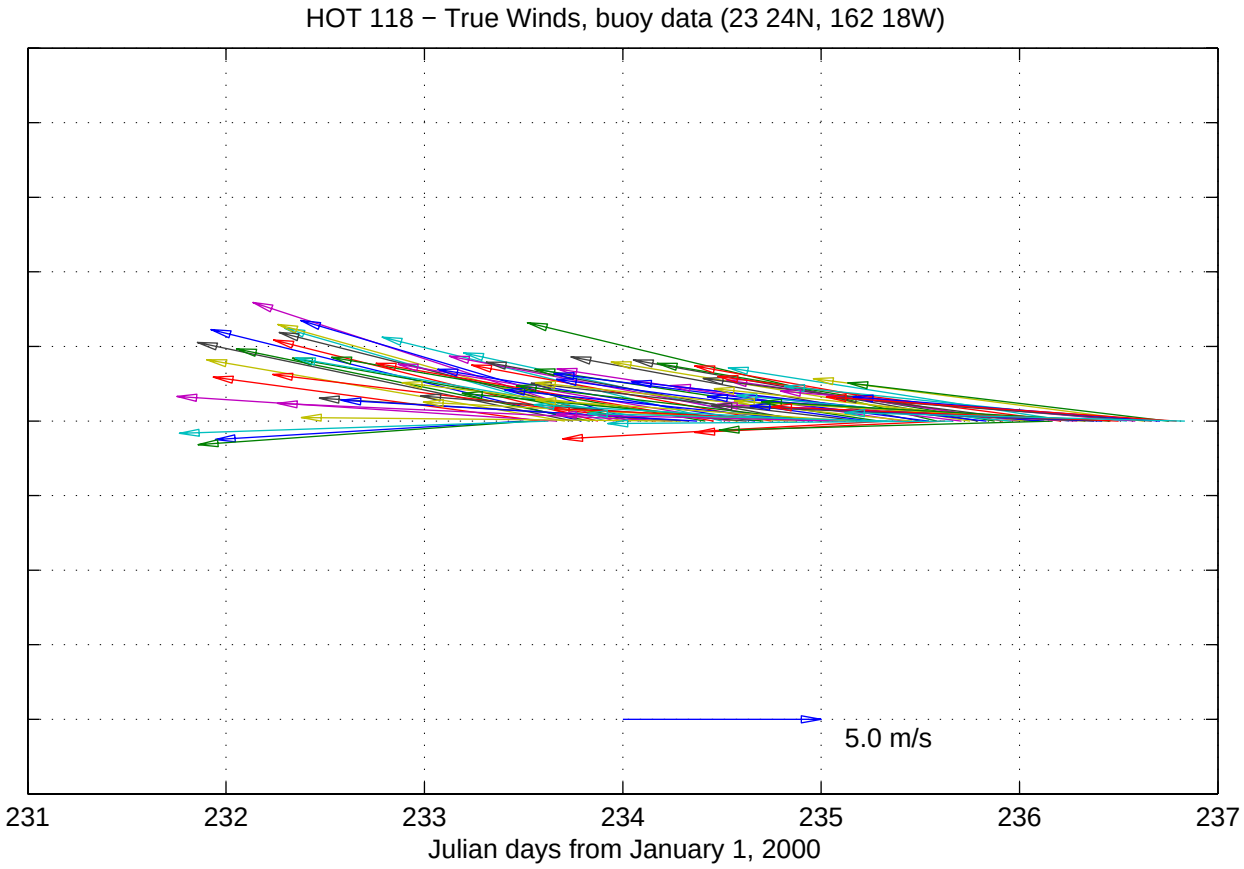
HOT 118 − True Winds, buoy data (23 24N, 162 18W)
5.0 m/s
231
232
233
234
235
236
237
Julian days from January 1, 2000

Figure 6.3.4h

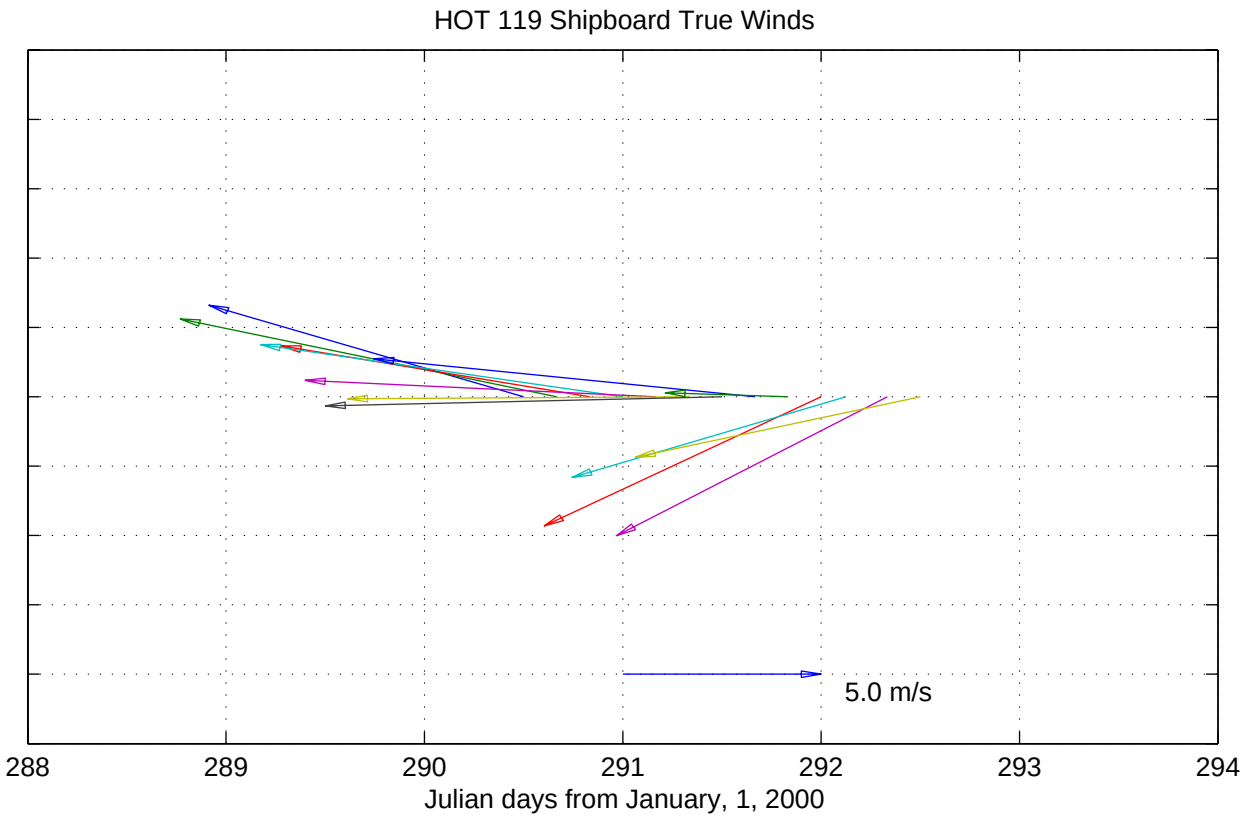
HOT 119 Shipboard True Winds
5.0 m/s
288
289
290
291
292
293
294
Julian days from January, 1, 2000

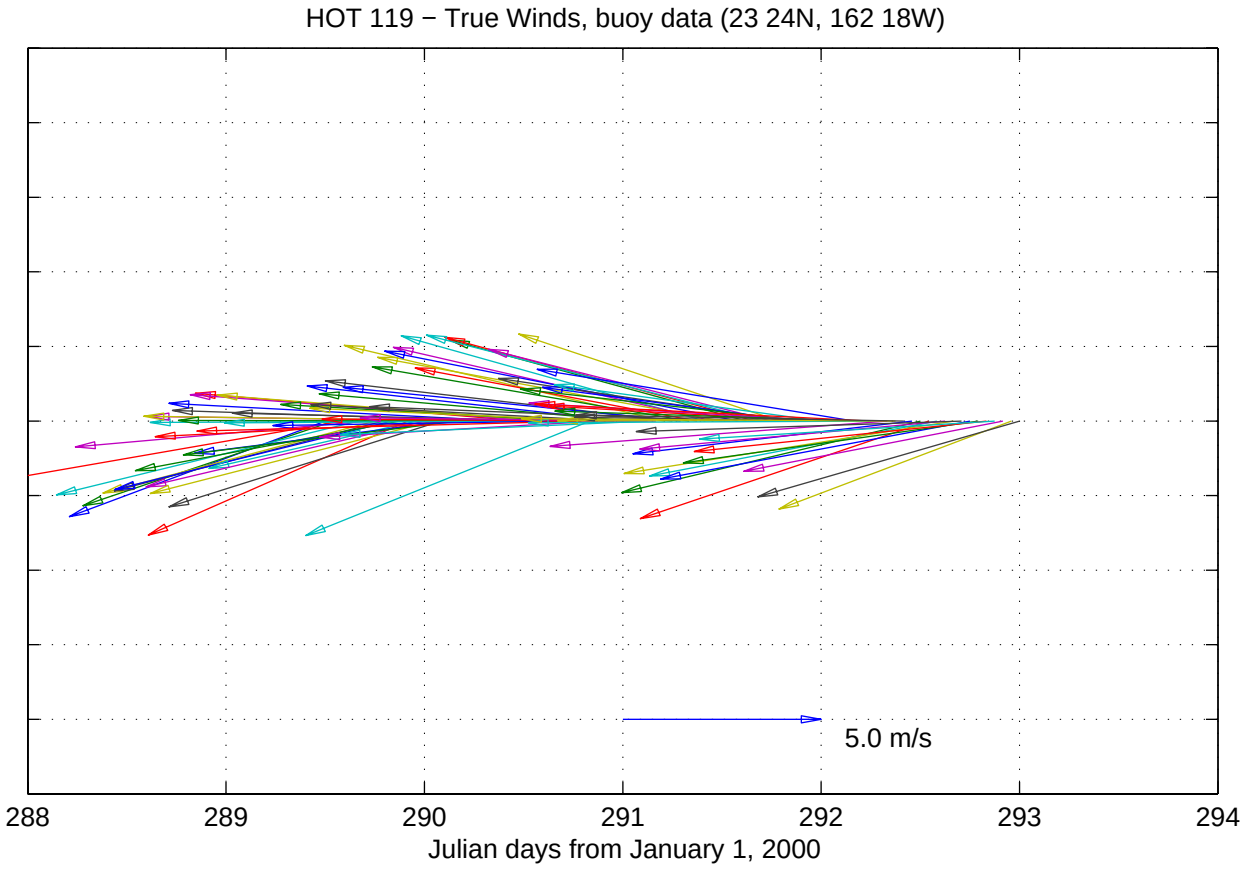
HOT 119 − True Winds, buoy data (23 24N, 162 18W)
5.0 m/s
288
289
290
291
292
293
294
Julian days from January 1, 2000

Figure 6.3.4i

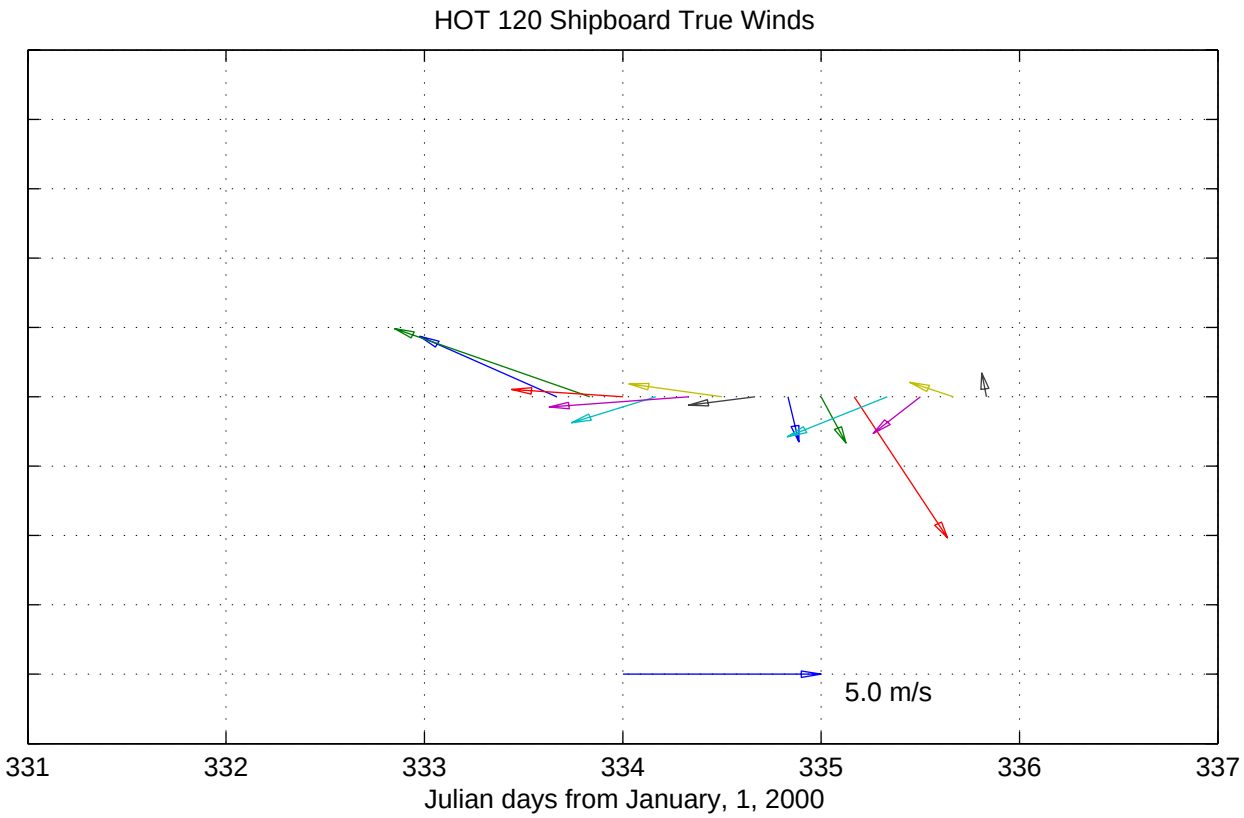
HOT 120 Shipboard True Winds
5.0 m/s
331
332
333
334
335
336
337
Julian days from January, 1, 2000

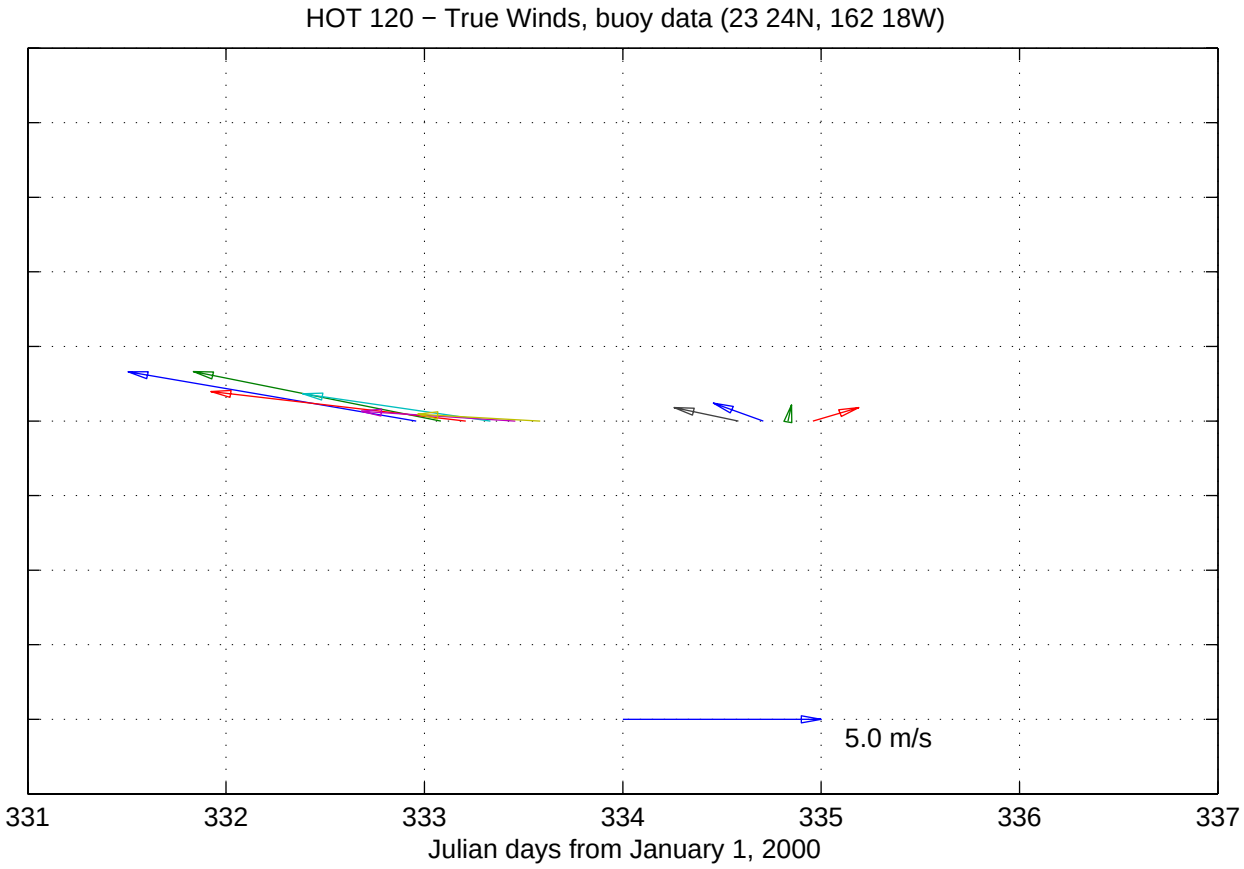
HOT 120 − True Winds, buoy data (23 24N, 162 18W)
5.0 m/s
331
332
333
334
335
336
337
Julian days from January 1, 2000

Figure 6.3.4j

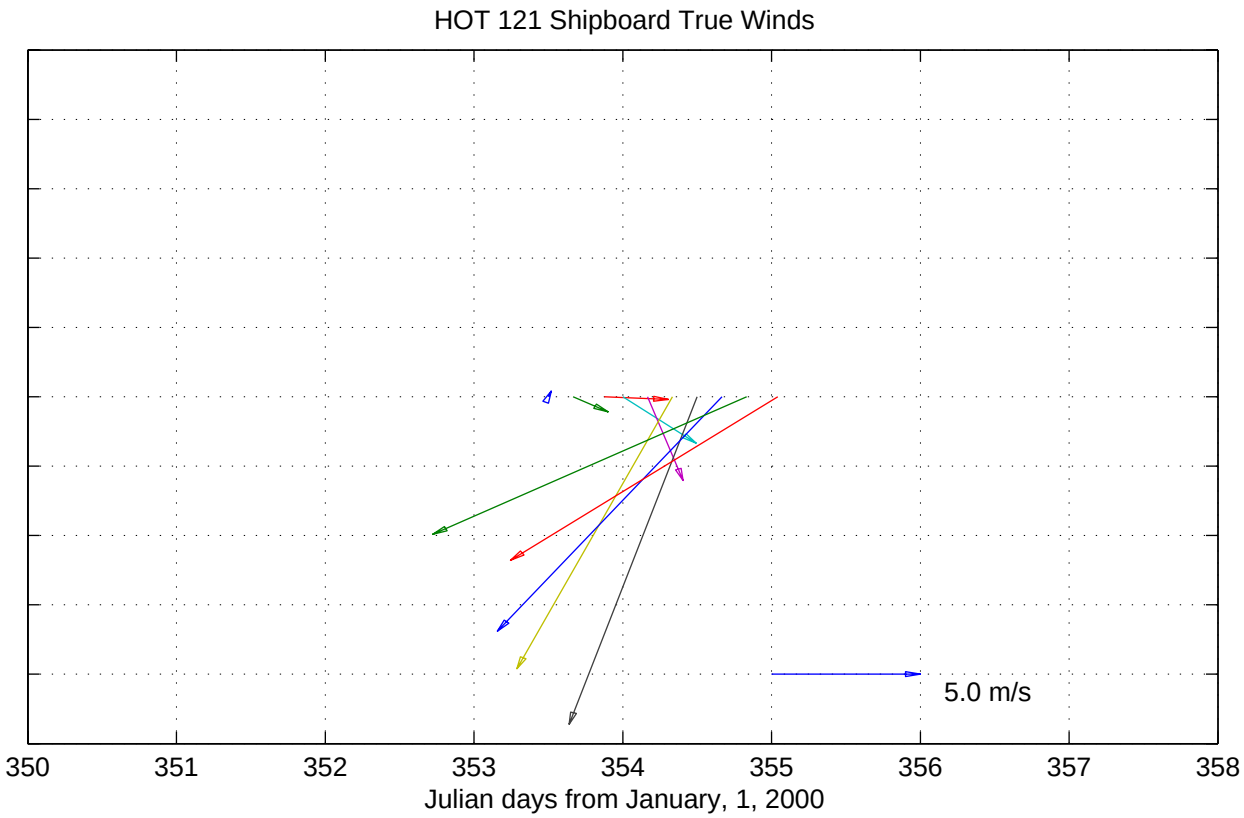
HOT 121 Shipboard True Winds
5.0 m/s
350
351
352
353
354
355
356
357
358
Julian days from January, 1, 2000

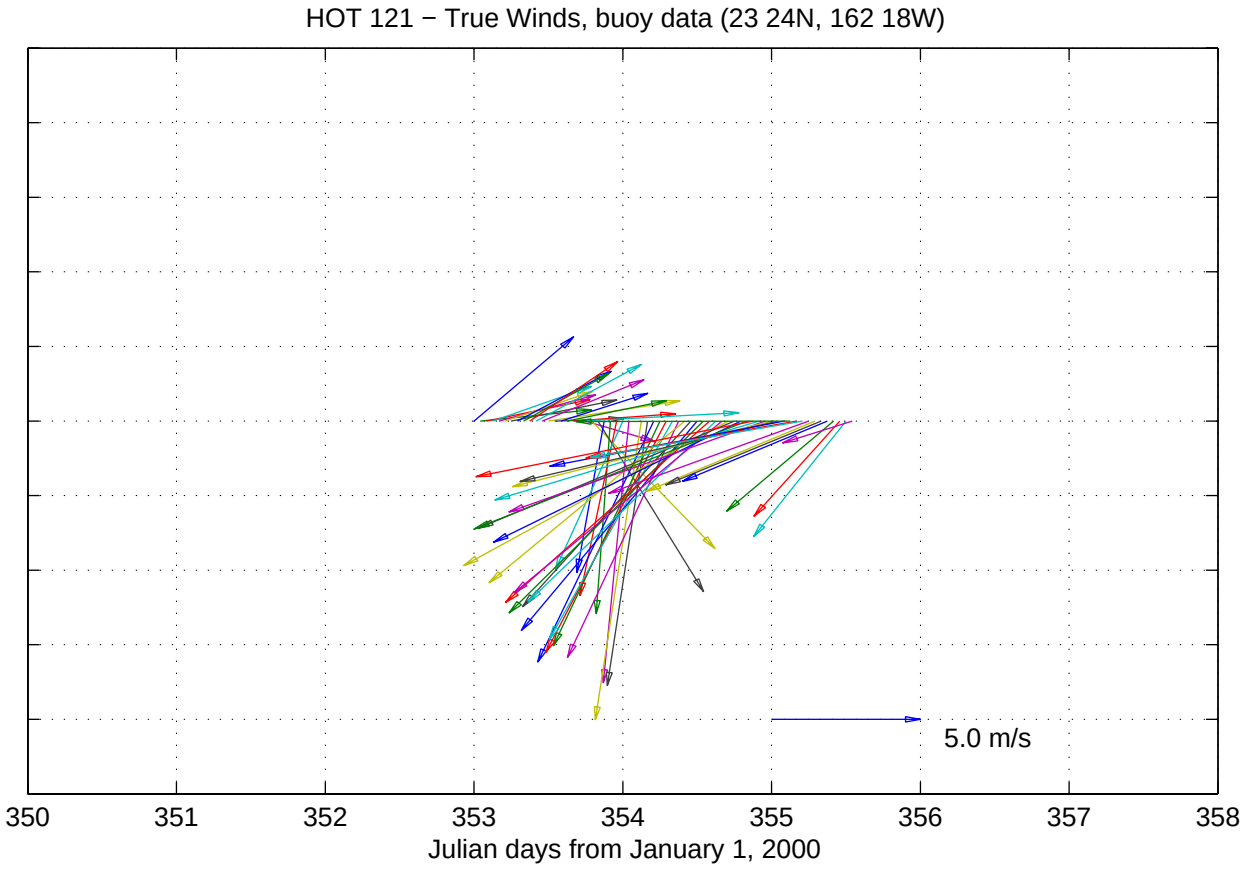
HOT 121 − True Winds, buoy data (23 24N, 162 18W)
5.0 m/s
350
351
352
353
354
355
356
357
358
Julian days from January 1, 2000

Figure 6.3.4k

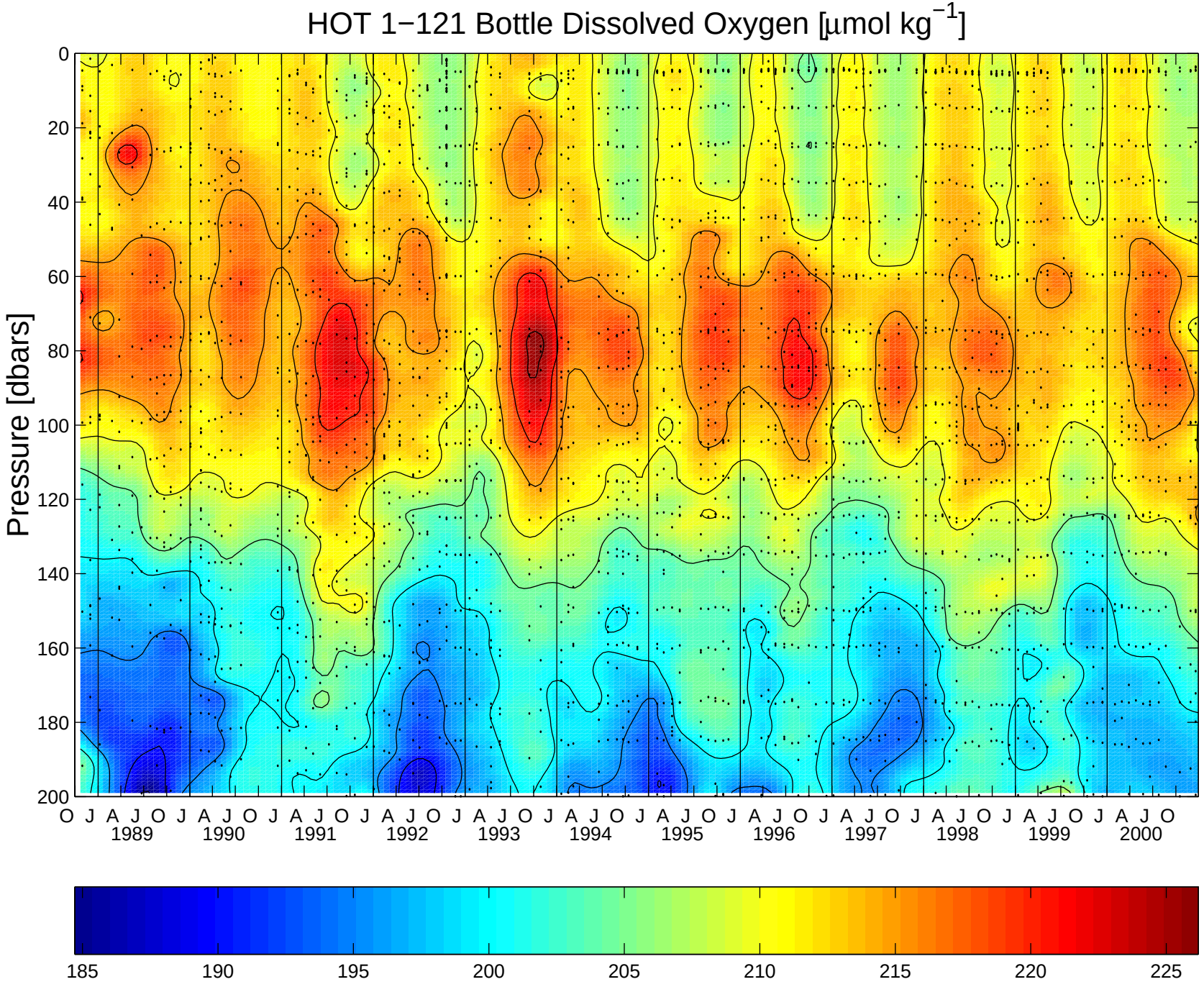
HOT 1−121 Bottle Dissolved Oxygen [µmol kg^{-1}]
Pressure [dbars]
0
20
40
60
80
100
120
140
160
180
200
O J A J O J A J O J A J O J A J O J A J O J A J O J A J O J A J O J A J O J A J O J A J O J A J O
1989
1990
1991
1992
1993
1994
1995
1996
1997
1998
1999
2000
185
190
195
200
205
210
215
220
225

Figure 6.4.1

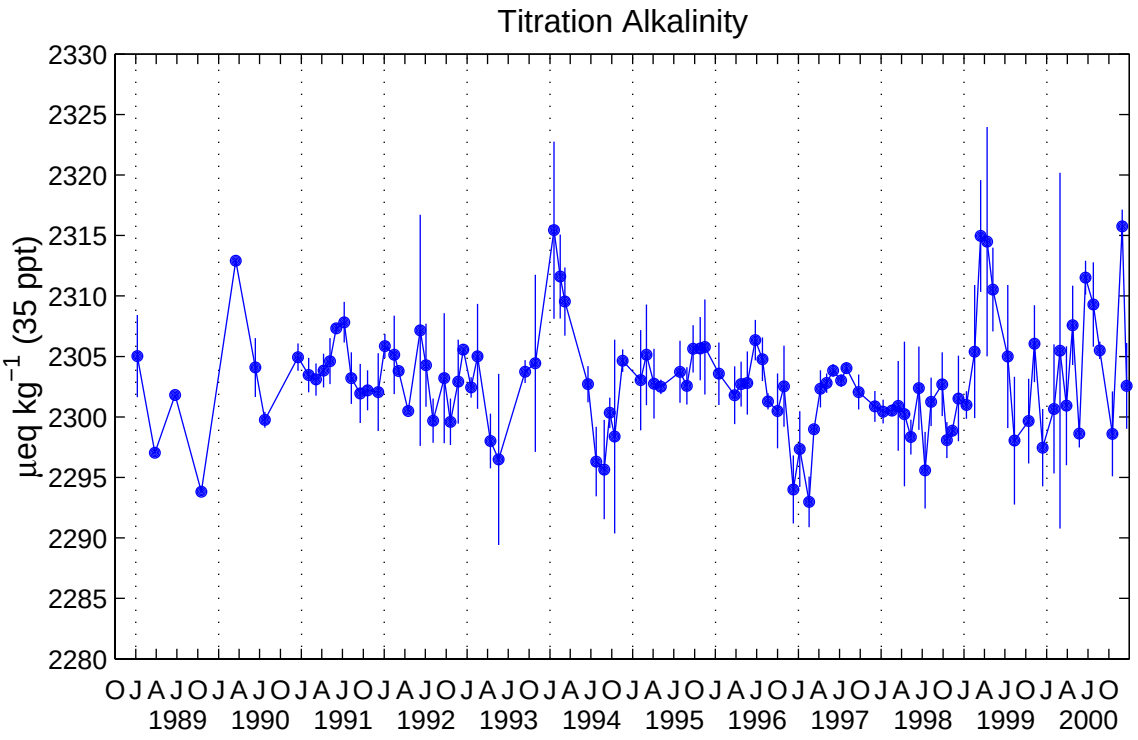
Titration Alkalinity
µeq kg^{-1} (35 ppt)
2330
2325
2320
2315
2310
2305
2300
2295
2290
2285
2280
O J A J O J A J O J A J O J A J O J A J O J A J O J A J O J A J O J A J O J A J O J A J O J A J O J A J O J A J O J A J O J A J O
1989 1990 1991 1992 1993 1994 1995 1996 1997 1998 1999 2000

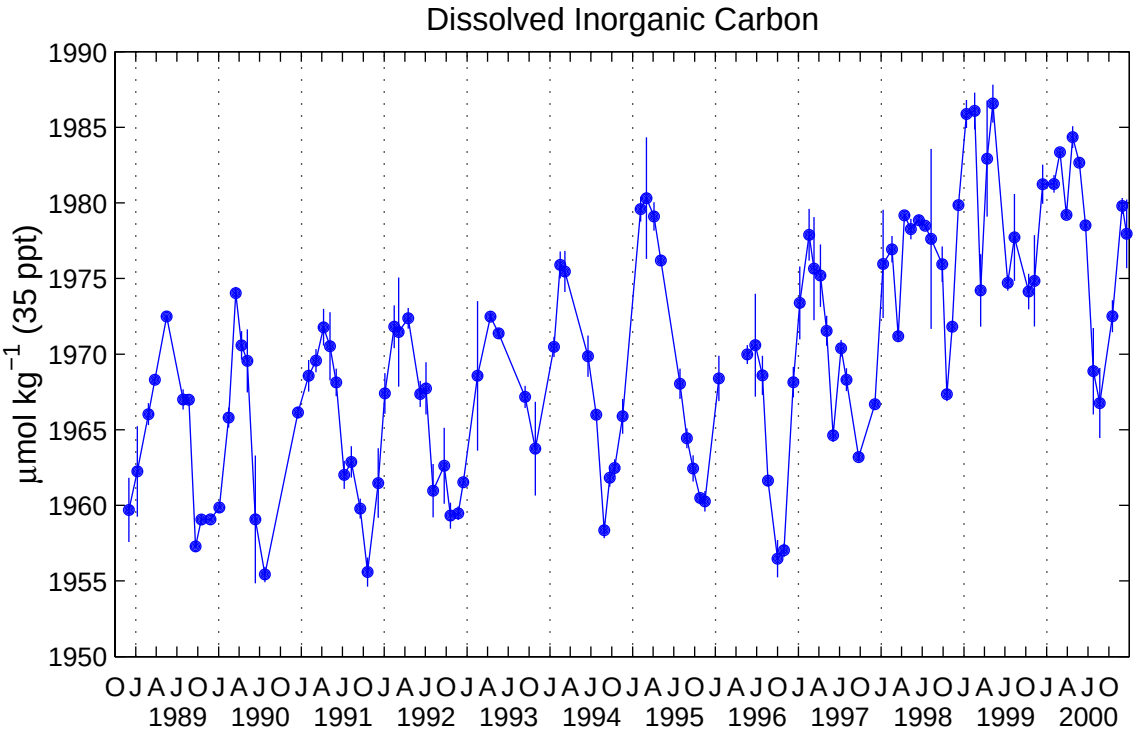
Dissolved Inorganic Carbon
µmol kg^{-1} (35 ppt)
1990
1985
1980
1975
1970
1965
1960
1955
1950
O J A J O J A J O J A J O J A J O J A J O J A J O J A J O J A J O J A J O J A J O J A J O J A J O J A J O J A J O J A J O J A J O
1989 1990 1991 1992 1993 1994 1995 1996 1997 1998 1999 2000

Figure 6.4.2

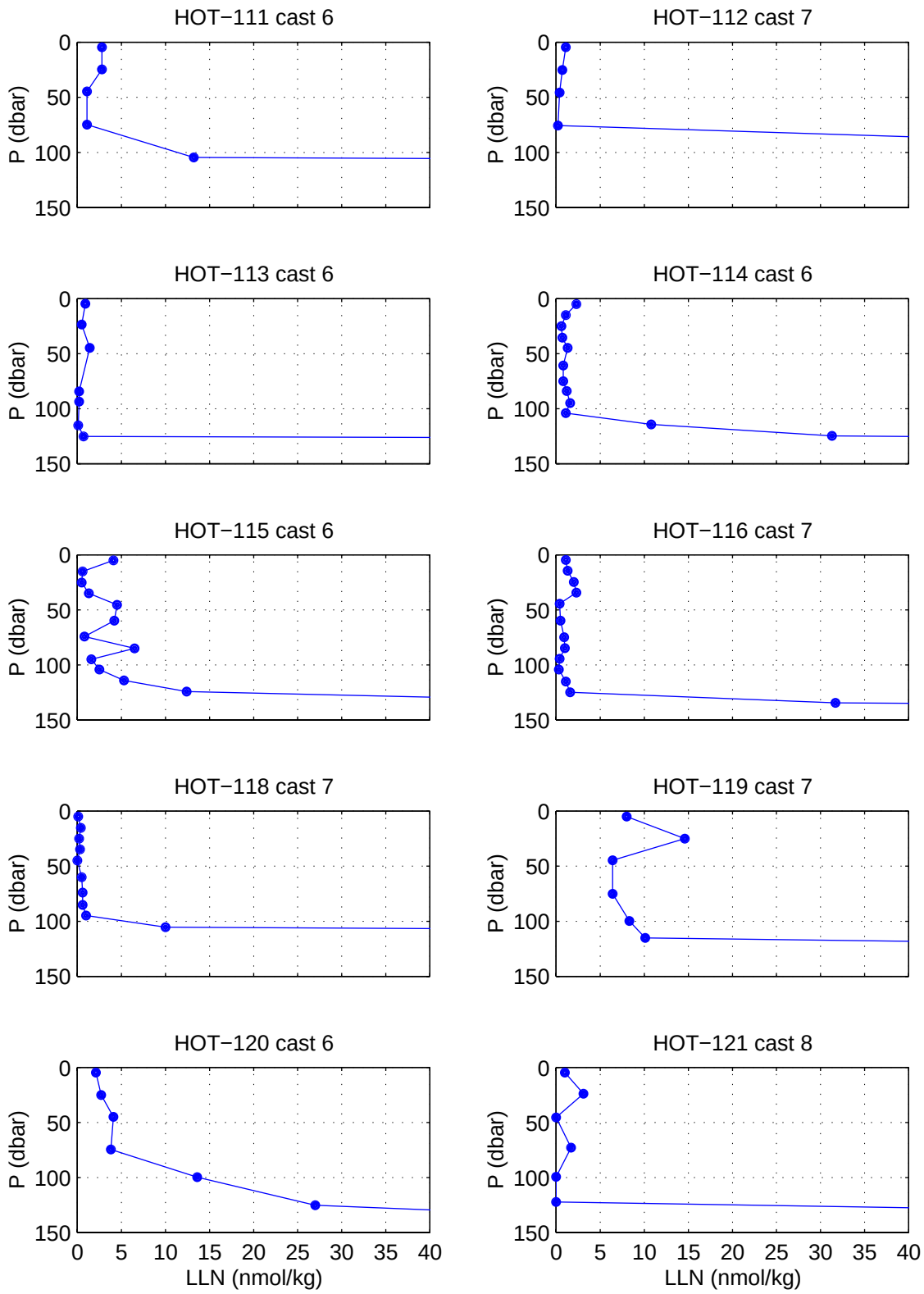
HOT−111 cast 6
HOT−112 cast 7
HOT−113 cast 6
HOT−114 cast 6
HOT−115 cast 6
HOT−116 cast 7
HOT−118 cast 7
HOT−119 cast 7
HOT−120 cast 6
HOT−121 cast 8
P (dbar)
0
50
100
150
0
5
10
15
20
25
30
35
40
LLN (nmol/kg)

Figure 6.4.3

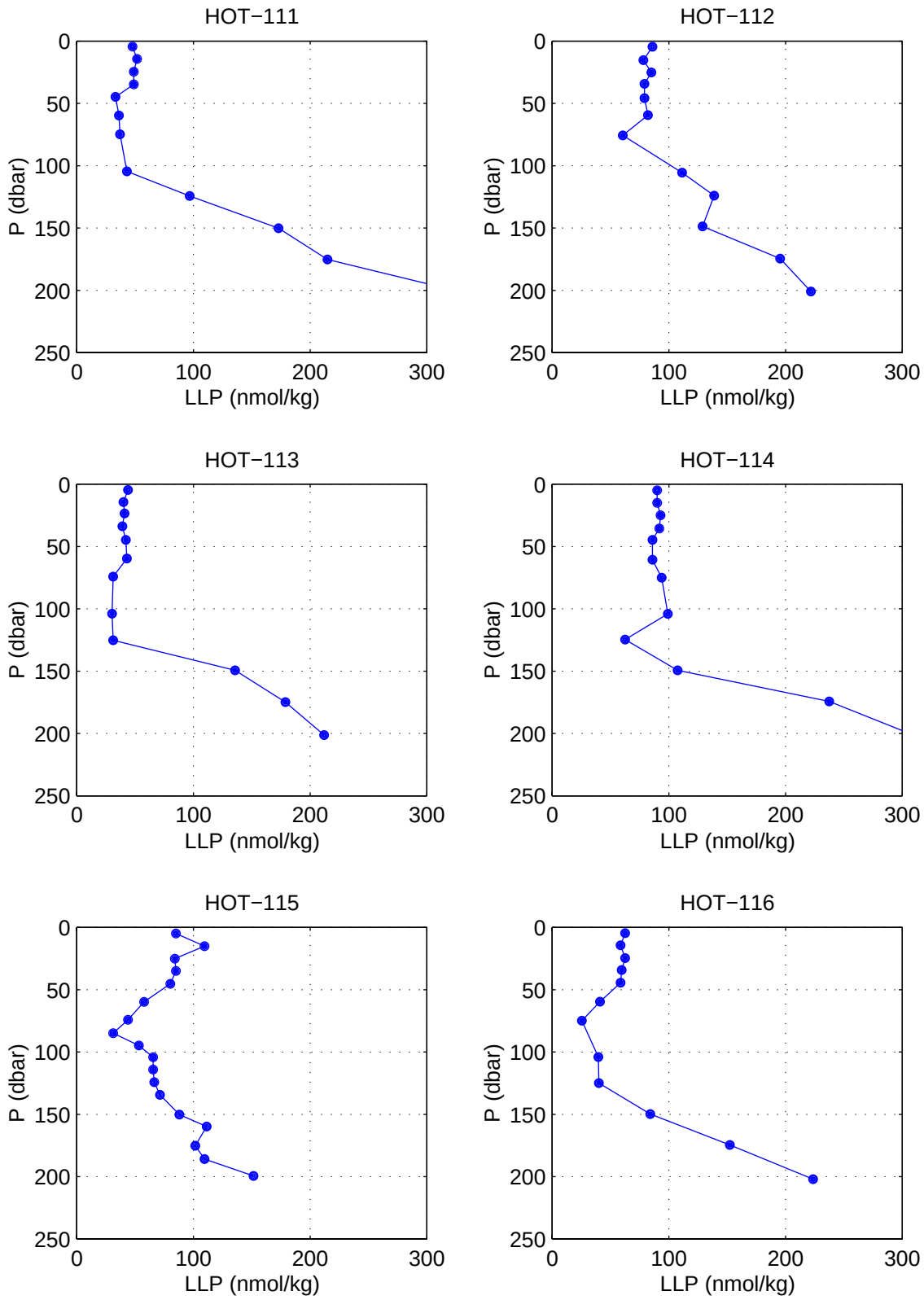
HOT−111
HOT−112
HOT−113
HOT−114
HOT−115
HOT−116
P (dbar)
LLP (nmol/kg)
0
50
100
150
200
250
0
100
200
300

Figure 6.4.4

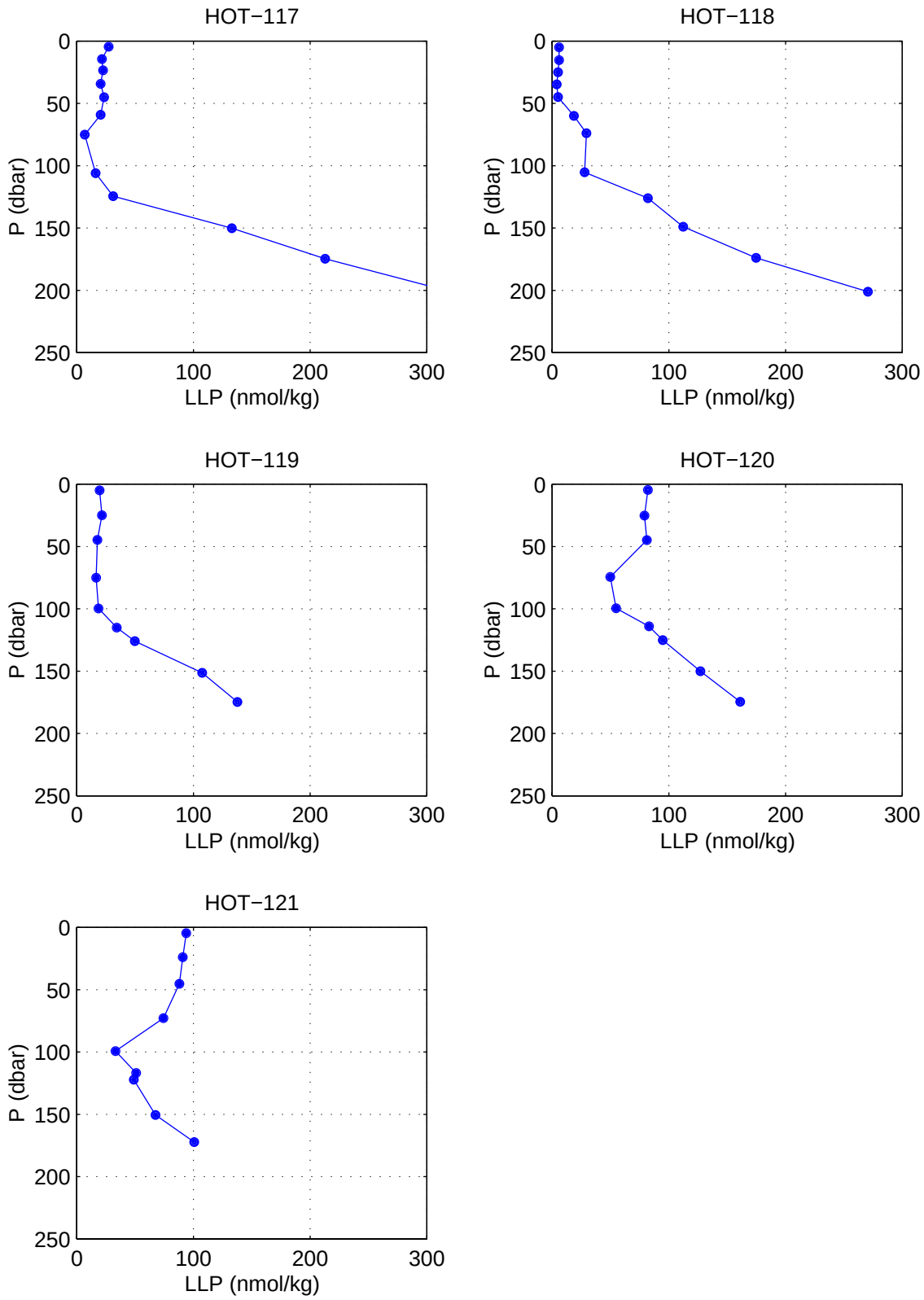

Figure 6.4.4 continued

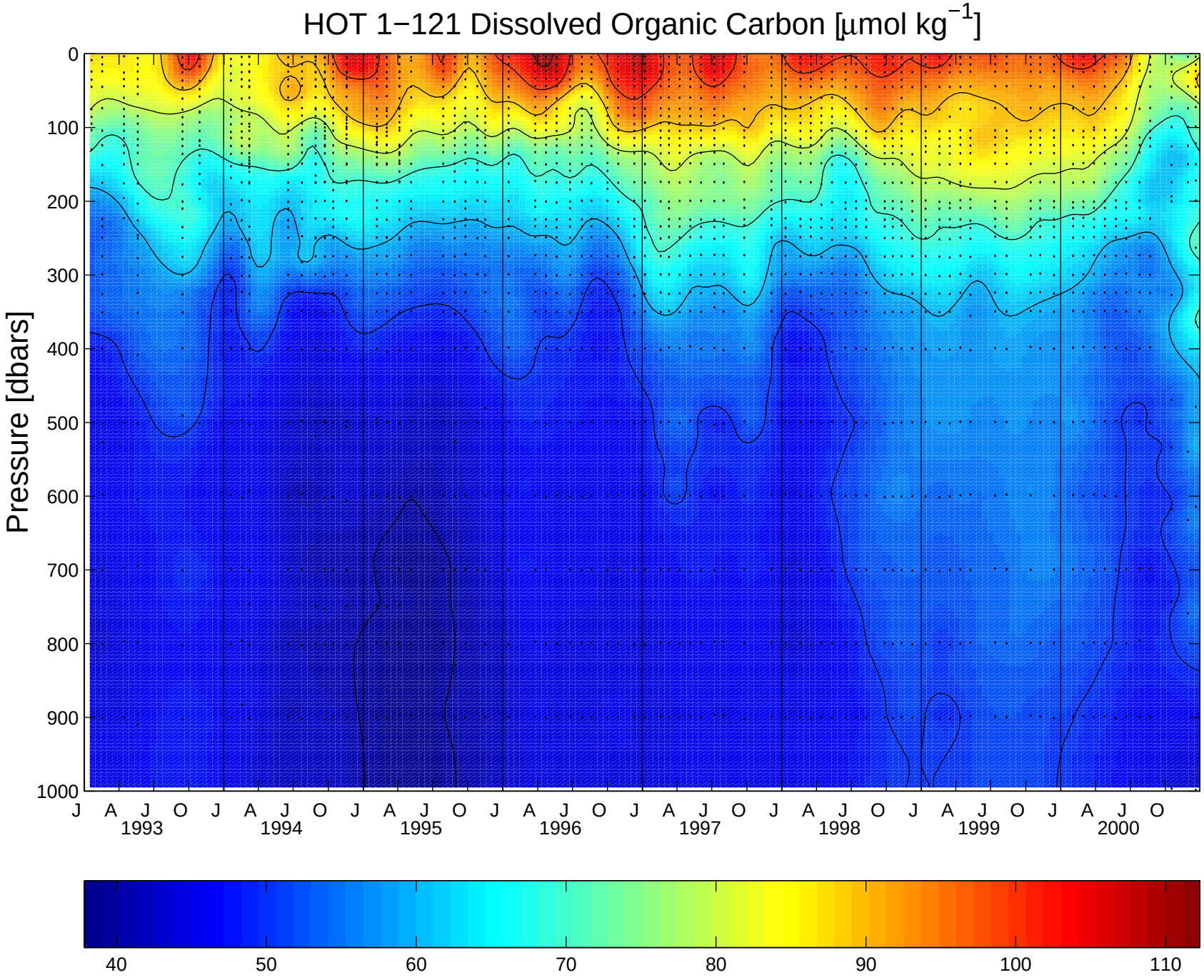
HOT 1−121 Dissolved Organic Carbon [µmol kg^{-1}]
Pressure [dbars]
0
100
200
300
400
500
600
700
800
900
1000
J A J O J A J O J A J O J A J O J A J O J A J O J A J O J A J O J A J O
1993
1994
1995
1996
1997
1998
1999
2000
40
50
60
70
80
90
100
110

Figure 6.4.5

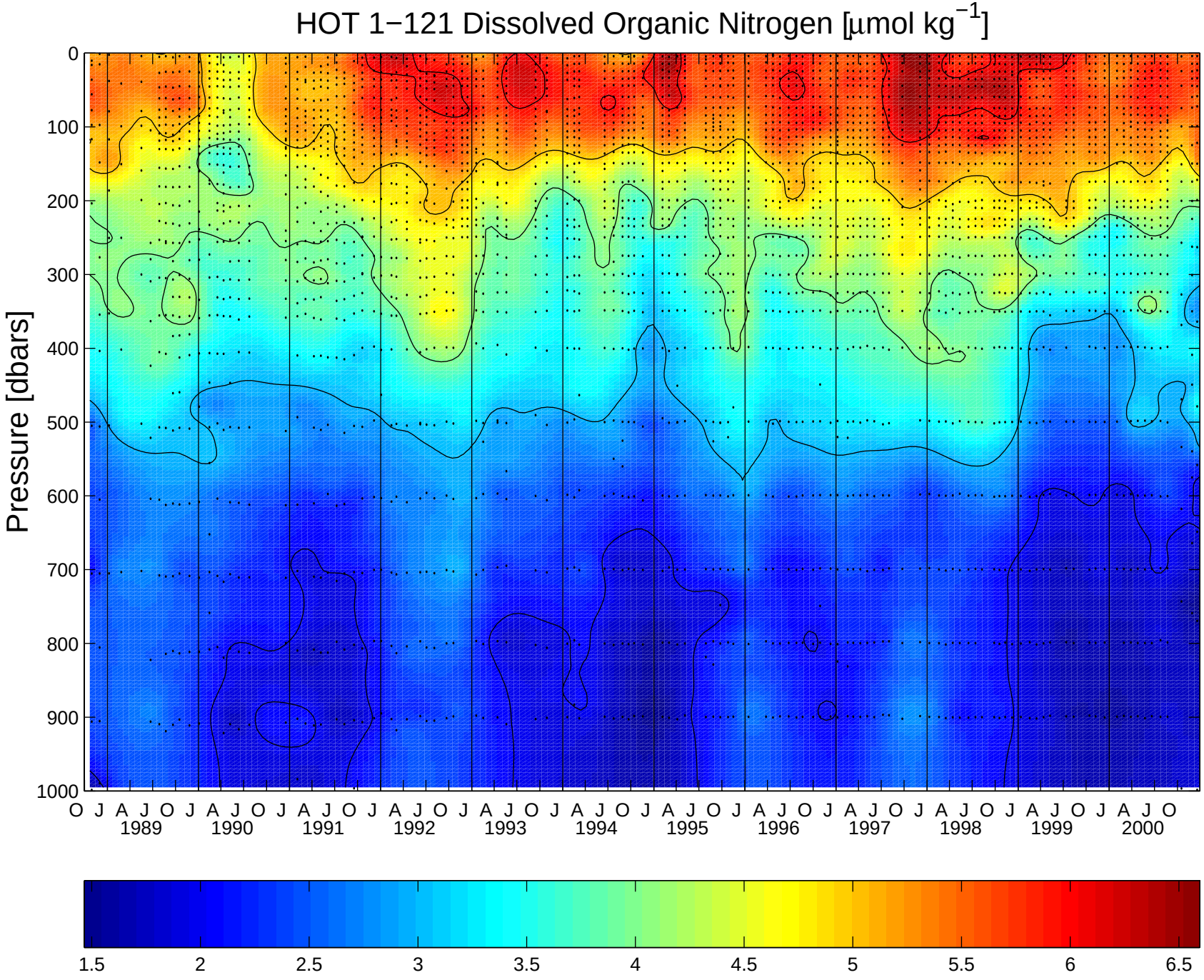
HOT 1−121 Dissolved Organic Nitrogen [µmol kg^{-1}]
Pressure [dbars]
0
100
200
300
400
500
600
700
800
900
1000
O J A J O J A J O J A J O J A J O J A J O J A J O J A J O J A J O J A J O J A J O J A J O J A J O
1989
1990
1991
1992
1993
1994
1995
1996
1997
1998
1999
2000
1.5
2
2.5
3
3.5
4
4.5
5
5.5
6
6.5

Figure 6.4.6

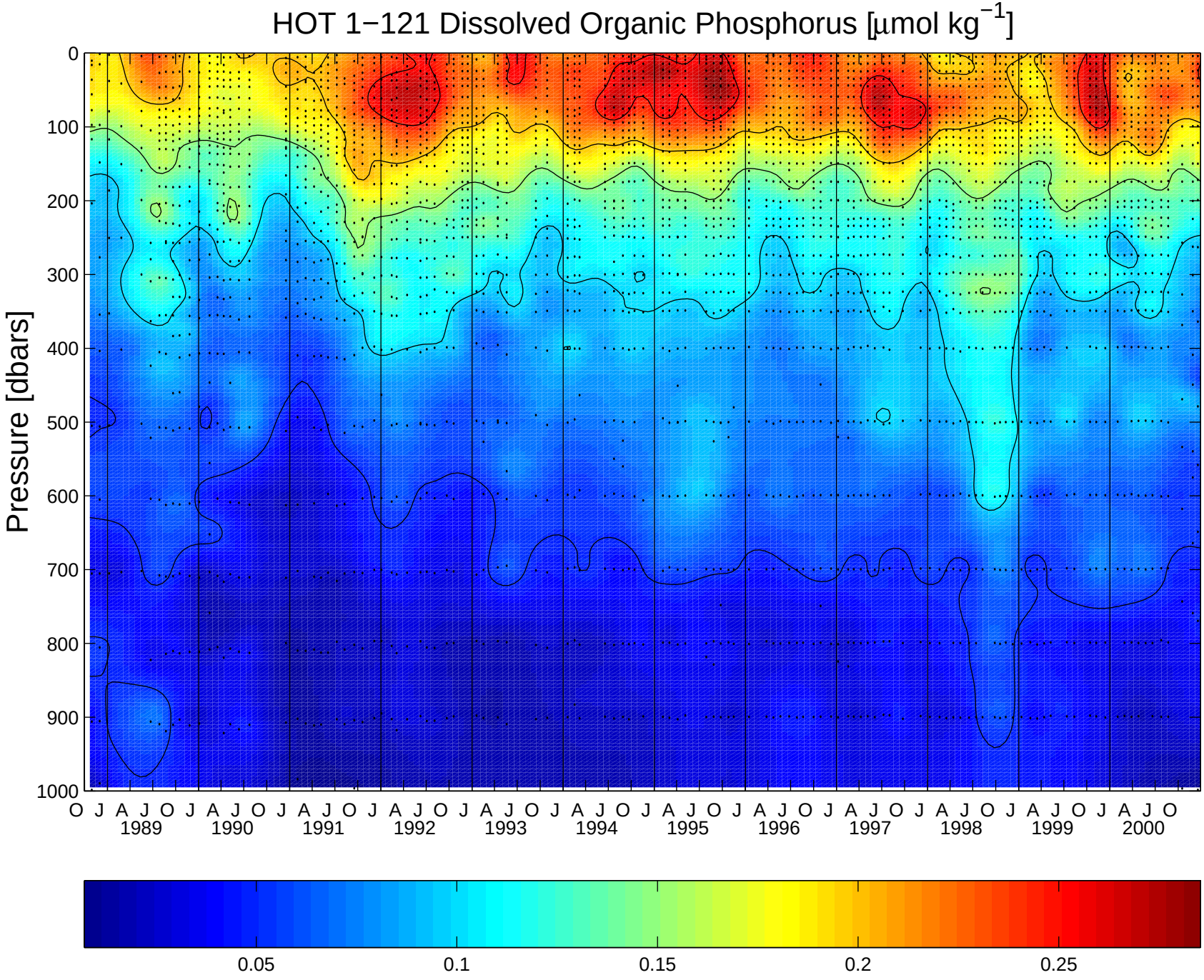
HOT 1−121 Dissolved Organic Phosphorus [µmol kg^{-1}]
Pressure [dbars]
0
100
200
300
400
500
600
700
800
900
1000
O J A J O J A J O J A J O J A J O J A J O J A J O J A J O J A J O J A J O J A J O J A J O J A J O
1989
1990
1991
1992
1993
1994
1995
1996
1997
1998
1999
2000
0.05
0.1
0.15
0.2
0.25

Figure 6.4.7

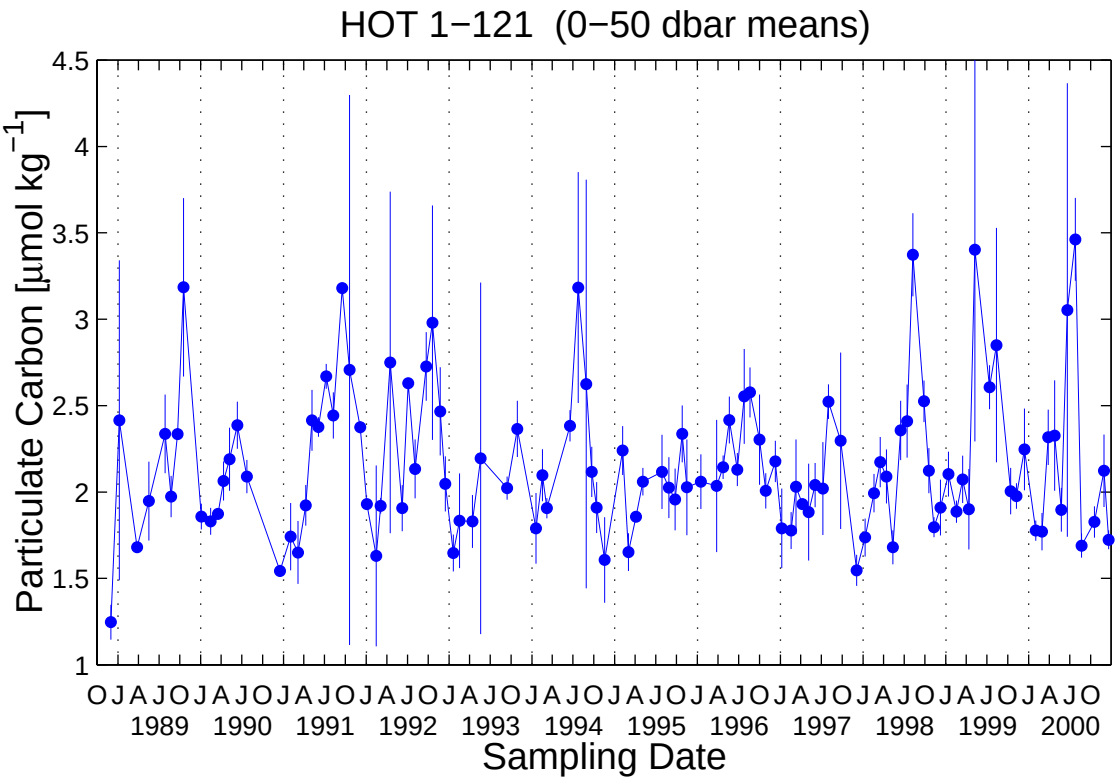
HOT 1−121 (0−50 dbar means)
Particulate Carbon [µmol kg^{-1}]
4.5
4
3.5
3
2.5
2
1.5
1
O J A J O J A J O J A J O J A J O J A J O J A J O J A J O J A J O J A J O J A J O J A J O J A J O J A J O J A J O
1989 1990 1991 1992 1993 1994 1995 1996 1997 1998 1999 2000
Sampling Date

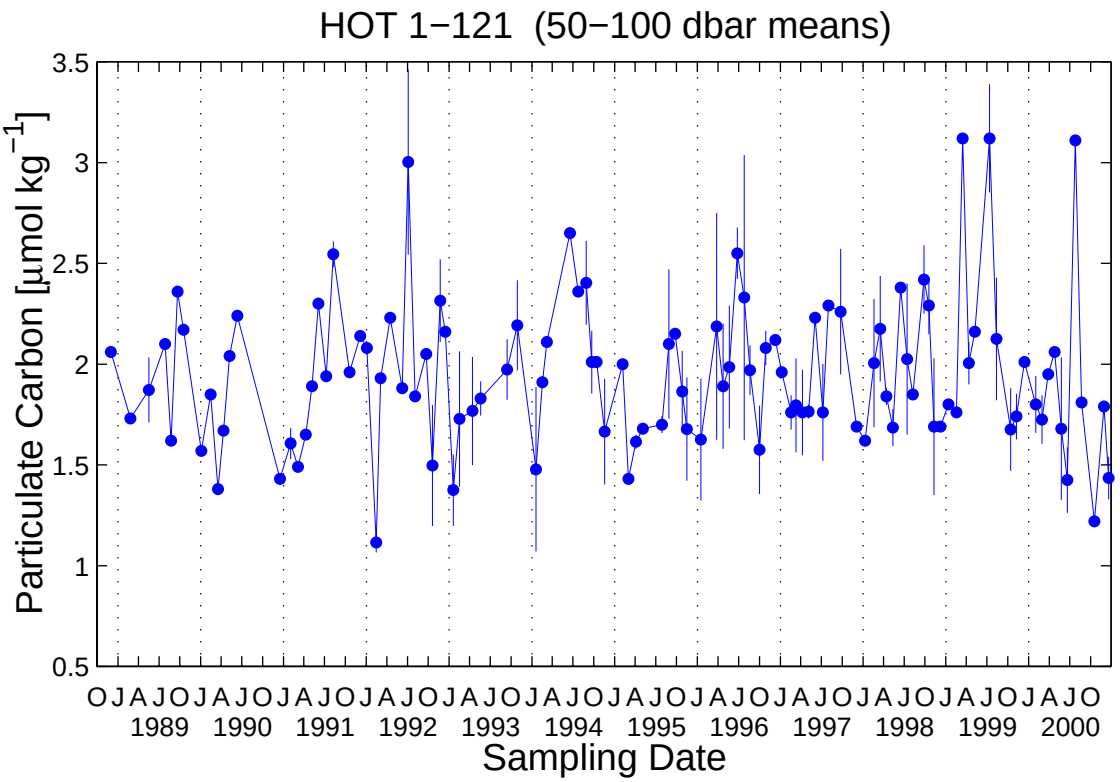
HOT 1−121 (50−100 dbar means)
Particulate Carbon [µmol kg^{-1}]
3.5
3
2.5
2
1.5
1
0.5
O J A J O J A J O J A J O J A J O J A J O J A J O J A J O J A J O J A J O J A J O J A J O J A J O J A J O J A J O
1989 1990 1991 1992 1993 1994 1995 1996 1997 1998 1999 2000
Sampling Date

Figure 6.4.8a

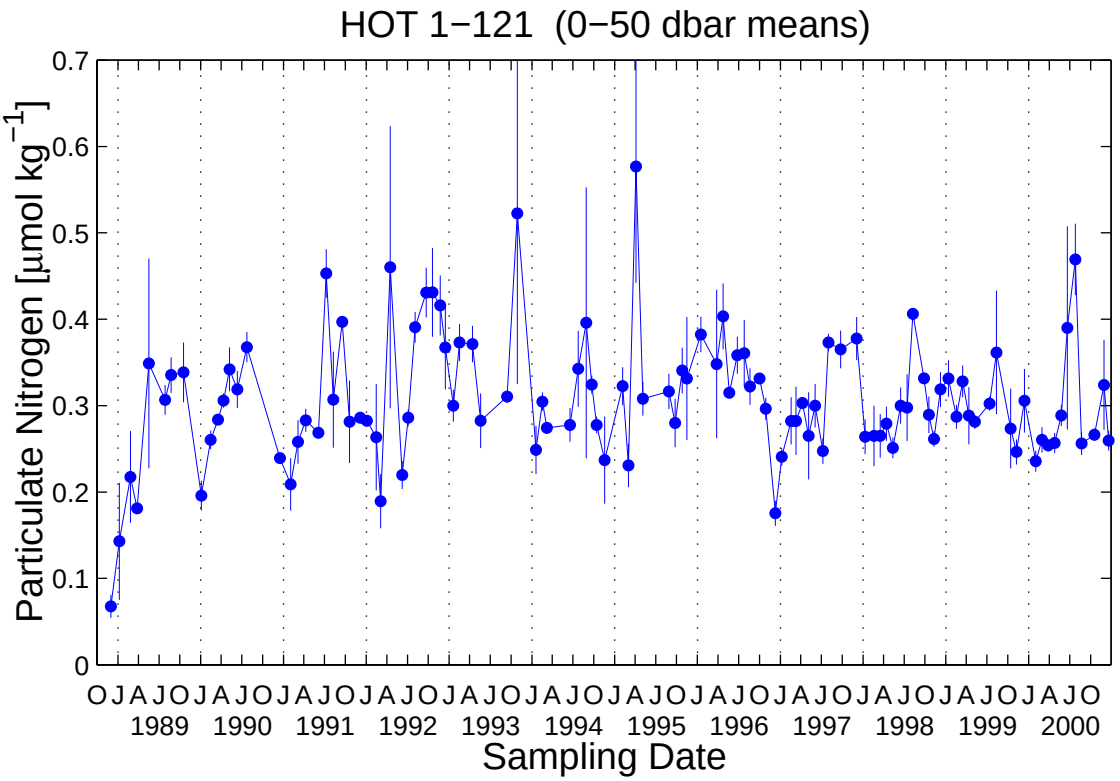
HOT 1−121 (0−50 dbar means)
Particulate Nitrogen [µmol kg^{-1}]
0
0.1
0.2
0.3
0.4
0.5
0.6
0.7
O J A J O J A J O J A J O J A J O J A J O J A J O J A J O J A J O J A J O J A J O J A J O J A J O J A J O
1989 1990 1991 1992 1993 1994 1995 1996 1997 1998 1999 2000
Sampling Date

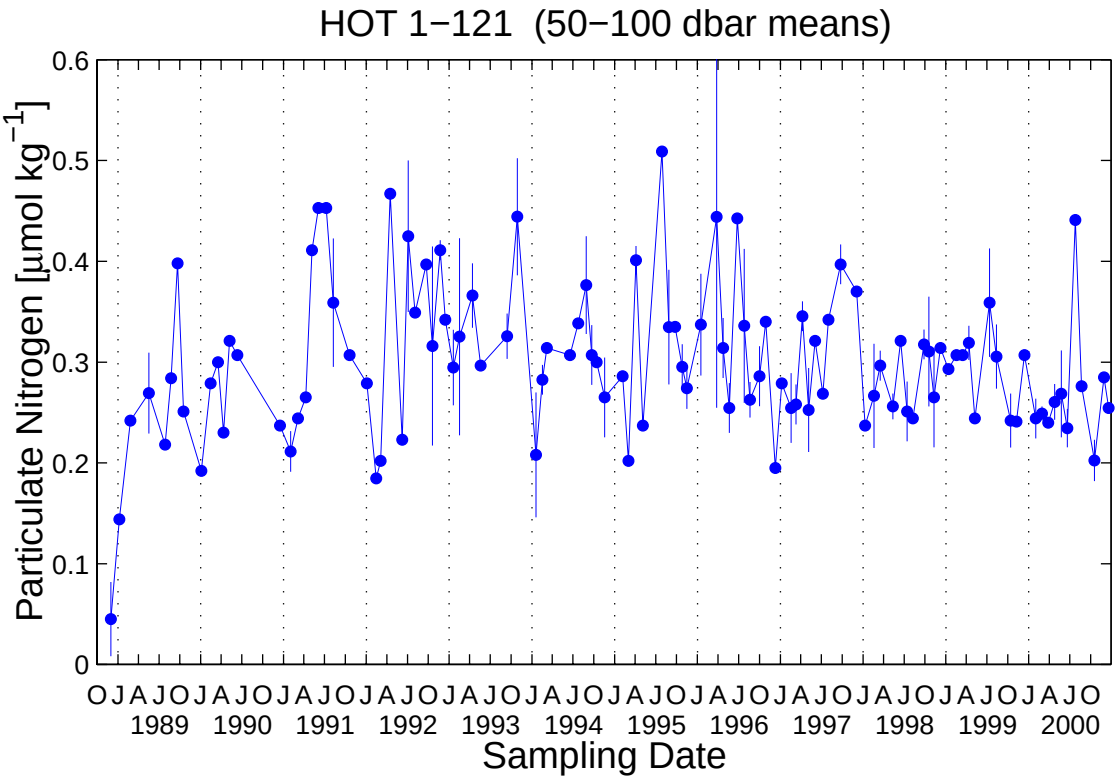
HOT 1−121 (50−100 dbar means)
Particulate Nitrogen [µmol kg^{-1}]
0
0.1
0.2
0.3
0.4
0.5
0.6
O J A J O J A J O J A J O J A J O J A J O J A J O J A J O J A J O J A J O J A J O J A J O J A J O J A J O
1989 1990 1991 1992 1993 1994 1995 1996 1997 1998 1999 2000
Sampling Date

Figure 6.4.8b

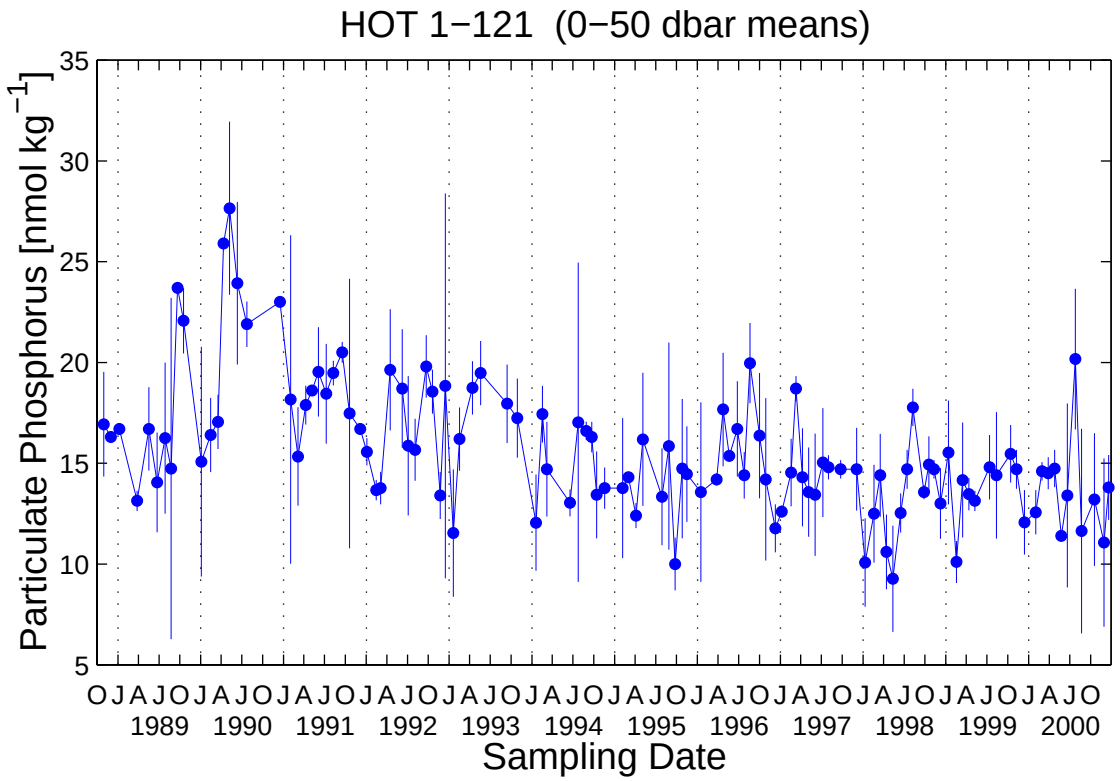
HOT 1−121 (0−50 dbar means)
Particulate Phosphorus [nmol kg^{-1}]
35
30
25
20
15
10
5
O J A J O J A J O J A J O J A J O J A J O J A J O J A J O J A J O J A J O J A J O J A J O J A J O J A J O
1989 1990 1991 1992 1993 1994 1995 1996 1997 1998 1999 2000
Sampling Date

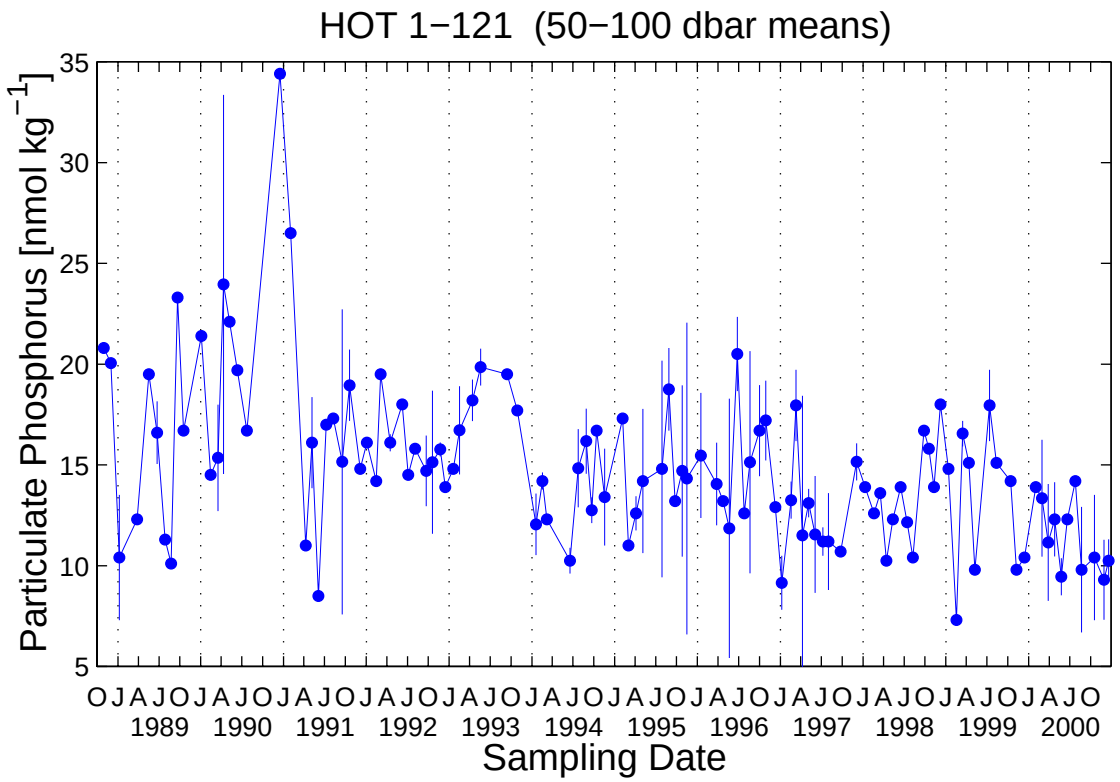
HOT 1−121 (50−100 dbar means)
Particulate Phosphorus [nmol kg^{-1}]
35
30
25
20
15
10
5
O J A J O J A J O J A J O J A J O J A J O J A J O J A J O J A J O J A J O J A J O J A J O J A J O J A J O
1989 1990 1991 1992 1993 1994 1995 1996 1997 1998 1999 2000
Sampling Date

Figure 6.4.8c

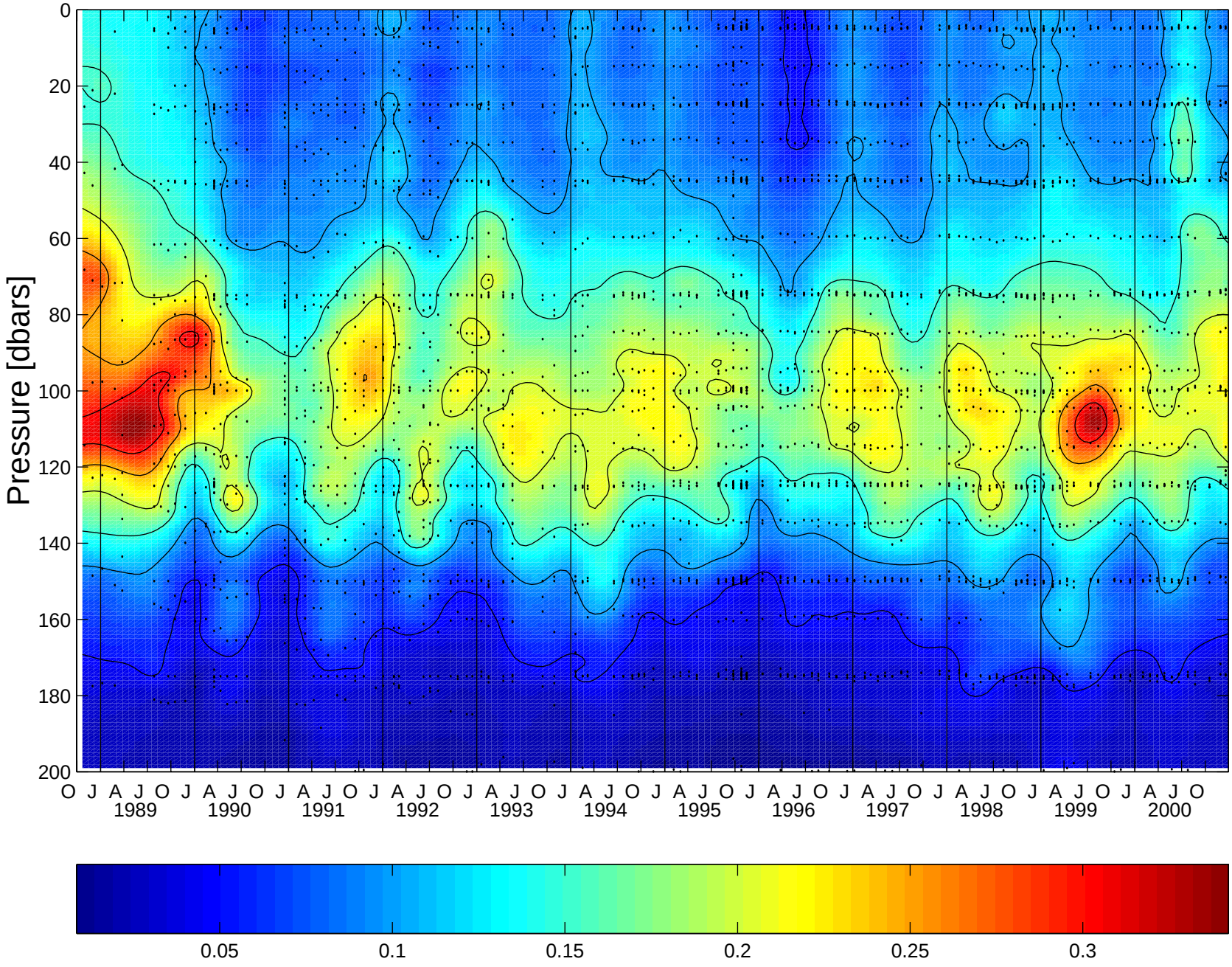
HOT 1−121 Fluorometric Chlorophyll a [mg m^{-3}]
Pressure [dbars]
0
20
40
60
80
100
120
140
160
180
200
O J A J O J A J O J A J O J A J O J A J O J A J O J A J O J A J O J A J O J A J O J A J O J A J O J A J O
1989
1990
1991
1992
1993
1994
1995
1996
1997
1998
1999
2000
0.05
0.1
0.15
0.2
0.25
0.3

Figure 6.4.9

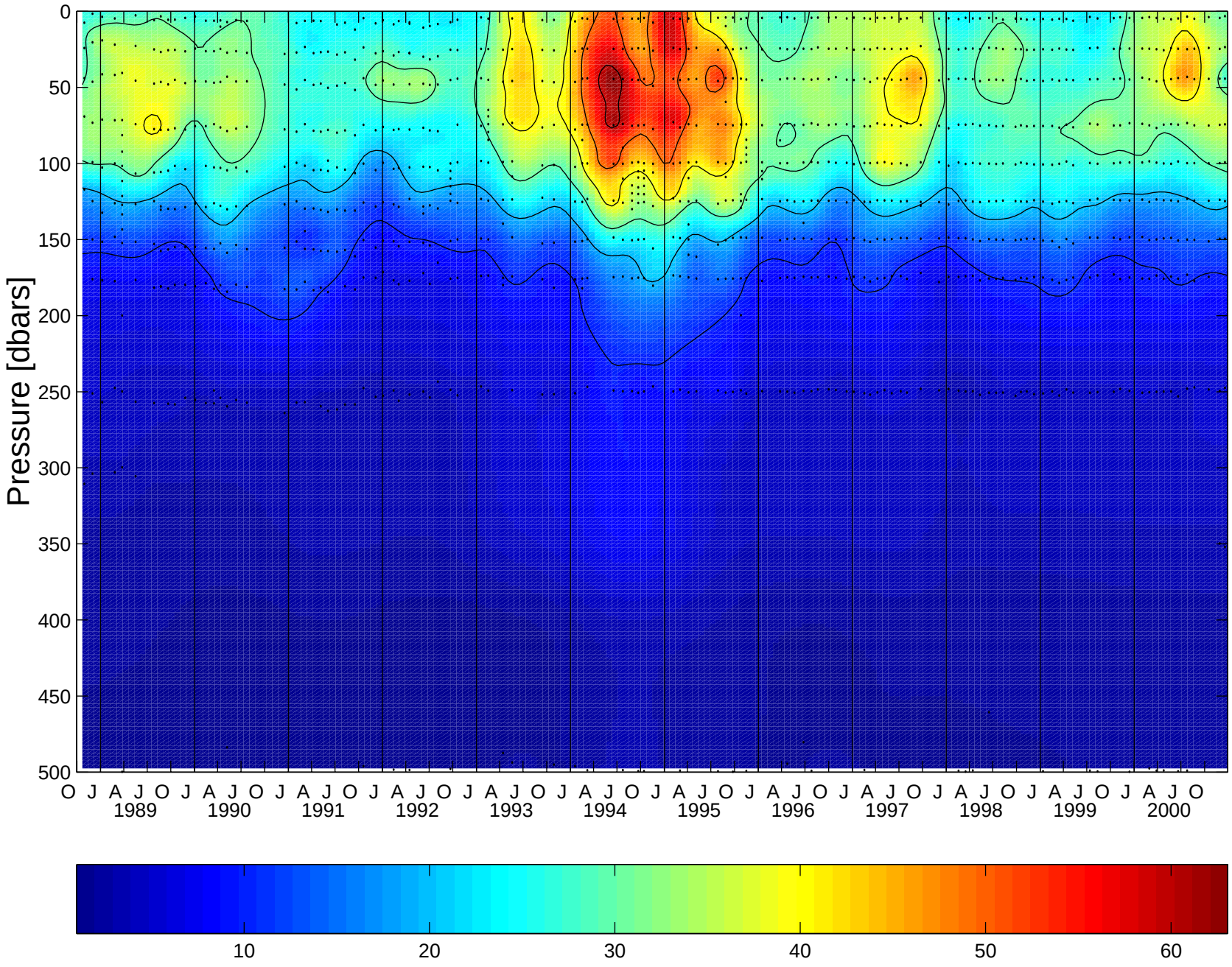
HOT 1−121 Adenosine 5'−Triphosphate [µg m^{-3}]
Pressure [dbars]
0
50
100
150
200
250
300
350
400
450
500
O J A J O J A J O J A J O J A J O J A J O J A J O J A J O J A J O J A J O J A J O J A J O J A J O J A J O J A J O J A J O
1989
1990
1991
1992
1993
1994
1995
1996
1997
1998
1999
2000
10
20
30
40
50
60

Figure 6.4.10

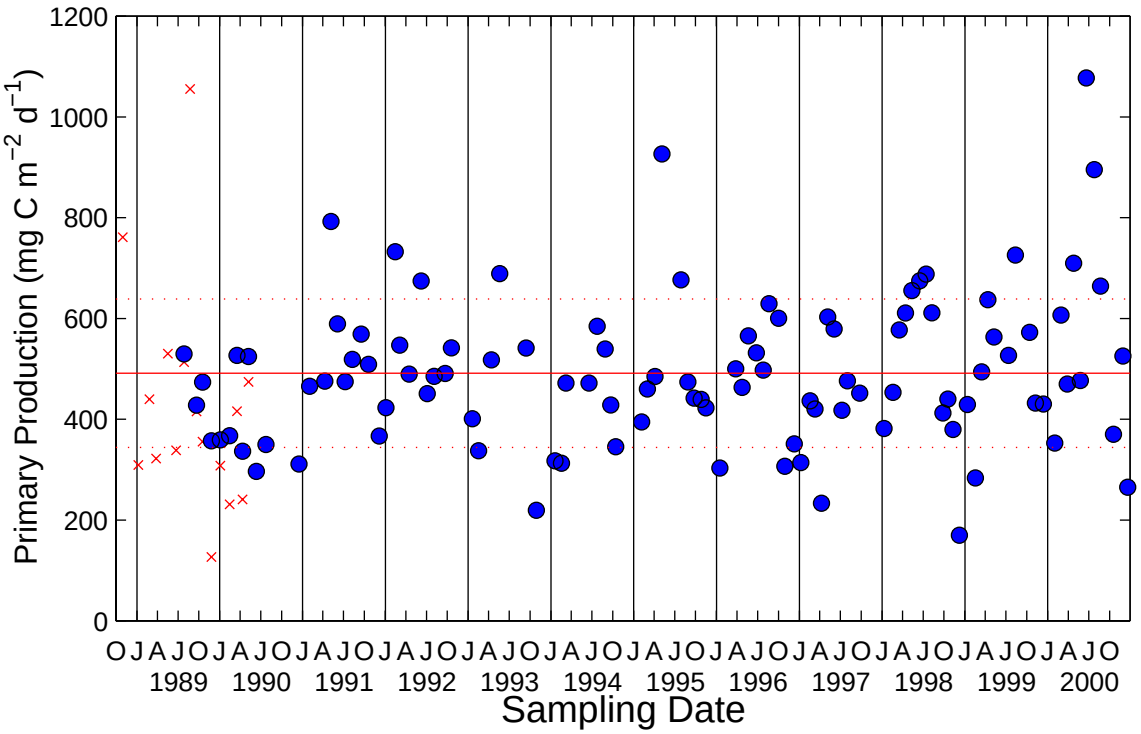
Primary Production (mg C m^{-2} d^{-1})
0
200
400
600
800
1000
1200
O J A J O J A J O J A J O J A J O J A J O J A J O J A J O J A J O J A J O J A J O J A J O J A J O J A J O J A J O
1989
1990
1991
1992
1993
1994
1995
1996
1997
1998
1999
2000
Sampling Date

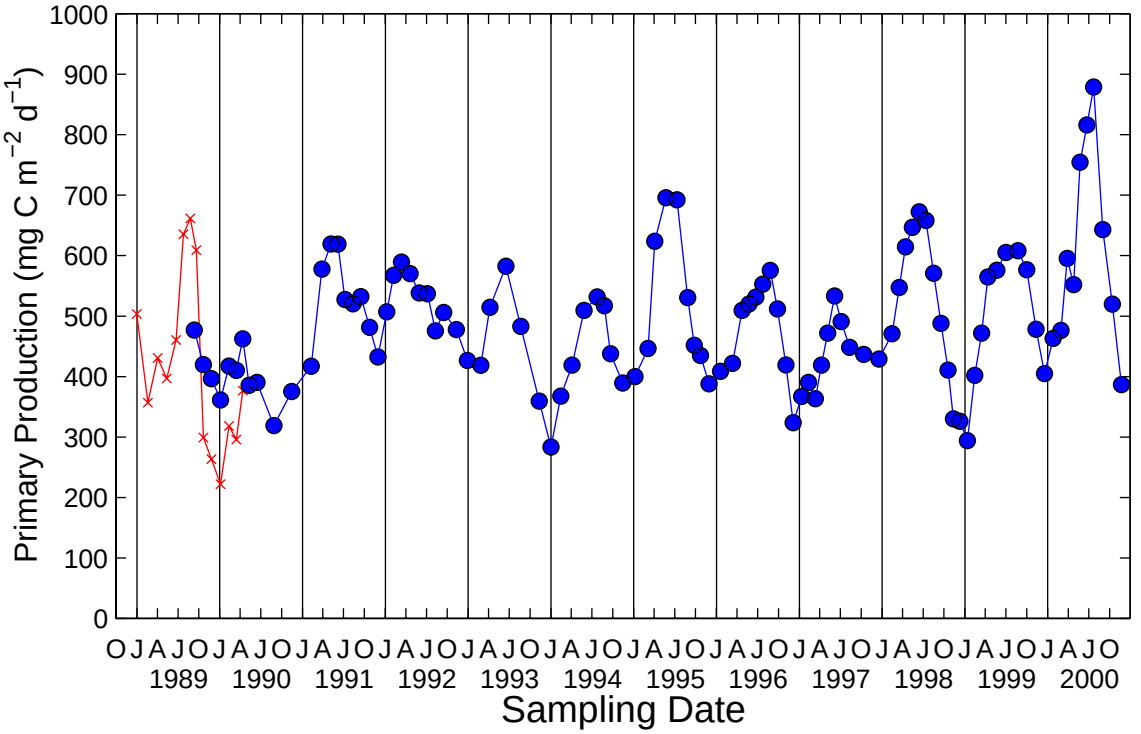
Primary Production (mg C m^{-2} d^{-1})
0
100
200
300
400
500
600
700
800
900
1000
O J A J O J A J O J A J O J A J O J A J O J A J O J A J O J A J O J A J O J A J O J A J O J A J O J A J O J A J O
1989
1990
1991
1992
1993
1994
1995
1996
1997
1998
1999
2000
Sampling Date

Figure 6.4.11

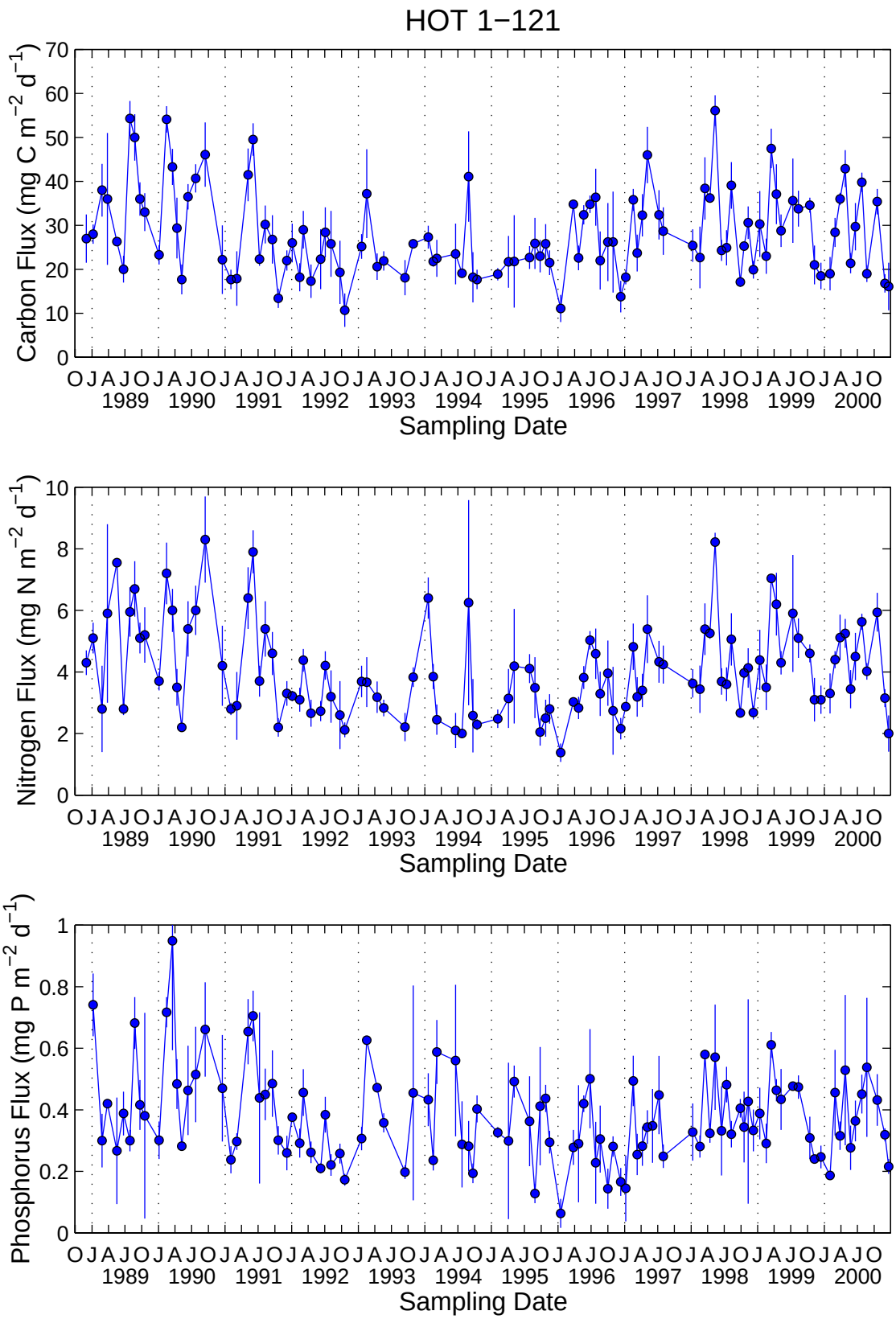
HOT 1−121
Carbon Flux (mg C m^{-2} d^{-1})
0
10
20
30
40
50
60
70
O J A J O J A J O J A J O J A J O J A J O J A J O J A J O J A J O J A J O J A J O J A J O J A J O J A J O
1989 1990 1991 1992 1993 1994 1995 1996 1997 1998 1999 2000
Sampling Date
Nitrogen Flux (mg N m^{-2} d^{-1})
0
2
4
6
8
10
O J A J O J A J O J A J O J A J O J A J O J A J O J A J O J A J O J A J O J A J O J A J O J A J O J A J O
1989 1990 1991 1992 1993 1994 1995 1996 1997 1998 1999 2000
Sampling Date
Phosphorus Flux (mg P m^{-2} d^{-1})
0
0.2
0.4
0.6
0.8
1
O J A J O J A J O J A J O J A J O J A J O J A J O J A J O J A J O J A J O J A J O J A J O J A J O J A J O
1989 1990 1991 1992 1993 1994 1995 1996 1997 1998 1999 2000
Sampling Date

Figure 6.4.12

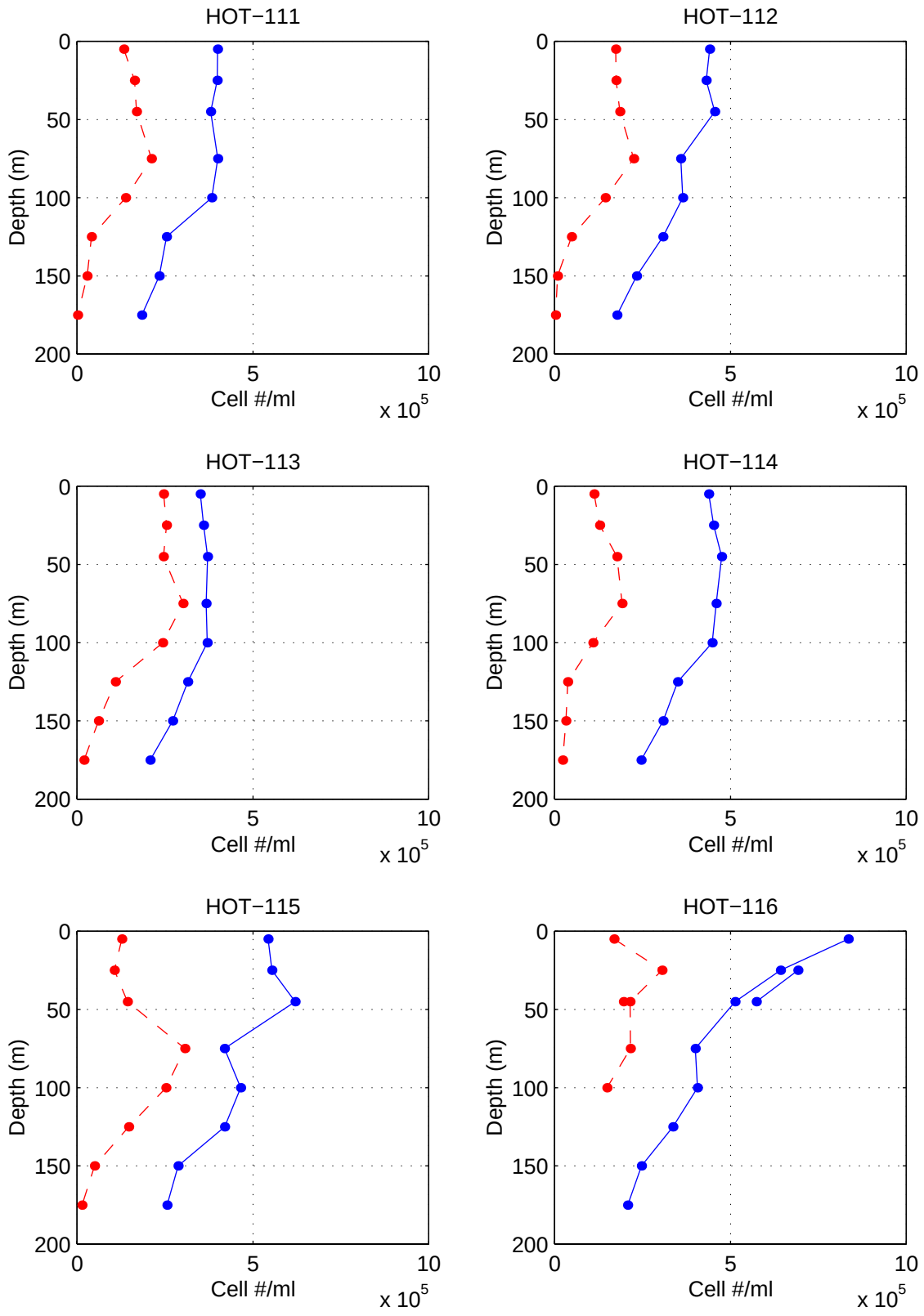
HOT−111
HOT−112
HOT−113
HOT−114
HOT−115
HOT−116
Depth (m)
0
50
100
150
200
0
5
10
Cell #/ml
x 10^5

Figure 6.4.13

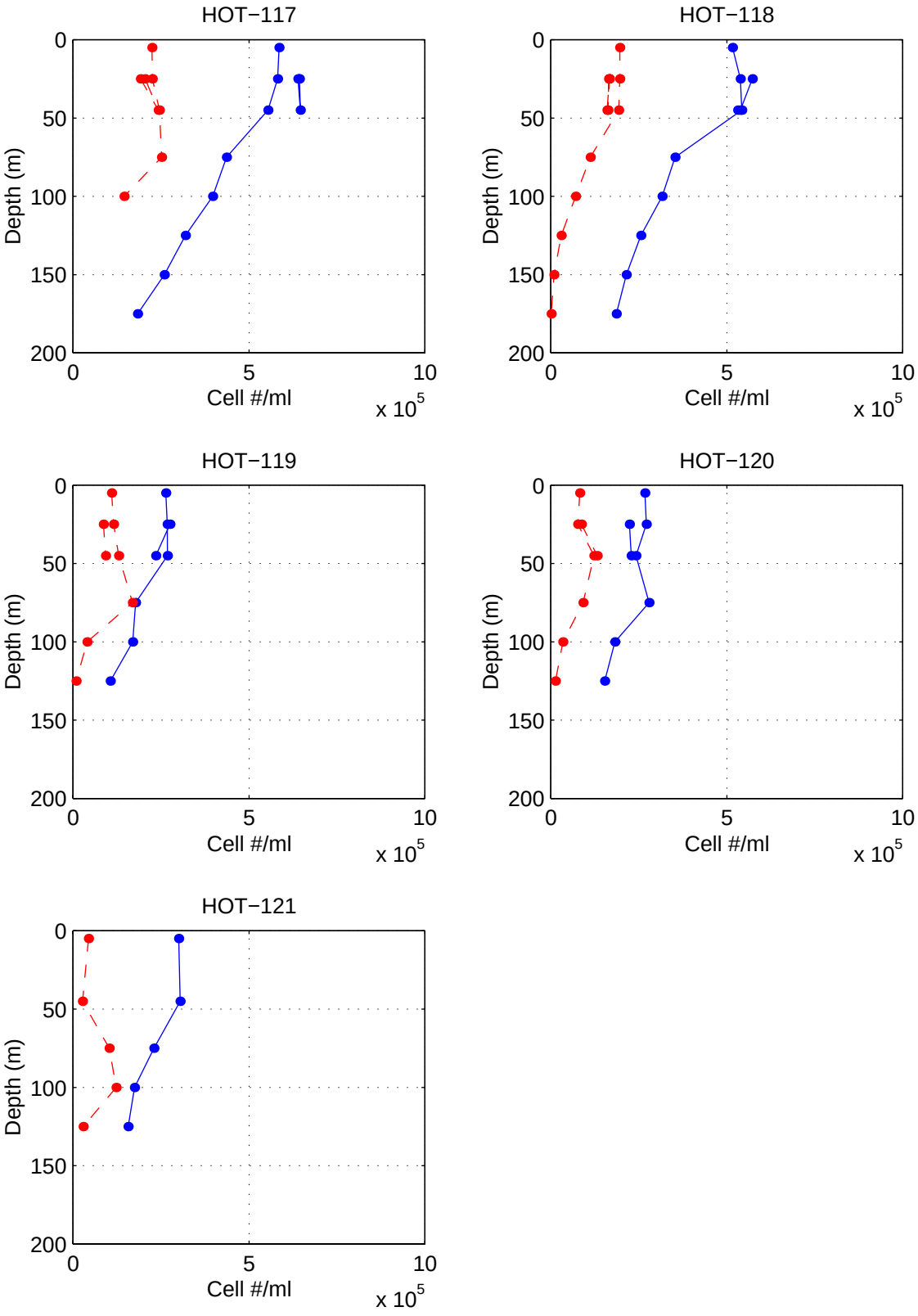

Figure 6.4.13 continued

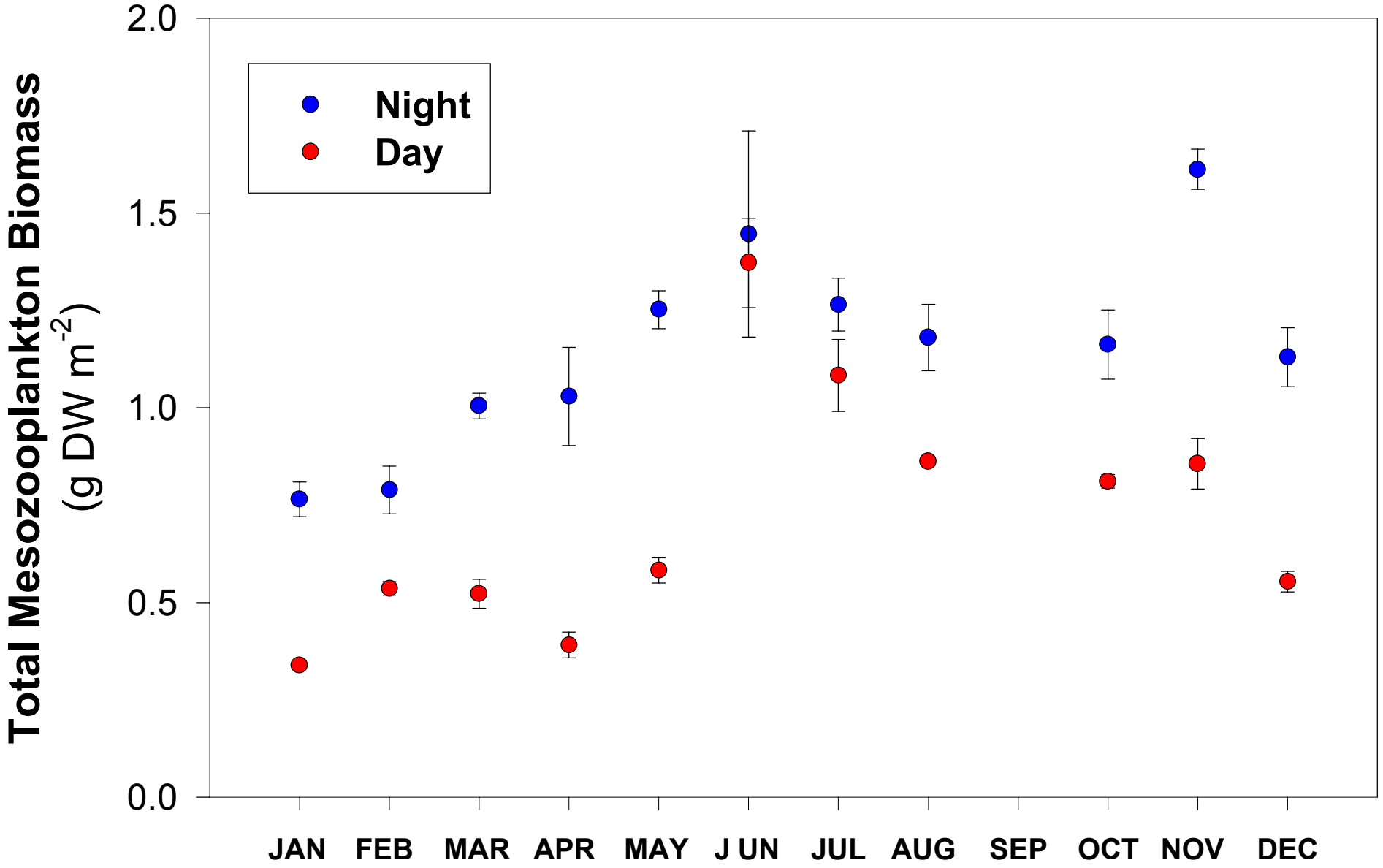
Total Mesozooplankton Biomass
(g DW m-2)
2.0
1.5
1.0
0.5
0.0
Night
Day
JAN
FEB
MAR
APR
MAY
J UN
JUL
AUG
SEP
OCT
NOV
DEC

Figure 6.4.14